Analysis of Parameter-Uniform Numerical Methods for Singularly Perturbed Differential Equations with Two Parameters

Mrityunjoy Barman

Department of Mathematics
Indian Institute of Technology Guwahati
Guwahati - 781039, India.

August, 2023

Analysis of Parameter-Uniform Numerical Methods for Singularly Perturbed Differential Equations with Two Parameters

A Thesis Submitted

in the Partial Fulfillment of the Requirements

for the Degree of

DOCTOR OF PHILOSOPHY

by

Mrityunjoy Barman

(Roll Number: 176123001)

Department of Mathematics

Indian Institute of Technology Guwahati

Guwahati - 781039, India.

August, 2023

DECLARATION

It is certified that the work contained in this thesis titled **"Analysis of Parameter-Uniform Numerical Methods for Singularly Perturbed Differential Equations with Two Parameters"** was completed by me, under the supervision of **Dr. Natesan Srinivasan, Professor, Department of Mathematics, Indian Institute of Technology Guwahati** for the award of the degree of Doctor of Philosophy and this work has not been submitted elsewhere for a degree.

August, 2023

Mrityunjoy Barman
(Roll No. 176123001)
Department of Mathematics
Indian Institute of Technology Guwahati.

CERTIFICATE

It is certified that the work contained in this thesis titled **"Analysis of Parameter-Uniform Numerical Methods for Singularly Perturbed Differential Equations with Two Parameters"** by **Mrityunjoy Barman**, a student of **Department of Mathematics, Indian Institute of Technology Guwahati**, for the award of the degree of Doctor of Philosophy has been carried out under my supervision and this work has not been submitted elsewhere for a degree.

August, 2023

Prof. Natesan Srinivasan
Professor
Department of Mathematics
Indian Institute of Technology Guwahati

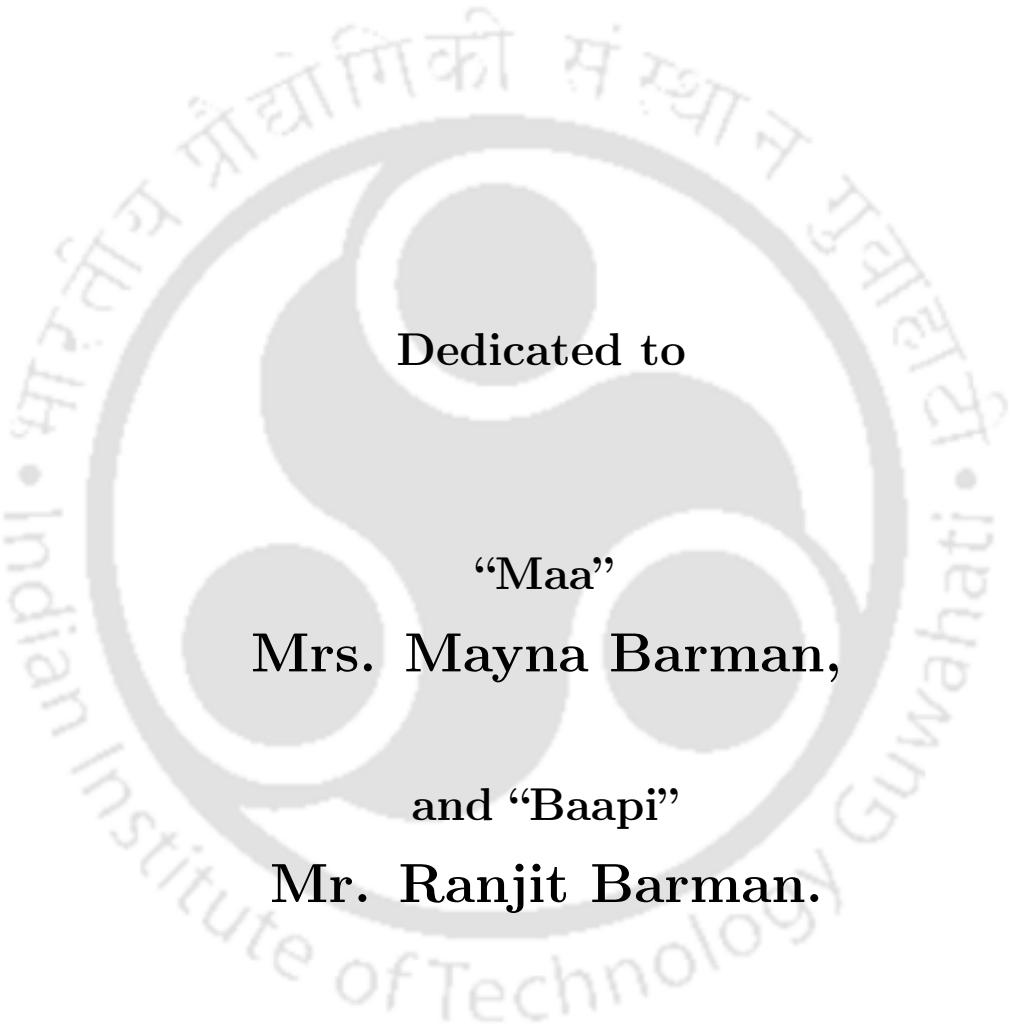

Dedicated to

"Maa"

Mrs. Mayna Barman,

and "Baapi"

Mr. Ranjit Barman.

ACKNOWLEDGMENT

At first, I would like to express my gratefulness to my thesis supervisor Prof. Natesan Srinivasan for his guidance and consistent encouragement to complete this thesis. I am deeply indebted to him for his support throughout this project. His expertise and suggestions have been invaluable to me, and I am grateful for his willingness to go above and beyond to help me succeed.

I would also like to thank my doctoral committee members, Prof. Swaroop Nandan Bora, Prof. Durga Charan Dalal and Prof. Rajen Kumar Sinha, for their valuable feedback and suggestions time to time. Their insights have helped me to improve my research and studies during the PhD tenure as well as my Masters course at IIT Guwahati

I am grateful to IIT Guwahati and Department of Education, Govt. of India for providing me financial support for carrying out research in this PhD program. I also acknowledge the support I have received from our Department staffs Mr. Santanu Da, Shridhar Da, Jayanta Da, Phatik Da, Pran Pratim Da, Pranab Jyoti Da, who helped me with the official and technical matters over the years.

I am also grateful to my friends and family for their support and encouragement. They have been there for me every step of the way, and I could not have done this without them. In particular, I would like to thank my parents, Mrs. Mayna Barman and Mr. Ranjit Barman, who always stood by me in every steps of this journey. They have always believed in me, and their sacrifices have made this journey possible. I am thankful to my siblings and cousins Chumki, Rinki, Nabonita, Jayita, and my uncle Mr. Bhombol Roy for their continuous encouragement for perusing with this journey.

I want to express my heartfelt gratitude for Nandita, who always kept me motivating with strong mental support throughout my PhD life. I know that it was not easy, but you have been there for me in all the ups and downs throughout the way. You have offered me words of encouragement, and helped me to stay on track. I am so grateful for your patience, understanding, and love.

I am indebted for life to my friends for their friendship and understanding during the whole journey. They have always been there to listen to me vent, celebrate my successes, and offer me a great mental support during my difficult times. I am thankful to my friends Avijit, Biplab, Buddha Dev, Koushik Kanti, Kuldeep and Araghni for sharing many cheerful memories at IIT Guwahati campus. I would like to take this opportunity to convey my gratitude to my seniors Dr. Gautam Singh, Dr. Anirban Majumdar, Dr. Abhishek Das, Dr. Swarup Barik, Dr. Abhijit Sarkar, Dr. Nilay Mondal, Dr. Ayan Chanda, Dr. Shyam Mondal and Dr. Ali Sendur for their valuable suggestions at various times. I also thank

my beloved juniors and friends Sandip, Aniruddha, Jaspreet, Saurabh, Aayushman, Sachin, Desta, Sagar, Mijanur, Rupchand, Gopinath, Kannan, Manali, and others for sharing a great bond of affection in the Department. My senior Dr. Mriganka Biswas deserves an special appreciation in this note for his brotherly love and affection that helped me stay peaceful during the stressful days.

I owe a lot to my teacher Mr. Manmohan Nath who taught me Mathematics with great care during my school days at Matalhat High School. I also recall the love and the active encouragement that I receive to pursue higher studies in Mathematics from my professor Prof. Asit Chakraborty and Mr. Sujoy Sarkar at Dinhata College.

I conclude my acknowledgment by recognizing the efforts of Babasaheb Dr. B. R. Ambedkar whose activism enabled a person like me to enter a noble profession like research which were difficult before.

I am truly grateful to all of the people who have helped me along the way. This thesis would not have been possible without their support.

Thank you.

Guwahati, August, 2023 **Mrityunjoy Barman.**

ABSTRACT

The aim of this thesis is to construct and analyze some simple, yet very efficient numerical methods that produce parameter-uniform approximate solutions to singularly perturbed differential equations (SPDEs) with two parameters. The SPDEs with two parameters are available in fields of applications in real life, for example fluid mechanics, chemical reactions, control theory, lubrication theory and electrical networks, etc. In most cases, due to the presence of the parameters and the prescribed boundary conditions, the solutions give rise to some interesting phenomena called 'boundary layers'. The problems having this kind of solution characteristics require some special adaptive strategies to compute sufficiently accurate numerical approximations.

We observe that the uniformly spaced grid cannot produce an approximate solution that properly reflects the boundary layer behaviour without using a large no. of mesh points. Thus, it is very difficult to compute the solution due to the limitations in our computing resources as well as the algorithm becomes inefficient. The adaptive mesh generation strategies help us to get rid of this issue by distributing a sufficient number of mesh points within the layer regions in the domain. In this thesis, we construct the layer-resolving Shishkin meshes for the spatial discretizations using the given problem data while the uniform grid for the time variable was sufficient.

The classical finite difference techniques usually fail to provide such reliable numerical solutions, and this is why the thesis studies some robust convergence finite difference methods that provide a fix. In this work, we describe some upwind finite difference schemes which supply some efficient solving methods for some solutions with parameter-independent accuracy. At first, we compute a uniformly stable and consistent numerical solution that approximates the solution to two-parameters degenerate boundary-value problems (BVPs) using this method. Then, we obtain a second-order accurate solution from this solution using Richardson extrapolation by preserving the consistency and stability in the solution. Then, we consider a degenerate parabolic problem involving two parameters as coefficients in the convection and diffusion term and use an implicit-Euler to approximate the time derivative and an upwind finite difference scheme for spatial derivatives to obtain the first-order accurate numerical solution. We also improve the accuracy of this solution by employing the Richardson extrapolation strategy to get a second-order convergent extrapolated solution. Then, we construct an Alternating Direction Implicit (ADI) scheme for singularly perturbed 2D parabolic convection-diffusion-reaction problems with two small parameters. We consider the operator-splitting ADI finite difference scheme for time stepping on a uniform mesh and a simple upwind-difference scheme for spatial discretization to compute a first-order convergent solution. Finally, we propose a method which is a combination of the backward-Euler method for the time variable and a hybrid method the space variables. The developed numerical method is proved to be first-order convergent in time and second order convergent in space. In each of the above studies, we discussed the error estimates on the Shishkin mesh with discrete maximum norm to establish the uniform convergence of the methods. We have also validated the convergence results by performing numerical experiments on some suitable examples.

Contents

Nomenclature **x**

List of Figures **xi**

List of Tables **xiii**

1 Introduction **1**
1.1 Preliminaries . . . 2
1.1.1 Singular perturbation problems . . . 4
1.1.2 Singular perturbation problems with two parameters . . . 6
1.2 Fitted numerical methods . . . 8
1.2.1 Shishkin mesh . . . 11
1.2.2 Bakhvalov mesh . . . 12
1.3 Background and motivation . . . 12
1.4 Model problems . . . 16
1.4.1 Singularly perturbed degenerate boundary-value problems of convection-reaction-diffusion type involving two small parameters . . . 16
1.4.2 Singularly perturbed degenerate time-dependent problems of convection-reaction-diffusion type with two parameters . . . 17
1.4.3 Singularly perturbed 2D parabolic convection-diffusion-reaction problems with two small parameters . . . 17
1.5 Structure of the thesis . . . 18

2 Second-order uniformly convergent numerical scheme for a singularly perturbed degenerate convection-diffusion-reaction problem with two parameters **21**
2.1 Introduction . . . 22
2.2 Properties of the continuous solution . . . 23
2.3 Spatial discretizations and the numerical scheme . . . 24
2.3.1 Motivation for Richardson extrapolation . . . 25

2.4 Convergence analysis . . . 26
2.4.1 Extrapolation in the smooth component . . . 27
2.4.2 Extrapolation in the singular components . . . 29
2.4.3 Error estimate for the extrapolated solution . . . 33
2.5 Numerical experiments . . . 34
2.6 Conclusions . . . 44

3 Richardson extrapolation of the numerical solution to singularly perturbed degenerate parabolic problems with two parameters 45
3.1 Introduction . . . 46
3.2 Properties of the continuous solution . . . 47
3.3 Numerical approximations . . . 49
3.4 Convergence analysis . . . 53
3.4.1 Error estimates in the regular component . . . 53
3.4.2 Error estimates in the singular components . . . 55
3.4.3 Error estimate for the extrapolated solution . . . 59
3.5 Numerical experiments . . . 59
3.6 Conclusions . . . 63

4 Alternating direction implicit methods for singularly perturbed 2D parabolic convection-diffusion-reaction problems with two small parameters 67
4.1 Introduction . . . 68
4.2 Application of the ADI finite difference scheme: Case I . . . 69
4.2.1 Temporal discretizations . . . 71
4.2.2 Spatial discretizations . . . 75
4.2.3 Convergence analysis . . . 79
4.2.4 Numerical experiments . . . 89
4.3 Application of the ADI finite difference scheme: Case II . . . 90
4.3.1 Temporal and spatial discretizations . . . 94
4.3.2 Convergence analysis . . . 96
4.3.3 Numerical experiments . . . 101
4.4 Conclusions . . . 102

5 A parameter-uniform hybrid method for singularly perturbed parabolic 2D convection-diffusion-reaction problems 107
5.1 Introduction . . . 108
5.2 Analysis of the hybrid scheme: Case I . . . 109
5.2.1 Temporal discretization and the semidiscrete problem . . . 110
5.2.2 Spatial discretization: fully-discrete scheme . . . 112
5.2.3 Convergence analysis . . . 116

5.2.4 Numerical experiments 127
5.3 Analysis of the hybrid scheme: Case II 128
5.3.1 Temporal and spatial discretizations 131
5.3.2 Convergence analysis 133
5.3.3 Numerical experiments 138
5.4 Conclusions 138

6 The summary and future scope of the thesis **143**
6.1 Summary of the thesis 144
6.2 Future scope of the thesis 145
6.2.1 Numerical approximations for a two-parameter singularly perturbed parabolic problem of convection-diffusion type with a discontinuous initial condition 145
6.2.2 A comparative study of singularly perturbed parabolic convection-diffusion-reaction problems on some layer-adapted meshes using streamline-diffusion finite element methods 146
6.2.3 Higher-order accurate numerical method for singularly perturbed parabolic problems of degenerate type with two perturbation parameters in 2D 147

Publications **155**

NOMENCLATURE

ADI	Alternating Direction Implicit
BVP	Boundary-value Problem
IBVP	Initial Boundary-value Problem
ODE	Ordinary Differential Equation
PDE	Partial Differential Equation
SPP	Singular Perturbation Problem
SPDE	Singularly Perturbed Differential Equation
TPSPP	Two-parameter Singular Perturbation Problem
FDM	Finite Difference Method
FEM	Finite Element Method
$\tau_x,\ \tau_y$	Transition parameter along the x-direction and y-direction respectively
$\tau_0,\ \tau_1$	Transition parameter based on the constants μ_0 and μ_1 respectively
$\mathcal{L}_\varepsilon, \mathcal{L}_{x,\varepsilon}, \mathcal{L}_{y,\varepsilon}$	Continuous differential operators
$L_\varepsilon^N, L_{x,\varepsilon}^N, L_{y,\varepsilon}^N$	Discrete operators corresponding to $\mathcal{L}_\varepsilon, \mathcal{L}_{x,\varepsilon}, \mathcal{L}_{y,\varepsilon}$ respectively
Ω_x	The domain $\{x : x \in (a,b)\}$ in the x-direction
Ω_y	The domain $\{y : y \in (a,b)\}$ in the y-direction
$\overline{\Omega}_x^N,\ \overline{\Omega}_y^N$	Shishkin mesh along the x-direction and y-direction respectively
$\overline{\Omega}_t^M$	Uniform mesh for the time variable
$\overline{\Omega}^N := \overline{\Omega}_x^N \times \overline{\Omega}_y^N$	The Shishkin mesh for the domain $\Omega = \Omega_x \times \Omega_y$
$L_{x,cd}^N,\ L_{y,cd}^N$	Central difference operator along the x-direction and y-direction respectively
$L_{x,mu}^N,\ L_{y,mu}^N$	Midpoint upwind operator along the x-direction and y-direction respectively
$E_{\varepsilon_1,\varepsilon_2}^N, E_{\varepsilon_1,\varepsilon_2}^{N,\Delta t}$	Pointwise maximum error for the parameters $\varepsilon_1,\ \varepsilon_2$
$E^N, E^{N,\Delta t}$	Parameter-independent maximum pointwise error
$p_{\varepsilon_1,\varepsilon_2}^{N,\Delta t},\ p_{\varepsilon_1,\varepsilon_2}^N$	Parameter-dependent order of convergence
$p^{N,\Delta t},\ p^N$	Parameter-uniform order of convergence

List of Figures

1.1 Comparison of the exact solution for Example 1.1.4 *vs* the solution of the reduced problem. 5

1.2 Significance of the boundary conditions for the solution with the parameters values $\varepsilon_1 = 2^{-10},\ \varepsilon_2 = 2^{-20}$ to exhibit boundary layers at various locations in the domain. 9

1.3 A typical Shishkin mesh construction with $N = 32$ for a convection-diffusion SPP with a boundary layer at $x = 0$. 11

1.4 A typical Shishkin mesh construction for a reaction-diffusion SPP with $N = 32$ with two boundary layers at $x = 0$ and $x = 1$. 12

1.5 The Bakhvalov mesh generating function. 13

2.1 Mesh structure along x : $\overline{\Omega}^N$. 24

2.2 Plot of the numerical approximation U^N for Example 2.5.1 with $p = 1$ and $\varepsilon_1 = 10^{-4},\ \varepsilon_2 = \dfrac{\sqrt{\varepsilon_1}}{10}$ for Case I. 36

2.3 Plot of the numerical approximation U^N for Example 2.5.1 with $p = 1$ and $\varepsilon_1 = 10^{-4}, \varepsilon_2 = \varepsilon_1^{1/4}$ for Case II. 36

2.4 Loglog plot of the pointwise maximum error obtained before using Richardson extrapolation for Case I for Example 2.5.1. 39

2.5 Loglog plot of the pointwise maximum error obtained before using Richardson extrapolation for Case II for Example 2.5.1. 39

2.6 Loglog plot visualization of the pointwise maximum error obtained after using Richardson extrapolation for Case I for Example 2.5.1. 40

2.7 Loglog plot visualization of the pointwise maximum error obtained after using Richardson extrapolation for Case II for Example 2.5.1. 40

3.1 Visualization of pointwise maximum error obtained before Richardson extrapolation for Case I. 61
3.2 Visualization of pointwise maximum error obtained before Richardson extrapolation for Case II. 61
3.3 Visualization of pointwise maximum error obtained after Richardson extrapolation for Case I. 62
3.4 Visualization of pointwise maximum error obtained after Richardson extrapolation for Case II. 62

4.1 Decomposition of the computational domain based on the occurrence of various layers. 70
4.2 A typical Shishkin mesh for (4.1.1) with $N = 16$. 76
4.3 Surface plot of the numerical solution with $N = 64$ and $\varepsilon_1 = 10^{-7}$ at $t = 1$. . 91
4.4 Graphical representation of the loglog plot of maximum pointwise errors in Table 4.2. 92
4.5 A sample Shishkin mesh for Case II with $N = 16$. 95
4.6 Numerical solution with $N = 64$ and $\varepsilon_1 = 10^{-7}$ at $t = 1$. 102
4.7 Visualization of the loglog plot of the maximum pointwise errors in Table 4.3. 103

5.1 Partition of the domain Ω based on the boundary layer appearance at various edges. 113
5.2 Visualization of the loglog plot of the maximum point-wise error with $\Delta t = \frac{1}{N}$. 129
5.3 Visualization of the loglog plot for the maximum point-wise error with $\Delta t = \frac{1}{2N^2}$. 129
5.4 Visualization of the loglog plot of the maximum pointwise error with $\Delta t = \frac{1}{N}$. 139
5.5 Visualization of the loglog plot for the pointwise error with $\Delta t = \frac{2}{N^2}$. 139

List of Tables

2.1 Maximum pointwise error and associated rate of convergence using standard upwind scheme for Example 2.5.1 with $p = 1$ for various values of ε_1 from the set S_1 for Case I. 37

2.2 Maximum pointwise error and associated rate of convergence using standard upwind scheme for Example 2.5.1 with $p = 1$ for various values of ε_1 from the set S_1 for Case II. 38

2.3 Maximum pointwise error and associated rate of convergence Example 2.5.1 with $p = 1$ for various values of ε_1 from the set S_1 after using Richardson extrapolation for Case I. 41

2.4 Maximum pointwise error and associated rate of convergence Example 2.5.1 with $p = 1$ for various values of ε_1 from the set S_2 after using Richardson extrapolation for Case II. 42

2.5 Maximum pointwise error and associated rate of convergence Example 2.5.1 with $\varepsilon_1 = 10^{-4}$, $\varepsilon_2 = \dfrac{\sqrt{\varepsilon_1}}{10}$ for various values of p before using Richardson extrapolation. 43

2.6 Maximum pointwise error and associated rate of convergence Example 2.5.1 with $\varepsilon_1 = 10^{-4}$, $\varepsilon_2 = \dfrac{\sqrt{\varepsilon_1}}{10}$ for various values of p after using Richardson extrapolation. 43

3.1 Maximum pointwise error and associated rate of convergence for various values of ε_1 before using Richardson extrapolation for Case I. 63

3.2 Maximum pointwise error and associated rate of convergence for various values of ε_1 before using Richardson extrapolation for Case II. 64

3.3 Maximum pointwise error and associated rate of convergence for various values of ε_1 after using Richardson extrapolation for Example 3.5.1 for Case I. . . . 65

3.4 Maximum pointwise error and associated rate of convergence for various values of ε_1 after using Richardson extrapolation for Case II 66

4.1 Maximum pointwise error and corresponding rate of convergence for Example 4.2.11 for the parameters defined in (4.2.61) with $\Delta t = 1/N$. 93
4.2 Maximum pointwise error and the rate of convergence for Example 4.2.11 for the parameters defined in (4.2.61) with $\Delta t = 2/N$. 94
4.3 Maximum pointwise error and corresponding rate of convergence for Example 4.2.11 for the parameters defined in (4.3.33) with $\Delta t = 1/N$. 104
4.4 Maximum pointwise error and the rate of convergence for Example 4.2.11 for the parameters defined in (4.3.33) with $\Delta t = 2/N$. 105

5.1 Error in max norm and rate of convergence for $\varepsilon_2 = \dfrac{\sqrt{\varepsilon_1}}{10}$ with $\Delta t = \dfrac{1}{N}$. . . . 128
5.2 Error in max norm and rate of convergence for $\varepsilon_2 = \dfrac{\sqrt{\varepsilon_1}}{10}$ with $\Delta t = \dfrac{2}{N^2}$. . . 130
5.3 *Error in discrete maximum norm and rate of convergence for* $\varepsilon_2 = {\varepsilon_1}^{1/4}$ with $\Delta t = \dfrac{1}{N}$. 140
5.4 *Error in discrete maximum norm and rate of convergence for* $\varepsilon_2 = \varepsilon^{1/4}$ *with* $\Delta t = \dfrac{2}{N^2}$. 141

CHAPTER 1

Introduction

Singular perturbation problems (SPPs) appear in many branches of science including computational fluid dynamics, financial modelling, heat transfer, hydrodynamics, chemical reactor theory, mathematical biology, and many others [1]. This type of problems is typically characterized by an arbitrarily small parameter multiplied with some or all of the highest order derivative terms in the governing differential equation. The study of singular perturbation problems initiated during the beginning of the 19^{th} century, when Ludwig Prandtl presented some articles on the boundary layer theory. In his work, he explained how a quantity as small as the viscosity of common fluids such as water and air can play a crucial role in determining their flow profile. He introduced the terminology 'boundary layer' which is a very familiar phenomenon in the concerned areas of Physics and Engineering.

Singular perturbation theory is of great importance in many fields of modern science. This type of problem attracted the attention of scientists mainly due to the interesting physical behavior of their solutions. Subsequently, the study of these problems has grown into a substantial field of study in applied mathematics for many decades. A good number of textbooks are written by various mathematicians on the analytical and numerical approaches of solving SPPs over the years. Unfortunately, the analytical methods have certain limitations, and hence, people started focusing on some effective ways to numerically solve the problems. Till date, many numerical ways including finite difference methods (FDMs), finite element methods (FEMs), and finite volume methods (FVMs), have been developed in order to solve these problems efficiently. The main goal of these methods is to develop a strategy for finding approximate solutions whose accuracy does not depend on the associated parameters.

1.1 Preliminaries

Let Ω be a bounded domain in $\mathbb{R}$, and $G = \overline{\Omega} \subset \mathbb{R}$. For each $k \geq 1$, let $C^k(G)$ be the space of all functions which are k-times continuously differentiable on G. The usual norm we are going to use for approximations is the sup norm (or max norm). Thus, for any $f \in C^k(G)$, we define the following norms and semi-norms as follows:

$$\|f\|_G = \sup_{x \in G} |f(x)|, \quad \|f\|_{k,G} = \max_{0 \leq l \leq k} \left\|f^{(l)}\right\|_G.$$

For $0 \leq l \leq k$, we also define

$$|f|_{l,G} = \left\|f^{(l)}\right\|_G.$$

Thus, we can see

$$\|f\|_{k,G} = \max_{0 \leq l \leq k} |f|_{l,G}.$$

In particular, when $k = 0$, we denote

$$\|f\|_{0,G} = \|f\|_G .$$

Now, we define the discrete norms in a similar way. We consider an arbitrary mesh,

$$\overline{\Omega}^N := \{x_j : 0 \leq j \leq N,\ x_0 \leq x_1 \leq \ldots \leq x_N\} \subseteq G,$$

where $x_0, x_N \in \partial\Omega$. For any mesh function S on this mesh, we define the discrete norm as,

$$\|S\|_{\infty,\overline{\Omega}^N} = \max_{0\leq i\leq N} |S_i|.$$

We now introduce the order notations "O" (read as **"big-oh"**) and "o" (read as **"little-oh"**) to describe the asymptotic growth of a function with respect to perturbation parameter. Suppose f and g are two real valued positive functions of the positive parameter ε.

Definition 1.1.1. (**"O"-notation**)
We call a function $f(\varepsilon)$ to have an asymptotic growth of $O(g(\varepsilon))$ as $\varepsilon \to 0$ if there exist $\varepsilon_0 > 0$ and $C > 0$ such that

$$f(\varepsilon) \leq Cg(\varepsilon), \quad \text{for all } 0 < \varepsilon \leq \varepsilon_0.$$

Equivalently, we write it as $f(\varepsilon) = O(g(\varepsilon))$ as $\varepsilon \to 0$. For example, $2\varepsilon^2 = O(\varepsilon^2)$ when ε approaches 0. Note that in this case, we have

$$\lim_{\varepsilon\to 0} \frac{f(\varepsilon)}{g(\varepsilon)} = C.$$

Definition 1.1.2. (**"o"-notation**)
We call a function $f(\varepsilon)$ to have an asymptotic growth of $o(g(\varepsilon))$ as $\varepsilon \to 0$ if there exist $\varepsilon_0 > 0$ such that for all $C > 0$,

$$f(\varepsilon) \leq Cg(\varepsilon), \quad \text{for all } 0 < \varepsilon \leq \varepsilon_0.$$

Equivalently, we express it as $f(\varepsilon) = o(g(\varepsilon))$ as $\varepsilon \to 0$. For example, $2\varepsilon^2 = o(\varepsilon)$ when ε approaches 0. Note that in this case

$$\lim_{\varepsilon\to 0} \frac{f(\varepsilon)}{g(\varepsilon)} = 0.$$

1.1.1 Singular perturbation problems

Let us take an example of the following equation in a bounded domain $\Omega \subseteq \mathbb{R}^n$:

$$\mathcal{L}_\varepsilon u(\mathbf{x}) = f(\mathbf{x}),\ \mathbf{x} \in \Omega \subseteq \mathbb{R}^n, \tag{1.1.1}$$

with some appropriate boundary conditions on u and $\mathcal{L}_\varepsilon$ is a differential operator that depends on ε, a small positive parameter. Usually we consider the parameter ε to be very small in magnitude, such as $0 < \varepsilon \ll 1$. We now define the associated regular problem by setting $\varepsilon = 0$ in (1.1.1) as

$$\mathcal{L}_0 u(\mathbf{x}) = f(\mathbf{x}), \quad \mathbf{x} \in \Omega. \tag{1.1.2}$$

Let the original problem (1.1.1) has a solution u_ε and the reduced problem (1.1.2) has a solution u_0. Then, we can define SPPs in the following manner.

Definition 1.1.3. (Singular Perturbation Problem)
The problem (1.1.1) *is called* ***a regular perturbation problem*** *with respect to some norm* $\|.\|$ *if the solutions* $u_\varepsilon,\ u_0$ *satisfy*

$$\lim_{\varepsilon \to 0} \|u_\varepsilon - u_0\| = 0 \quad as \quad \varepsilon \to 0.$$

The problem (1.1.1) *is called* ***a singular perturbation problem or singularly perturbed problem*** *if it is not a regular perturbation problem.*

Let us consider the following example to elaborate the above definition.

Example 1.1.4. *Suppose* u_ε *satisfies the following boundary-value problem in the domain* $(0,\ 1)$*:*

$$\begin{cases} -\varepsilon u''(x) + 2u'(x) = 2, \quad for \quad 0 < x < 1, \\ u(0) = 0, \quad u(1) = 0, \end{cases} \tag{1.1.3}$$

where ε *is a very small parameter such that* $0 < \varepsilon \ll 1$.

The exact solution of the above is given by

$$u_\varepsilon(x) = x - \frac{e^{-2(1-x)/\varepsilon} - e^{-2/\varepsilon}}{1 - e^{-2/\varepsilon}}, \quad 0 < x < 1,$$

while the reduced problem has the solution $u_0(x) = x$ with the zero boundary condition. From Figure 1.1, we clearly observe that in a narrow region of the domain, there is a significant difference in the behavior of the corresponding solutions of the original problem and

the reduced problem, while they mostly agree in the remaining part. This indicates that the problem is not regularly perturbed as $\|u_\varepsilon - u_0\|_\infty = 1$ with respect to the *sup*-norm. Therefore, Example 1.1.4 is singularly perturbed ordinary differential equation for the given boundary conditions in (1.1.3) in the domain $(0, 1)$. This phenomenon that the solution making a abrupt change in a small part of the domain is usually known as a boundary layer occurrence.

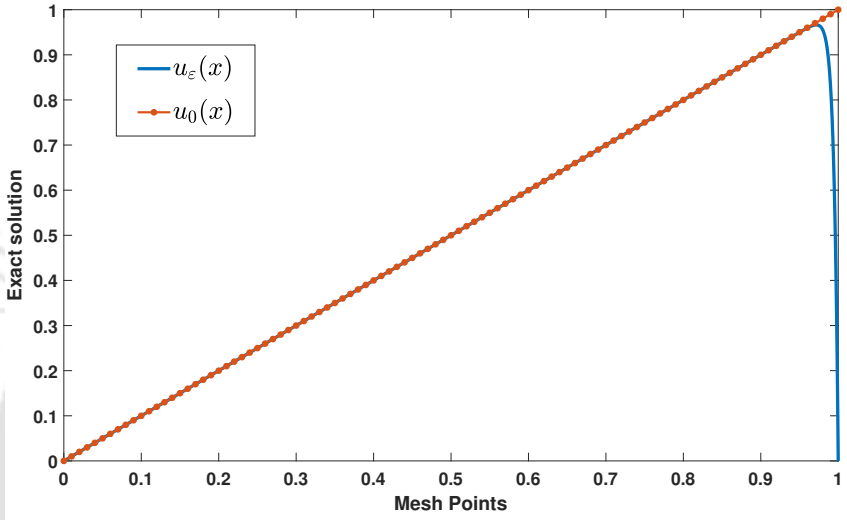

Figure 1.1: Comparison of the exact solution for Example 1.1.4 *vs* the solution of the reduced problem.

We can formally state the following definition of a boundary layer formed by the solution of an SPP based on the nature of the gradient of the solution.

Definition 1.1.5. (Boundary Layer: A Mathematical Definition)
Suppose, $u_\varepsilon(x)$ is the solution of an SPP and $x_0 \in \overline{\Omega}$. Then, we say that $u_\varepsilon(x)$ creates ***a boundary layer*** *near $x = x_0$ if*

(i) $\lim_{\varepsilon \to 0} u'_\varepsilon(x_0)$ *is either ∞ or $-\infty$,*

(ii) $\lim_{\varepsilon \to 0} u'_\varepsilon(x)$ *exits finitely for $0 < |x - x_0| < \delta$ for some $\delta > 0$ independent of ε.*

We note that the boundary layer happens in a narrow subdomain of the SPP and its width is very small. Its width can be mathematically defined in several ways. For example, for the boundary layer function $e^{-x/\varepsilon}$, we define the thickness/width of the boundary layer to be the smallest value w such that

$$e^{-x/\varepsilon} \leq \varepsilon \text{ for all } x \geq w.$$

Another way of defining the width is that we choose w such that for all $1 \leq k \leq 3$,

$$\left| \frac{d^k}{dx^k} e^{-x/\varepsilon} \right| \leq C \quad \text{for all } x \geq w,$$

for some positive constant C. In both cases, we can see that the thickness of layer region is given by $w = O(\varepsilon \ln 1/\varepsilon)$.

The presence of small positive parameters in the highest-order terms of the equation causes the exact solution to exhibit boundary layers of certain widths. As a result, the classical numerical approaches fail to provide a reasonably accurate approximate solution to these problems [2, 3]. Sometimes a numerical method on uniform mesh may fail to properly resolve the boundary layers and produce less accurate numerical solution to the problem. Therefore, we need to devise some suitable numerical schemes on some properly designed discrete mesh that adapt to the boundary layers behavior of the exact solution and give better approximations.

We note that all SPPs do not necessarily have just one single perturbation parameter. There are many problems in which the associated differential operator contains multiple parameters. In this thesis, we will confine our discussions to the two-parameter singularly perturbed problems only.

1.1.2 Singular perturbation problems with two parameters

Let us consider the following singularly perturbed second-order linear differential equation.

$$\begin{cases} -\varepsilon u''(x) + a(x)u'(x) + b(x)u(x) = f(x), \quad x \in \Omega = (0,1), \\ u(0) = u_0, \quad u(1) = u_1, \end{cases} \tag{1.1.4}$$

where ε is the perturbation parameter. The associated coefficient functions are assumed to be smooth enough. In this case, the boundary layer formation depends on the parameter ε, the given conditions and the convection coefficients. We also observe the following under some appropriate boundary conditions.

- If $a(x) \geq \alpha > 0$, the solution causes a boundary layer at $x = 1$ of width $O(\varepsilon)$.
- If $a(x) \leq -\alpha < 0$, the solution creates a boundary layer at $x = 0$ of width $O(\varepsilon)$.
- If $a(x_0) = 0$, for some $x_0 \in (0,1)$, the solution forms an interior layer at $x = x_0$.
- If $a(x) \equiv 0$ in $[0,1]$, there are twin boundary layers of width $O(\sqrt{\varepsilon})$ at both boundaries.

But in the case of two parameters, the form of boundary layers is determined in some different way. To discuss about the layer formation in this case, let us consider the following linear SPP with two parameters in 1D. Similar analysis may be generalized for higher dimensions also.

$$\begin{cases} -\varepsilon_1 u''(x) + \varepsilon_2\ a(x)u'(x) + b(x)u(x) = f(x), \quad x \in \Omega = (0,1), \\ u(0) = u_0, \quad u(1) = u_1. \end{cases} \tag{1.1.5}$$

The nature of the boundary layer depends on the following characteristic equation.

$$-\varepsilon_1 \lambda^2(x) + \varepsilon_2\ a(x)\lambda(x) + b(x) = 0, \quad 0 < x < 1. \tag{1.1.6}$$

The roots of the equation are given by

$$\begin{aligned} \lambda(x) &= \frac{\varepsilon_2 a(x) \pm \sqrt{\varepsilon_2^2 a^2(x) + 4\varepsilon_1 b(x)}}{2\varepsilon_1} \\ &= \frac{\varepsilon_2 a(x)}{2\varepsilon_1}\left[1 \pm \sqrt{1 + \frac{4\varepsilon_1 b(x)}{\varepsilon_2^2 a^2(x)}}\right]. \end{aligned}$$

When $\dfrac{\varepsilon_1}{\varepsilon_2^2} \to 0$ as $\varepsilon_2 \to 0$, using binomial expansion, the roots of the above equation are computed as

$$\begin{aligned} \lambda_0(x) &= \frac{1}{\varepsilon_2}\left[-\frac{b(x)}{a(x)} + \left(\frac{\varepsilon_1}{\varepsilon_2^2}\right)\frac{b^2(x)}{a^3(x)} - \cdots\right], \\ \lambda_1(x) &= \frac{\varepsilon_2}{\varepsilon_1}\left[a(x) + \left(\frac{\varepsilon_1}{\varepsilon_2^2}\right)\frac{b(x)}{a(x)} - \cdots\right]. \end{aligned}$$

The constants

$$\mu_0 = \min_{0\le x\le 1} |\lambda_0(x)|, \quad \mu_1 = \min_{0\le x\le 1} \lambda_1(x),$$

determine the decay of the boundary layers at $x = 0$ and $x = 1$ respectively. The layer function near the point left boundary behaves like $e^{-\mu_0 x}$ while the layer function near the right boundary has the behavior resembles that of $e^{-\mu_1(1-x)}$. On the other hand, when $\dfrac{\varepsilon_2^2}{\varepsilon_1} \to 0$ as $\varepsilon_1 \to 0$, the roots of the characteristic equation are given by

$$\lambda(x) = \frac{\varepsilon_2 a(x)}{2\varepsilon_1} \pm \sqrt{\frac{b(x)}{\varepsilon_1}}\left\{1 + \frac{\varepsilon_2^2 a^2(x)}{4\varepsilon_1 b(x)}\right\}^{1/2}$$

$$= \sqrt{\frac{b(x)}{\varepsilon_1}} \left[\sqrt{\frac{\varepsilon_2^2 a^2(x)}{\varepsilon_1 b(x)}} \pm \left\{ 1 + \sqrt{\frac{\varepsilon_2^2 a^2(x)}{4\varepsilon_1 b(x)}} \right\}^{1/2} \right].$$

Therefore, $\lambda(x) \longrightarrow \pm\sqrt{\frac{b(x)}{\varepsilon_1}}$, as $\varepsilon_1 \to 0$. Hence, in this case, $\mu_0 = \mu_1 = O(1/\sqrt{\varepsilon_1})$ and the boundary layers at both boundaries have the same structure and width.

The occurrence of boundary layers in a solution significantly depends on the prescribed boundary conditions as well. A differential equation with a given set of boundary conditions may exhibit layers in certain parts of the domain, but if we alter the conditions, the layers may even disappear. We elaborate the dependence of the formation of the layers on the prescribed boundary conditions by taking an example of a two-point boundary-value problem with Dirichlet boundary conditions.

Example 1.1.6. *Suppose, u is the solution of the following equation for the positive parameters $\varepsilon_1,\ \varepsilon_2$.*

$$-\varepsilon_1 u''(x) + \varepsilon_2 u'(x) + u(x) = x, \quad 0 < x < 1. \tag{1.1.7}$$

We consider a set of four different boundary conditions for u for the above problem, namely

(i) $u(0) = 1,\ u(1) = 1$, (ii) $u(0) = 0,\ u(1) = 0$,

(iii) $u(0) = 1,\ u(1) = 0$, (iv) $u(0) = 0,\ u(1) = 1$.

We observe the following solution profiles corresponding to the above prescribed boundary conditions.

From Figure 1.2, it is clear that the solution forms boundary layers when we have considered the first three conditions, while for the last condition $u(0) = 0,\ u(1) = 1$, there is no such phenomenon. This means that the problem is regularly perturbed for the last condition. In this case, the solution coincides with the straight line $y = x$. Moreover, the boundary conditions prescribed at each of the points $x = 0$ and $x = 1$ separately affect the boundary layer formations at the corresponding boundaries.

1.2 Fitted numerical methods

It is generally very difficult to solve a singularly perturbed equation for a closed-form solution using analytical ways, for example, in the case of multiple parameters and the higher-dimensional problems. With numerical approaches of solving SPPs, we attempt to construct

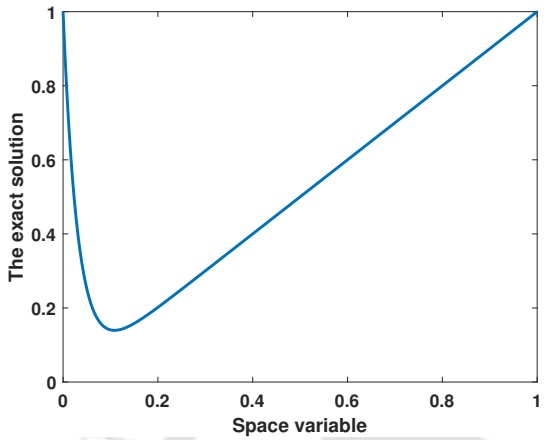

(a) The exact solution with $u(0) = 1,\ u(1) = 1.$

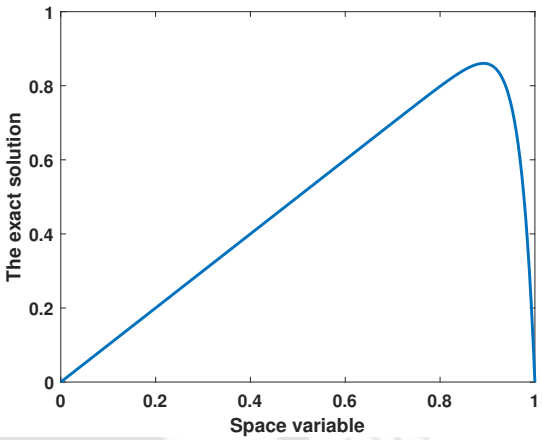

(b) The exact solution with $u(0) = 0,\ u(1) = 0.$

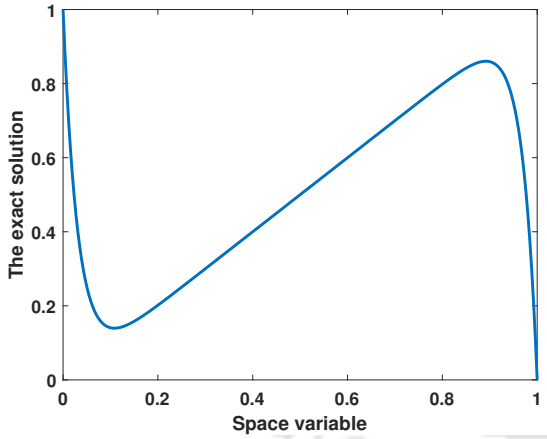

(c) The exact solution with $u(0) = 1,\ u(1) = 0.$

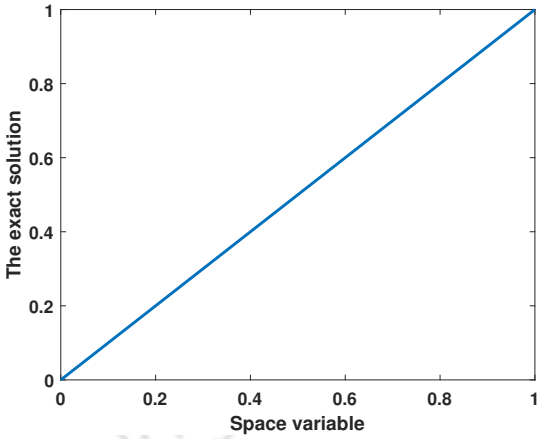

(d) The exact solution with $u(0) = 0,\ u(1) = 1.$

Figure 1.2: Significance of the boundary conditions for the solution with the parameters values $\varepsilon_1 = 2^{-10},\ \varepsilon_2 = 2^{-20}$ to exhibit boundary layers at various locations in the domain.

admissible approximations to the exact solution to the problem even for asymptotically smaller values of the parameter ε. Usually, for solving regular differential equations using some numerical methods with standard finite difference operators, the uniform mesh distribution are sufficient to get a solution with good accuracy. But, in case of SPPs, when the perturbation parameter tends to become extremely small, these methods often fail to produce a solution with a reliable accuracy. Even too much refinement of the mesh is not a good option, as in that case, the methods become inefficient for including a huge number of grid points in a small computational domain. Moreover, the space complexity and the time complexity of these finite difference algorithms worsen with the increasing number of the grid points. Therefore, we need to think of construction of some suitable numerical approaches that use lesser mesh points, yet provide robust approximate solutions for all values of the singular perturbation parameters. Here comes the concept of ε-uniform numerical methods.

Definition 1.2.1. (Convergence of numerical approximations)
Let us consider an SPP with a perturbation parameter ε, where $0 < \varepsilon \ll 1$. Let the problem have a solution u_ε which is approximated by a sequence of numerical approximations $\left\{U_\varepsilon^N : N \geq 16\right\}$ on the mesh $\overline{\Omega}^N$, where N denotes the mesh parameter. Then, we say that the numerical approximations U_ε^N converge ε-uniformly to u_ε, if there exist positive constants C, p and $N_0 \in \mathbb{N}$, all independent of ε and N, such that

$$\sup_{0<\varepsilon\leq 1} \left\|U_\varepsilon^N - u_\varepsilon\right\|_{\overline{\Omega}^N} \leq CN^{-p} \quad \text{for all } N \geq N_0.$$

The constant p is called the uniform rate of convergence.

We could rely upon the standard finite difference methods for solving SPPs provided their accuracy in the solution and order of convergence are parameter-independent. Unfortunately, it appears that most of these methods do not satisfy that criteria, because the continuously declining magnitude of the parameters affects the stability of the methods. Generally there are two main approaches to alleviate these limitations, namely fitted mesh methods (FMMs) and fitted operator methods (FOMs). A finite difference FMM approach involves the construction of an adaptive numerical scheme applied on the problem on a layer-adapted piecewise-uniform or non-uniform mesh. It should be noted that the creation of the computational mesh has a great significance in determining the convergence of the employed methods. Examples of some frequently used mesh include the piecewise-uniform Shishkin mesh, the non-uniform Bakhvalov mesh, B-S mesh, exponentially graded mesh, etc. There are numerous works on the FMM approaches of solving various class of SPPs by many authors in [3, 2, 4, 5, 6, 7, 8, 9, 10, 11] and others till date. There are also a good numbers

works available on the FOM methods by several authors in [12, 13, 14, 15, 16] and others.

We briefly describe the FMM approach and how to construct a Shishkin mesh and a Bakhvalov mesh for an one-dimensional problem in the following.

1.2.1 Shishkin mesh

A piecewise uniform mesh on the domain $\Omega = (0, 1)$, suggested by G. I. Shishkin, was constructed as follows. Let $N+1$ be the total number of grid points in the mesh for an SPP with a boundary layer of width $O(\varepsilon)$ in Ω. Usually, we choose the number of mesh points $N \geq 16$ and it is taken to be a multiple of 4. We define a transition parameter τ to separate the layer region(s) and the smooth region in the domain, and it is defined as

$$\tau = \min\left\{q,\ \sigma\varepsilon \ln N\right\},$$

where q, σ are two positive constants chosen by the user. The parameter $q \in (0, 1)$ is chosen according to the number boundary layer regions and $\sigma > 0$ depends on the given data and it adjusts the position of the transition point for better convergence of the method.

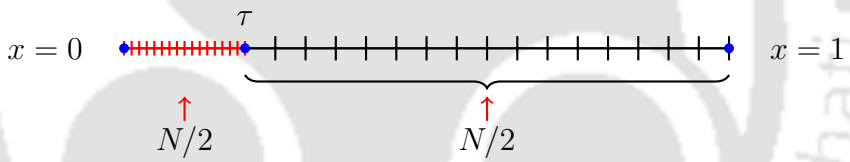

Figure 1.3: A typical Shishkin mesh construction with $N = 32$ for a convection-diffusion SPP with a boundary layer at $x = 0$.

In the case of convection-diffusion problems with single parameter, where typically one boundary layer appears at one of the boundaries, the domain Ω is divided in two subregions, namely layer region and the smooth region. We choose $q = 1/2$ to equally distribute the grid points between the layer region and the non-layer region. If the layer arises at $x = 0$, we construct the Shishkin mesh by discretizing the layer region $(0,\ \tau)$ into $N/2$ subintervals and $(\tau,\ 1)$ into $N/2$ subintervals. The resulting grid is a piecewise-uniform mesh with N elements and it is denoted by $\overline{\Omega}^N$.

For reaction-diffusion problems with single parameter, we observe two layer regions at $x = 0$ as well as at $x = 1$. In this case, we use $q = 1/4$ to define the transition points that separate three subregions, namely $(0,\ \tau)$, $(\tau,\ 1-\tau)$ and $(1-\tau,\ 1)$. Then, we put $N/2$ points in the smooth region and from the remaining $N/2$ points, we distribute an equal number of grid points in each of the layer regions.

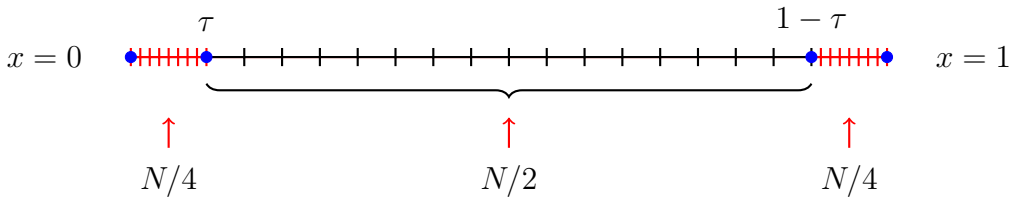

Figure 1.4: A typical Shishkin mesh construction for a reaction-diffusion SPP with $N = 32$ with two boundary layers at $x = 0$ and $x = 1$.

1.2.2 Bakhvalov mesh

In 1969, Bakhvalov first introduced the use of non-uniform meshes for the numerical method of solving SPPs. The mesh generating function $\lambda(t)$, associated with the exponential boundary layer at $x = 0$, is defined as

$$\lambda(t) = \begin{cases} \psi(t) := \sigma\varepsilon\phi(t), & 0 \le t < \alpha, \\ \psi(\alpha) + \psi'(\alpha)(t-\alpha), & \alpha \le t \le 1, \end{cases} \tag{1.2.1}$$

where $\phi(t) = \ln \dfrac{q}{q-t}$, $0 \le t < q$ and $\sigma > 0$, $q \in (0,1)$ are user chosen parameters. It can be easily seen that the mesh is graded inside the layer region, while there is uniform mesh spacing outside the location. The mesh transition parameter α is taken such that the point $(\alpha, \psi(\alpha))$ is the point of contact of the tangent from the point $(1,1)$ to the curve $\psi(t)$. Thus, α is given by the following implicit relation

$$\frac{1-\psi(\alpha)}{1-\alpha} = \psi'(\alpha). \tag{1.2.2}$$

The generated Bakhvalov grid points are defined by

$$x_i = \lambda(t_i),\ t_i = i/N, \quad 0 \le i \le N.$$

1.3 Background and motivation

The aim of thesis is to construct and analyze some numerical methods which produce parameter-uniform convergent approximate solution to SPPs with two parameters. The works in this thesis are motivated by several research works with various approaches for solving SPPs involving two parameters. Here is a brief overview of the such works in the

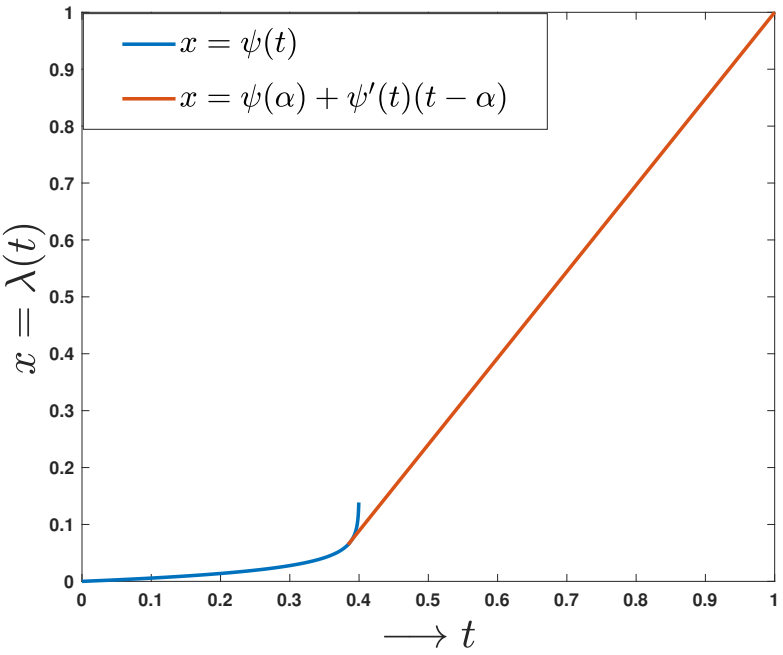

Figure 1.5: The Bakhvalov mesh generating function.

following discussions.

SPPs with two parameters was studied in detail by O'Malley in his books [17, 18] in the late 1970's. He presented some rigorous analysis of the analytical solution to these problems based on asymptotic expansion technique. This method seeks the solution in the form of an infinite series with respect to some asymptotic sequence of the perturbation parameters, such as $\{1, \varepsilon, \varepsilon^2, \varepsilon^3, \dots\}$. Although the approach is not so easy to generalize for SPPs with multiple parameters in higher dimensions, it may reveal some insights about the boundary layer nature of the solution. For a singularly perturbed boundary-value problem (BVP) with two parameters $\varepsilon_1,\ \varepsilon_2$, O'Malley [17] showed that the ratio $\frac{\varepsilon_2^2}{\varepsilon_1}$ has a decisive role to determine the boundary layer formation by the solution. He completed the analysis in two separate cases, namely $\varepsilon_2^2 \leq C\varepsilon_1$ and $\varepsilon_2^2 \geq C\varepsilon_1$, where C is a positive constant. Later, this idea has been used by many authors to properly design layer-adapted mesh for the computation of the numerical approximation.

Over the decades, many researchers have been involved in formulation and analysis of uniformly convergent numerical solution of SPPs using finite difference techniques. A detailed literature on the construction of parameter-uniform numerical schemes for singular perturbation problems is available in many books [2, 1, 3, 19], etc. There are also many articles [6, 20, 21, 22, 23, 24] which studied the single parameter SPPs using various finite

difference methods. In FMMs, some well-known layer resolving fitted meshes includes the Bakhvalov mesh, the Shishkin mesh, Bakhvalov-Shishkin (B-S) type mesh and the meshes based on some adaptive algorithm. An extensive amount of works analyzing various methods on Shishkin mesh has been published by many authors. A review paper addressing the numerical solution of computationally challenging singularly perturbed differential equations on Shishkin mesh has been published by Kopteva *et al.* [25] in 2010. A study of numerical approximations for a class of singularly perturbed convection-diffusion type problems with a moving interior layer was done by Shishkin *et al.* in 2004. Some notable works using the Bakhvalov mesh are also published till date by Roos *et al.* [26, 27], Kellog *et al.* [28], Brdar and Zarin [29], Zhang and Liu [30], etc.

In 2006, O'Riordan e*t al.* [31] analyzed an upwind finite difference method by combining the implicit-Euler and the classical upwind finite difference operator on a piecewise-uniform mesh in one dimension and achieved parameter-uniform convergence of first-order in both space and time variables. In recent times, some robust layer adapted finite difference methods with first-order convergence combining an implicit-Euler method for time discretization and an upwind scheme on the B-S mesh was proposed for a parabolic problem by Jha and Kadalbajoo in [32]. A uniformly convergent numerical method of second-order in both space and time variables was constructed and analyzed in [33]. Moreover, an adaptive finite difference scheme by employing implicit-Euler method with upwind scheme using a moving mesh-adaptive algorithm for a 1D linear time-dependent problem was proposed by Das and Mehrmann [8]. A fitted mesh finite difference scheme for a two-point boundary-value problem (BVP) with two parameters having discontinuous source function was studied by Shanthi *et al.* in [34].

Q. Sloan in [35] presented very interesting analysis of the finite difference approximations to a singularly perturbed two-point BVP on an adaptive mesh in 1999. Following him, Kopteva *et al.* discussed the quasi-linear convection-diffusion problem in one dimensional case on this mesh in [36]. In recent times, Kopteva and Stynes considered a semi-linear reaction-diffusion two-point BVP with a positive parameter to deduce a ε-uniform numerical scheme. In 2001, a quasilinear two-point boundary-value problem was studied using a simple upwind finite difference scheme on this mesh by T. Linß [37], where he derives a sufficient conditions on the monitor function that guarantee uniform convergence in the discrete maximum norm. In 2005, Kopteva *et al.* [38] presented a linear singularly-perturbed reaction–diffusion BVP and proposed a new monitor function, and they explained why the standard arc-length monitor function was not suitable for that problem. In 2011, Mohapatra and Natesan [24] studied a numerical method comprising of upwind finite difference operator on an adaptive grid, which is formed by equidistributing the arc-length monitor function

and proved the robustness of the solution. In 2012, Das and Natesan [7] considered a singularly perturbed reaction-diffusion problem with Robin boundary conditions. They observed that classical forward–backward approximation for mixed type boundary conditions gives first-order convergence, whereas their proposed cubic spline scheme provides second order accuracy independent of the perturbation parameter. They also employed the Richardson extrapolation technique to improve the accuracy in the computed solution. In the last decade, Pratibhamoy and Natesan [39] and Gowrisankar and Natesan [40] presented an impressive study of the equidistribution algorithm for constructing the adaptive mesh with its application for solving parabolic and elliptic SPPs.

For stationary two-parameter SPPs, Shishkin and Titov [41] studied parameter-uniform methods on the basis of special fitted finite difference operators on uniform meshes. Stynes and Roos applied a hybrid scheme on the Shishkin mesh and proved that the algorithm gives almost second-order accurate numerical solution in [42]. O'Riordan *et al.* analyzed a numerical scheme with an upwind finite difference operator on an appropriate piecewise-uniform mesh. Some different types of two-parameter elliptic convection-diffusion problems were considered by Shishkin in [43]. More studies on two-parameters problems using finite difference methods also available in the articles [32, 44, 45, 46], etc.

Some researchers has also proposed other numerical schemes, such as spline difference schemes [47], layer adapted finite difference methods [32] to solve non-stationary two-parameter SPPs. Among them, Clavero *et al.* studied a monotone finite difference scheme by combining the implicit-Euler method on a uniform mesh together with the classical upwind finite difference scheme on a non-uniform mesh in [48]. Chandru *et al.* developed an almost first order parameter uniform numerical scheme by using an adaptive mesh in [49]. Kumar and Kumari proposed a numerical solution by using the Crank-Nicolson method on a equispaced mesh and an upwind difference scheme on a Shishkin mesh in [50].

In recent studies, Mukherjee and Natesan [51, 22, 52, 53, 21] analyzed some standard upwind and hybrid schemes with second-order convergence for solving parabolic problems one and two dimensions. Das and Natesan [54, 55, 56, 57] also considered some time-dependent parabolic problem with positive delays and proposed some robust convergent finite different methods with higher-order accuracy for solving them. These works are contemporary with the studies of higher-order hybrid numerical methods and ADI schemes for parabolic problems of degenerate type by Majumdar and Natesan [58, 59, 60, 61, 62].

1.4 Model problems

In this section, we introduce the singularly perturbed differential equations we have considered in the thesis and briefly discuss the assumptions on the associated functions and the parameters in order to find uniformly convergent solution for the same.

1.4.1 Singularly perturbed degenerate boundary-value problems of convection-reaction-diffusion type involving two small parameters

We study the following parabolic SPP:

$$\begin{cases} \varepsilon_1 u''(x) + \varepsilon_2 x^p a(x) u'(x) - c(x)u(x) = f(x), \quad x \in \Omega = (0,1), \\ u(0) = u_0, \quad u(1) = u_1, \end{cases} \tag{1.4.1}$$

where the perturbation parameters $0 < \varepsilon_1, \varepsilon_2 \ll 1$, and

$$b(x) = x^p a(x),\ 0 \le x \le 1,\ p \ge 1,$$
$$c(x) \ge \gamma > 0,\ \text{and}\ c(x) - \frac{1}{2}\varepsilon_2 b'(x) \ge \gamma_0 > 0.$$

We also assume that $a(x) \ge \alpha > 0$ in Ω. Depending on the roots $\lambda_0(x) < 0,\ \lambda_1(x) > 0$ of the characteristic equation $\varepsilon_1\lambda^2 + \varepsilon_2 b(x)\lambda - c(x) = 0$, the solution exhibits boundary layers of certain widths at both boundaries $x = 0$ and $x = 1$. Further, if we define the constants $\mu_0,\ \mu_1$ as

$$\mu_0 = \min_{0\le x\le 1} |\lambda_0(x)| = \sqrt{\frac{\gamma}{\varepsilon_1}}, \quad \mu_1 = \min_{0\le x\le 1} \lambda_1(x) = \frac{-\varepsilon_2 A + \sqrt{\varepsilon_2^2 A^2 + 4\varepsilon_1\gamma}}{2\varepsilon_1}, \tag{1.4.2}$$

where $A = \|b\|_\infty$, we observe that the width of the boundary layer at $x = 0$ is $O(1/\mu_0)$ and that at $x = 1$ is $O(1/\mu_1)$. In this problem, the boundary conditions are chosen such a way that the solution produces regular boundary layers at the boundary points. The analysis is presented in two separate cases, *viz.* when $\varepsilon_2^2 \le C\varepsilon_1$ and $\varepsilon_2^2 \ge C\varepsilon_1$.

1.4.2 Singularly perturbed degenerate time-dependent problems of convection-reaction-diffusion type with two parameters

We consider the following time-dependent convection-reaction-diffusion problem with the parameters $\varepsilon_1,\ \varepsilon_2$ in the domain $(0,1)\times(0,T]$.

$$\begin{cases} \varepsilon_1\dfrac{\partial^2 u}{\partial x^2}+\varepsilon_2 x^p a(x,t)\dfrac{\partial u}{\partial x}-c(x,t)u(x,t)-\dfrac{\partial u}{\partial t}=f(x,t), \quad x\in\Omega=(0,1), \quad t\in(0,T], \\ u(0,t)=u_0(t), \quad u(1,t)=u_1(t), \quad 0\le t\le T, \\ u(x,0)=\phi(x), \quad x\in\overline{\Omega}. \end{cases} \tag{1.4.3}$$

The convection coefficient is given as $b(x,t)=x^p a(x,t)$ for some $p\ge 1$ and $a(x,t)\ge\beta>0$ in Ω. The functions $a,\ c\ f$ are assumed to be sufficiently smooth and the function ϕ needs to be a continuous function. We also assume that $c(x,t)\ge\gamma>0$ and $c(x,t)-\dfrac{1}{2}\varepsilon_2 b_x(x,t)\ge\gamma_0>0$ for the existence of a unique solution to the problem. In this case also, the boundary layer occurrence depends on the characteristic equation and its roots. The boundary layer structure is also determined by the relations between the given parameters $\varepsilon_1,\ \varepsilon_2$. Therefore, we study the convergence analysis in two separate cases, *viz.* when $\varepsilon_2^2\le C\varepsilon_1$ and $\varepsilon_2^2\ge C\varepsilon_1$.

1.4.3 Singularly perturbed 2D parabolic convection-diffusion-reaction problems with two small parameters

$$\begin{cases} u_t+\mathcal{L}_\varepsilon u=f(x,y,t), & (x,y)\in\Omega=\Omega_x\times\Omega_y,\ t\in\Omega_t, \\ u(x,y,t)=0, & (x,y)\in\partial\Omega=\overline{\Omega}\backslash\Omega,\ t\in\overline{\Omega}_t, \\ u(x,y,0)=\phi(x,y), & (x,y)\in\Omega, \end{cases} \tag{1.4.4}$$

where we consider the domains $\Omega_x=\{x:0<x<1\}$, $\Omega_y=\{y:0<y<1\}$, $\Omega_t=(0,T]$ and $\varepsilon_1,\varepsilon_2$ are the perturbation parameters such that $0<\varepsilon_1,\varepsilon_2\ll 1$ and the operator $\mathcal{L}_\varepsilon$ is defined as,

$$\mathcal{L}_\varepsilon u:=-\varepsilon_1\Delta u+\varepsilon_2\mathbf{b}(x,y)\cdot\nabla u+c(x,y)u. \tag{1.4.5}$$

The convection coefficient $\mathbf{b}$ is defined as $\mathbf{b}(x,y)=\big(b_1(x,y),\ b_2(x,y)\big)$ such that $b_i(x,y)\ge\beta_i>0$, for $i=1,2$ and $c(x,y)\ge c_0>0$. We also assume that $f=f_1+f_2$ is a sufficiently

smooth function that satisfies the following compatibility property:

$$f_1(x,0,t) = f_1(x,1,t) = f_2(0,y,t) = f_2(1,y,t) = 0. \tag{1.4.6}$$

Let $\beta = \min\left\{\beta_1, \beta_2\right\}$ and $\gamma < \min\limits_{\overline{\Omega}} \left\{ \dfrac{c(x,y)}{2b_1(x,y)}, \ \dfrac{c(x,y)}{2b_2(x,y)} \right\}$. We split the problem (4.1.1) into the following two cases, namely $\varepsilon_2^2 \leq \dfrac{\gamma\varepsilon_1}{\beta}$, and $\varepsilon_2^2 \geq \dfrac{\gamma\varepsilon_1}{\beta}$.

In the case when $\varepsilon_2^2 \leq \dfrac{\gamma\varepsilon_1}{\beta}$, we usually notice regular boundary layers of width $O(\sqrt{\varepsilon_1})$ near all four edges along with the corner layers appearing near every corner of the domain Ω. On the other hand, for $\varepsilon_2^2 \geq \dfrac{\gamma\varepsilon_1}{\beta}$, we have regular boundary layers of width $O(\varepsilon_2)$ near the inflow boundaries $x = 0$ and $y = 0$, while there are boundary layers of width $O\Big(\varepsilon_1/\varepsilon_2\Big)$ condensing at the outflow boundaries $x = 1$ and $y = 1$.

1.5 Structure of the thesis

The thesis has been composed of several chapters discussing various uniformly convergent numerical methods for the model problems presented in the previous section. We present a brief outline of the thesis in the following.

In **Chapter 2**, we consider two-point boundary-value problem in a bounded domain, where the diffusion and convection terms are affected by perturbation parameters, as described in the section 1.4.1. The convection coefficient consists of a degenerate term that affects the boundary layer nature in the domain. We create a layer-resolving Shishkin mesh with the help of a characteristic equation that governs the boundary layer behavior of the solution. We use an standard upwind scheme on the constructed Shishkin mesh and produce a first-order accurate approximation to solution. We consider the same problem with this scheme and improved the accuracy to obtain second-order convergent solution by employing Richardson extrapolation tool. We also have presented some results based on the performed numerical computations to validate each of the above theoretical results.

In **Chapter 3**, we consider a degenerate parabolic problem involving two parameters as coefficients in the convection and diffusion terms. We setup a combination of a piecewise-uniform Shishkin in the space direction, and a uniform grid along the time direction to calculate the approximate solution. We use an implicit-Euler to approximate the time derivative on the equispaced temporal grid to obtain the semidiscrete problem. Then, we apply upwind finite difference scheme on this semidiscrete problem on the Shishkin mesh to get a numerical solution that is first-order convergent in both time and space variables. Then,

we use Richardson extrapolation method to enhance the order of convergence for the same problem. We obtain parameter-uniform convergent solution with second-order accuracy in both variables in the extrapolated solution.

In **Chapter 4**, we construct and analyze an ADI scheme for singularly perturbed 2D parabolic convection-diffusion-reaction problems with two small parameters. We consider the operator-splitting ADI finite difference scheme for time stepping on a uniform mesh and a simple upwind-difference scheme for spatial discretization on a specially designed piecewise-uniform Shishkin mesh. The resulting scheme is proved to be uniformly convergent of order $O(N^{-1}\ln N + M^{-1})$, where N, M are the spatial and temporal parameters respectively. Numerical experiments confirm the theoretical results and the effectiveness of the proposed method.

In **Chapter 5**, we consider the same model problem discussed in **Chapter 4**, and study a parameter-uniform operator-splitting ADI scheme to efficiently solve the parabolic singularly perturbed problems with two positive parameters a two-dimensional domain. The proposed model is a combination of the backward-Euler method on a uniform mesh in time and a hybrid method in space. The analysis is presented on a layer adapted piecewise-uniform Shishkin mesh. The developed numerical method is proved to be first-order convergent in time and second order convergent in space. The numerical experiments are performed to validate the theoretical convergence results and illustrate the efficiency of the current strategy.

We finally summarize the works in this thesis and then conclude with a note on some proposed future works in this direction.

CHAPTER 2

Second-order uniformly convergent numerical scheme for a singularly perturbed degenerate convection-diffusion-reaction problem with two parameters

This chapter considers a convection-reaction-diffusion boundary-value problem (BVP) of degenerate type with two perturbation parameters. We use a standard upwind scheme on a suitably designed Shishkin mesh to obtain a uniformly convergent first-order accurate solution. We also apply the Richardson extrapolation technique to increase the upwind scheme's convergence order. Based on the relations between the parameters, we consider the study in two different cases due to the different boundary layer behavior of the solution in those cases. Numerical results validate the theoretical results and the effectiveness of the proposed extrapolation tool.

2.1 Introduction

We study the following parabolic singularly perturbed degenerate problem,

$$\begin{cases} \varepsilon_1 u''(x) + \varepsilon_2 b(x)u'(x) - c(x)u(x) = f(x), \quad x \in \Omega = (0,1), \\ u(0) = u_0, \quad u(1) = u_1, \end{cases} \tag{2.1.1}$$

where the perturbation parameters $0 < \varepsilon_1, \varepsilon_2 \ll 1$. The convection coefficient is given as $b(x) = x^p a(x)$ for some $p \geq 1$ and $a \geq \alpha > 0$ in Ω. We also assume that $c(x) \geq \beta > 0$ and use $\mathcal{L}_\varepsilon$ to define the continuous operator

$$\mathcal{L}_\varepsilon \kappa = \varepsilon_1 \kappa'' + \varepsilon_2 \kappa' - c\kappa.$$

We split the analysis of the numerical solution and its accuracy into the following two cases:

$$\text{Case I:} \quad \varepsilon_2^2 \leq C\varepsilon_1, \quad \text{Case II:} \quad \varepsilon_2^2 \geq C\varepsilon_1.$$

The characteristics equation associated with the BVP (2.1.1) is defined as

$$\varepsilon_1 \lambda^2 + \varepsilon_2 b(x)\lambda - c(x) = 0, \tag{2.1.2}$$

which has two roots of opposite signs. Suppose, the roots of the above are given by

$$\lambda_0(x) = \frac{-\varepsilon_2 b(x) - \sqrt{\varepsilon_2^2 b^2(x) + 4\varepsilon_1 c(x)}}{2\varepsilon_1},$$

$$\lambda_1(x) = \frac{-\varepsilon_2 b(x) + \sqrt{\varepsilon_2^2 b^2(x) + 4\varepsilon_1 c(x)}}{2\varepsilon_1}.$$

Then, we define the constants $\mu_0,\ \mu_1$ as

$$\mu_0 = \min_{0\leq x\leq 1} |\lambda_0(x)| = \sqrt{\frac{\beta}{\varepsilon_1}}, \quad \mu_1 = \min_{0\leq x\leq 1} \lambda_1(x) = \frac{-\varepsilon_2 A + \sqrt{\varepsilon_2^2 A^2 + 4\varepsilon_1 \beta}}{2\varepsilon_1}, \tag{2.1.3}$$

where $A = \|b\|_\infty$. It is observed that the width of the boundary layer at $x = 0$ is $O(1/\mu_0)$ and that at $x = 1$ is $O(1/\mu_1)$ [4].

Remark 2.1.1. *In Case I, we note that both the constants $\mu_0 = O(\varepsilon_1^{-1/2})$ and $\mu_1 = O(\varepsilon_1^{-1/2})$, while in the other case, μ_0 has the same growth, but $\mu_1 = O(\varepsilon_2^{-1})$.*

2.2 Properties of the continuous solution

The differential operator satisfies the standard minimum principle.

Lemma 2.2.1. Minimum principle: *If* $\omega \in C^2(\Omega)$ *and* $\mathcal{L}_\varepsilon \omega(x) \leq 0$ *for all* $x \in \Omega$ *with* $\omega(0) \geq 0,\ \omega(1) \geq 0$, *then it follows that*

$$\omega(x) \geq 0, \quad \text{for all } x \in \overline{\Omega}. \tag{2.2.1}$$

Lemma 2.2.2. *Suppose* u *is the exact solution of the problem* (2.1.1) *and* u *is decomposed as*

$$u = v + w_L + w_R, \tag{2.2.2}$$

where v *is the smooth component, and* $w_L,\ w_R$ *are the singular components of the solution. For* $\varepsilon_2^2 \leq C\varepsilon_1$, *we have the following bounds for the smooth component* v*:*

$$\left\|v^{(k)}\right\|_\infty \leq C, \quad 0 \leq k \leq 3, \quad \left\|v^{(4)}\right\|_\infty \leq C\left(1 + \frac{1}{\sqrt{\varepsilon_1}}\right). \tag{2.2.3}$$

On the other hand, for the case when $\varepsilon_2^2 \geq C\varepsilon_1$, v *satisfies*

$$\left\|v^{(k)}\right\|_\infty \leq C\left(1 + \left(\frac{\varepsilon_1}{\varepsilon_2}\right)^{3-k}\right), \tag{2.2.4}$$

for $0 \leq k \leq 4$.

Proof. If $\varepsilon_2^2 \leq C\varepsilon_1$, we further decompose the smooth component as $v = v_0 + \sqrt{\varepsilon_1}v_1 + \varepsilon_1 v_2 + \varepsilon_1^{3/2}v_3$. Then for $0 \leq k \leq 4$, following the approaches in Gracia *et al.* [63], we deduce

$$\left\|v_i^{(k)}\right\|_\infty \leq C, \quad \text{for } 0 \leq i \leq 2, \tag{2.2.5}$$

$$\left\|v_3^{(k)}\right\|_\infty \leq C\varepsilon_1^{-k/2}\left(1 + \left(\frac{\varepsilon_2}{\sqrt{\varepsilon_1}}\right)^k\right). \tag{2.2.6}$$

Using $\varepsilon_2^2 \leq C\varepsilon_1$ in (2.2.5)-(2.2.6), we obtain the desired estimates.

Further, when $\varepsilon_2^2 \geq C\varepsilon_1$, expressing the smooth component as $v = v_0 + \varepsilon_1 v_1 + \varepsilon_1^2 v_2 + \varepsilon_1^3 v_3$, we obtain the required estimates for v for $0 \leq k \leq 4$. □

We also have the following estimates for the derivatives of the components $w_L,\ w_R$ available in Linß et al. [64].

Lemma 2.2.3. *The singular components $w_L,\ w_R$ satisfy the following bounds*

$$\left|w_L^{(k)}(x)\right| \leq C\mu_0^k\ e^{-\mu_0 x},$$
$$\left|w_R^{(k)}(x)\right| \leq C\mu_1^k\ e^{-\mu_1(1-x)}, \quad 0 \leq k \leq 4.$$

2.3 Spatial discretizations and the numerical scheme

The space domain $\overline{\Omega} = [0,1]$ is now discretized as

$$\overline{\Omega}^N = \Big\{x_i : x_i = x_{i-1} + h_i, \quad x_0 = 0,\ x_N = 1, \quad 1 \leq i \leq N\Big\},$$

where the step-lengths are defined as $h_i = x_i - x_{i-1}$.

In order to construct the Shishkin mesh $\overline{\Omega}^N$, we first define the transition parameter $\tau_0,\ \tau_1$ as

$$\tau_0 = \min\left\{\frac{1}{4},\ \frac{2}{\mu_0}\ln N\right\}, \quad \tau_1 = \min\left\{\frac{1}{4},\ \frac{2}{\mu_1}\ln N\right\}. \tag{2.3.1}$$

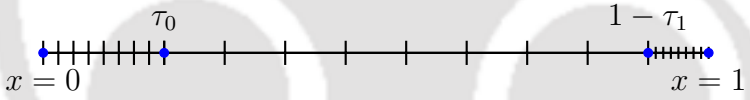

Figure 2.1: Mesh structure along x : $\overline{\Omega}^N$.

The continuous domain $\overline{\Omega} = [0,1]$ is divided into the three subintervals $[0,\ \tau_0]$, $[\tau_0,\ 1-\tau_1]$ and $[1-\tau_1,\ 1]$ by the transitions points τ_0 and $(1-\tau_1)$ to distribute $N/2$ grid points in the layer regions and the remaining $N/2$ grids in the outer regions. The generated Shishkin grid is given by

$$x_i = \begin{cases} \dfrac{4i\tau_0}{N}, & 0 \leq i \leq N/4, \\ \tau_0 + 2\left(i - \dfrac{N}{4}\right)\dfrac{1-\tau_0-\tau_1}{N}, & N/4 < i < 3N/4, \\ 1-\tau_1 + 4\left(i - \dfrac{3N}{4}\right)\dfrac{\tau_1}{N}, & 3N/4 \leq i \leq N. \end{cases} \tag{2.3.2}$$

Clearly, the step-length in the layer regions is given by $h = \dfrac{4\tau_0}{N} \leq 1/N$, and that outside the regions is $H = \dfrac{2(1-\tau_0-\tau_1)}{N}$. Therefore, the step-size outside the layer regions satisfy $1/N \leq H \leq 2/N$.

For a mesh function $\mathcal{S} : \overline{\Omega}^N \longrightarrow \mathbb{R}$, we define the standard finite difference approximations by

$$\delta^+\mathcal{S}_i = \frac{\mathcal{S}_{i+1} - \mathcal{S}_i}{h_{i+1}}, \quad \delta^-\mathcal{S}_i = \frac{\mathcal{S}_i - \mathcal{S}_{i-1}}{h_i},$$
$$\delta^2\mathcal{S}_i = \frac{2}{h_i + h_{i+1}}\Big(\delta^+\mathcal{S}_i - \delta^-\mathcal{S}_i\Big).$$

The standard upwind scheme can now be applied to obtain the discrete equations as:

$$\begin{cases} L_\varepsilon^N U_i^N := \varepsilon_1\delta^2 U_i^N + \varepsilon_2 b(x_i)\ \delta^+ U_i^N - c(x_i)U_i^N = f(x_i), \quad 1 \le i \le N-1, \\ U^N(x_0) = u_0, \quad U^N(x_N) = u_1. \end{cases} \tag{2.3.3}$$

Lemma 2.3.1. Discrete minimum principle *Suppose, Z_i be a mesh function on $\overline{\Omega}^N$ such that $L_\varepsilon^N Z_i \le 0$ for all $1 \le i \le N-1$. Then for $Z_0 \ge 0,\ Z_N \ge 0$, we have*

$$Z_i \ge 0, \quad \forall 0 \le i \le N. \tag{2.3.4}$$

The standard upwind scheme described above has the following convergence property.

Theorem 2.3.2. *If U^N is the numerical approximation of the exact solution $u(x)$ of the problem (2.1.1), and the perturbation parameter satisfies $\varepsilon_1 \le CN^{-1}$. Then, there exist $C > 0$ and $N_0 \in \mathbb{N}$ such that*

$$\left\|U^N - u|_{\Omega^N}\right\|_\infty \le CN^{-1}(\ln N)^2, \quad \textit{for some } N \ge N_0. \tag{2.3.5}$$

Proof. The proof is analogous to the main convergence proof in O'Riordan *et al.* [65] with minimal changes in $\mu_0,\ \mu_1$. □

2.3.1 Motivation for Richardson extrapolation

From Theorem 2.3.2, we have

$$U_i^N - u(x_i) = CN^{-1}(\ln N)^2 + R_N(x_i), \quad 1 \le i \le N-1, \tag{2.3.6}$$

where $R_N(x_i) = o(N^{-1}(\ln N)^2)$, and C is independent of the perturbation parameters and the mesh parameter N. Keeping the transition points in (2.3.1) fixed, we refine the Shishkin mesh $\overline{\Omega}^N$ by bisecting every mesh intervals to create a new Shishkin grid $\widetilde{\Omega}^{2N}$. Let $\widetilde{U}^{2N}$ be the numerical approximation on this grid without changing the transition points $\tau_0,\ \tau_1$.

From Theorem (2.3.2), with $\mu_0,\ \mu_1$ defined in (2.1.3), the error equation can be rewritten as

$$U_i^N - u(x_i) = CN^{-1}\left(\frac{\tau_0\mu_0}{2}\right)^2 + o\left(N^{-1}\left(\frac{\tau_0\mu_0}{2}\right)^2\right), \quad 1 \le i \le N-1,$$

since $\ln N = \dfrac{\tau_0\mu_0}{2}$ is constant. Clearly from the above, we have for $x_i \in \overline{\Omega}^N$

$$\widetilde{U}_i^{2N} - u(x_i) = C(2N)^{-1}\left(\frac{\tau_0\mu_0}{2}\right)^2 + o\left(N^{-1}\left(\frac{\tau_0\mu_0}{2}\right)^2\right), \quad 1 \le i \le N-1,$$

which gives

$$2\widetilde{U}_i^{2N} - U_i^N - u(x_i) = o\left(N^{-1}(\ln N)^2\right). \tag{2.3.7}$$

Therefore, we define the following extrapolation formula, known as the Richardson extrapolation formula, as

$$\widehat{U}^N(x_i) = \left(2\widetilde{U}^{2N} - U^N\right)(x_i), \quad \forall x_i \in \overline{\Omega}^N, \tag{2.3.8}$$

having almost second-order accuracy in approximation of the exact solution.

2.4 Convergence analysis

We decompose the numerical approximation U^N of the exact solution $u(x)$ as

$$U^N = V^N + W_l^N + W_r^N,$$

where $V^N,\ W_l^N,\ W_r^N$ denote the smooth, the left singular and the right singular components of U^N respectively. These components satisfy the following discrete equations:

$$\begin{cases} L_\varepsilon^N V^N(x_i) = f(x_i), \quad x_i \in (0,1), \\ V^N(0) = v(0), \quad V^N(1) = v(1), \end{cases} \quad \begin{cases} L_\varepsilon^N W_l^N(x_i) = 0, \quad x_i \in (0,1), \\ W_l^N(0) = w_L(0), \quad W_l^N(1) = 0, \end{cases} \tag{2.4.1}$$

and

$$\begin{cases} L_\varepsilon^N W_r^N(x_i) = 0, \quad x_i \in (0,1), \\ W_r^N(0) = 0, \quad W_r^N(1) = w_R(1), \end{cases} \tag{2.4.2}$$

Similarly, we also decompose the solution $\widetilde{U}^{2N}$ as

$$\widetilde{U}^{2N} = \widetilde{V}^{2N} + \widetilde{W_l}^{2N} + \widetilde{W_r}^{2N}.$$

2.4.1 Extrapolation in the smooth component

Lemma 2.4.1. *For $x_i \in \Omega^N$, the truncation error in the smooth component satisfies*

$$L_\varepsilon^N(V_i^N - v(x_i)) = h_i\eta(x_i) + O(\varepsilon_2 h_i^2), \tag{2.4.3}$$

where $V_i^N = V^N(x_i)$, and $\eta(x) = \dfrac{1}{2}\varepsilon_2 b(x)v''(x)$.

Proof. A straightforward Taylor series expansion deduces the following for the smooth component v:

$$\begin{aligned} L_\varepsilon^N(V_i^N - v(x_i)) &= \frac{\varepsilon_1}{4!}h_i^2\left[v^{(4)}(\xi_1) + v^{(4)}(\xi_2)\right] + \varepsilon_2 b(x_i)\left[\frac{h_i}{2}v''(x_i) + \frac{h_i^2}{3!}v^{(3)}(\xi_3)\right], \\ &= h_i\eta(x_i) + \varepsilon_2 b(x_i)\frac{h_i^2}{3!}v^{(3)}(\xi_3) + \frac{\varepsilon_1}{4!}h_i^2\left[v^{(4)}(\xi_1) + v^{(4)}(\xi_2)\right], \end{aligned} \tag{2.4.4}$$

for some $\xi_1 \in (x_i, x_{i+1})$, $\xi_2, \xi_3 \in (x_{i-1}, x_i)$. Now using the estimates of $v^{(3)}$, $v^{(4)}$ from Lemma 2.2.2, we obtain the required estimate. □

We define the following auxiliary problem:

$$\begin{cases} \mathcal{L}_\varepsilon E(x) = \eta(x), \quad 0 < x < 1, \\ E(0) = 0, \quad E(1) = 0. \end{cases} \tag{2.4.5}$$

The function $E(x)$ can be further decomposed as $E = E_0 + E_1 + E_2$, where E_0 is the smooth component, while E_1, E_2 are the left and right singular layers parts of E respectively. The

components satisfy

$$\begin{cases} \mathcal{L}_\varepsilon E_0(x) = \eta(x), \ 0 < x < 1, \\ E_0(0) = -E_l(0), \ E_0(1) = -E_r(1), \end{cases} \tag{2.4.6}$$

where

$$\begin{cases} \mathcal{L}_\varepsilon E_l(x) = 0, \quad 0 < x < 1, \\ |E_l(0)| \le C, \quad E_l(1) = 0, \end{cases} \quad \begin{cases} \mathcal{L}_\varepsilon E_r(x) = 0, \quad 0 < x < 1, \\ E_r(0) = 0, \quad |E_r(1)| \le C. \end{cases} \tag{2.4.7}$$

Lemma 2.4.2. *For $\varepsilon_2 \le CN^{-1}$, the smooth component of the approximate solution satisfy the following error equation:*

$$V_i^N - v(x_i) = h_i E_0(x_i) + O(N^{-2}), \quad \text{for } x_i \in \overline{\Omega}^N. \tag{2.4.8}$$

Proof. From Lemma 2.4.1 and (2.4.5), we obtain

$$\begin{aligned} L_\varepsilon^N (V_i^N - v(x_i)) &= h_i \mathcal{L}_\varepsilon E_0(x_i) + O(\varepsilon_2 H^2), \\ &= h_i \left[L_\varepsilon^N E_0(x_i) + O(H) \right] + O(\varepsilon_2 H^2). \end{aligned}$$

Thus, assuming $\varepsilon_2 \le CN^{-1} \le H$ and $h_i \le H$, we have

$$L_\varepsilon^N (V_i^N - v(x_i) - h_i E_0(x_i)) = O(N^{-2}).$$

We define the discrete function

$$\Psi_i = C_1(1 - x_i)N^{-2} \pm \left(V_i^N - v(x_i) - h_i E_0(x_i) \right), \quad 1 \le i \le N - 1 \tag{2.4.9}$$

for some $C_1 > 0$ with $\Psi_0 = 0 = \Psi_N$. We have

$$L_\varepsilon^N \Psi_i = C_1 N^{-2} L_\varepsilon^N (1 - x_i) \pm L_\varepsilon^N \left(V_i^N - v(x_i) - h_i E_0(x_i) \right).$$

We choose C_1 such that $L_\varepsilon^N \Psi_i \le 0$. By using discrete minimum principle and $1/N \le H \le 2/N$, we have

$$\left| \left(V_i^N - v(x_i) \right) - h_i E_0(x_i) \right| \le CN^{-2}. \tag{2.4.10}$$

Therefore, $V_i^N - v(x_i) - h_i E_0(x_i) = O(N^{-2})$. □

Theorem 2.4.3. *For $\varepsilon_2 \leq CN^{-1}$, the error after the extrapolation in the smooth component satisfies*

$$\left|\left(2\widetilde{V}_i^{2N} - V_i^N\right) - v(x_i)\right| \leq CN^{-2}, \text{ for } 1 \leq i \leq N-1. \tag{2.4.11}$$

Proof. From Lemma 2.4.1, we have on the Shishkin mesh $\widetilde{\Omega}^{2N}$

$$\widetilde{V}_i^{2N} - v(x_i) = \frac{h_i}{2}E_0(x_i) + O(N^{-2}), \quad 1 \leq i \leq N-1. \tag{2.4.12}$$

Using the equation (2.4.8) and (2.4.12), we obtain

$$2(\widetilde{V}_i^{2N} - v(x_i)) - (V_i^N - v(x_i)) = O(N^{-2}),$$

which gives the required error estimate. □

We now proceed to obtain the estimates for the error after extrapolation in the singular components.

2.4.2 Extrapolation in the singular components

We first define the following problem, which will be used in the estimation of the extrapolated solution in $(0, \tau_0)$.

$$\begin{cases} \mathcal{L}_\varepsilon F(x) = \dfrac{4\varepsilon_2}{\mu_0} b(x) w_L''(x), & 0 < x < \tau_0, \\ F(0) = 0, \quad F(\tau_0) = 0. \end{cases} \tag{2.4.13}$$

It can be easily verified that

$$\begin{aligned} L_\varepsilon^N F(x_i) &= \mathcal{L}_\varepsilon F(x_i) + O(\varepsilon_1 h_i \mu_0^3 e^{-\mu_0 x_i}), \\ &= \mathcal{L}_\varepsilon F(x_i) + O((N^{-1}\ln N)\, e^{-\mu_0 x_i}), \end{aligned} \tag{2.4.14}$$

using $\varepsilon_1 \mu_0^2 \leq C$ and $h_i = O(N^{-1}\mu_0^{-1}\ln N)$.

Lemma 2.4.4. *Let us define $S_i = \prod_{j=1}^{i}(1+\mu_0 h_j)$, $S_0 = 1$. Then there exists a positive constant C such that*

$$L_\varepsilon^N S_i \leq C S_i, \quad 1 \leq i \leq N-1.$$

Proof. We have

$$\frac{S_{i+1}-S_i}{h_{i+1}} = \mu_0 S_i, \quad \frac{S_i - S_{i-1}}{h_i} = \mu_0 S_{i-1},$$
$$\text{and } S_{i-1} = \frac{\mu_0 h_i}{1+\mu_0 h_i} S_i.$$

Thus,

$$\begin{aligned} L_\varepsilon^N S_i &= \frac{2\varepsilon_1 \mu_0}{h_i + h_{i+1}}(S_i - S_{i-1}) + \varepsilon_2 b(x_i)\mu_0 S_i, \\ &= \frac{2\varepsilon_1 h_i \mu_0^2}{h_i + h_{i+1}} \frac{S_i}{1+\mu_0 h_i} + \varepsilon_2 b(x_i)\mu_0 S_i, \\ &\le \frac{C S_i}{1+\mu_0 h_i} + C\varepsilon_2 \mu_0 S_i. \end{aligned}$$

Now for Case I: $\varepsilon_2 \le C\sqrt{\varepsilon_1}$, it is clear that

$$\varepsilon_2 \mu_0 \le C\mu_0 \sqrt{\varepsilon_1} \le C,$$

and for Case II: $\varepsilon_2 \le C\sqrt{\varepsilon_1}$, we use $\mu_1 \ge \mu_0$ and $\mu_1 = O(1/\varepsilon_2)$ to deduce $\varepsilon_2 \mu_0 \le C$.

Hence, in either cases, we have $L_\varepsilon^N S_i \le C S_i$, for all $1 \le i \le N-1$. □

Lemma 2.4.5. *For $x_i \in (0, \tau_0)$, the error after extrapolation in the left singular part satisfies the following*

$$\left| \left(2\widetilde{W_l}^{2N} - W_l^N \right)(x_i) - w_L(x_i)) \right| \le C(N^{-1}\ln N)^2, \text{ for } 1 \le i \le N/4. \tag{2.4.15}$$

Proof. For $0 < x_i < \tau_0$, using Taylor series expansion, we have for some $\xi_1 \in (x_i, x_{i+1})$, and $\xi_2, \xi_3 \in (x_{i-1}, x_i)$,

$$\begin{aligned} L_\varepsilon^N (W_l^N - w_L)(x_i) &= \frac{\varepsilon_1}{4!} h_i^2 \left[w_L^{(4)}(\xi_1) + w_L^{(4)}(\xi_2) \right] + \varepsilon_2 b(x_i) \left[\frac{h_i}{2} w_L''(x_i) + \frac{h_i^2}{3!} w_L^{(3)}(\xi_3) \right], \\ &= \frac{4\varepsilon_2}{N\mu_0} b(x) \ln N w_L''(x_i) + O(\varepsilon_1 h_i^2 \mu_0^4 e^{-\mu_0 x_i}), \\ &= (N^{-1}\ln N)\mathcal{L}_\varepsilon F(x_i) + O((N^{-1}\ln N)^2\, e^{-\mu_0 x_i}). \end{aligned}$$

Using (2.4.14), we obtain

$$L_\varepsilon^N (W_l^N - w_L)(x_i) = (N^{-1}\ln N) L_\varepsilon^N F(x_i) + O((N^{-1}\ln N)^2\, e^{-\mu_0 x_i}),$$

which gives

$$L_\varepsilon^N(W_l^N - w_L - (N^{-1}\ln N)F)(x_i) = O((N^{-1}\ln N)^2\ e^{-\mu_0 x_i}). \tag{2.4.16}$$

Let $\Lambda_i = (W_l^N - w_L - (N^{-1}\ln N)F)(x_i),\ 0 \le i \le N/4.$

We now define the discrete mesh function

$$\Gamma_i = C_2(1-x_i)N^{-2} + (N^{-1}\ln N)^2 \prod_{j=1}^{i}(1+\mu_0 h_j)^{-1}, \quad 1 \le i \le N/4,$$

where $C_2 > 0$.

Using the fact $L_\varepsilon^N S_i \le CS_i$, we can prove

$$L_\varepsilon^N \Gamma_i \le L_\varepsilon^N \Lambda_i, \quad 1 \le i \le N/4.$$

Also, $\Gamma_0 \ge 0 = \Lambda_0$ and $\Gamma_{N/4} \ge C_2 N^{-2} \ge \Lambda_{N/4}$ for some $C_2 > 0$.

Therefore, Γ_i is a barrier function for the function Λ_i. Hence, using discrete minimum principle for the operator L_ε^N, we get

$$\left|(W_l^N - w_L - (N^{-1}\ln N)F)(x_i)\right| \le \Gamma_i \le C(N^{-1}\ln N)^2, \quad 0 \le i \le N/4. \tag{2.4.17}$$

Therefore, we have

$$(W_l^N - w_L)(x_i) = (N^{-1}\ln N)F(x_i) + O((N^{-1}\ln N)^2), \tag{2.4.18}$$

$$= N^{-1}\frac{\tau_0\mu_0}{2}F(x_i) + O((N^{-1}\ln N)^2). \tag{2.4.19}$$

Similarly, we also obtain

$$(\widetilde{W}_l^{2N} - w_L)(x_i) = (2N)^{-1}\frac{\tau_0\mu_0}{2}F(x_i) + O((N^{-1}\ln N)^2). \tag{2.4.20}$$

From the last two equations, it follows that

$$2(\widetilde{W}_l^{2N} - w_L)(x_i) - (W_l^N - w_L)(x_i) = O((N^{-1}\ln N)^2), \tag{2.4.21}$$

which leads to the desired error estimate. □

Lemma 2.4.6. *For $x_i \in (\tau_0,\ 1)$, the error after extrapolation in the left singular part satisfies*

the following error equation:

$$\left|\left(2\widetilde{W}_l^{2N} - W_l^N\right)(x_i) - w_L(x_i)\right| \leq CN^{-2}, \text{ for } N/4 < i \leq N-1. \tag{2.4.22}$$

Proof. Let us start with the notations

$$\chi_L(x_i) = \prod_{j=1}^{i} \frac{1}{1+\mu_0 h_j}, \quad \chi_R(x_i) = \prod_{j=i+1}^{N} \frac{1}{1+\mu_1 h_j}, \quad 1 \leq i \leq N-1. \tag{2.4.23}$$

Following the approach in O'Riordan *et al.* [65], it can be proved that

$$\left|W_l^N(x_i)\right| \leq C\chi_L(x_i), \quad \text{and } |W_r(x_i)| \leq C\chi_R(x_i), \ \forall i.$$

Then, we observe for $i \geq N/4$,

$$\begin{aligned}\left|W_l^N(x_i)\right| &\leq C\chi_L(x_i) \leq C\chi_L(x_{N/4}) = C\prod_{j=1}^{N/4}(1+\mu_0 H)^{-1}, \\ &\leq \left(1+8N^{-1}\ln N\right)^{-N/4} \leq CN^{-2}.\end{aligned}$$

We also observe from Lemma 2.2.2 that for $x_i \geq \tau_0$,

$$|w_L(x_i)| \leq Ce^{-\mu_0 x_i} \leq Ce^{-\mu_0\tau_0} \leq CN^{-2}.$$

Therefore combining these two, we have

$$\left|(W_l^N - w_L)(x_i)\right| \leq CN^{-2}, \quad \text{for } x_i \in (\tau_0, 1). \tag{2.4.24}$$

Similarly, we also have

$$\left|(\widetilde{W}_l^{2N} - w_L)(x_i)\right| \leq CN^{-2}, \quad \text{for } x_i \in (\tau_0, 1). \tag{2.4.25}$$

From (2.4.24)-(2.4.25), it follows that

$$\begin{aligned}\left|\left(2\widetilde{W}_l^{2N} - W_l^N\right)(x_i) - w_L(x_i)\right| &\leq \left|(W_l^N - w_L)(x_i)\right| + 2\left|(\widetilde{W}_l^{2N} - w_L)(x_i)\right|, \\ &\leq CN^{-2}, \text{ for } x_i \in (\tau_0, 1).\end{aligned}$$

This completes the proof. □

Combining the error estimates established in Lemma 2.4.5 and Lemma 2.4.6, we prove the following global estimate for the extrapolation of the left singular component.

Theorem 2.4.7. *For $x_i \in \overline{\Omega}^N$, the error after extrapolation in the left singular part satisfies the following estimate*

$$\left|\left(2\widetilde{W_l}^{2N} - W_l^N\right)(x_i) - w_L(x_i)\right| \leq C(N^{-1}\ln N)^2, \text{ for } 1 \leq i \leq N-1. \tag{2.4.26}$$

Theorem 2.4.8. *For $x_i \in \overline{\Omega}^N$, the numerical error after extrapolation in the right singular component satisfies the following*

$$\left|\left(2\widetilde{W_r}^{2N} - W_r^N\right)(x_i) - w_R(x_i)\right| \leq C(N^{-1}\ln N)^2, \text{ for } 1 \leq i \leq N-1. \tag{2.4.27}$$

Proof. Using the estimates $|W_r(x_i)| \leq C\chi_R(x_i)$, $\forall i$, and proceeding in the same way as in Lemma 2.4.6, we can prove that

$$\left|\left(2\widetilde{W_r}^{2N} - W_r^N\right)(x_i) - w_R(x_i)\right| \leq CN^{-2}, \text{ for } 0 < i < \frac{3N}{4}. \tag{2.4.28}$$

Also by using the same approach as in Lemma 2.4.5, we can prove

$$\left|\left(2\widetilde{W_r}^{2N} - W_r^N\right)(x_i) - w_R(x_i)\right| \leq C(N^{-1}\ln N)^2, \text{ for } i \geq \frac{3N}{4}. \tag{2.4.29}$$

The required convergence result follows by combining the last two equations. □

2.4.3 Error estimate for the extrapolated solution

Theorem 2.4.9. (Main convergencet theorem) *If $\widehat{U}^N$ is the Richardson extrapolation of the numerical solution U^N of the problem (2.1.1) on $\overline{\Omega}^N$, and the perturbation parameter satisfies $\varepsilon_2 \leq CN^{-1}$. Then, we have the following accuracy:*

$$\left\|\widehat{U}^N - u\right\|_{\infty,\overline{\Omega}^N} \leq CN^{-2}(\ln N)^2, \quad \text{for some } N \geq N_0. \tag{2.4.30}$$

where $C > 0$ and $N_0 \in \mathbb{N}$.

Proof. Suppose, V^N, W_r^N, W_l^N are the smooth and singular components of the numerical solution U^N of the exact solution $u(x)$ on $\overline{\Omega}^N$, and $\widetilde{V}^{2N}$, $\widetilde{W_l}^{2N}$, $\widetilde{W_r}^{2N}$ are those of the approximate solution $\widetilde{U}^{2N}$ on the mesh $\widetilde{\Omega}^{2N}$. Then, from Theorem 2.4.3, Theorem 2.4.7 and

Theorem 2.4.8, we have the following

$$\begin{aligned}\left|\widehat{U}_i^N - u(x_i)\right| &= \left|(2\widetilde{V}_i^{2N} - V_i^N) - v(x_i)\right| + \left|((2\widetilde{W}_l^{2N} - W_l^N) - w_L)(x_i)\right| \\ &\quad + \left|((2\widetilde{W}_r^{2N} - W_r^N) - w_R)(x_i)\right| \\ &\leq C\left[N^{-2} + N^{-2}(\ln N)^2 + N^{-2}(\ln N)^2\right] \leq CN^{-2}(\ln N)^2.\end{aligned}$$

for each $x_i \in \overline{\Omega}^N$. Adding the above equations and using (2.3.8), we prove the required convergence result. □

2.5 Numerical experiments

For validation of the theoretical convergence results, we consider a convection-reaction-diffusion problem with two parameters, where the diffusion coefficient is affected by parameter ε_1 and the convection coefficient function contains the second parameters ε_2. We first choose two sets of parameters to test the parameter-uniform convergence of the underlying standard-upwind scheme. Then, we extrapolate the numerical solution to observe the enhanced accuracy for the same of parameters.

Example 2.5.1. *We take the following example for computing the numerical results.*

$$\begin{cases} \varepsilon_1 u''(x) + \varepsilon_2 x^p(1+x)\ u'(x) - u(x) = 1 - x^2, \quad x \in \Omega = (0,1), \\ u(0) = 1, \quad u(1) = 1. \end{cases} \tag{2.5.1}$$

We consider the set

$$S_1 = \left\{(\varepsilon_1, \varepsilon_2) : \varepsilon_1 = 10^{-k-2}, \quad \varepsilon_2 = \frac{\sqrt{\varepsilon_1}}{10}, \quad k = 1, 2, \ldots, 5\right\}, \tag{2.5.2}$$

$$S_2 = \left\{(\varepsilon_1, \varepsilon_2) : \varepsilon_1 = 10^{-k}, \quad \varepsilon_2 = {\varepsilon_1}^{1/4}, \quad k = 1, 2, \ldots, 5\right\}, \tag{2.5.3}$$

for the parameters that satisfy the condition in Case I and for Case II, respectively.

The maximum pointwise error in the approximate solution U^N can be computed using the formula

$$E^N_{\varepsilon_1,\varepsilon_2} = \max_{x_i \in \overline{\Omega}^N} \left|U^N_{\varepsilon_1,\varepsilon_2}(x_i) - u(x_i)\right|. \tag{2.5.4}$$

Since we do not have the exact solution in this example, we use double mesh principle to

calculate the pointwise maximum error in the numerical solution U^N as

$$E^N_{\varepsilon_1,\varepsilon_2} = \max_{x_i \in \overline{\Omega}^N} \left| U^N_{\varepsilon_1,\varepsilon_2}(x_i) - \widetilde{U}^{2N}_{\varepsilon_1,\varepsilon_2}(x_i) \right|. \tag{2.5.5}$$

We also define the parameter-independent maximum error E^N and the parameter-uniform rate of convergence p^N by

$$E^N = \max_{\varepsilon_1,\varepsilon_2} E^N_{\varepsilon_1,\varepsilon_2}, \quad p^N = \log_2 \left(\frac{E^N}{E^{2N}} \right). \tag{2.5.6}$$

From Figure 2.2, we see that the thickness of the boundary layers at both boundaries are same when we consider Case I. However from Figure 2.3, for Case II, it is clear that the boundary layers at $x = 0$ and $x = 1$ are not of the same width. This happens because the sharpness of the layers depends directly of the constants μ_0, μ_1 and in this case, we have $\mu_0 \gg \mu_1$.

We first observe the convergence phenomena before employing the Richardson extrapolation for the example. We notice from Table 2.1 and Table 2.2 that the approximation error have consistently decreased with increasing number of mesh points. Also, the error remains bounded even after significantly decreasing the parameters values along the columns. This ensures the parameter-independent stability of the upwind scheme. The data in the tables successfully reflect the almost first-order accuracy of the scheme in discrete maximum norm. The order of accuracy of the method can also be easily noticed from loglog plot visualizations in Figure 2.4 and Figure 2.5.

After using the Richardson extrapolation technique, we note that there is a significant improve in the pointwise-maximum error as well as the rate of convergence in both cases for the same set of parameters. The method retains the consistency as well as the parameter-uniform stability of the upwind scheme. From Table 2.3 and Table 2.4, the almost second-order convergence of the scheme are verified. Graphically, the same can also be visualized from the loglog figures in Figure 2.6 and Figure 2.7. Therefore, the theoretical estimates proved in the previous sections are successfully validate with these numerical results.

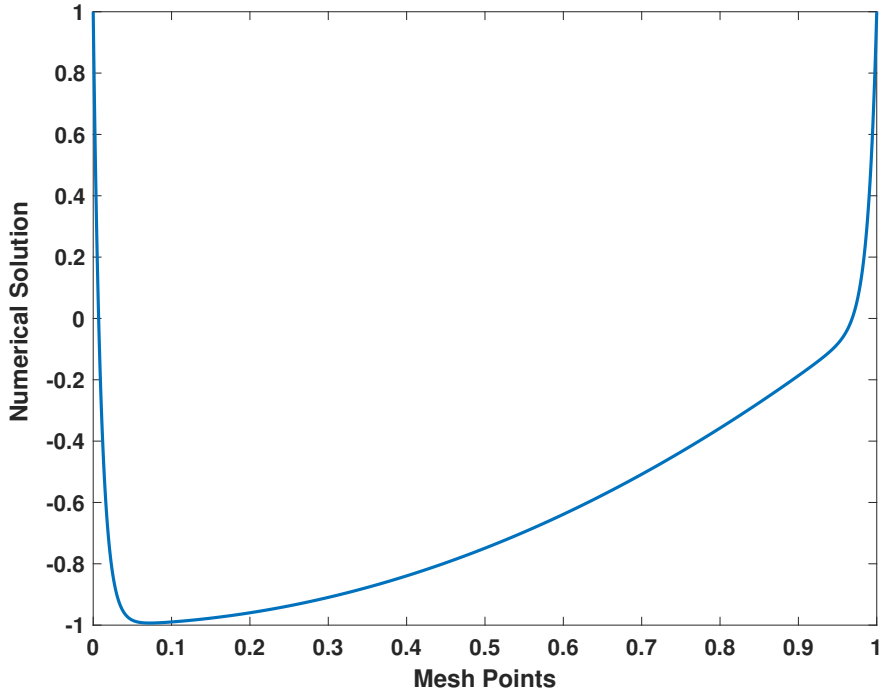

Figure 2.2: Plot of the numerical approximation U^N for Example 2.5.1 with $p = 1$ and $\varepsilon_1 = 10^{-4}$, $\varepsilon_2 = \dfrac{\sqrt{\varepsilon_1}}{10}$ for Case I.

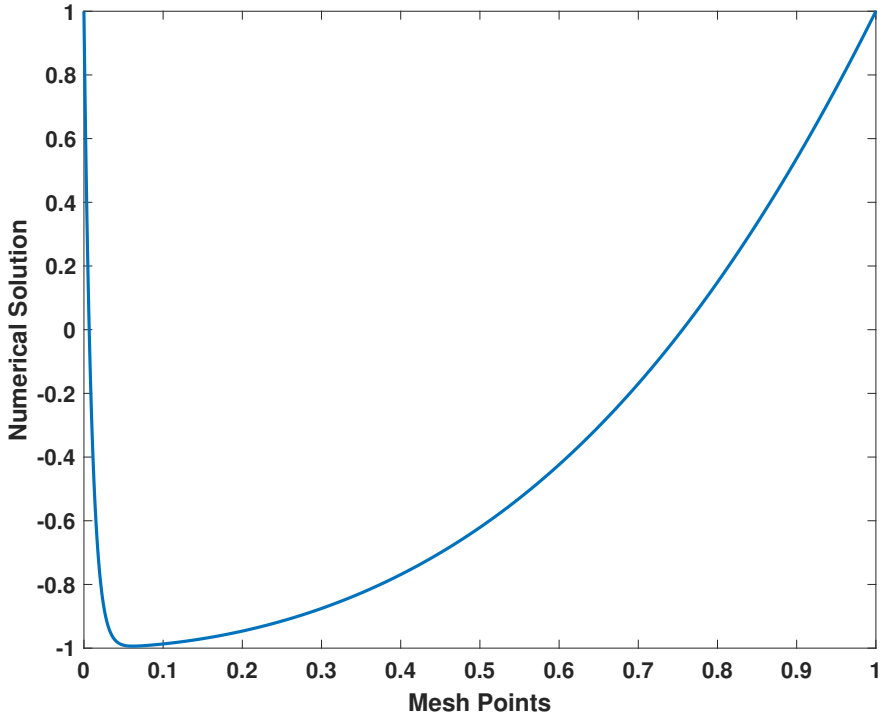

Figure 2.3: Plot of the numerical approximation U^N for Example 2.5.1 with $p = 1$ and $\varepsilon_1 = 10^{-4}, \varepsilon_2 = \varepsilon_1^{1/4}$ for Case II.

Table 2.1: Maximum pointwise error and associated rate of convergence using standard upwind scheme for Example 2.5.1 with $p = 1$ for various values of ε_1 from the set S_1 for Case I.

ε_1	$N = 64$	128	256	512	1024
10^{-3}	6.3449e-03	2.5847e-03	1.1369e-03	5.2666e-04	2.5283e-04
	1.295	1.184	1.110	1.058	-
10^{-4}	8.0929e-03	3.9311e-03	1.9664e-03	1.0073e-03	5.2738e-04
	1.041	0.999	0.965	0.933	-
10^{-5}	8.1787e-03	3.9726e-03	1.9892e-03	1.0191e-03	5.3370e-04
	1.041	0.997	0.965	0.933	0
10^{-6}	8.2063e-03	3.9860e-03	1.9967e-03	1.0229e-03	5.3576e-04
	1.041	0.997	0.964	0.933	-
10^{-7}	8.2151e-03	3.9903e-03	1.9990e-03	1.0241e-03	5.3642e-04
	1.041	0.997	0.964	0.932	-
10^{-8}	8.2179e-03	3.9917e-03	1.9998e-03	1.0245e-03	5.3663e-04
	1.041	0.997	0.964	0.932	-
10^{-9}	8.2188e-03	3.9921e-03	2.0000e-03	1.0246e-03	5.3670e-04
	1.041	0.997	0.964	0.932	-
10^{-10}	8.2190e-03	3.9922e-03	2.0001e-03	1.0247e-03	5.3672e-04
	1.041	0.997	0.964	0.932	-

Table 2.2: Maximum pointwise error and associated rate of convergence using standard upwind scheme for Example 2.5.1 with $p = 1$ for various values of ε_1 from the set S_1 for Case II.

ε_1	$N = 64$	128	256	512	1024
10^{-3}	9.0359e-03	3.6544e-03	1.6136e-03	7.5427e-04	3.6450e-04
	1.3060	1.1794	1.0971	1.0492	-
10^{-4}	1.0155e-02	5.3257e-03	2.7271e-03	1.3799e-03	6.9413e-04
	0.9312	0.9656	0.9828	0.9913	-
10^{-5}	2.3788e-02	1.3050e-02	6.8544e-03	3.5207e-03	1.7844e-03
	0.8662	0.9289	0.9612	0.9805	-
10^{-6}	3.4001e-02	2.2046e-02	1.3549e-02	7.9447e-03	4.0898e-03
	0.6250	0.7024	0.7701	0.9580	-
10^{-7}	3.5106e-02	2.2779e-02	1.4000e-02	8.2157e-03	4.6848e-03
	0.6240	0.7023	0.7689	0.8104	-
10^{-8}	3.5620e-02	2.3121e-02	1.4210e-02	8.3401e-03	4.7559e-03
	0.6235	0.7024	0.7688	0.8103	-
10^{-9}	3.5859e-02	2.3281e-02	1.4307e-02	8.3979e-03	4.7890e-03
	0.6231	0.7024	0.7686	0.8103	-
10^{-10}	3.5970e-02	2.3355e-02	1.4353e-02	8.4247e-03	4.8044e-03
	0.6231	0.7024	0.7686	0.8103	-

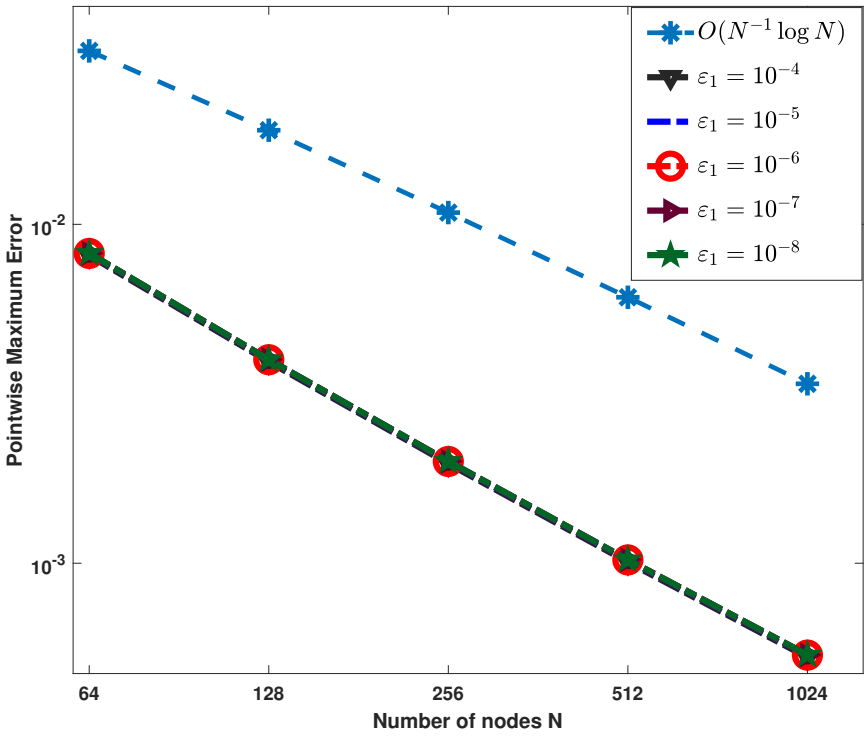

Figure 2.4: Loglog plot of the pointwise maximum error obtained before using Richardson extrapolation for Case I for Example 2.5.1.

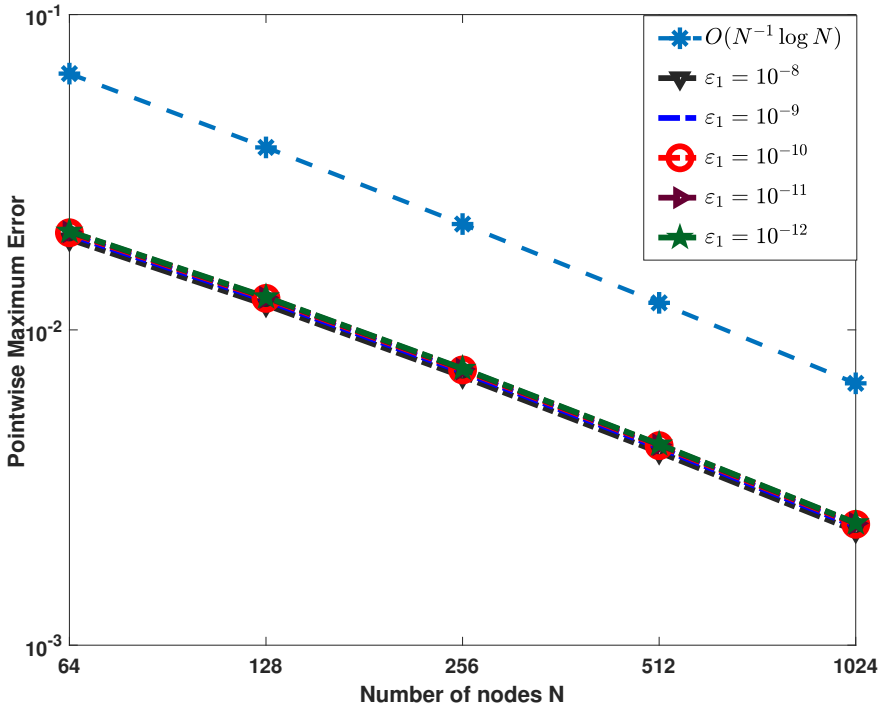

Figure 2.5: Loglog plot of the pointwise maximum error obtained before using Richardson extrapolation for Case II for Example 2.5.1.

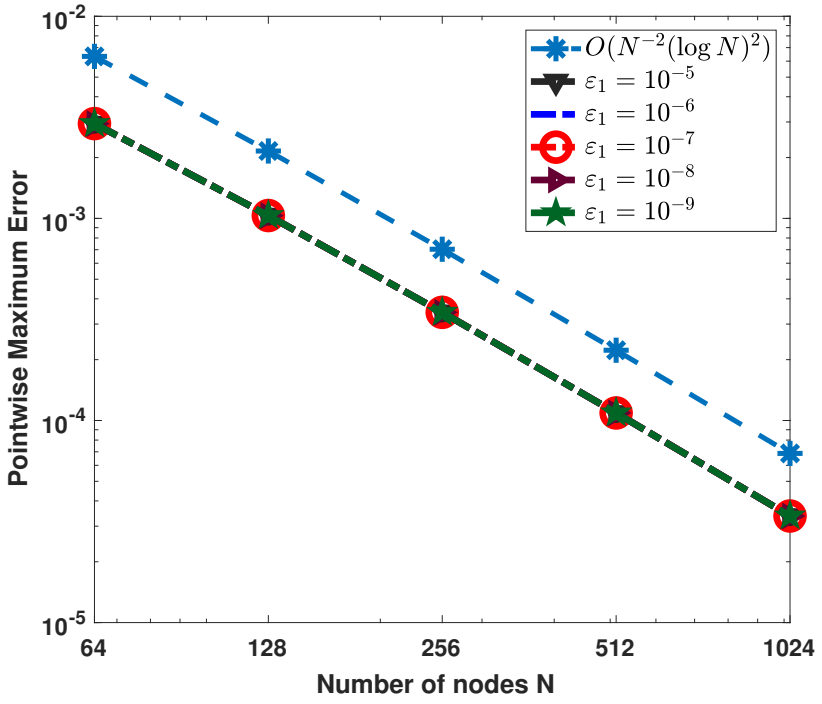

Figure 2.6: Loglog plot visualization of the pointwise maximum error obtained after using Richardson extrapolation for Case I for Example 2.5.1.

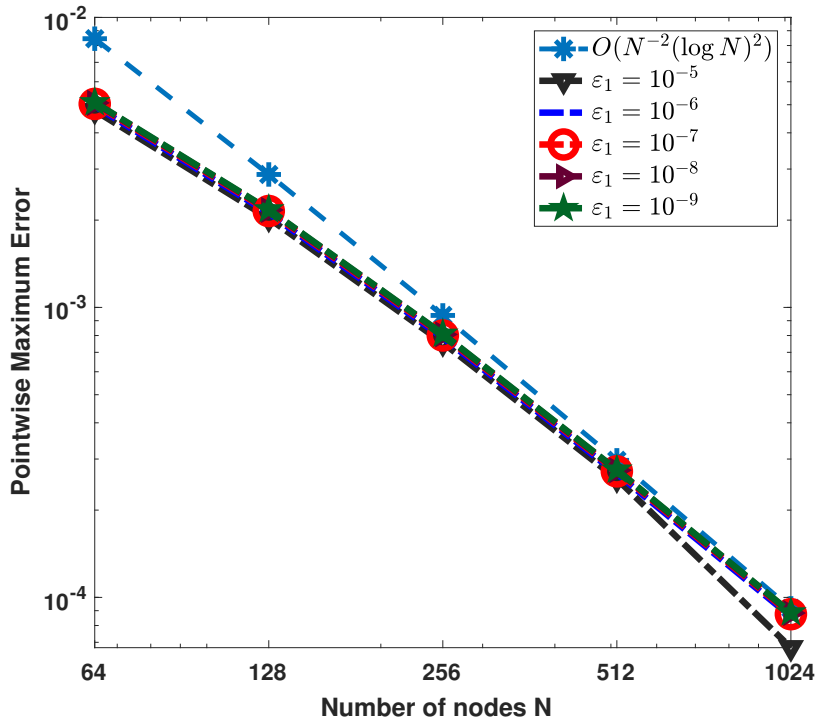

Figure 2.7: Loglog plot visualization of the pointwise maximum error obtained after using Richardson extrapolation for Case II for Example 2.5.1.

Table 2.3: Maximum pointwise error and associated rate of convergence Example 2.5.1 with $p = 1$ for various values of ε_1 from the set S_1 after using Richardson extrapolation for Case I.

ε_1	$N = 64$	128	256	512	1024
10^{-3}	2.6513e-03	6.8674e-04	1.7319e-04	4.3388e-05	1.0852e-05
	1.9489	1.9874	1.9970	1.9993	-
10^{-4}	2.9375e-03	1.0305e-03	3.4196e-04	1.0868e-04	3.3587e-05
	1.5112	1.5915	1.6537	1.6942	-
10^{-5}	2.9424e-03	1.0323e-03	3.4261e-04	1.0889e-04	3.3652e-05
	1.5111	1.5913	1.6537	1.6941	-
10^{-6}	2.9439e-03	1.0329e-03	3.4281e-04	1.0895e-04	3.3672e-05
	1.5111	1.5912	1.6537	1.6941	-
10^{-7}	2.9443e-03	1.0330e-03	3.4287e-04	1.0897e-04	3.3678e-05
	1.5111	1.5912	1.6537	1.6941	-
10^{-8}	2.9444e-03	1.0331e-03	3.4289e-04	1.0898e-04	3.3680e-05
	1.5111	1.5912	1.6537	1.6941	-
10^{-9}	2.9445e-03	1.0331e-03	3.4290e-04	1.0898e-04	3.3681e-05
	1.5111	1.5911	1.6537	1.6941	-
10^{-10}	2.9445e-03	1.0331e-03	3.4290e-04	1.0898e-04	3.3681e-05
	1.5111	1.5911	1.6537	1.6941	-

Table 2.4: Maximum pointwise error and associated rate of convergence Example 2.5.1 with $p = 1$ for various values of ε_1 from the set S_2 after using Richardson extrapolation for Case II.

ε_1	$N = 64$	128	256	512	1024
10^{-3}	1.9995e-03	4.9935e-04	1.2403e-04	3.0740e-05	7.6481e-06
	2.0015	2.0094	2.0125	2.0069	-
10^{-4}	2.6202e-03	9.1404e-04	2.9946e-04	9.5012e-05	2.9285e-05
	1.5193	1.6099	1.6562	1.6980	-
10^{-5}	2.7981e-03	9.7935e-04	3.2331e-04	1.0268e-04	3.1700e-05
	1.5146	1.5989	1.6547	1.6957	-
10^{-6}	4.7749e-03	2.0285e-03	7.5493e-04	2.5601e-04	6.7089e-05
	1.2351	1.4260	1.5602	1.9320	-
10^{-7}	4.9511e-03	2.1111e-03	7.8581e-04	2.6701e-04	8.5912e-05
	1.2298	1.4257	1.5573	1.6360	-
10^{-8}	5.0337e-03	2.1499e-03	8.0032e-04	2.7205e-04	8.7543e-05
	1.2274	1.4256	1.5567	1.6358	-
10^{-9}	5.0738e-03	2.1679e-03	8.0710e-04	2.7441e-04	8.8306e-05
	1.2268	1.4255	1.5564	1.6357	-
10^{-10}	5.0932e-03	2.1763e-03	8.1026e-04	2.7550e-04	8.8661e-05
	1.2267	1.4255	1.5563	1.6357	-

Table 2.5: Maximum pointwise error and associated rate of convergence Example 2.5.1 with $\varepsilon_1 = 10^{-4},\ \varepsilon_2 = \dfrac{\sqrt{\varepsilon_1}}{10}$ for various values of p before using Richardson extrapolation.

p	$N = 64$	128	256	512	1024
1	3.2196e-2	1.6186e-2	7.8622e-3	3.9327e-3	2.0145e-3
	0.9922	1.0417	0.9994	0.9651	-
2	3.1978e-2	1.6060e-2	7.8012e-3	3.8978e-3	1.9964e-3
	0.9936	1.0417	1.0010	0.9653	-
3	3.1762e-2	1.5937e-2	7.7410e-3	3.8633e-3	1.9785e-3
	0.9950	1.0418	1.0027	0.9654	-
4	3.1549e-2	1.5814e-2	7.6814e-3	3.8293e-3	1.9608e-3
	0.9964	1.0418	1.0043	0.9656	-
5	3.1439e-2	1.5694e-2	7.6225e-3	3.7956e-3	1.9434e-3
	1.0024	1.0419	1.0059	0.9658	-
6	3.1439e-2	1.5575e-2	7.5643e-3	3.7624e-3	1.9261e-3
	1.0134	1.0419	1.0075	0.9660	-

Table 2.6: Maximum pointwise error and associated rate of convergence Example 2.5.1 with $\varepsilon_1 = 10^{-4},\ \varepsilon_2 = \dfrac{\sqrt{\varepsilon_1}}{10}$ for various values of p after using Richardson extrapolation.

p	64	128	256	512	1024
1	7.3463e-3	2.9375e-3	1.0305e-3	3.4196e-4	1.0868e-4
	1.3224	1.5112	1.5915	1.6537	-
2	7.3600e-3	2.9441e-3	1.0330e-3	3.4285e-4	1.0897e-4
	1.3219	1.5110	1.5912	1.6537	-
3	7.3602e-3	2.9442e-3	1.0330e-3	3.4286e-4	1.0897e-4
	1.3219	1.5110	1.5911	1.6537	-
4	7.3602e-3	2.9442e-3	1.0330e-3	3.4286e-4	1.0897e-4
	1.3219	1.5110	1.5911	1.6537	-
5	7.3602e-3	2.9442e-3	1.0330e-3	3.4286e-4	1.0897e-4
	1.3219	1.5110	1.5911	1.6537	-
6	7.3602e-3	2.9442e-3	1.0330e-3	3.4286e-4	1.0897e-4
	1.3219	1.5110	1.5911	1.6537	-

2.6 Conclusions

In this work, we have considered a convection-reaction-diffusion BVP of degenerate type with two perturbations and used standard upwind scheme to find the approximate solution. We have also employed the Richardson extrapolation tool on the solution to obtain higher-order accuracy in the solution. It turns out that the degeneracy does not affect the uniform convergence of the numerical method if we carefully construct the layer-resolving Shishkin mesh based on the characteristics of the degenerate solution.

CHAPTER 3

Richardson extrapolation of the numerical solution to singularly perturbed degenerate parabolic problems with two parameters

This chapter considers a parabolic initial boundary-value problem (IBVP) of convection-reaction-diffusion type with two perturbation parameters. We use a standard upwind scheme on a Shishkin mesh for the space variable and a backward-Euler scheme for the time variable. We employ the Richardson extrapolation method to improve the upwind scheme's convergence order. The resulting scheme is established as a second-order convergent one with parameter-independent stability. Numerical results validate the proposed extrapolation tool's theoretical results and effectiveness.

3.1 Introduction

We study the following parabolic SPP:

$$\begin{cases} \varepsilon_1 \dfrac{\partial^2 u}{\partial x^2} + \varepsilon_2 b(x,t)\dfrac{\partial u}{\partial x} - c(x,t)u(x,t) - \dfrac{\partial u}{\partial t} = f(x,t), \quad (x,t) \in Q, \\ u(0,t) = u_0(t), \quad u(1,t) = u_1(t), \quad 0 \le t \le T, \\ u(x,0) = \phi(x), \quad x \in \overline{\Omega}, \end{cases} \tag{3.1.1}$$

where $\Omega = (0,1), \quad Q = \Omega \times (0,T]$. We denote the differential operator as

$$\mathcal{L}_\varepsilon \zeta = \varepsilon_1 \frac{\partial^2 \zeta}{\partial x^2} + \varepsilon_2 b \frac{\partial \zeta}{\partial x} - c\zeta - \frac{\partial \zeta}{\partial t}$$

for convenience.

The convection coefficient is given as $b(x,t) = x^p a(x,t)$ for some $p \ge 1$ and $a(x,t) \ge \beta > 0$ in Ω. We also assume that the associated coefficient functions as well as the source function are smooth enough. We also consider the following conditions, known as the compatibility conditions, as follows:

$$u_0(0) = \phi(0), \quad u_1(0) = \phi(1), \tag{3.1.2}$$

$$\varepsilon_1 \phi''(0) - c(0,0)\phi(0) = f(0,0), \tag{3.1.3}$$

$$\varepsilon_1 \phi''(1) + \varepsilon_2 a(1,0)\phi'(1) - c(1,0)\phi(1) = f(1,0). \tag{3.1.4}$$

Because of the presence of the perturbation parameters $\varepsilon_1,\ \varepsilon_2$, the exact solution of the IBVP creates boundary layers along both boundaries $x = 0$ and $x = 1$. However, the width of these two layers depend on the following characteristic equation

$$\varepsilon_1 \lambda^2 + \varepsilon_2 b(x,t)\lambda - c(x,t) = 0$$

for each fixed t. The above equation in λ has two roots, say $\lambda_0(x) < 0$ and $\lambda_1(x) > 0$. Then, the width of the layers depends on the constants

$$\mu_0 = \min_{0 \le x \le 1} |\lambda_0(x)|, \quad \mu_1 = \min_{0 \le x \le 1} |\lambda_1(x)|. \tag{3.1.5}$$

Like the previous work in Chapter 2, the width of the associated boundary layers at $x = 0$ and $x = 1$ are respectively $O(1/\mu_0)$ and $O(1/\mu_1)$. Depending on the relations between the

parameters $\varepsilon_1,\ \varepsilon_2$, the boundary layer behaviour changes significantly. Therefore, we need to study those cases separately.

We complete the analysis of the problem into the following two cases:

$$\textbf{Case I:}\quad \varepsilon_2 \leq C\sqrt{\varepsilon_1}, \quad \textbf{Case II:}\quad \varepsilon_2 \geq C\sqrt{\varepsilon_1}.$$

We organize the rest of the chapter as follows. In Section 2, we prove some a priori estimates on the derivatives of the continuous solution and its components. In Section 3, we describe the semidiscrete problem on a uniformly spaced temporal mesh and find the estimates due to the time discretizations. Section 4 discusses about the construction of a suitably designed Shishkin with the help of the constants $\mu_0,\ \mu_1$, and the fully-discrete scheme using classical upwind method. Then, we employ the Richardson extrapolation technique and analyze its effectiveness on the accuracy of the approximated solution. Finally compare the numerical results obtained before and after the application of Richardson extrapolation.

3.2 Properties of the continuous solution

The associated differential operator $(\mathcal{L}_\varepsilon)$ satisfies the following standard comparison principle.

Lemma 3.2.1. Minimum Principle: *If $\omega \in C^{2,1}(\overline{Q})$ such that $\omega(x,t) \geq 0,\ (x,t) \in \partial\overline{Q}$ and $\mathcal{L}_\varepsilon\omega(x,t) \leq 0, \quad (x,t) \in Q$, then $\omega(x,t) \geq 0$ for all $(x,t) \in \overline{Q}$.*

For rigorous analysis of the boundary layer behaviour of the exact solution, we decompose it as follows.

$$u(x,t) = v(x,t) + w_L(x,t) + w_R(x,t),\ \text{in } \overline{Q}. \tag{3.2.1}$$

Here, v is the regular component and $w_L,\ w_R$ are respectively the left and right layers parts of u. These components solve the following equations

$$\begin{cases} \mathcal{L}_\varepsilon v = f(x,t), \quad (x,t) \in Q, \\ v(0,t), v(1,t) \text{ are bounded for } 0 \leq t \leq T, \\ v(x,0) = \phi(x), \quad x \in \overline{\Omega}, \end{cases} \tag{3.2.2}$$

$$\begin{cases} \mathcal{L}_\varepsilon w_R = 0, \quad (x,t) \in Q, \\ w_R(0,t) = 0, \quad w_R(1,t) = u_1 - v(1,t), \text{ for } 0 \le t \le T, \\ w_R(x,0) = 0, \quad x \in \overline{\Omega}, \end{cases} \tag{3.2.3}$$

and

$$\begin{cases} \mathcal{L}_\varepsilon w_L = 0, \quad (x,t) \in Q, \\ w_L(0,t) = u_0 - v(0,t), \quad w_L(1,t) = 0, \text{ for } 0 \le t \le T, \\ w_L(x,0) = 0, \quad x \in \overline{\Omega}. \end{cases} \tag{3.2.4}$$

The smooth and layer parts of the exact solution satisfy the following error bounds.

Lemma 3.2.2. *For $0 \le i + 2j \le 6$, the smooth part v and the singular parts w_L, w_R satisfy the following derivative estimates*

$$\left\| \frac{\partial^{i+j} v}{\partial x^i \partial t^j} \right\|_\infty \le C \left(1 + \varepsilon_1^{(3-i)/2} \right), \tag{3.2.5}$$

$$\left| \frac{\partial^{i+j} w_L}{\partial x^i \partial t^j} \right| \le C \mu_0^i e^{-\mu_0 x}, \tag{3.2.6}$$

$$\left| \frac{\partial^{i+j} w_R}{\partial x^i \partial t^j} \right| \le C \mu_1^i e^{-\mu_1 (1-x)}, \tag{3.2.7}$$

for all $(x,t) \in \overline{Q}$.

Proof. The proof can be done by fixing t and following the same approach for the estimates proved in Lemma 2.2.2 and Lemma 2.2.3 in Chapter 2. □

We denote the spatial operator $\mathcal{L}_{x,\varepsilon}$ in (3.1.1) at $t = t_{n+1}$ as

$$\mathcal{L}_{x,\varepsilon} u^{n+1}(x) := \varepsilon_1 \frac{d^2}{dx^2} u^{n+1}(x) + \varepsilon_2 b(x, t_{n+1}) \frac{d}{dx} u^{n+1}(x) - c(x, t_{n+1}) u^{n+1}(x),$$

and the corresponding discrete operator as

$$L^N_{x,\varepsilon} Z_i = \varepsilon_1 \delta^2 Z_i + \varepsilon_2 b(x_i, t_n)\ \delta^+ Z_i - c(x_i, t_n) Z_i, \tag{3.2.8}$$

for each fixed t_n.

We define the semidiscrete problem corresponding to the IBVP (3.1.1) as follows: For every $0 \leq n \leq M-1$, find $u^{n+1}(x)$ such that $u^0 = \phi(x)$ and

$$\begin{cases} \Big[-I + \Delta t \mathcal{L}_{x,\varepsilon} \Big] u^{n+1}(x) = -u^n(x) + \Delta t f(x, t_{n+1}), \quad x \in \Omega, \\ u^{n+1}(0) = u_0(t_{n+1}), \quad u^{n+1}(1) = u_1(t_{n+1}). \end{cases} \tag{3.2.9}$$

Theorem 3.2.3. *Let u be the exact solution of the problem (3.1.1). Suppose that for $0 \leq i \leq 2$, $\left| \dfrac{\partial^i u}{\partial t^i}(x,t) \right| \leq C, \quad \forall (x,t) \in \overline{Q}$. Then, the local error due to time discretization satisfies*

$$\|u(t_n) - \widehat{u}^n\|_{\infty,\overline{\Omega}} \leq C\Delta t^2, \quad \forall\ n = 1, \ldots, M, \tag{3.2.10}$$

and the global error satisfies

$$\sup_{n\Delta t \leq T} \|u(t_n) - u^n\|_{\infty,\overline{\Omega}} \leq C\Delta t, \tag{3.2.11}$$

where $\widehat{u}^n$ satisfies

$$\begin{cases} \Big[-I + \Delta t \mathcal{L}_{x,\varepsilon} \Big] \widehat{u}^{n+1}(x) = -u(t_n) + \Delta t f(x, t_{n+1}), \quad x \in \Omega, \\ \widehat{u}^{n+1}(0) = u_0(t_{n+1}), \quad \widehat{u}^{n+1}(1) = u_1(t_{n+1}), \end{cases} \tag{3.2.12}$$

for every $n = 0, 1, \ldots, M-1$.

Proof. The proof of this theorem is available in [59]. □

3.3 Numerical approximations

The domain of the time variable is discretized as

$$\overline{\Omega}_t^M := \big\{ t_k : t_k = k\Delta t, \quad k = 0, 1, \ldots, M, \quad \Delta t = T/M \big\},$$

where we consider only the uniform time step-length Δt. Suppose the roots of the characteristic equation $\varepsilon_1 \lambda^2 + \varepsilon_2 b - c = 0$ are given by $\lambda_0(x) < 0$ and $\lambda_1(x) > 0$. In order to generate the layer resolving Shishkin mesh, we use the transition parameters defined in the following

way

$$\tau_0 = \min\left\{\frac{1}{4}, \frac{2}{\mu_0}\ln N\right\}, \quad \tau_1 = \min\left\{\frac{1}{4}, \frac{2}{\mu_1}\ln N\right\}, \tag{3.3.1}$$

where

$$\mu_0 = \sqrt{\frac{\beta}{\varepsilon_1}}, \quad \mu_1 = \frac{-\varepsilon_1 A + \sqrt{\varepsilon_1^2 A^2 + 4\varepsilon_1\beta}}{2\varepsilon_1}, \tag{3.3.2}$$

with $A = \left\|\widehat{b}\right\|_\infty$, $c(x) \geq \beta$.

For spatial discretization, we use the similar Shishkin grid $\overline{\Omega}^N$ with $(N+1)$ mesh points designed as in Section 3.1, with the same transition points $\tau_0,\ \tau_1$ in (3.3.1) and the constants $\mu_0,\ \mu_1$ defined by

$$\mu_0 = -\max_{0\leq x\leq 1}\lambda_0(x), \quad \mu_1 = \min_{0\leq x\leq 1}\lambda_1(x). \tag{3.3.3}$$

We define the fully-discrete problem as follows:

The fully-discrete approximation U that solves following problem

$$\begin{cases} L_\varepsilon^N U_i^{n+1} = f(x_i, t_{n+1}), \quad 1 \leq i \leq N-1, \\ U_0^{n+1} = u_0(t_{n+1}), \quad U_N^{n+1} = u_1(t_{n+1}), \\ U_i^0 = \phi(x_i),\ x_i \in \overline{\Omega}^N, \end{cases} \tag{3.3.4}$$

for every $n = 0, 1, \ldots, M-1$, where the fully-discrete operator L_ε^N is defined by

$$L_\varepsilon^N Z_i^n = \varepsilon_1\delta^2 Z_i^n + \varepsilon_2 b(x_i, t_n)\ \delta^+ Z_i^n - c(x_i, t_n)Z_i^n - \delta_t^- Z_i^n. \tag{3.3.5}$$

Let us denote the fully-discrete solution obtained by solving the problem (3.3.4) on the mesh $D^{N,M} := \overline{\Omega}^N \times \overline{\Omega}_t^M$ by $U^{N,M}$. With this notation, we state the results related to the truncation errors associated with the above fully-discrete problem.

Let us decompose $U^{N,M}$ as

$$U^{N,M} = V^{N,M} + W_r^{N,M} + W_l^{N,M},$$

where $V^{N,M}$, $W_r^{N,M}$ and $W_l^{N,M}$ respectively denote the smooth part, right singular part, and the left singular part of $U^{N,M}$.

The discrete operator satisfies the following discrete minimum principle.

Lemma 3.3.1. (Discrete minimum principle) *Suppose, the mesh function Z satisfies $Z \geq 0$ on $\partial D^{N,M}$ and $L_\varepsilon^N Z \leq 0$ for every $(x_i, t_n) \in Q \cap D^{N,M}$. Then, we have*

$$Z \geq 0 \quad \text{for all} \quad (x_i, t_n) \in D^{N,M}. \tag{3.3.6}$$

The standard upwind scheme for the present model problem has the following convergence properties:

Theorem 3.3.2. *Suppose, $U^{N,M}$ be the fully-discrete approximation of the exact solution $u(x,t)$ on $D^{N,M}$, and $\varepsilon_1 \leq CN^{-1}$, then we have following error estimate:*

$$\left\| U^{N,M} - u \right\|_{\infty, D^{N,M}} \leq C \left(N^{-1} (\ln N)^2 + \Delta t \right). \tag{3.3.7}$$

Proof. The semidiscrete problem (3.2.12) can be rewritten as

$$\begin{aligned} \varepsilon_1 \frac{d^2}{dx^2} \widehat{u}^{n+1}(x) + \varepsilon_2 b(x, t_{n+1}) \frac{d}{dx} \widehat{u}^{n+1}(x) - \left(\frac{1}{\Delta t} + c(x, t_{n+1}) \right) \widehat{u}^{n+1}(x) \\ = -\frac{1}{\Delta t} \widehat{u}^n(x) + f(x, t_{n+1}), \quad x \in \Omega. \end{aligned} \tag{3.3.8}$$

The above problem in x is a two-parameter BVP and is similar to the model problem studied in O'Riordan *et al.* [65]. Therefore, for every $t = t_n$, the following error equation holds good:

$$\left| \widehat{U}^n(x_i) - \widehat{u}(x_i, t_n) \right| \leq C \; N^{-1} (\ln N)^2, \quad \forall x_i \in \Omega^N, \tag{3.3.9}$$

where $\widehat{U}^n$ satisfies the discrete form of (3.2.12).

We first observe the error equation in the form

$$U^n - u(t_n)|_{\overline{\Omega}^N} = \left(U^n - \widehat{U}^n \right) + \left(\widehat{U}^n - \widehat{u}^n|_{\overline{\Omega}^N} \right) + \left(\widehat{u}^n|_{\overline{\Omega}^N} - u(t_n)|_{\overline{\Omega}^N} \right), \tag{3.3.10}$$

where $\widehat{U}^n$ is the solution of the discrete form of the problem (3.2.12).

We recall the results from Theorem 3.2.3 to obtain

$$\left\| \widehat{u}^n|_{\overline{\Omega}^N} - u(t_n)|_{\overline{\Omega}^N} \right\|_{\infty, \overline{\Omega}^N} \leq C \Delta t^2, \quad \left\| \widehat{U}^n - \widehat{u}^n|_{\overline{\Omega}^N} \right\|_{\infty, \overline{\Omega}^N} \leq C \Delta t N^{-1} (\ln N)^2.$$

Using these estimates and discrete minimum principle $\left\|\left(-I+\Delta t L^N_{x,\varepsilon}\right)^{-1}\right\| \leq C$, we have

$$\begin{aligned}\left\|U^n - u(t_n)|_{\overline{\Omega}^N}\right\|_{\infty,\overline{\Omega}^N} &\leq C\Delta t\big(\Delta t + N^{-1}(\ln N)^2\big) + C\left\|U^{n-1} - u(t_{n-1})|_{\overline{\Omega}^N}\right\|_{\infty,\overline{\Omega}^N}\\ &\leq Cn\Delta t\big(\Delta t + N^{-1}(\ln N)^2\big) \leq C\big(\Delta t + N^{-1}(\ln N)^2\big),\end{aligned}$$

since $n\Delta t \leq T$. □

Suppose, $U^{N,M}$ be the fully-discrete approximation of the exact solution $u(x,t)$ on the discrete mesh $D^{N,M} := \overline{\Omega}^N \times \overline{\Omega}^M_t$. From Theorem 3.3.2, we have

$$\begin{aligned}\left(U^{N,M} - u\right)(x_i,t_n) &= C\left(N^{-1}\ln N + \Delta t\right) + R^{N,M}(x_i,t_n),\\ &= C\left(N^{-1}\Big(\frac{\mu_0\tau_0}{2}\Big) + \Delta t\right) + R^{N,M}(x_i,t_n),\end{aligned} \tag{3.3.11}$$

for all $(x_i,t_n) \in D^{N,M}$, where $R^{N,M}(x_i,t_n) = O\left(N^{-2}(\ln N)^2 + \Delta t^2\right)$.

Now, let us fix the transition parameters $\tau_0,\ \tau_1$ in the Shishkin mesh $\overline{\Omega}^N$ and refine it by creating new grid points $\widetilde{x}_i = \dfrac{x_{i-1}+x_i}{2}$ in each element $[x_{i-1},x_i]$. We also bisect every mesh interval in time direction and create new grid points $\widetilde{t}_j = \dfrac{t_{j-1}+t_j}{2}$ in every element $[t_{j-1},t_j]$. Thus, the refinement of the original mesh can be described as

$$D^{2N,2M} := \widetilde{\Omega}^{2N} \times \widetilde{\Omega}^{2M}_t, \tag{3.3.12}$$

where $\widetilde{\Omega}^{2N} := \overline{\Omega}^N \cup \{\widetilde{x}_i : 1 \leq i \leq N\}$, and $\widetilde{\Omega}^{2M}_t := \overline{\Omega}^M_t \cup \{\widetilde{t}_j : 1 \leq j \leq M\}$.

Suppose, $\widehat{U}^{2N,2M}$ be the approximate solution on $D^{2N,2M}$ with the same transition points $x_i = \tau_0$ and $x_i = 1-\tau_1$ in space. Then, from Equation (3.3.11), we have

$$\left(\widetilde{U}^{2N,2M} - u\right)(x_i,t_n) = C\left((2N)^{-1}\Big(\frac{\mu_0\tau_0}{2}\Big) + \frac{\Delta t}{2}\right) + \widetilde{R}^{2N,2M}(x_i,t_n), \tag{3.3.13}$$

where $\widetilde{R}^{2N,2M}(x_i,t_n) = O\left(N^{-2}(\ln N)^2 + \Delta t^2\right)$.

From Equations (3.3.11) and (3.3.13), we get

$$\begin{aligned}\left(2\widetilde{U}^{2N,2M} - U^{N,M}\right)(x_i,t_n) - u(x_i,t_n) &= (2\widetilde{R}^{2N,2M} - R^{N,M}(x_i,t_n))(x_i,t_n),\\ &= O\left(N^{-2}(\ln N)^2 + \Delta t^2\right).\end{aligned} \tag{3.3.14}$$

Thus, we have a new approximation formula with a higher accuracy given as follows:

$$\widehat{U}^{N,M}(x_i,t_n)=\left(2\widetilde{U}^{2N,2M}-U^{N,M}\right)(x_i,t_n),\quad \text{for } (x_i,t_n)\in G^{N,M}. \tag{3.3.15}$$

3.4 Convergence analysis

3.4.1 Error estimates in the regular component

We deduce the following truncation error bounds for the smooth part of the numerical solution on the mesh $D^{N,M}$.

Lemma 3.4.1. *The truncation error corresponding to the smooth component can be expressed as*

$$L_\varepsilon^{N,M}\left(V^{N,M}-v\right)(x_i,t_{n+1})=-h_{i+1}\chi_1(x_i,t_{n+1})-\Delta t\chi_2(x_i,t_{n+1})+O(H^2+\Delta t^2), \tag{3.4.1}$$

where

$$\chi_1(x,t)=\frac{\varepsilon_2 h_{i+1}}{2}b(x,t)\frac{\partial^2 v}{\partial x^2}(x,t),\quad \chi_2(x,t)=\frac{1}{2}\frac{\partial^2 v}{\partial t^2}(x,t).$$

Proof. From straightforward Taylor series expansion about the point (x_i,t_{n+1}), we obtain

$$\begin{aligned}L_\varepsilon^{N,M}\left(V^{N,M}-v\right)(x_i,t_{n+1})=&-\frac{\varepsilon_1}{3(h_i+h_{i+1})}\left[h_{i+1}^2\frac{\partial^3 v}{\partial x^3}(\kappa_1,t_{n+1})-h_i^2\frac{\partial^3 v}{\partial x^3}(\kappa_2,t_{n+1})\right]\\&-\frac{\varepsilon_2 h_{i+1}}{2}b(x_i,t_{n+1})\frac{\partial^2 v}{\partial x^2}(x_i,t_{n+1})-\frac{\varepsilon_2 h_{i+1}^2}{3!}b(x_i,t_{n+1})\frac{\partial^3 v}{\partial x^3}(\kappa_3,t_{n+1})\\&-\frac{\Delta t}{2}\frac{\partial^2 v}{\partial t^2}(x_i,t_{n+1})+\frac{\Delta t^2}{3!}\frac{\partial^3 v}{\partial t^3}(x_i,\nu_0),\end{aligned}$$

where $x_i<\kappa_1,\kappa_3<x_{i+1}\quad x_{i-1}<\kappa_2<x_i$, and $t_n<\nu_0<t_{n+1}$. Now applying the bounds for the derivatives of the smooth part v, the result follows. □

Now following the approach by Natividad and Stynes [5], we define the following auxiliary problems for $k=1,2$:

$$\begin{cases}\mathcal{L}_\varepsilon F_k(x,t)=\chi_k(x,t), & (x,t)\in Q,\\ F_k(x,0)=0, & x\in\overline{\Omega},\\ F_k(0,t)=F_k(1,t)=0,\forall t.\end{cases} \tag{3.4.2}$$

We also decompose each F_k as $F_k = \xi_k + \eta_k + \zeta_k$ such that the smooth part satisfies

$$\begin{cases} \mathcal{L}_\varepsilon \xi_k = \chi_k, \quad (x,t) \in Q, \\ |\xi_k(0,t)| \le C, \quad |\xi_k(1,t)| \le C, \end{cases} \tag{3.4.3}$$

and the layer parts satisfy

$$\begin{cases} \mathcal{L}_\varepsilon \eta_k = 0, \quad (x,t) \in Q, \\ \eta_k(0,t) = -\xi_k(0,t), \quad \eta_k(1,t) = 0, \end{cases} \qquad \begin{cases} \mathcal{L}_\varepsilon \zeta_k = 0, \quad (x,t) \in Q, \\ \zeta_k(0,t) = 0, \quad \zeta_k(1,t) = -\xi_k(1,t), \end{cases} \tag{3.4.4}$$

with ξ_k, η_k, ζ_k all vanishes at $t = 0$.

Lemma 3.4.2. *The smooth part $V^{N,M}$ of the approximate solution satisfies*

$$\begin{aligned} \left(V^{N,M} - v\right)(x_i, t_{n+1}) &= -(h_{i+1}\xi_1 + \Delta t \xi_2)(x_i, t_{n+1}) \\ &\quad + O(N^{-2} + \Delta t^2), \ 1 \le i \le N-1, \ 1 \le n \le M. \end{aligned} \tag{3.4.5}$$

Proof. We have from Lemma 3.4.1,

$$L_\varepsilon^{N,M}\left(V^{N,M} - v\right)(x_i, t_{n+1}) = -h_{i+1}\mathcal{L}_\varepsilon \xi_1(x_i, t_{n+1}) - \Delta t \mathcal{L}_\varepsilon \xi_2(x_i, t_{n+1}) + O(H^2 + \Delta t^2).$$

We can also show that

$$\begin{aligned} \left|\left(\mathcal{L}_\varepsilon - L_\varepsilon^{N,M}\right)\xi_k(x_i, t_{n+1})\right| &\le C\left[\varepsilon_1(h_i + h_{i+1})\left\|\frac{\partial^3 \xi_k}{\partial x^3}\right\|_\infty + \frac{\varepsilon_2 b(x_i, t_{n+1}) h_i}{2}\left\|\frac{\partial^2 \xi_k}{\partial x^2}\right\|_\infty\right] \\ &\quad + C\,\frac{\Delta t}{2}\left\|\frac{\partial^2 \xi_k}{\partial t^2}\right\|_\infty. \end{aligned}$$

Thus, we find

$$\left|h_{i+1}\left(\mathcal{L}_\varepsilon - L_\varepsilon^{N,M}\right)\xi_1(x_i, t_{n+1}) + \Delta t\left(\mathcal{L}_\varepsilon - L_\varepsilon^{N,M}\right)\xi_2(x_i, t_{n+1})\right| \le C(H^2 + \Delta t^2).$$

Therefore,

$$L_\varepsilon^{N,M}\left(V^{N,M} - v + h_{i+1}\xi_1 + \Delta t \xi_2\right)(x_i, t_{n+1}) \le C(H^2 + \Delta t^2).$$

Finally, using the barrier function

$$\Lambda(x_i, t_n) = C_1(N^{-2} + \Delta t^2)(1 - x_i)$$

for $1 \leq i \leq N-1, 1 \leq n \leq M-1$ with $\Lambda = 0$ on $\partial D^{N,M}$, we prove the required estimate. □

Theorem 3.4.3. *If $\widetilde{V}^{2N,2M}$ be the smooth component of the numerical solution on the discrete mesh $D^{2N,2M}$ and v is the smooth part of the continuous solution u, then*

$$\left|\left(2\widetilde{V}^{2N,2M} - V^{N,M} - v\right)(x_i, t_n)\right| \leq C\left(N^{-2} + \Delta t^2\right), \tag{3.4.6}$$

for all $(x_i, t_n) \in D^{N,M}$.

Proof. From Lemma 3.4.2, we derive the following

$$\left(\widetilde{V}^{2N,2M} - v\right)(x_i, t_{n+1}) = -\frac{1}{2}(h_{i+1}\xi_1 + \Delta t\xi_2)(x_i, t_{n+1}) + O(N^{-2} + \Delta t^2),$$
$$1 \leq i \leq N-1,\ 1 \leq n \leq M. \tag{3.4.7}$$

From (3.4.5) and (3.4.7), we get

$$\left(2\widetilde{V}^{2N,2M} - V^{N,M} - v\right)(x_i, t_{n+1}) = O(N^{-2} + \Delta t^2),\ 1 \leq i \leq N-1,\ 1 \leq n \leq M. \tag{3.4.8}$$

Hence the proof. □

3.4.2 Error estimates in the singular components

We present the bound for the error after extrapolation in the singular component $W_l^{N,M}$, while similar proof follows for the other singular part also.

Lemma 3.4.4. *For $x_i \in [\tau_0, 1]$, the following error equation holds*

$$\left|(W_l^{N,M} - w_L)(x_i, t_n)\right| \leq CN^{-2}, \tag{3.4.9}$$

for every $1 \leq n \leq M$.

Proof. The proof follows exactly in a similar way in Lemma 2.4.6 in Chapter 2 following the fact that for each t_n,

$$\left|W_l^{N,M}(x_i, t_n)\right| \leq C\prod_{j=1}^{i}(1 + \mu_0 h_i)^{-1}.$$

We prove that both $W_l^{N,M}$, w_L have an upper bound $O(N^{-2})$ and the remaining part of the proof are same. □

Theorem 3.4.5. *For $x_i \in [\tau_0, 1]$, the left singular component of the extrapolated solution satisfies*

$$\left|\left(2\widetilde{W}_l^{2N,2M} - W_l^{N,M} - w_L\right)(x_i, t_n)\right| \leq CN^{-2}. \tag{3.4.10}$$

Proof. Using Lemma 3.4.4, we also have

$$\left|(\widetilde{W}_l^{2N,2M} - w_L)(x_i, t_n)\right| \leq CN^{-2}, \tag{3.4.11}$$

and combining it with (3.4.9), we get

$$\left|2(\widetilde{W}_l^{2N,2M} - w_L)(x_i, t_n) - (W_l^{N,M} - w_L)(x_i, t_n)\right| \leq CN^{-2}.$$

This is the desired result. □

Now we consider the case when $0 < x_i < \tau_0$. We prove the estimate with the help of the following lemmas.

Lemma 3.4.6. *For $0 < x_i < \tau_0$, the following error estimates hold:*

$$\begin{aligned} L_\varepsilon^{N,M}\left(W_l^{N,M} - w_L\right)(x_i, t_{n+1}) = &-(N^{-1}\ln N\ \mathcal{L}_\varepsilon F_1 + \Delta t\ \mathcal{L}_\varepsilon F_2)(x_i, t_{n+1}) \\ &+ O(N^{-2}(\ln N)^2 e^{-\mu_0 x_i} + \Delta t^2 e^{-\mu_0 x_i}), \end{aligned} \tag{3.4.12}$$

where $\mathcal{L}_\varepsilon F_1 = \dfrac{4\varepsilon_2}{\mu_0} b(x,t)\dfrac{\partial^2 w_L}{\partial x^2}$, *and* $\mathcal{L}_\varepsilon F_2 = \dfrac{1}{2}\dfrac{\partial^2 w_L}{\partial t^2}$.

Proof. We obtain from Taylor series formula the following:

$$\begin{aligned} L_\varepsilon^{N,M}\left(W_l^{N,M} - w_L\right)(x_i, t_{n+1}) = &-\frac{\varepsilon_1 h_i^2}{4!}\left[\frac{\partial^4 w_L}{\partial x^4}(\kappa_1, t_{n+1}) + \frac{\partial^4 w_L}{\partial x^4}(\kappa_2, t_{n+1})\right] \\ &- \frac{\varepsilon_2 h_{i+1}}{2} b(x_i, t_{n+1})\frac{\partial^2 w_L}{\partial x^2}(x_i, t_{n+1}) - \frac{\varepsilon_2 h_{i+1}^2}{3!} b(x_i, t_{n+1})\frac{\partial^3 w_L}{\partial x^3}(\kappa_3, t_{n+1}) \\ &- \frac{\Delta t}{2}\frac{\partial^2 w_L}{\partial t^2}(x_i, t_{n+1}) + \frac{\Delta t^2}{3!}\frac{\partial^3 w_L}{\partial t^3}(x_i, \nu_0), \end{aligned}$$

where $x_i < \kappa_1, \kappa_3 < x_{i+1}$ $x_{i-1} < \kappa_2 < x_i$, and $t_n < \nu_0 < t_{n+1}$. Thus, we rewrite the

truncation error as

$$\begin{aligned}
&L_\varepsilon^{N,M}\left(W_l^{N,M}-w_L\right)(x_i,t_{n+1})\\
&=-(N^{-1}\ln N\ \mathcal{L}_\varepsilon F_1+\Delta t\ \mathcal{L}_\varepsilon F_2)(x_i,t_{n+1})+O(\varepsilon_1 h_i^2\mu_0^4 e^{-\mu_0 x_i}+\Delta t^2 e^{-\mu_0 x_i}),\\
&=-(N^{-1}\ln N\ \mathcal{L}_\varepsilon F_1+\Delta t\ \mathcal{L}_\varepsilon F_2)(x_i,t_{n+1})+O(N^{-2}(\ln N)^2 e^{-\mu_0 x_i}+\Delta t^2 e^{-\mu_0 x_i}).
\end{aligned}$$

This completes the proof. □

Lemma 3.4.7. *For $0<x_i<\tau_0$, the singular layer part $W_l^{N,M}$ satisfies the following error equation:*

$$\begin{aligned}
\left(W_l^{N,M}-w_L\right)(x_i,t_{n+1})=&-(N^{-1}\ln N\ F_1+\Delta t\ F_2)(x_i,t_{n+1})\\
&+O(N^{-2}(\ln N)^2+\Delta t^2),
\end{aligned}\tag{3.4.13}$$

where F_1, F_2 are defined in the previous lemma.

Proof. We first recall the result that for each $k=1,2$, the function F_k satisfies

$$\left|\frac{\partial^{i+j}F_k}{\partial x^i\partial t^j}\right|\le C\mu_0^i e^{-\mu_0 x},\ \text{for}\ (x,t)\in\overline{Q},\tag{3.4.14}$$

for $0\le i+2j\le 6$. Using this, we can easily verify that

$$\begin{aligned}
\left|\left(\mathcal{L}_\varepsilon-L_\varepsilon^{N,M}\right)F_1(x_i,t_{n+1})\right|&\le C\left[\varepsilon_1 h_i\left\|\frac{\partial^3 F_k}{\partial x^3}\right\|_\infty+\Delta t e^{-\mu_0 x_i}\right]\\
&\le C\left[\varepsilon_1\mu_0^3 h_i e^{-\mu_0 x}+\Delta t e^{-\mu_0 x_i}\right]\\
&\le C\left[(N^{-1}\ln N+\Delta t)e^{-\mu_0 x_i}\right],
\end{aligned}\tag{3.4.15}$$

since $\varepsilon_1\mu_0^2\le C$ and $h_i=O(N^{-1}\mu_0^{-1}\ln N)$.

Similarly,

$$\left|\left(\mathcal{L}_\varepsilon-L_\varepsilon^{N,M}\right)F_2(x_i,t_{n+1})\right|\le C\Delta t)e^{-\mu_0 x_i}.\tag{3.4.16}$$

Using the last two equations, it follows that

$$\begin{aligned}
L_\varepsilon^{N,M}\left(W_l^{N,M}-w_L\right)(x_i,t_{n+1})=&-(N^{-1}\ln N\ L_\varepsilon^{N,M}F_1+\Delta t\ \ L_\varepsilon^{N,M}F_2)(x_i,t_{n+1})\\
&+O(N^{-2}(\ln N)^2 e^{-\mu_0 x_i}+\Delta t^2 e^{-\mu_0 x_i}),
\end{aligned}\tag{3.4.17}$$

which gives

$$L_{\varepsilon}^{N,M}\left(W_l^{N,M}-w_L+(N^{-1}\ln N)F_1+\Delta tF_2\right)(x_i,t_{n+1})=O(N^{-2}(\ln N)^2e^{-\mu_0x_i}+\Delta t^2e^{-\mu_0x_i}). \tag{3.4.18}$$

Let us now define the barrier function

$$Z_i=C_1(1-x_i)N^{-2}+(N^{-2}(\ln N)^2+\Delta t^2)\prod_{j=1}^{i}(1+\mu_0h_j)^{-1} \tag{3.4.19}$$

and using the fact that $e^{-\mu_0x_i}\leq C\prod_{j=1}^{i}(1+\mu_0h_j)^{-1}$, we prove the required estimate. □

We now present the error estimate after the extrapolation in the singular layer part.

Theorem 3.4.8. *For* $0<x_i<\tau_0$,

$$\left|\left(2\widetilde{W}_l^{2N,2M}-W_l^{N,M}-w_L\right)(x_i,t_n)\right|\leq C\left(N^{-2}(\ln N)^2+\Delta t^2\right), \tag{3.4.20}$$

for each $1\leq n\leq M$.

Proof. From the last lemma, we can write

$$\left(W_l^{N,M}-w_L+(N^{-1}\frac{\mu_0\tau_0}{2})F_1+\Delta tF_2\right)(x_i,t_{n+1})=O(N^{-2}(\ln N)^2+\Delta t^2). \tag{3.4.21}$$

Similarly for the extrapolated solution, we have

$$\left(\widetilde{W}_l^{N,M}-w_L+(2N)^{-1}(\frac{\mu_0\tau_0}{2})F_1+\frac{\Delta t}{2}F_2\right)(x_i,t_{n+1})=O(N^{-2}(\ln N)^2+\Delta t^2). \tag{3.4.22}$$

From the last two equations, we get

$$\left[2\left(\widetilde{W}_l^{N,M}-w_L\right)-\left(W_l^{N,M}-w_L\right)\right](x_i,t_n)=O(N^{-2}(\ln N)^2+\Delta t^2).$$

Hence the proof. □

Combining Theorem 3.4.5 and Theorem 3.4.8, we finally present the following theorem.

Theorem 3.4.9. *If* $\widetilde{W}_l^{2N,2M}$ *be the left singular component of the numerical solution on the discrete mesh* $D^{2N,2M}$ *and* w_L *is the left singular part of the continuous solution* u*, then we get*

$$\left|\left(2\widetilde{W}_l^{2N,2M}-W_l^{N,M}-w_L\right)(x_i,t_n)\right|\leq C\left(N^{-2}(\ln N)^2+\Delta t^2\right), \tag{3.4.23}$$

for all $(x_i, t_n) \in D^{N,M}$.

We also prove the following error estimate after the extrapolation of the singular component $W_r^{N,M}$ in a very similar way.

Theorem 3.4.10. *If* $\widetilde{W}_r^{2N,2M}$ *be the right singular component of the numerical solution on the discrete mesh* $D^{2N,2M}$ *and* w_R *is the right singular part of the continuous solution* u*, then we have*

$$\left|\left(2\widetilde{W}_r^{2N,2M} - W_r^{N,M} - w_R\right)(x_i, t_n)\right| \leq C\left(N^{-2}(\ln N)^2 + \Delta t^2\right), \tag{3.4.24}$$

for all $(x_i, t_n) \in D^{N,M}$.

3.4.3 Error estimate for the extrapolated solution

Combining all the error estimates proved in Theorem 3.4.3, Theorem 3.4.8 and Theorem 3.4.10, the following global convergence result follows.

Theorem 3.4.11. (Main convergence result) *If* $\varepsilon_1 \leq CN^{-1}$*, then the fully-discrete solution* $\widehat{U}^{2N,2M}$ *on the discrete mesh* $D^{N,M}$ *satisfies the following global convergence result:*

$$\left|\left(\widehat{U}^{2N,2M} - u\right)(x_i, t_n)\right| \leq C\left(N^{-2}(\ln N)^2 + \Delta t^2\right), \tag{3.4.25}$$

for all $(x_i, t_n) \in D^{N,M}$.

3.5 Numerical experiments

Example 3.5.1. *For verification of the theoretical bounds, we have proved in the previous section, we consider the following example.*

$$\begin{cases} u_t - \varepsilon_1 u_{xx} - \varepsilon_2(1+x^2)x^3 u_x + u = -16x^2(1-x)^2, \quad (x,t) \in (0,1)\times(0,1], \\ u(0,t) = 0, \quad u(1,t) = 0, \ t \in (0,1], \\ u(x,0) = 0, \quad 0 \leq x \leq 1. \end{cases} \tag{3.5.1}$$

If the exact solution are known to use, we use the following error formula

$$E_{\varepsilon_1,\varepsilon_2}^{N,M} = \max_{(x_i,t_n)\in D^{N,M}} \left|U_{\varepsilon_1,\varepsilon_2}^{N,M}(x_i,t_n) - u(x_i,t_n)\right|. \tag{3.5.2}$$

In this case, the exact solution of the above parabolic IBVP is unknown, hence we use double mesh formula to compute the error. In order to calculate the pointwise maximum error, we define

$$E^{N,M}_{\varepsilon_1,\varepsilon_2} = \max_{(x_i,t_n)\in D^{N,M}} \left| U^{N,M}_{\varepsilon_1,\varepsilon_2}(x_i,t_n) - \widetilde{U}^{2N,2M}_{\varepsilon_1,\varepsilon_2}(x_i,t_n) \right|. \tag{3.5.3}$$

The associated order of convergence can be defined as,

$$p^{N,M}_{\varepsilon_1,\varepsilon_2} = \log_2 \left(\frac{E^{N,M}_{\varepsilon_1,\varepsilon_2}}{E^{2N,2M}_{\varepsilon_1,\varepsilon_2}} \right). \tag{3.5.4}$$

The parameter-independent error and rate of convergence are defined by

$$E^{N,M} = \max_{\varepsilon_1,\varepsilon_2} E^{N,M}_{\varepsilon_1,\varepsilon_2}, \quad p^{N,M} = \log_2 \left(\frac{E^{N,M}}{E^{2N,2M}} \right). \tag{3.5.5}$$

We can use similar formulas to calculate the extrapolation error also. In that case, the error formula is given by

$$E^{N,M}_{\varepsilon_1,\varepsilon_2} = \max_{(x_i,t_n)\in D^{N,M}} \left| \widehat{U}^{N,M}_{\varepsilon_1,\varepsilon_2}(x_i,t_n) - u(x_i,t_n) \right|. \tag{3.5.6}$$

Here, we consider the various values of the parameters satisfying the conditions for Case I and Case II separately and obtain the results as follows.

We solve Example 3.5.1 by using the classical upwind numerical method for spatial derivatives and implicit-Euler method for the time derivative on the Shihskin mesh $D^{N,M}$. We calculate the error in discrete maximum norm for the example and present them in Table 3.1 and Table 3.2 for both cases. The associated order of convergence are also given in each case for various values of the perturbation parameters. The loglog plots presented in Figure 3.1 and Figure 3.3 reveals the almost first-order accuracy of the error. Then, we apply the Richardson extrapolation technique for the same example and obtain significantly improved results. From Table 2.4 and Table 3.3, it appears that after extrapolation, the convergence of the scheme is not affected and the magnitude of the error has reduced nicely. It is easily noticeable that the rate of convergence is almost doubled after the extrapolation and the same can be visualized from the loglog plots in Figure 3.2 and Figure 3.4. Therefore, this ensures that the accuracy of the numerical scheme has been improved from $O\left(N^{-1}\ln N + \Delta t\right)$ to $(N^{-2}(\ln N)^2 + \Delta t^2)$ after application of the extrapolation formula.

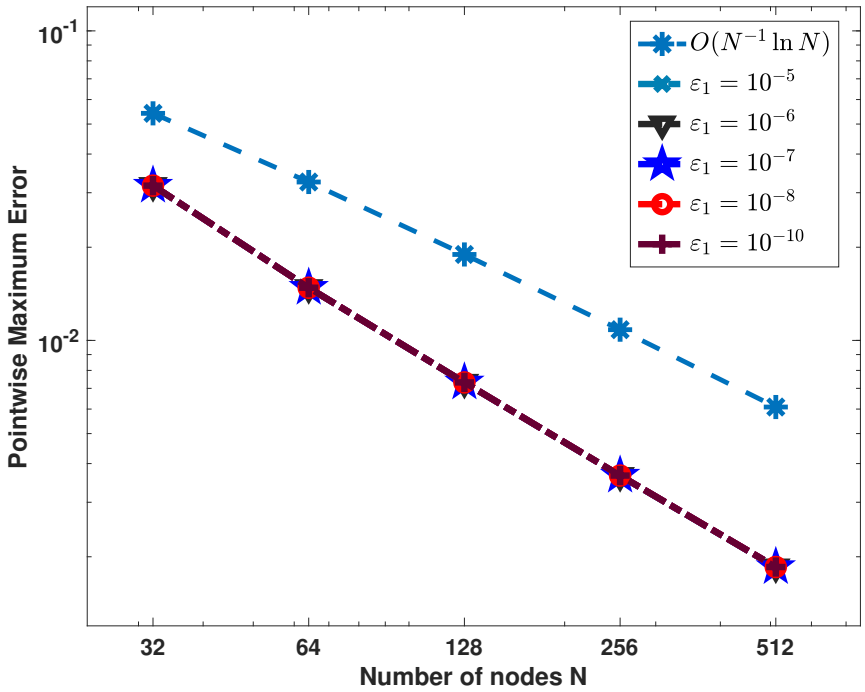

Figure 3.1: Visualization of pointwise maximum error obtained before Richardson extrapolation for Case I.

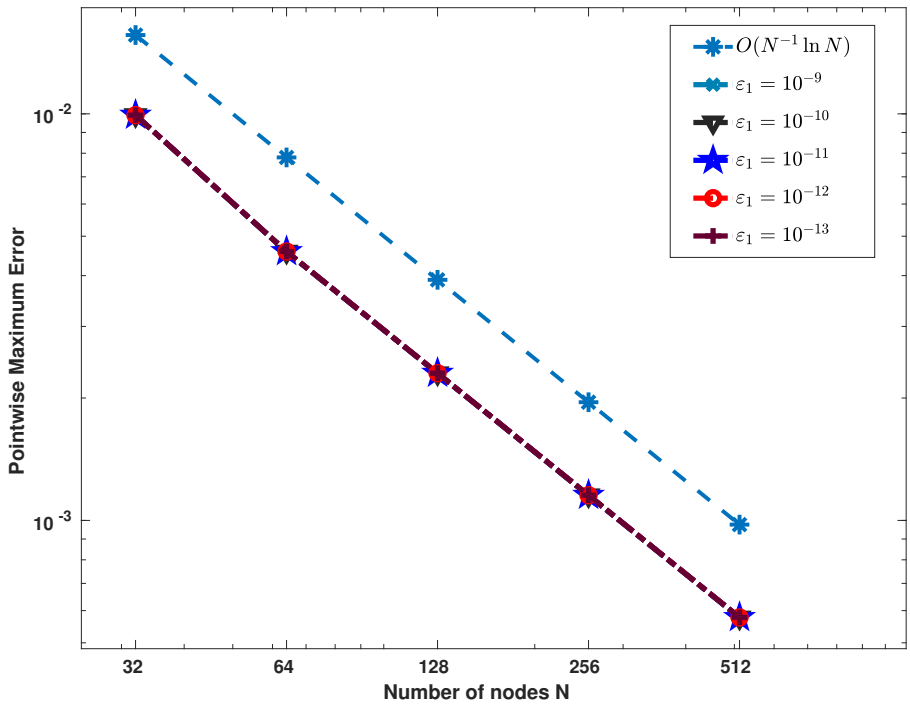

Figure 3.2: Visualization of pointwise maximum error obtained before Richardson extrapolation for Case II.

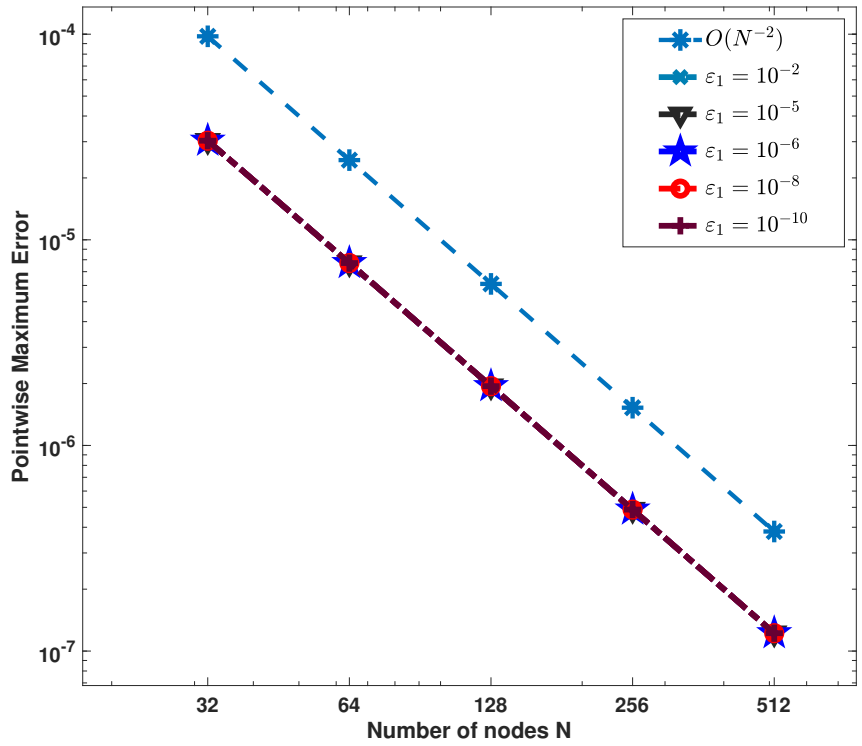

Figure 3.3: Visualization of pointwise maximum error obtained after Richardson extrapolation for Case I.

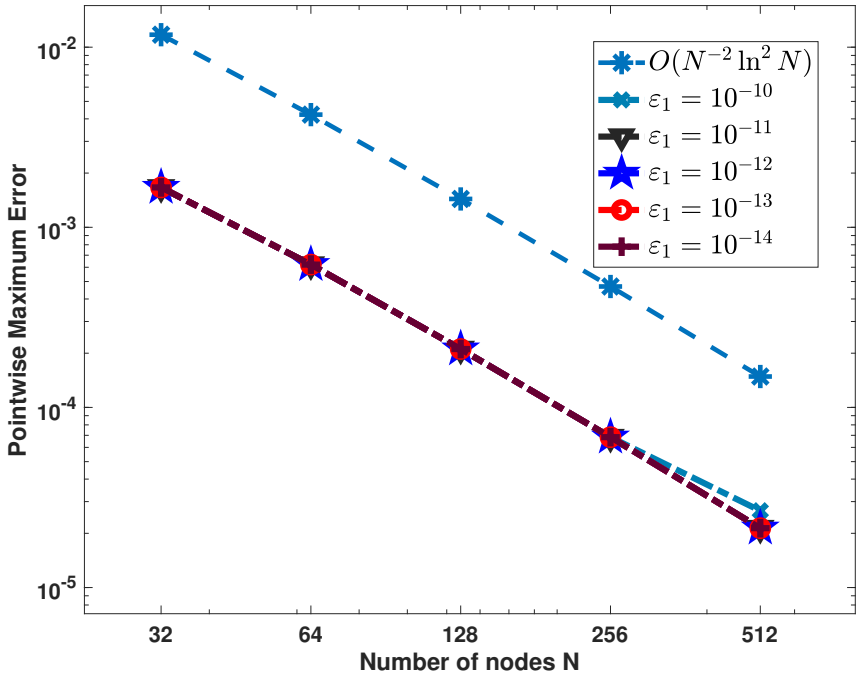

Figure 3.4: Visualization of pointwise maximum error obtained after Richardson extrapolation for Case II.

Table 3.1: Maximum pointwise error and associated rate of convergence for various values of ε_1 before using Richardson extrapolation for Case I.

ε_1	$N = 32$	64	128	256	512
	$\Delta t = 1/32$	$1/64$	$1/128$	$1/256$	$1/512$
10^{-3}	3.1486e-02	1.2614e-02	5.1412e-03	2.2779e-03	1.0580e-03
	1.319	1.294	1.174	1.106	
10^{-4}	3.1582e-02	1.4745e-02	7.2538e-03	3.6103e-03	1.8222e-03
	1.098	1.023	1.006	0.986	
10^{-5}	3.1612e-02	1.4782e-02	7.2970e-03	3.6434e-03	1.8433e-03
	1.096	1.018	1.002	0.983	
10^{-6}	3.1621e-02	1.4793e-02	7.3107e-03	3.6539e-03	1.8501e-03
	1.096	1.016	1.000	0.982	
10^{-7}	3.1624e-02	1.4797e-02	7.3150e-03	3.6572e-03	1.8522e-03
	1.095	1.016	1.000	0.982	
10^{-8}	3.1625e-02	1.4798e-02	7.3164e-03	3.6583e-03	1.8529e-03
	1.095	1.016	0.999	0.981	
10^{-9}	3.1625e-02	1.4798e-02	7.3168e-03	3.6586e-03	1.8531e-03
	1.095	1.016	0.999	0.981	
10^{-10} to 10^{-12}	3.1625e-02	1.4798e-02	7.3169e-03	3.6587e-03	1.8532e-03
	1.095	1.016	0.999	0.981	
$E^{N,\Delta t}$	**3.1625e-02**	**1.4798e-02**	**7.3170e-03**	**3.6588e-03**	**1.8532e-03**
$p^{N,\Delta t}$	**1.095**	**1.016**	**0.999**	**0.981**	

3.6 Conclusions

In this chapter, we have considered a parabolic IBVP of degenerate type with two parameters and used upwind scheme for space and backward-Euler method for calculation of the numerical solution. We have constructed layer-adapted Shishkin mesh using the constants $\mu_0,\ \mu_1$ which determine sharpness of the layers. The almost first-order accurate solution has been significantly improved using the Richardson extrapolation. The resulting approximate solution is found to be almost second-order convergent.

Table 3.2: Maximum pointwise error and associated rate of convergence for various values of ε_1 before using Richardson extrapolation for Case II.

ε_1	$N = 32$	64	128	256	512
	$\Delta t = 1/32$	$1/64$	$1/128$	$1/256$	$1/512$
10^{-7}	9.9259e-03	4.5577e-03	2.2887e-03	1.1102e-03	5.4535e-04
	1.123	0.9938	1.043	1.023	
10^{-8}	9.9246e-03	4.5689e-03	2.2940e-03	1.1494e-03	5.7531e-04
	1.119	0.994	0.997	0.998	
10^{-9}	9.9242e-03	4.5754e-03	2.2974e-03	1.1511e-03	5.7618e-04
	1.117	0.994	0.997	0.998	
10^{-10}	9.9241e-03	4.5802e-03	2.2998e-03	1.1523e-03	5.7673e-04
	1.115	0.994	0.997	0.998	
10^{-11}	9.9241e-03	4.5834e-03	2.3010e-03	1.1529e-03	5.7705e-04
	1.114	0.994	0.997	0.998	
10^{-12}	9.9241e-03	4.5851e-03	2.3019e-03	1.1533e-03	5.7725e-04
	1.114	0.994	0.997	0.998	
10^{-13}	9.9241e-03	4.5860e-03	2.3024e-03	1.1535e-03	5.7736e-04
	1.113	0.994	0.997	0.998	
10^{-14}	9.9241e-03	4.5865e-03	2.3026e-03	1.1537e-03	5.7742e-04
	1.113	0.994	0.997	0.998	
10^{-15}	9.9241e-03	4.5868e-03	2.3028e-03	1.1537e-03	5.7746e-04
	1.113	0.994	0.997	0.998	
$E^{N,\Delta t}$	**9.9241e-03**	**4.5868e-03**	**2.3028e-03**	**1.1537e-03**	**5.7746e-04**
$p^{N,\Delta t}$	**1.113**	**0.994**	**0.997**	**0.998**	

Table 3.3: Maximum pointwise error and associated rate of convergence for various values of ε_1 after using Richardson extrapolation for Example 3.5.1 for Case I.

ε_1	$N = 32$	64	128	256	512
	Δt 1/32	1/64	1/128	1/256	1/512
10^{-7}	3.0340e-5	7.7088e-6	1.9427e-6	4.8765e-7	1.2216e-7
	1.977	1.988	1.994	1.997	
10^{-8}	3.0339e-5	7.7088e-6	1.9427e-6	4.8765e-7	1.2216e-7
	1.977	1.988	1.994	1.997	
10^{-9}	3.0339e-5	7.7088e-6	1.9427e-6	4.8766e-7	1.2216e-7
	1.977	1.988	1.994	1.997	
10^{-10}	3.0339e-5	7.7088e-6	1.9427e-6	4.8766e-7	1.2216e-7
	1.977	1.988	1.994	1.997	
10^{-11}	3.0339e-5	7.7088e-6	1.9427e-6	4.8766e-7	1.2216e-7
	1.977	1.988	1.994	1.997	
10^{-12}	3.0339e-5	7.7088e-6	1.9427e-6	4.8766e-7	1.2216e-7
	1.977	1.988	1.994	1.997	
10^{-13} to 10^{-15}	3.0339e-5	7.7088e-6	1.9427e-6	4.8766e-7	1.2216e-7
	1.977	1.988	1.994	1.997	
$E^{N,\Delta t}$	**3.0339e-5**	**7.7088e-6**	**1.9427e-6**	**4.8766e-7**	**1.2216e-7**
$p^{N,\Delta t}$	**1.977**	**1.988**	**1.994**	**1.997**	

Table 3.4: Maximum pointwise error and associated rate of convergence for various values of ε_1 after using Richardson extrapolation for Case II

ε_1	$N = 32$	64	128	256	512
	$\Delta t = 1/32$	$1/64$	$1/128$	$1/256$	$1/512$
10^{-8}	1.6651e-03	6.2080e-04	2.1097e-04	6.8383e-05	2.6678e-05
	1.423	1.557	1.625	1.357	
10^{-9}	1.6651e-03	6.2080e-04	2.1097e-04	6.8383e-05	2.6679e-05
	1.423	1.557	1.625	1.357	
10^{-10}	1.6651e-03	6.2080e-04	2.1097e-04	6.8383e-05	2.6680e-05
	1.423	1.557	1.625	1.357	
10^{-11}	1.6651e-03	6.2080e-04	2.1097e-04	6.8383e-05	2.1364e-05
	1.423	1.557	1.625	1.678	
10^{-12}	1.6651e-03	6.2080e-04	2.1097e-04	6.8383e-05	2.1364e-05
	1.423	1.557	1.625	1.678	
10^{-13}	6.2080e-04	2.1097e-04	6.8383e-05	2.1364e-05	2.1364e-05
	1.423	1.557	1.625	1.678	
10^{-14}	1.6651e-03	6.2080e-04	2.1097e-04	6.8383e-05	2.1364e-05
	1.423	1.557	1.625	1.678	
$E^{N,\Delta t}$	**1.6651e-03**	**6.2080e-04**	**2.1097e-04**	**6.8383e-05**	**2.1364e-05**
$p^{N,\Delta t}$	**1.423**	**1.423**	**1.557**	**1.625**	

CHAPTER 4

Alternating direction implicit methods for singularly perturbed 2D parabolic convection-diffusion-reaction problems with two small parameters

In this chapter, we construct and analyze an ADI scheme for singularly perturbed 2D parabolic convection-diffusion-reaction problems with two small parameters. We consider the operator-splitting ADI finite difference scheme for time stepping on a uniform mesh and a simple upwind-difference scheme for spatial discretization on a specially designed piecewise-uniform Shishkin mesh. The resulting scheme is proved to be uniformly convergent of order $O(N^{-1}\ln N + M^{-1})$*, where* N, M *are the spatial and temporal parameters respectively. Numerical experiments confirm the theoretical results and the effectiveness of the proposed method.*

4.1 Introduction

The aim of this chapter is to solve singularly perturbed 2D parabolic convection-diffusion-reaction problems using the operator-splitting ADI finite difference scheme on piecewise-uniform mesh, where the diffusion and convection terms are affected by two small parameters. Also, we derive the truncation error for the proposed scheme. Stability analysis is carried out. Parameter-uniform error estimates are obtained, and numerical examples are provided to validate the theoretical results.

In this work, we study the following singularly perturbed 2D parabolic initial-boundary-value problem (IBVP):

$$\begin{cases} u_t + \mathcal{L}_\varepsilon u = f(x,y,t), & (x,y) \in \Omega = \Omega_x \times \Omega_y,\ t \in \Omega_t, \\ u(x,y,t) = 0, & (x,y) \in \partial\Omega = \overline{\Omega}\backslash\Omega,\ t \in \overline{\Omega}_t, \\ u(x,y,0) = \phi(x,y), & (x,y) \in \Omega, \end{cases} \tag{4.1.1}$$

where we consider the domains $\Omega_x = \{x : 0 < x < 1\}$, $\Omega_y = \{y : 0 < y < 1\}$, $\Omega_t = (0,T]$ and $\varepsilon_1, \varepsilon_2$ are the perturbation parameters such that $0 < \varepsilon_1, \varepsilon_2 \ll 1$ and the operator $\mathcal{L}_\varepsilon$ is defined as

$$\mathcal{L}_\varepsilon u := -\varepsilon_1 \Delta u + \varepsilon_2 \mathbf{b}(x,y) \cdot \nabla u + c(x,y)u. \tag{4.1.2}$$

The convection coefficient $\mathbf{b}$ is defined as $\mathbf{b}(x,y) = \big(b_1(x,y),\ b_2(x,y)\big)$ such that $b_i(x,y) \geq \beta_i > 0$, for $i = 1,2$ and $c(x,y) \geq c_0 > 0$. We also assume that $f = f_1 + f_2$ is a sufficiently smooth function that satisfies the following compatibility property:

$$f_1(x,0,t) = f_1(x,1,t) = f_2(0,y,t) = f_2(1,y,t) = 0. \tag{4.1.3}$$

Let $\beta = \min\{\beta_1, \beta_2\}$ and $\gamma < \min\limits_{\overline{\Omega}} \left\{ \dfrac{c(x,y)}{2b_1(x,y)}, \dfrac{c(x,y)}{2b_2(x,y)} \right\}$. We complete the analysis of the problem (4.1.1) into the following two cases:

$$\textbf{Case I:}\quad \varepsilon_2^2 \leq \frac{\gamma\varepsilon_1}{\beta}, \quad \textbf{Case II:}\quad \varepsilon_2^2 \geq \frac{\gamma\varepsilon_1}{\beta}.$$

We organize the rest of the chapter as follows: We divide the study into two main sections, namely Section 4.2 and Section 4.3 depending on the relation between the perturbation parameters $\varepsilon_1, \varepsilon_2$. We first consider the case with the assumption $\varepsilon_2^2 \leq C\varepsilon_1$ in Section 4.2.1 and estimate the local and global errors for the time semi-discretization. The construction

of Shishkin mesh and the ADI operator-splitting numerical scheme are described in Section 4.2.2. We prove the theoretical results related to the convergence analysis in Section 4.2.3 and the numerical examples are given in Section 4.2.4. We present similar discussions in Section 4.3 for the second case, *i.e.*, $\varepsilon_2^2 \geq C\varepsilon_1$. Here, C denotes a generic positive constant independent of all the parameters.

In the subsequent sections, we will consider each case separately to study the convergence analysis of the problem (4.1.1) with the associated layer structures.

4.2 Application of the ADI finite difference scheme: Case I

In this section, we first confine the discussion to Case I: $\varepsilon_2^2 \leq \dfrac{\gamma\varepsilon_1}{\beta}$. In this case, we usually notice regular boundary layers of width $O(\sqrt{\varepsilon_1})$ near all four edges along with the corner layers appearing near every corner of the domain Ω.

For more rigorous analysis, we consider the following decomposition of the solution u of the problem (4.1.1):

$$u = v + w_L + w_R + w_T + w_B + w_{LT} + w_{RB} + w_{RT} + w_{LB}, \tag{4.2.1}$$

where v is the regular component of the solution while w_L, w_R, w_B, w_T are the boundary layer components appearing near the edges S_{10}, S_{11}, S_{20}, S_{21} respectively and w_{LB}, w_{LT}, w_{RB}, w_{RT} are the respective corner layer components condensing at the four corners $(0,0)$, $(1,0)$, $(0,1)$, $(1,1)$, where

$$S_{10} = \big\{(0,y):\ 0 \leq y \leq 1\big\}, \quad S_{11} = \big\{(1,y):\ 0 \leq y \leq 1\big\},$$
$$S_{20} = \big\{(x,0):\ 0 \leq x \leq 1\big\}, \quad S_{21} = \big\{(x,1):\ 0 \leq x \leq 1\big\}.$$

In Figure 4.1, we present the subdivision of the spatial domain $[0,1]^2$ into different layer and non-layer regions according to the appearance of various boundary and corner layers for the continuous solution. The regions C_{10}, C_{11}, C_{20} and C_{21} indicate the corner layer regions near the vertices $(0,0)$, $(1,0)$, $(0,1)$ and $(1,1)$ respectively. Also, the regions E_{10}, E_{11}, E_{20}, E_{21} represent the regular boundary layer locations near the boundaries S_{10}, S_{11}, S_{20}, S_{21} respectively while the region E_{00} lies outside all the layer regions.

The following explicit bounds for the various components of the continuous solution u of the problem (4.1.1) are established by Clavero *et al.* [66]. If the compatibility conditions

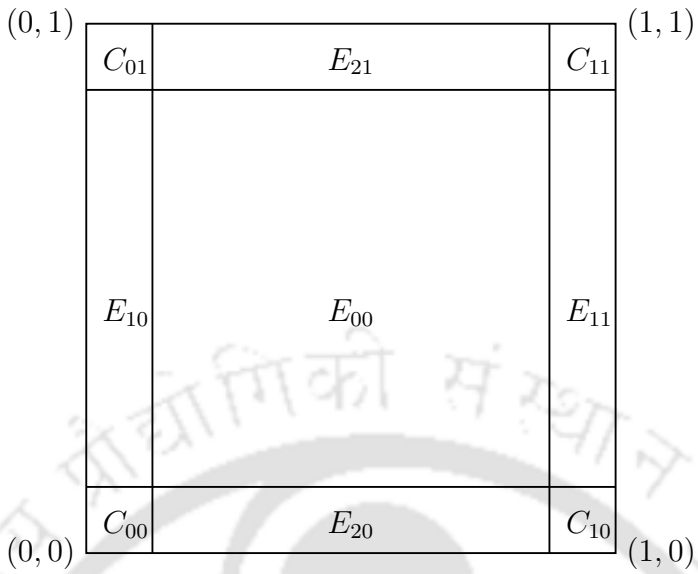

Figure 4.1: Decomposition of the computational domain based on the occurrence of various layers.

in (4.1.3) hold, then the boundary layer components satisfy the following bounds

$$\left|\frac{\partial^{k_s+k_t} v}{\partial x^{k_1}\partial y^{k_2}\partial t^{k_t}}\right| \leq C, \quad \left|\frac{\partial^{k_s+k_t} w_L}{\partial x^{k_1}\partial y^{k_2}\partial t^{k_t}}\right| \leq C\varepsilon_1^{-k_1/2} e^{-\sqrt{\frac{\beta\gamma}{\varepsilon_1}}x}, \tag{4.2.2}$$

$$\left|\frac{\partial^{k_s+k_t} w_R}{\partial x^{k_1}\partial y^{k_2}\partial t^{k_t}}\right| \leq C\varepsilon_1^{-k_1/2} e^{-\sqrt{\frac{\beta\gamma}{\varepsilon_1}}(1-x)}, \tag{4.2.3}$$

$$\left|\frac{\partial^{k_s+k_t} w_B}{\partial x^{k_1}\partial y^{k_2}\partial t^{k_t}}\right| \leq C\varepsilon_1^{-k_2/2} e^{-\sqrt{\frac{\beta\gamma}{\varepsilon_1}}y}, \tag{4.2.4}$$

$$\left|\frac{\partial^{k_s+k_t} w_T}{\partial x^{k_1}\partial y^{k_2}\partial t^{k_t}}\right| \leq C\varepsilon_1^{-k_2/2} e^{-\sqrt{\frac{\beta\gamma}{\varepsilon_1}}(1-y)}, \tag{4.2.5}$$

while the corner layer parts satisfy the followings

$$\left|\frac{\partial^{k_s+k_t} w_{LB}}{\partial x^{k_1}\partial y^{k_2}\partial t^{k_t}}\right| \leq C\varepsilon_1^{-(k_1+k_2)/2} \min\left\{e^{-\sqrt{\frac{\beta\gamma}{\varepsilon_1}}x}, \; e^{-\sqrt{\frac{\beta\gamma}{\varepsilon_1}}y}\right\}, \tag{4.2.6}$$

$$\left|\frac{\partial^{k_s+k_t} w_{RB}}{\partial x^{k_1}\partial y^{k_2}\partial t^{k_t}}\right| \leq C\varepsilon_1^{-(k_1+k_2)/2} \min\left\{e^{-\sqrt{\frac{\beta\gamma}{\varepsilon_1}}(1-x)}, \; e^{-\sqrt{\frac{\beta\gamma}{\varepsilon_1}}y}\right\}, \tag{4.2.7}$$

$$\left|\frac{\partial^{k_s+k_t} w_{LT}}{\partial x^{k_1}\partial y^{k_2}\partial t^{k_t}}\right| \leq C\varepsilon_1^{-(k_1+k_2)/2} \min\left\{e^{-\sqrt{\frac{\beta\gamma}{\varepsilon_1}}x}, \; e^{-\sqrt{\frac{\beta\gamma}{\varepsilon_1}}(1-y)}\right\}, \tag{4.2.8}$$

$$\left|\frac{\partial^{k_s+k_t} w_{RT}}{\partial x^{k_1}\partial y^{k_2}\partial t^{k_t}}\right| \leq C\varepsilon_1^{-(k_1+k_2)/2} \min\left\{e^{-\sqrt{\frac{\beta\gamma}{\varepsilon_1}}(1-x)}, \; e^{-\sqrt{\frac{\beta\gamma}{\varepsilon_1}}(1-y)}\right\}, \tag{4.2.9}$$

where $k_s = k_1 + k_2$, $0 \leq k_1 + k_2 + 2k_t \leq 4$.

4.2.1 Temporal discretizations

As we have mentioned previously, we use the operator-splitting ADI finite difference scheme, we split the differential operator $\mathcal{L}_\varepsilon$ in (4.1.1) as $\mathcal{L}_\varepsilon := \mathcal{L}_{x,\varepsilon} + \mathcal{L}_{y,\varepsilon}$ where

$$\mathcal{L}_{x,\varepsilon}u := -\varepsilon_1\frac{\partial^2 u}{\partial x^2} + \varepsilon_2 b_1(x,y)\frac{\partial u}{\partial x} + c_1(x,y)u,$$
$$\mathcal{L}_{y,\varepsilon}u := -\varepsilon_1\frac{\partial^2 u}{\partial y^2} + \varepsilon_2 b_2(x,y)\frac{\partial u}{\partial y} + c_2(x,y)u,$$

where $c = c_1 + c_2$ with $c_1 > 0$, $c_2 > 0$.

The domain of the time variable is discretized as

$$\overline{\Omega}_t^M := \big\{t_k : t_k = k\Delta t, \quad k = 0, 1, \ldots, M, \quad \Delta t = T/M\big\}.$$

where we consider only the uniform time step size Δt.

Then, the time semi-discretization of problem (4.1.1) is carried out using the following alternating direction scheme:

Let $u^0 = \phi(x,y)$ and u^{n+1} is defined by the following equations

$$\begin{cases} \begin{cases} \Big[I + \Delta t\mathcal{L}_{x,\varepsilon}\Big]u^{n+1/2} = u^n + \Delta t f_1(x,y,t_{n+1}), & \text{(4.2.10.a)} \\ u^{n+1/2}(0,y) = u^{n+1/2}(1,y) = 0, \quad 0 \le y \le 1, \end{cases} \\ \begin{cases} \Big[I + \Delta t\mathcal{L}_{y,\varepsilon}\Big]u^{n+1} = u^{n+1/2} + \Delta t f_2(x,y,t_{n+1}), \\ u^{n+1}(x,0) = u^{n+1}(x,1) = 0, \quad 0 \le x \le 1. \end{cases} & \text{(4.2.10.b)} \end{cases}$$

for $n = 0, 1, \ldots, M-1$.

We state the maximum principle for the operators $\big(I + \Delta t\mathcal{L}_{k,\varepsilon}\big)$ for $k = x, y$ in the following lemma.

Lemma 4.2.1. (Maximum principle) *Let $\eta(x,y) \in C^2(\Omega)$ with $\eta(x,y) \ge 0$ on the boundary $\partial\Omega$ and*

$$\big(I + \Delta t\mathcal{L}_{k,\varepsilon}\big)\eta(x,y) \ge 0, \quad (x,y) \in \Omega, \quad k = x, y. \tag{4.2.11}$$

Then, the function $\eta(x,y)$ is non-negative for every $(x,y) \in \overline{\Omega}$.

The operator $\big(I + \Delta t\mathcal{L}_{x,\varepsilon} + \Delta t\mathcal{L}_{y,\varepsilon}\big)$ also satisfies the same maximum principle on the domain $\overline{\Omega}$.

Proof. We only give the proof for the operator $\big(I+\Delta t\mathcal{L}_{x,\varepsilon}\big)$ while the proof for $\big(I+\Delta t\mathcal{L}_{y,\varepsilon}\big)$ can be achieved by following similar steps.

Suppose, $(x_*, y_*) \in \Omega$ satisfies

$$\eta(x_*, y_*) = \min_{\overline{\Omega}} \eta(x, y) < 0.$$

Since (x_*, y_*) is a point of minimum, we have $\eta_x(x_*, y_*) = 0$, $\eta_{xx}(x_*, y_*) > 0$ and hence

$$\begin{aligned}
&(I + \Delta t\mathcal{L}_{x,\varepsilon})\,\eta(x_*, y_*) \\
&= \eta(x_*, y_*) + \Delta t\big[-\varepsilon_1\eta_{xx}(x_*, y_*) + \varepsilon_2 b_1(x_*, y_*)\eta_x(x_*, y_*) + c_1(x_*, y_*)\eta(x_*, y_*)\big] \\
&< 0.
\end{aligned}$$

This leads to a contradiction. Hence, the result follows.

For the operator $\big(I+\Delta t\mathcal{L}_{x,\varepsilon}+\Delta t\mathcal{L}_{y,\varepsilon}\big)$, let us consider the function $\xi \in C^2(\Omega)$ with $\xi \geq 0$ on the boundary. If there is a point $(\tilde{x}, \tilde{y}) \in \Omega$ such that

$$\xi(\tilde{x}, \tilde{y}) = \min_{\overline{\Omega}} \xi(x, y) < 0.$$

Thus, we have $\xi_x(\tilde{x}, \tilde{y}) = 0 = \xi_y(\tilde{x}, \tilde{y})$, and $\xi_{xx}(\tilde{x}, \tilde{y}) > 0$, $\xi_{yy}(\tilde{x}, \tilde{y}) > 0$ with the condition $\big(\xi_{xx}\xi_{yy} - \xi_{xy}^2\big)(\tilde{x}, \tilde{y}) > 0$. Hence,

$$\begin{aligned}
&\big(I + \Delta t\mathcal{L}_{x,\varepsilon} + \Delta t\mathcal{L}_{y,\varepsilon}\big)(\tilde{x}, \tilde{y}) \\
&= \xi(\tilde{x}, \tilde{y}) + \Delta t\big[-\varepsilon_1\xi_{xx} - \varepsilon_1\xi_{yy} + \varepsilon_2 b_1\xi_x + \varepsilon_2 b_2\xi_y + c(\tilde{x}, \tilde{y})\xi\big](\tilde{x}, \tilde{y}) < 0,
\end{aligned}$$

which contradicts the hypothesis $\big(I + \Delta t\mathcal{L}_{x,\varepsilon} + \Delta t\mathcal{L}_{y,\varepsilon}\big)\xi(x, y) \geq 0$, $(x, y) \in \Omega$. Hence, the maximum principle is valid for this operator also. □

As a consequence of the above maximum principle, we have the following stability estimates

$$\begin{aligned}
\Big\|\big(I + \Delta t\mathcal{L}_{k,\varepsilon}\big)^{-1}\Big\|_{\infty,\overline{\Omega}} &\leq \frac{1}{1+\beta\Delta t} \text{ for } k = x, y, \\
\Big\|\big(I + \Delta t\mathcal{L}_{x,\varepsilon} + \Delta t\mathcal{L}_{y,\varepsilon}\big)^{-1}\Big\|_{\infty,\overline{\Omega}} &\leq C.
\end{aligned}$$

Let $\widehat{u}^{n+1}$ solves the following semi-discrete problem

$$\begin{cases} \Big[I + \Delta t \mathcal{L}_{x,\varepsilon}\Big]\widehat{u}^{n+1/2} = u(t_n) + \Delta t f_1(x,y,t_{n+1}), \\ \widehat{u}^{n+1/2}(0,y) = \widehat{u}^{n+1/2}(1,y) = 0, \quad 0 \le y \le 1, \end{cases} \tag{4.2.12.a}$$

$$\begin{cases} \Big[I + \Delta t \mathcal{L}_{y,\varepsilon}\Big]\widehat{u}^{n+1} = \widehat{u}^{n+1/2} + \Delta t f_2(x,y,t_{n+1}), \\ \widehat{u}^{n+1}(x,0) = \widehat{u}^{n+1}(x,1) = 0, \quad 0 \le x \le 1, \end{cases} \tag{4.2.12.b}$$

for $n = 0, 1, \ldots, M-1$.

We define the local truncation error at the n-th time level as,

$$e_n = u(t_n) - \widehat{u}^n, \quad 1 \le n \le M. \tag{4.2.13}$$

Then, the following consistency result holds true.

Lemma 4.2.2. *Let u be the solution of the problem (4.1.1). If $\left|\dfrac{\partial^k u}{\partial t^k}\right| \le C$, $0 \le k \le 2$, then, the local truncation error e_{n+1} for time semi-discretization satisfies the following bound*

$$\|e_{n+1}\|_{\infty,\overline{\Omega}} \le C\Delta t^2, \quad n = 0, 1, \ldots, M-1. \tag{4.2.14}$$

Proof. Let the function $\widehat{u}^{n+1}$ satisfy the equation (4.2.12.a) and (4.2.12.b). Then we get,

$$\begin{aligned} u(t_n) &= \Big[I + \Delta t \mathcal{L}_{x,\varepsilon}\Big]\widehat{u}^{n+1/2} - \Delta t f_1(x,y,t_{n+1}) \\ &= \Big[I + \Delta t \mathcal{L}_{x,\varepsilon}\Big]\Big(\Big[I + \Delta t \mathcal{L}_{y,\varepsilon}\Big]\widehat{u}^{n+1} - \Delta t f_2(x,y,t_{n+1})\Big) - \Delta t f_1(x,y,t_{n+1}) \\ &= \widehat{u}^{n+1/2} + \Delta t\big(\mathcal{L}_{x,\varepsilon} + \mathcal{L}_{y,\varepsilon}\big)\widehat{u}^{n+1/2} - \Delta t f_1(x,y,t_{n+1}) - \Delta t f_2(x,y,t_{n+1}) \\ &\quad + \Delta t^2\big[\mathcal{L}_{x,\varepsilon}\mathcal{L}_{y,\varepsilon}\widehat{u}^{n+1/2} - \mathcal{L}_{x,\varepsilon} f_2(x,y,t_{n+1})\big] \\ &= \big[I + \Delta t\big(\mathcal{L}_{x,\varepsilon} + \mathcal{L}_{y,\varepsilon}\big)\big]\widehat{u}^{n+1/2} - \Delta t f(x,y,t_{n+1}) + O(\Delta t^2). \end{aligned} \tag{4.2.15}$$

Using the Taylor series expansion for $u(t_n)$ with an integral form of remainder, we obtain

$$u(t_n) = u(t_{n+1}) - \Delta t \ \frac{\partial u}{\partial t}(t_{n+1}) + \int_{t_{n+1}}^{t_n} (t_n - s)\frac{\partial^2 u}{\partial t^2}(s)ds.$$

On the other hand, since u is the solution of problem (4.1.1), one can write

$$u(t_n) = u(t_{n+1}) + \Delta t\big[\big(\mathcal{L}_{x,\varepsilon} + \mathcal{L}_{y,\varepsilon}\big)u(t_{n+1}) - f_1(x,y,t_{n+1}) - f_2(x,y,t_{n+1})\big] + \int_{t_{n+1}}^{t_n}(t_n - s)\frac{\partial^2 u}{\partial t^2}(s)ds.$$

The uniform boundedness of $\dfrac{\partial^2 u}{\partial t^2}$ also ensures that $\left|(t_n - s)\dfrac{\partial^2 u}{\partial t^2}(s)\right| \leq C\Delta t$. Therefore,

$$u(t_n) = u(t_{n+1}) + \Delta t\big[\big(\mathcal{L}_{x,\varepsilon} + \mathcal{L}_{y,\varepsilon}\big)u(t_{n+1}) - f(x,y,t_{n+1})\big] + O(\Delta t^2). \tag{4.2.16}$$

From (4.2.15) and (4.2.16), we get,

$$\Big[I + \Delta t\mathcal{L}_{x,\varepsilon} + \Delta t\mathcal{L}_{y,\varepsilon}\Big]e_{n+1} = O(\Delta t^2) \tag{4.2.17}$$

with $e_{n+1}(x,0) = 0 = e_{n+1}(x,1)$ and $e_{n+1}(0,y) = 0 = e_{n+1}(1,y)$.

Finally, applying the maximum principle given in Lemma 4.2.1 for the operator $\big(I + \Delta t\mathcal{L}_{x,\varepsilon} + \Delta t\mathcal{L}_{y,\varepsilon}\big)$, we obtain the desired estimate. □

In order to establish the uniform convergence of (4.2.10), we define the global error E_n by

$$E_n = u(t_n) - u^n, \quad 1 \leq n \leq M. \tag{4.2.18}$$

And the following theorem shows that the global error for the time semi-discretization process has first-order convergence.

Theorem 4.2.3. *The global error E_n in (4.2.18) satisfies the following bound*

$$\max_{1\leq n\leq M}\|E_n\|_{\infty,\overline{\Omega}} \leq CM^{-1}. \tag{4.2.19}$$

Proof. We can rewrite the global error as,

$$\begin{aligned} E_n &= u(t_n) - u^n \\ &= \big(u(t_n) - \widehat{u}^n\big) + \big(\widehat{u}^n - u^n\big) \\ &= e_n + \big(\widehat{u}^n - u^n\big). \end{aligned}$$

From the equations (4.2.10) and (4.2.12) we get,

$$\Big(I+\Delta t\mathcal{L}_{x,\varepsilon}\Big)\Big[\Big(I+\Delta t\mathcal{L}_{y,\varepsilon}\Big)\widehat{u}^{n+1}-\Delta t f_2(x,y,t_n)\Big]=u(t_n)+\Delta t f_1(x,y,t_n),$$
$$\Big(I+\Delta t\mathcal{L}_{x,\varepsilon}\Big)\Big[\Big(I+\Delta t\mathcal{L}_{y,\varepsilon}\Big)u^{n+1}-\Delta t f_2(x,y,t_n)\Big]=u^{n}+\Delta t f_1(x,y,t_n).$$

From the above equations, one can easily obtain that

$$\begin{aligned}E_n&=\Big[I+\Delta t\mathcal{L}_{x,\varepsilon}\Big]\Big[I+\Delta t\mathcal{L}_{y,\varepsilon}\Big]\big(\widehat{u}^{n+1}-u^{n+1}\big)\\&=\Big[I+\Delta t\mathcal{L}_{x,\varepsilon}\Big]\Big[I+\Delta t\mathcal{L}_{y,\varepsilon}\Big]\big(E_{n+1}-e_{n+1}\big).\end{aligned}$$

We can express the above equality as

$$E_{n+1}=e_{n+1}+\mathcal{R}E_n,$$

where $\mathcal{R}=\Big[I+\Delta t\mathcal{L}_{y,\varepsilon}\Big]^{-1}\Big[I+\Delta t\mathcal{L}_{x,\varepsilon}\Big]^{-1}$. Thus, we have the following recurrence relation,

$$E_{n+1}=\sum_{i=1}^{n+1}\mathcal{R}^{n-i-1}e_i$$

Following the techniques given in [67], and using the fact that $\|\mathcal{R}\|_{\infty,\overline{\Omega}}\leq C$, we get

$$\|E_{n+1}\|_{\infty,\overline{\Omega}}\ \leq C\Delta t$$

for $n=0,1,\ldots,M-1$. Finally, substituting $\Delta t=T/M$ in previous inequality, we obtain

$$\max_{1\leq n\leq M}\|E_n\|_{\infty,\overline{\Omega}}\ \leq CM^{-1},$$

which is the required estimate. □

4.2.2 Spatial discretizations

In this section, we present the fully-discrete scheme based on the discretization of the spatial domain. We discretize the domain $\overline{\Omega}=[0,1]^2$ to construct the piecewise-uniform Shishkin mesh, which is generated as follows. First, we define the transition parameter for the x-grid

as

$$\tau_x = \min\left\{\frac{1}{4},\ 2\sqrt{\frac{\varepsilon_1}{\beta\gamma}}\ln N\right\}.$$

The domain $[0,1]$ along the x-axis is divided into the three subintervals $[0,\tau_x]$, $[\tau_x, 1-\tau_x]$ and $[1-\tau_x, 1]$ by the transitions points τ_x and $(1-\tau_x)$ to distribute $N/2$ grid points in the layer regions and the remaining $N/2$ grids outside the region. Thus, the grids can be defined as follows

$$x_i = \begin{cases} \dfrac{4i\tau_x}{N}, & 0 \le i \le N/4, \\ \tau_x + 2\left(i - \dfrac{N}{4}\right)\dfrac{1-2\tau_x}{N}, & N/4 < i \le 3N/4, \\ 1-\tau_x + 4\left(i - \dfrac{3N}{4}\right)\dfrac{\tau_x}{N}, & 3N/4 < i \le N. \end{cases} \tag{4.2.20}$$

We also construct the grid along y-axis using the transition parameter τ_y, where $\tau_y = \tau_x$. Thus, the domain $\overline{\Omega} = [0,1]^2$ is now discretized using the tensor product of the meshes $\overline{\Omega}_x^N$ and $\overline{\Omega}_y^N$ as $\overline{\Omega}^N := \overline{\Omega}_x^N \times \overline{\Omega}_y^N$, where

$$\overline{\Omega}_x^N = \left\{x_i : x_i = x_{i-1} + h_i^x, \quad x_0 = 0,\ x_N = 1, \quad 1 \le i \le N\right\},$$
$$\overline{\Omega}_y^N = \left\{y_j : y_j = y_{j-1} + h_j^y, \quad y_0 = 0,\ y_N = 1, \quad 1 \le j \le N\right\}.$$

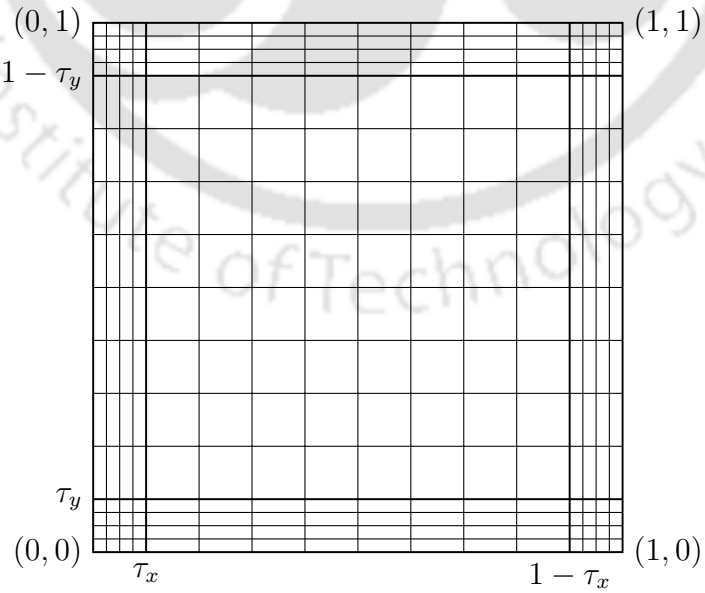

Figure 4.2: A typical Shishkin mesh for (4.1.1) with $N = 16$.

For a mesh function v, we define the following finite difference operators:

$$\delta_x^+ v_{ij}^n = \frac{v_{i+1,j}^n - v_{ij}^n}{h_{i+1}^x}, \quad \delta_x^- v_{ij}^n = \frac{v_{ij}^n - v_{i-1,j}^n}{h_i^x}$$
$$\text{and} \quad \Delta_x v_{ij}^n = \frac{2}{h_i^x + h_{i+1}^x}\Big[\delta_x^+ v_{ij}^n - \delta_x^- v_{ij}^n\Big],$$

where $v(x_i, y_j, t_n) = v_{i,j}^n$. By using the above definitions, the operators corresponding to the derivatives with respect to y can be defined analogously. Let us also define the discrete operators $L_{i,\varepsilon}^N$, for $i = x, y$ by

$$L_{x,\varepsilon}^N U_{ij}^n = \Big[-\varepsilon_1 \Delta_x + \varepsilon_2 b_1(x_i, y_j)\delta_x^- + c_1(x_i, y_j) I\Big] U_{ij}^n,$$
$$L_{y,\varepsilon}^N U_{ij}^n = \Big[-\varepsilon_1 \Delta_y + \varepsilon_2 b_2(x_i, y_j)\delta_y^- + c_2(x_i, y_j) I\Big] U_{ij}^n.$$

The fully-discrete problem on $\overline{\Omega}^N \times \overline{\Omega}_t^M$ can be presented as follows: U_{ij}^{n+1} is the solution of the following

$$\begin{cases} U_{ij}^0 = \phi(x_i, y_j), \ \ 0 \le i, j \le N, \\ \begin{cases} \Big[I + \Delta t L_{x,\varepsilon}^N\Big] U_{ij}^{n+1/2} = r_{ij}^- U_{i-1,j}^{n+1/2} + r_{ij}^0 U_{ij}^{n+1/2} + r_{ij}^+ U_{i+1,j}^{n+1/2} \\ \qquad\qquad\qquad\qquad = U_{ij}^n + \Delta t f_{1_{ij}}^{n+1}, \\ U_{0,j}^{n+1/2} = U_{N,j}^{n+1/2} = 0, \quad 1 \le j \le N-1, \end{cases} \qquad (4.2.21) \\ \begin{cases} \Big[I + \Delta t L_{y,\varepsilon}^N\Big] U_{ij}^{n+1} = s_{ij}^- U_{i,j-1}^{n+1} + s_{ij}^0 U_{ij}^{n+1} + s_{ij}^+ U_{i,j+1}^{n+1} \\ \qquad\qquad\qquad\qquad = U_{ij}^{n+1/2} + \Delta t f_{2_{ij}}^{n+1}, \\ U_{i,0}^{n+1} = U_{i,N}^{n+1} = 0, \quad 1 \le i \le N-1, \end{cases} \qquad (4.2.22) \\ n = 0, 1, \ldots, M-1. \end{cases}$$

where the associated coefficients are defined for $1 \le i, j \le N-1$ as,

$$r_{ij}^- = -\frac{2\varepsilon_1}{(h_i^x + h_{i+1}^x)}\frac{\Delta t}{h_i^x}, \quad r_{ij}^+ = -\left(\frac{2\varepsilon_1}{h_i^x + h_{i+1}^x} + \varepsilon_2 b_{1,ij}\right)\frac{\Delta t}{h_{i+1}^x}, \qquad (4.2.23)$$

$$r_{ij}^0 = \left(1 + \Delta t c_{1,ij} - r_{ij}^+ - r_{ij}^-\right), \ b_{1,ij} = b_1(x_i, y_j), \ c_{1,ij} = c_1(x_i, y_j), \qquad (4.2.24)$$

and

$$s_{ij}^{-} = -\frac{2\varepsilon_1}{(h_j^y + h_{j+1}^y)}\frac{\Delta t}{h_j^y}, \quad s_{ij}^{+} = -\left(\frac{2\varepsilon_1}{h_j^y + h_{j+1}^y} + \varepsilon_2 b_{2,ij}\right)\frac{\Delta t}{h_{j+1}^y}, \tag{4.2.25}$$

$$s_{ij}^{0} = \left(1 + \Delta t c_{2,ij} - s_{ij}^{+} - s_{ij}^{-}\right), \; b_{2,ij} = b_2(x_i, y_j), \; c_{2,ij} = c_2(x_i, y_j). \tag{4.2.26}$$

Lemma 4.2.4. *The coefficient matrices associated with the difference equations* (4.2.21) *and* (4.2.22) *are M-matrices.*

Proof. Suppose R_j, S_i are the coefficient matrices corresponding to the discrete equations (4.2.21) and (4.2.22) respectively for each fixed j and i. Since they are of similar structure, it is sufficient to prove that R_j is an M-matrix.

From the coefficients defined in (4.2.23)-(4.2.24), it is clear that for each fixed j, the matrix R_j is a tridiagonal matrix with $r_{ij}^0 > 0$, $r_{ij}^+ < 0$, $r_{ij}^- < 0$. We also note that

$$\left|r_{ij}^0\right| > \left|r_{ij}^+\right| + \left|r_{ij}^-\right|, \quad \forall i = 1, 2, \ldots, N-1,$$

for each j. Therefore, the matrix R_j ia an M-matrix for every $1 \le j \le N-1$. Hence, the claim is proved. □

Since the associated matrices are M-matrices, the discrete operators defined above satisfy the following discrete maximum principle, which ensures the parameter-uniform stability of the numerical scheme. It is also easy to solve each of the finite difference equations with the help of an efficient tridiagonal matrix solver.

Lemma 4.2.5. (Discrete maximum principle) *Let V be an arbitrary mesh function defined on $\overline{\Omega}_x^N$ (or $\overline{\Omega}_y^N$) and $V_k \ge 0$ for $k = 0, N$. If*

$$\left(I + \Delta t L_{i,\varepsilon}^N\right)V_k \; \ge 0, \;\; 1 \le k \le N-1, \quad i = x, y,$$

then we have, $V_k \ge 0$ for $0 \le k \le N$.

Proof. Let us proceed with the proof by contradiction. Suppose, there is a natural number k, where $1 \le k \le N-1$, such that

$$V_k = \min_{0 \le i \le N} V_i < 0.$$

By hypothesis, we have, $V_{k+1} \geq V_k$ and $V_k \leq V_{k-1}$. Thus,

$$\Delta_x V_k = \frac{2}{h_k^x + h_{k+1}^x}\left[\frac{V_{k+1}-V_k}{h_{k+1}^x} - \frac{V_k - V_{k-1}}{h_k^x}\right] \geq 0, \quad \delta_x^- V_k = \frac{V_k - V_{k-1}}{h_k^x} \leq 0.$$

Since $b_1 > 0,\ c_1 > 0$, we have

$$V_k + \Delta t L_{x,\varepsilon}^N V_k \ < 0,$$

which contradicts to our assumption. Hence, we get the desired result.

Similar arguments also apply for the discrete operator $\left(I + \Delta t L_{y,\varepsilon}^N\right)$ on $\overline{\Omega}_y^N$. □

The above lemma immediately gives the following

$$\left\|\left(I + \Delta t L_{i,\varepsilon}^N\right)^{-1}\right\|_{\infty,\overline{\Omega}_i^N} \leq C, \quad i = x, y.$$

4.2.3 Convergence analysis

Lemma 4.2.6. *Suppose the perturbation parameters satisfy the relation* $\varepsilon_2^2 \leq \frac{\gamma\varepsilon_1}{\beta}$ *and* $\widehat{u}^{n+1/2}$ *satisfies the equation* (4.2.12) *for* $n = 0, 1, \ldots, M-1$. *Then for* $0 \leq i \leq 4$, *we have*

$$\left|\frac{\partial^i \widehat{u}^{n+1/2}}{\partial x^i}\right| \leq C\left[1 + \varepsilon_1^{-i/2}\left(e^{-\sqrt{\frac{\beta\gamma}{\varepsilon_1}}x} + e^{-\sqrt{\frac{\beta\gamma}{\varepsilon_1}}(1-x)}\right)\right]. \tag{4.2.27}$$

Proof. Let us first consider the case $i = 0$. Since the operator $\left(I + \Delta t \mathcal{L}_{x,\varepsilon}\right)$ satisfies the maximum principle and the right-hand side of the semi-discrete problem (4.2.12) is bounded, the result follows by using the fact that

$$\left\|\left(I + \Delta t \mathcal{L}_{x,\varepsilon}\right)^{-1}\right\|_{\infty,\overline{\Omega}} \ \leq \frac{1}{1+\beta\Delta t}.$$

Now consider the case $i = 1$, *i.e.,* we need to find the estimate for $\dfrac{\partial \widehat{u}^{n+1/2}}{\partial x}$. To begin with, let us define the following function

$$\omega = \frac{\widehat{u}^{n+1/2} - u(t_n)}{\Delta t}.$$

One can easily verify that the function ω satisfies

$$\begin{aligned}\omega + \Delta t\mathcal{L}_{x,\varepsilon}\omega &= \frac{\widehat{u}^{n+1/2} - u(t_n)}{\Delta t} + \mathcal{L}_{x,\varepsilon}\widehat{u}^{n+1/2} - \mathcal{L}_{x,\varepsilon}u(t_n)\\ &= \frac{\widehat{u}^{n+1/2} + \Delta t\mathcal{L}_{x,\varepsilon}\widehat{u}^{n+1/2}}{\Delta t} - \frac{u(t_n)}{\Delta t} - \mathcal{L}_{x,\varepsilon}u(t_n)\\ &= \frac{u(t_n) + \Delta t f_1(x,y,t_{n+1})}{\Delta t} - \frac{u(t_n)}{\Delta t} - \mathcal{L}_{x,\varepsilon}u(t_n).\end{aligned}$$

Thus, $\omega + \Delta t\mathcal{L}_{x,\varepsilon}\ \omega = f_1(x,y,t_{n+1}) - \mathcal{L}_{x,\varepsilon}u(t_n)$.

Since the right-hand side of the previous equation is bounded, we can use the maximum principle for the operator $\left(I + \Delta t\mathcal{L}_{x,\varepsilon}\right)$ to get $|\omega| \leq c$.

On the other hand, we can rewrite the equation (4.2.12.a) as

$$\begin{cases}\mathcal{L}_{x,\varepsilon}\widehat{u}^{n+1/2} = -\omega + f_1(x,y,t_{n+1}), \quad x \in (0,1),\\ \widehat{u}^{n+1/2}(0,y) = 0, \quad \widehat{u}^{n+1/2}(1,y) = 0.\end{cases} \tag{4.2.28}$$

One can observe that the equation (4.2.28) is essentially a two-parameter singularly perturbed problem in one-dimension with a bounded right-hand side function for each fixed $y \in [0,1]$ is considered to be a parameter. The width of the boundary layers for this problem can be determined by the following characteristic equation

$$-\varepsilon_1\zeta^2(x) + \varepsilon_2 b_1(x,y)\zeta(x) + c_1(x,y) = 0 \tag{4.2.29}$$

considering y as a parameter and define

$$\mu_0 = -\max_{x\in[0,1]} \frac{\varepsilon_2 b_1(x,y) - \sqrt{\varepsilon_2^2 b_1(x,y)^2 + 4\varepsilon_1 c_1(x,y)}}{2\varepsilon_1}, \tag{4.2.30}$$

$$\mu_1 = \min_{x\in[0,1]} \frac{\varepsilon_2 b_1(x,y) + \sqrt{\varepsilon_2^2 b_1(x,y)^2 + 4\varepsilon_1 c_1(x,y)}}{2\varepsilon_1}. \tag{4.2.31}$$

Following the techniques given in [64] and using the fact that $\mu_0 = O(\varepsilon_1^{-1/2})$, $\mu_1 = O(\varepsilon_1^{-1/2})$ for $\varepsilon_2^2 \leq \dfrac{\gamma\varepsilon_1}{\beta}$, we can deduce the followings

$$\left|\frac{\partial^i \widehat{u}^{n+1/2}}{\partial x^i}(0,y)\right| \leq C\varepsilon_1^{-i/2}, \quad \left|\frac{\partial^i \widehat{u}^{n+1/2}}{\partial x^i}(1,y)\right| \leq C\varepsilon_1^{-i/2}, \quad 0 \leq i \leq 4.$$

To bound the term $\left|\dfrac{\partial \widehat{u}^{n+1/2}}{\partial x}(x,y)\right|$ for $0<x<1$, we differentiate (4.2.12) with respect to x. Thus, we have

$$\left(I+\varepsilon_2\Delta t\frac{\partial b_1}{\partial x}+\Delta t\mathcal{L}_{x,\varepsilon}\right)\frac{\partial \widehat{u}^{n+1/2}}{\partial x} = \frac{\partial u(t_n)}{\partial x}+\Delta t\frac{\partial f_1}{\partial x}(x,y,t_{n+1})-\widehat{u}^{n+1/2}\frac{\partial c_1}{\partial x}\Delta t.$$

Let us define $g(x,y):=\dfrac{\partial u(t_n)}{\partial x}+\Delta t\dfrac{\partial f_1}{\partial x}(x,y,t_{n+1})-\widehat{u}^{n+1/2}\dfrac{\partial c_1}{\partial x}\Delta t.$

We know that the operator $\left(I+\varepsilon_2\Delta t\dfrac{\partial b_1}{\partial x}+\Delta t\mathcal{L}_{x,\varepsilon}\right)$ satisfies the maximum principle for $\dfrac{\partial b_1}{\partial x}\geq\delta>0$. Then, using the results in (4.2.2)-(4.2.3) we have

$$|g(x,y)|\leq C\left[1+\varepsilon_1^{-1/2}\left(e^{-\sqrt{\frac{\beta\gamma}{\varepsilon_1}}x}+e^{-\sqrt{\frac{\beta\gamma}{\varepsilon_1}}(1-x)}\right)\right].$$

On the other hand, let us consider the following functions

$$\eta_1(x)=1+x,$$
$$\eta_2(x)=\varepsilon_1^{-1/2}\left(e^{-\sqrt{\frac{\beta\gamma}{\varepsilon_1}}x}+e^{-\sqrt{\frac{\beta\gamma}{\varepsilon_1}}(1-x)}\right).$$

Now, we can choose two sufficiently large constants $C_1,\ C_2$ such that

$$\left|\left(I+\varepsilon_2\Delta t\frac{\partial b_1}{\partial x}+\Delta t\mathcal{L}_{x,\varepsilon}\right)\frac{\partial \widehat{u}^{n+1/2}}{\partial x}\right| \leq |g(x,y)|\leq\left(I+\varepsilon_2\Delta t\frac{\partial b_1}{\partial x}+\Delta t\mathcal{L}_{x,\varepsilon}\right)\Big(C_1\eta_1(x)+C_2\eta_2(x)\Big),$$
$$\left|\frac{\partial \widehat{u}^{n+1/2}}{\partial x}(0,y)\right|\leq\ C\varepsilon_1^{-1/2}\leq C_1\eta_1(0)+C_2\eta_2(0),$$
$$\left|\frac{\partial \widehat{u}^{n+1/2}}{\partial x}(1,y)\right|\leq\ C\varepsilon_1^{-1/2}\leq C_1\eta_1(1)+C_2\eta_2(1).$$

Finally, by using the maximum principle in Lemma 4.2.1, we conclude that

$$\left|\frac{\partial \widehat{u}^{n+1/2}}{\partial x}\right|\leq\Big(C_1\eta_1(x)+C_2\eta_2(x)\Big)\leq C\left[1+\varepsilon_1^{-1/2}\left(e^{-\sqrt{\frac{\beta\gamma}{\varepsilon_1}}x}+e^{-\sqrt{\frac{\beta\gamma}{\varepsilon_1}}(1-x)}\right)\right]. \tag{4.2.32}$$

We note that by using similar techniques, one can prove (5.2.15) for the cases $i=2,\ 3,\ 4$. □

We also prove the following estimates of the derivatives of the semi-discrete solution $\widehat{u}^{n+1}$ with respect to y analogously.

Lemma 4.2.7. *Let $\widehat{u}^{n+1}$ be the semi-discrete solution of the problem (4.2.12) for $0 \leq n \leq M-1$. Then,*

$$\left|\frac{\partial^j \widehat{u}^{n+1}}{\partial y^j}\right| \leq C\left[1+\varepsilon_1^{-j/2}\left(e^{-\sqrt{\frac{\beta\gamma}{\varepsilon_1}}y}+e^{-\sqrt{\frac{\beta\gamma}{\varepsilon_1}}(1-y)}\right)\right] \tag{4.2.33}$$

holds for $0 \leq j \leq 4$.

In order to prove the uniform convergence of the fully-discrete scheme (4.2.21) and (4.2.22), we discretize the semidiscrete problems (4.2.12) first and then find the associated truncation error estimates. Suppose, the totally discrete form of (4.2.12) is defined as

$$\begin{cases} \left[I+\Delta t L_{x,\varepsilon}^N\right]\widehat{U}_{ij}^{n+1/2} := r_{ij}^-\widehat{U}_{i-1,j}^{n+1/2}+r_{ij}^0\widehat{U}_{ij}^{n+1/2}+r_{ij}^+\widehat{U}_{i+1,j}^{n+1/2} = u(x_i,y_j,t_n)+\Delta t f_{1_{ij}}^{n+1}, \\ \widehat{U}_{0,j}^{n+1/2} = \widehat{U}_{N,j}^{n+1/2} = 0, \quad 1 \leq j \leq N-1, \end{cases} \tag{4.2.34}$$

for every fixed y_j and

$$\begin{cases} \left[I+\Delta t L_{x,\varepsilon}^N\right]\widehat{U}_{ij}^{n+1} := s_{ij}^-\widehat{U}_{i,j-1}^{n+1}+s_{ij}^0\widehat{U}_{ij}^{n+1/2}+s_{ij}^+\widehat{U}_{i,j+1}^{n+1} = \widehat{U}_{ij}^{n+1/2}+\Delta t f_{2_{ij}}^{n+1}, \\ \widehat{U}_{i,0}^{n+1} = \widehat{U}_{i,N}^{n+1} = 0, \quad 1 \leq i \leq N-1, \end{cases} \tag{4.2.35}$$

for every fixed x_i.

Lemma 4.2.8. *Let $\widehat{U}^{n+1/2}$ be the solution of the totally discrete form of (4.2.12) and $\widehat{u}^{n+1/2}$ be the semidiscrete solution of (4.2.12) on $\overline{\Omega}^N$. Then the following estimates hold*

$$\left\|\widehat{U}^{n+1/2}-\widehat{u}^{n+1/2}\big|_{\overline{\Omega}^N}\right\|_{\infty,\overline{\Omega}^N} \leq C\Delta t N^{-1}\ln N. \tag{4.2.36}$$

Proof. We estimate the error in maximum norm on the mesh $\overline{\Omega}_x^N$ for each fixed y_j by defining the truncation error as

$$\theta_i = \left(I+\Delta t L_{x,\varepsilon}^N\right)\widehat{u}^{n+1/2}(x_i,y_j)-\left(I+\Delta t\mathcal{L}_{x,\varepsilon}\right)\widehat{u}^{n+1/2}(x_i,y_j), \ 1 \leq i \leq N-1. \tag{4.2.37}$$

Recall that from (4.2.12), we have

$$\left[I+\Delta t\mathcal{L}_{x,\varepsilon}\right]\widehat{u}^{n+1/2} = u(t_n)+\Delta t f_1(x,y,t_{n+1}), \quad 0 \leq x,y \leq 1.$$

We introduce the notation $R_n(g, x_1, x_2) = \dfrac{1}{n!}\displaystyle\int_{x_1}^{x_2}(x_2 - s)^n g^{(n+1)}(s)ds$ to denote the integral remainder in the Taylor series expression of the function g about the point x_1 after the $(n+1)$-th term. Thus, we have

$$\begin{aligned}\theta_i &= -\varepsilon_1\Delta t\left(\Delta_x\widehat{u}^{n+1/2} - \frac{\partial^2\widehat{u}^{n+1/2}}{\partial x^2}\right)(x_i, y_j) + \Delta t\varepsilon_2 b_{1,ij}\left(\delta_x^-\widehat{u}^{n+1/2} - \frac{\partial\widehat{u}^{n+1/2}}{\partial x}\right)(x_i, y_j)\\ &= -\frac{\varepsilon_1\Delta t}{3}\big(h_{i+1}^x - h_i^x\big)\frac{\partial^3\widehat{u}^{n+1/2}}{\partial x^3}(x_i, y_j) + r_{ij}^+\ R_3\big(\widehat{u}^{n+1/2}, x_i, x_{i+1}\big)\\ &+ r_{ij}^-\ R_3\big(\widehat{u}^{n+1/2}, x_i, x_{i-1}\big) + \varepsilon_2\Delta t\ b_{1,ij}\left(-\frac{h_i^x}{2}\frac{\partial^2\widehat{u}^{n+1/2}}{\partial x^2}(x_i, y_j) + \frac{(h_i^x)^2}{3!}\frac{\partial^3\widehat{u}^{n+1/2}}{\partial x^3}(x_i, y_j)\right),\end{aligned} \tag{4.2.38}$$

where the coefficients r_{ij}^+, r_{ij}^- are given in (4.2.23). Clearly, $h_{i+1}^x - h_i^x = 0$ for $i \notin \Big\{N/4,\ 3N/4\Big\}$.

We find the estimate for θ_i for the values of x_i in each region, namely inside and outside the layer regions. We will consider the following three typical cases:

Case (i): Consider the case when $0 < x_i < \tau_x$.

In this case, we have

$$h_{i+1}^x = h_i^x = \frac{8}{N}\sqrt{\frac{\varepsilon_1}{\beta\gamma}}\ln N \le C\varepsilon_1^{1/2}N^{-1}\ln N.$$

Using the previous inequality and the fact that $\varepsilon_2 \le C\varepsilon_1^{1/2}$, one can easily deduce

$$\begin{aligned}&\left|\varepsilon_2\Delta t\ b_1(x_i, y_j)\left(-\frac{h_i^x}{2}\frac{\partial^2\widehat{u}^{n+1/2}}{\partial x^2}(x_i, y_j) + \frac{(h_i^x)^2}{3!}\frac{\partial^3\widehat{u}^{n+1/2}}{\partial x^3}(x_i, y_j)\right)\right|\\ &\qquad\le\ C\varepsilon_1\Delta t\ N^{-1}\ln N\left[1 + \varepsilon_1^{-1}\left(e^{-\sqrt{\frac{\beta\gamma}{\varepsilon_1}}x_i} + e^{-\sqrt{\frac{\beta\gamma}{\varepsilon_1}}(1-x_i)}\right)\right]\\ &\qquad+\ C\varepsilon_1^{3/2}\Delta t\big(N^{-1}\ln N\big)^2\left[1 + \varepsilon_1^{-3/2}\left(e^{-\sqrt{\frac{\beta\gamma}{\varepsilon_1}}x_i} + e^{-\sqrt{\frac{\beta\gamma}{\varepsilon_1}}(1-x_i)}\right)\right]\\ &\qquad\le\ C\Delta t\left[N^{-1}\ln N + \varepsilon_1^{3/2}\big(N^{-1}\ln N\big)^2\right] \le\ C\Delta t\ N^{-1}\ln N.\end{aligned} \tag{4.2.39}$$

On the other hand, we have

$$\begin{aligned}
\left|r_{ij}^{+}\ R_3\big(\widehat{u}^{n+1/2}, x_i, x_{i+1}\big)\right| &= \left|-\frac{2\varepsilon_1}{(h_i^x + h_{i+1}^x)}\frac{\Delta t}{h_{i+1}^x}\right| \left|\frac{1}{3!}\int_{x_i}^{x_{i+1}} (x_{i+1}-s)^3 \frac{\partial^4 \widehat{u}^{n+1/2}}{\partial x^4}(s, y_j)ds\right| \\
&\leq\ C\varepsilon_1 \Delta t \big(h_{i+1}^x\big)^2 \left[1 + \varepsilon_1^{-2}\left(e^{-\sqrt{\frac{\beta\gamma}{\varepsilon_1}}x_i} + e^{-\sqrt{\frac{\beta\gamma}{\varepsilon_1}}(1-x_{i+1})}\right)\right] \\
&\leq\ C\Delta t \big(\varepsilon_1^{1/2} N^{-1}\ln N\big)^2 \left[1 + \varepsilon_1^{-1}\left(e^{-\sqrt{\frac{\beta\gamma}{\varepsilon_1}}x_i} + e^{-\sqrt{\frac{\beta\gamma}{\varepsilon_1}}(1-x_{i+1})}\right)\right] \leq\ C\Delta t \big(N^{-1}\ln N\big)^2.
\end{aligned} \tag{4.2.40}$$

Similarly, one can deduce the following

$$\left|r_{ij}^{-}\ R_3\big(\widehat{u}^{n+1/2}, x_i, x_{i-1}\big)\right| \leq C\Delta t \big(N^{-1}\ln N\big)^2. \tag{4.2.41}$$

Therefore, from (4.2.39)-(4.2.41) we obtain

$$|\theta_i| \leq C\Delta t\ N^{-1}\ln N, \tag{4.2.42}$$

when $0 < x_i < \tau_x$.

Case (ii): Let us now consider the case when $\tau_x < x_i < 1-\tau_x$.

To find the estimate for the truncation error in this region, we recall that the spatial step-lengths are given by

$$h_{i+1}^x = h_i^x = \frac{2}{N}\Big(1-2\tau_x\Big) = \frac{2}{N}\Big(1 - 4\sqrt{\frac{\varepsilon_1}{\beta\gamma}}\ln N\Big)$$

and observe that $h_i^x \leq N^{-1}$ for the current case.

Therefore, we obtain the following

$$\begin{aligned}
\left|r_{ij}^{+}\ R_3\big(\widehat{u}^{n+1/2}, x_i, x_{i+1}\big)\right| &\leq C\varepsilon_1\Delta t\ h_{i+1}^x \left|\int_{x_i}^{x_{i+1}} \frac{\partial^4 \widehat{u}^{n+1/2}}{\partial x^4}(s, y_j)ds\right| \\
&\leq\ C\varepsilon_1\Delta t\ h_{i+1}^x \int_{x_i}^{x_{i+1}} \left[1 + \varepsilon_1^{-2}\left(e^{-\sqrt{\frac{\beta\gamma}{\varepsilon_1}}s} + e^{-\sqrt{\frac{\beta\gamma}{\varepsilon_1}}(1-s)}\right)ds\right] \\
&\leq\ C\varepsilon_1\Delta t\ {h_{i+1}^x}^2 + C\varepsilon_1^{-1}\Delta t\ h_{i+1}^x \left[-\frac{e^{-\sqrt{\frac{\beta\gamma}{\varepsilon_1}}s}}{\sqrt{\frac{\beta\gamma}{\varepsilon_1}}}\right]_{s=x_i}^{x_{i+1}} + C\varepsilon_1^{-1}\Delta t\ h_{i+1}^x \left[\frac{e^{-\sqrt{\frac{\beta\gamma}{\varepsilon_1}}(1-s)}}{\sqrt{\frac{\beta\gamma}{\varepsilon_1}}}\right]_{s=x_i}^{x_{i+1}}
\end{aligned}$$

$$\leq C\varepsilon_1\Delta t\ N^{-2} + C\Delta t N^{-1}\frac{1}{\sqrt{\varepsilon_1}}\left(e^{-\sqrt{\frac{\beta\gamma}{\varepsilon_1}}x_i} + e^{-\sqrt{\frac{\beta\gamma}{\varepsilon_1}}x_{i+1}}\right)$$
$$+ C\Delta t N^{-1}\frac{1}{\sqrt{\varepsilon_1}}\left(e^{-\sqrt{\frac{\beta\gamma}{\varepsilon_1}}(1-x_i)} + e^{-\sqrt{\frac{\beta\gamma}{\varepsilon_1}}(1-x_{i+1})}\right).$$

Using the fact that $\frac{1}{\sqrt{\varepsilon_1}}e^{-\frac{\alpha}{\sqrt{\varepsilon_1}}} \leq \frac{C}{\alpha}$ for any $\alpha > 0$, we have

$$\left|r_{ij}^{+}\ R_3\big(\widehat{u}^{n+1/2}, x_i, x_{i+1}\big)\right| \leq C\varepsilon_1\Delta t N^{-2} + C\Delta t N^{-1}\left(\frac{1}{x_i} + \frac{1}{x_{i+1}}\right)$$
$$+ C\Delta t N^{-1}\left(\frac{1}{1-x_i} + \frac{1}{1-x_{i+1}}\right).$$

Since $\tau_x < x_i < 1-\tau_x$, we have the following

$$\frac{1}{x_i} < \frac{1}{\tau_x} \leq C\Big(\sqrt{\varepsilon_1}\ln N\Big)^{-1}, \quad \text{and} \quad \frac{1}{1-x_i} < \frac{1}{\tau_x} \leq C\Big(\sqrt{\varepsilon_1}\ln N\Big)^{-1}.$$

Therefore, it follows that

$$\left|r_{ij}^{+}\ R_3\big(\widehat{u}^{n+1/2}, x_i, x_{i+1}\big)\right| \leq C\varepsilon_1\Delta t\ N^{-2} + C\Delta t N^{-1}\Big(\sqrt{\varepsilon_1}\ln N\Big)^{-1}.$$

Now using the fact that $1/\sqrt{\varepsilon_1} \leq C\ln N$ when $\varepsilon_2^2 \leq C\varepsilon_1$, we have

$$\left|r_{ij}^{+}\ R_3\big(\widehat{u}^{n+1/2}, x_i, x_{i+1}\big)\right| \leq C\varepsilon_1\Delta t\ N^{-2} + C\Delta t N^{-1} \leq C\Delta t N^{-1}. \tag{4.2.43}$$

Similarly, one can also get the following inequality

$$\left|r_{ij}^{-}\ R_3\big(\widehat{u}^{n+1/2}, x_i, x_{i-1}\big)\right| \leq C\Delta t N^{-1}. \tag{4.2.44}$$

We also have

$$\left|\varepsilon_2\Delta t\ b_1(x_i,y_j)\left(-\frac{h_i^x}{2}\frac{\partial^2\widehat{u}^{n+1/2}}{\partial x^2}(x_i,y_j) + \frac{h_i^{x2}}{3!}\frac{\partial^3\widehat{u}^{n+1/2}}{\partial x^3}(x_i,y_j)\right)\right|$$
$$\leq C\varepsilon_2\Delta t\ h_i^x\left[1+\varepsilon_1^{-1}\left(e^{-\sqrt{\frac{\beta\gamma}{\varepsilon_1}}x_i} + e^{-\sqrt{\frac{\beta\gamma}{\varepsilon_1}}(1-x_i)}\right)\right]$$
$$+\ C\varepsilon_2\Delta t\ \left(h_i^x\right)^2\left[1+\varepsilon_1^{-3/2}\left(e^{-\sqrt{\frac{\beta\gamma}{\varepsilon_1}}x_i} + e^{-\sqrt{\frac{\beta\gamma}{\varepsilon_1}}(1-x_i)}\right)\right]$$

$$\leq C\varepsilon_2\Delta t\left[h_i^x+\left(h_i^x\right)^2+\frac{N^{-1}}{\sqrt{\varepsilon_1}}\left(\frac{1}{x_i}+\frac{1}{1-x_i}\right)+\frac{N^{-2}}{\varepsilon_1}\left(\frac{1}{x_i}+\frac{1}{1-x_i}\right)\right]$$
$$\leq C\frac{\varepsilon_2}{\sqrt{\varepsilon_1}}\Delta t\left(\sqrt{\varepsilon_1}N^{-1}+N^{-1}\left(\sqrt{\varepsilon_1}\ln N\right)^{-1}\right).$$

Using $1/\sqrt{\varepsilon_1}\leq C\ln N$ and $\varepsilon_2^2\leq C\varepsilon_1$, we have

$$\left|\varepsilon_2\Delta t\ b_1(x_i,y_j)\left(-\frac{h_i^x}{2}\frac{\partial^2\widehat{u}^{n+1/2}}{\partial x^2}(x_i,y_j)+\frac{(h_i^x)^2}{3!}\frac{\partial^3\widehat{u}^{n+1/2}}{\partial x^3}(x_i,y_j)\right)\right|\leq C\Delta t\ N^{-1}. \quad (4.2.45)$$

From the above estimates, it follows that

$$|\theta_i|\leq C\Delta t\ N^{-1}. \quad (4.2.46)$$

Case (iii): We now consider the case when $1-\tau_x<x_i<1$. The bounds for this case follows directly by the application of the estimates in Case (i) because we have the same boundary layer width and the same grid structure in Case (i) and Case (iii). Thus, the estimate in (4.2.42) also holds for the current case.

Case (iv): Finally, we consider the estimates at $x_i=\tau_x$ or $x_i=1-\tau_x$. In this case, the step-lengths on the left and right to x_i are either $h_i^x=\dfrac{4\tau_x}{N}$ or $h_i^x=\dfrac{2(1-2\tau_x)}{N}$. Thus, $\left|h_i^x-h_{i+1}^x\right|=\dfrac{2(1-4\tau_x)}{4}\leq CN^{-1}$. We now bound the following term in (4.2.38) as

$$\left|\frac{\varepsilon_1\Delta t}{3}\left(h_{i+1}^x-h_i^x\right)\frac{\partial^3\widehat{u}^{n+1/2}}{\partial x^3}(x_i,y_j)\right|$$
$$\leq\frac{C\varepsilon_1\Delta t}{N}\left[1+\varepsilon_1^{-3/2}\left(e^{-\sqrt{\frac{\beta\gamma}{\varepsilon_1}}\tau_x}+e^{-\sqrt{\frac{\beta\gamma}{\varepsilon_1}}(1-\tau_x)}\right)\right]$$
$$\leq\frac{C\Delta t}{N}\left[\varepsilon_1+\varepsilon_1^{-1/2}\left(e^{-\sqrt{\frac{\beta\gamma}{\varepsilon_1}}\tau_x}+e^{-\sqrt{\frac{\beta\gamma}{\varepsilon_1}}(1-\tau_x)}\right)\right]\leq C\Delta tN^{-1}, \quad (4.2.47)$$

where we use the property $e^{-t}<C/t^k$, $t>0$, $k\in\mathbb{N}$ to show the boundedness of the term inside the square bracket. We also prove that

$$\left|r_{ij}^+\ R_3\left(\widehat{u}^{n+1/2},x_i,x_{i+1}\right)\right|\leq C\Delta tN^{-1}\ln N,\quad \left|r_{ij}^-\ R_3\left(\widehat{u}^{n+1/2},x_i,x_{i-1}\right)\right|\leq C\Delta t\ N^{-1}\ln N, \quad (4.2.48)$$

$$\left|\varepsilon_2\Delta t\ b_1(x_i,y_j)\left(-\frac{h_i^x}{2}\frac{\partial^2\widehat{u}^{n+1/2}}{\partial x^2}(x_i,y_j)+\frac{h_i^{x2}}{3!}\frac{\partial^3\widehat{u}^{n+1/2}}{\partial x^3}(x_i,y_j)\right)\right|\leq C\Delta t\ N^{-1}\ln N, \quad (4.2.49)$$

similarly as in **Case (i)** or **Case (ii)**.

From (4.2.47)-(4.2.49), it follows that

$$|\theta_i| \leq C\Delta t\ N^{-1} \ln N. \tag{4.2.50}$$

Therefore, from the above discussions, it is clear that

$$\left|\left[\left(I + \Delta t L^N_{x,\varepsilon}\right) - \left(I + \Delta t \mathcal{L}_{x,\varepsilon}\right)\right] \widehat{u}^{n+1/2}(x_i, y_j)\right| = |\theta_i| \leq C\Delta t N^{-1} \ln N, \tag{4.2.51}$$

for every fixed $y_j \in \overline{\Omega}^N_y$.

Therefore, the truncation error for the complete discretization of the semidiscrete problem (4.2.12) has the following estimate

$$|\theta_i| \leq \begin{cases} C\Delta t\ N^{-1}, & \tau_x < x_i < 1 - \tau_x \\ C\Delta t\ N^{-1} \ln N, & x_i \leq \tau_x, \quad x_i \geq 1 - \tau_x. \end{cases} \tag{4.2.52}$$

Thus, $|\theta_i| \leq C\Delta t\ N^{-1} \ln N, \quad x_i \in \overline{\Omega}^N_x$. We now define the discrete barrier function $\Phi = C_1 \Delta t\ N^{-1} \ln N$ on the mesh $\overline{\Omega}^N_x$ for some $C_1 > 0$. Then,

$$\begin{aligned} &\left(I + \Delta t L^N_{x,\varepsilon}\right) \left[\Phi \pm (\widehat{U}^{n+1/2}_{ij} - \widehat{u}^{n+1/2}(x_i, y_j))\right] \\ &= C_1(1 + \Delta t c_{1,ij})\Delta t\ N^{-1} \ln N \pm \left(I + \Delta t L^N_{x,\varepsilon}\right) \left[\widehat{U}^{n+1/2}_{ij} - \widehat{u}^{n+1/2}(x_i, y_j)\right] \geq 0, \end{aligned}$$

for sufficiently large values of C_1. Using discrete maximum principle for the operator $\left(I + \Delta t L^N_{x,\varepsilon}\right)$ one can easily have,

$$\left|\widehat{U}^{n+1/2}_{ij} - \widehat{u}^{n+1/2}(x_i, y_j)\right| \leq C\Delta t\ N^{-1} \ln N, \quad x_i \in \overline{\Omega}^N_x. \tag{4.2.53}$$

Hence, the result follows. □

Theorem 4.2.9. *Let $\widehat{U}^{n+1}$ be the solution of the discrete form of the problem (4.2.12) at $t = t_{n+1}$ and $\widehat{u}^{n+1}$ be the solution of (4.2.12). Then, we have the following estimate*

$$\left\|\widehat{U}^{n+1} - \widehat{u}^{n+1}|_{\overline{\Omega}^N}\right\|_{\infty,\overline{\Omega}^N} \leq C\Delta t N^{-1} \ln N. \tag{4.2.54}$$

Proof. Recalling the function defined $\widehat{u}^{n+1/2}$ in (4.2.12.a) and the corresponding discrete version $\widehat{U}^{n+1/2}$ in (4.2.21) and using the Lemma 4.2.8, we have

$$\left\|\widehat{U}^{n+1/2} - \widehat{u}^{n+1/2}|_{\overline{\Omega}^N}\right\|_{\infty,\overline{\Omega}^N} \leq C\Delta t N^{-1} \ln N.$$

We introduce the following problem

$$\begin{cases} \left(I + \Delta t L^N_{y,\varepsilon}\right)\tilde{U}^{n+1}_{ij} = \widehat{u}^{n+1/2}_{ij}\Big|_{\overline{\Omega}^N} + \Delta t f^{n+1}_{2_{i,j}}, \\ \widetilde{U}^{n+1}_{i,0} = 0, \quad \widetilde{U}^{n+1}_{i,N} = 0, \quad 1 \le i \le N-1. \end{cases} \tag{4.2.55}$$

A similar argument in Lemma 4.2.8 gives,

$$\left\| \widetilde{U}^{n+1} - \widehat{u}^{n+1}|_{\overline{\Omega}^N} \right\|_{\infty,\overline{\Omega}^N} \le C\Delta t N^{-1} \ln N. \tag{4.2.56}$$

We also have

$$\widehat{U}^{n+1} - \widehat{u}^{n+1}|_{\overline{\Omega}^N} = \left(\widehat{U}^{n+1} - \widetilde{U}^{n+1}\right) + \left(\widetilde{U}^{n+1} - \widehat{u}^{n+1}|_{\overline{\Omega}^N}\right),$$

$$\text{and} \quad \left(\widehat{U}^{n+1} - \widetilde{U}^{n+1}\right) = \left(I + \Delta t L^N_{y,\varepsilon}\right)^{-1}\left(\widehat{U}^{n+1/2} - \widehat{u}^{n+1/2}|_{\overline{\Omega}^N}\right).$$

Finally using the property $\left\|\left(I + \Delta t L^N_{y,\varepsilon}\right)^{-1}\right\|_{\infty,\overline{\Omega}^N} \le C$, we obtain the desired result. □

Theorem 4.2.10. *Let U^n be the solution of the fully-discrete problem (4.2.21)-(4.2.22) at the time level t_n and u is the exact solution of the main problem (4.1.1). Then, we have the following global error estimate*

$$\left\|U^n - u(t_n)|_{\overline{\Omega}^N}\right\|_{\infty,\overline{\Omega}^N} \;\le\; C\big(\Delta t + N^{-1}\ln N\big). \tag{4.2.57}$$

Proof. We first express the error in the following form

$$U^n - u(t_n)|_{\overline{\Omega}^N} = \left(U^n - \widehat{U}^n\right) + \left(\widehat{U}^n - \widehat{u}^n|_{\overline{\Omega}^N}\right) + \left(\widehat{u}^n|_{\overline{\Omega}^N} - u(t_n)|_{\overline{\Omega}^N}\right), \tag{4.2.58}$$

where $\widehat{U}^n$ is the solution of the discrete form of the problem (4.2.12) using $u(t_{n-1})|_{\Omega^N}$ as the starting value for the n-th iteration.

We recall the results from Lemma 4.2.2 and Theorem 4.2.9 to obtain

$$\left\|\widehat{u}^n|_{\overline{\Omega}^N} - u(t_n)|_{\overline{\Omega}^N}\right\|_{\infty,\overline{\Omega}^N} \le C\Delta t^2, \quad \left\|\widehat{U}^n - \widehat{u}^n|_{\overline{\Omega}^N}\right\|_{\infty,\overline{\Omega}^N} \le C\Delta t N^{-1}\ln N.$$

Using these estimates and the fact $\left\|\left(I+\Delta t L_{i,\varepsilon}^{N}\right)^{-1}\right\| \leq C, \quad i=x,y$, we have

$$\begin{aligned}\left\|U^{n}-u(t_n)|_{\overline{\Omega}^N}\right\|_{\infty,\overline{\Omega}^N} &\leq C\Delta t\big(\Delta t+N^{-1}\ln N\big)+C\left\|U^{n-1}-u(t_{n-1})|_{\overline{\Omega}^N}\right\|_{\infty,\overline{\Omega}^N}\\ &\leq Cn\Delta t\big(\Delta t+N^{-1}\ln N\big)\leq C\big(\Delta t+N^{-1}\ln N\big),\end{aligned}$$

since $n\Delta t\leq T$. □

4.2.4 Numerical experiments

In this section, we present some numerical results obtained by the fully-discrete scheme (4.2.21)-(4.2.22) for the following test problem on the Shishkin mesh $\overline{\Omega}^N$ defined in (4.2.20) with different time step sizes Δt.

Example 4.2.11. *Consider the following 2D parabolic IBVP:*

$$\begin{cases} u_t-\varepsilon_1\Delta u+\varepsilon_2\big(1+\dfrac{xy}{2}\big)\big(u_x+u_y\big)+u=t^2\Big(x^2+y^2-x-y\Big), & (x,y)\in\Omega,\quad 0<t\leq 1,\\ u(x,y,t)=0, & (x,y)\in\partial\Omega,\quad 0\leq t\leq 1,\\ u(x,y,0)=0, & (x,y)\in\Omega,\end{cases}$$

where we have $\beta_1=1,\ \beta_2=1$ and hence, $\beta=1$. Thus,

$$\gamma<\min_{\overline{\Omega}}\left\{\frac{c}{2b_1},\ \frac{c}{2b_2}\right\}=\frac{1}{2}.$$

Since the exact solution for this example is not known, we use double mesh principle to find the error in the computation to demonstrate parameter-uniform convergence rate. Suppose $U_{\varepsilon_1,\varepsilon_2}^{N,\Delta t}(x_i,y_j,t_n)$ is the computed numerical solution at the point (x_i,y_j,t_n) on the grid $\overline{\Omega}^N\times\overline{\Omega}_t^M$ with the uniform time step size $\Delta t=T/M$ while $\widetilde{U}_{\varepsilon_1,\varepsilon_2}^{2N,\Delta t/2}(x_i,y_j,t_n)$ denotes the approximated value at the same point on the Shishkin mesh $\widetilde{\Omega}^{2N}\times\widetilde{\Omega}_t^{2M}$ obtained by bisecting every subinterval of $\overline{\Omega}^N\times\overline{\Omega}_t^M$ with $2N$ subintervals in each space direction and $\Delta t/2$ uniform step-length in the time direction. Then, we define the pointwise error by

$$E_{\varepsilon_1,\varepsilon_2}^{N,\Delta t}=\max_{\substack{(x_i,y_j)\in\overline{\Omega}^N\\ t_n\in\overline{\Omega}_t^M}}\left|U_{\varepsilon_1,\varepsilon_2}^{N,\Delta t}(x_i,y_j,t_n)-\widetilde{U}_{\varepsilon_1,\varepsilon_2}^{2N,\Delta t/2}(x_i,y_j,t_n)\right|. \tag{4.2.59}$$

The corresponding order of convergence is defined as,

$$p^{N,\Delta t}_{\varepsilon_1,\varepsilon_2} = \log_2\left(\frac{E^{N,\Delta t}_{\varepsilon_1,\varepsilon_2}}{E^{2N,\Delta t/2}_{\varepsilon_1,\varepsilon_2}}\right). \tag{4.2.60}$$

Here, we use the following set of parameters satisfying the condition on the parameters for Case I:

$$S_\varepsilon = \left\{(\varepsilon_1,\varepsilon_2) : \varepsilon_1 = 10^{-k-1}, \quad \varepsilon_2 = \frac{\sqrt{\varepsilon_1}}{10}, \quad k = 1, 2, \ldots, 6\right\}. \tag{4.2.61}$$

The values of the maximum error $E^{N,\Delta t}$ and the corresponding rate $p^{N,\Delta t}$ defined in (4.2.62) for Example 4.2.11 are displayed in Table 4.2 for different pair of values of $(\varepsilon_1,\varepsilon_2) \in S_\varepsilon$, N and Δt. The associated loglog plot of the numerical error is also given for various values of the mesh parameters N, Δt. For each N, the number of points in each spatial direction and fixed time step Δt, we define the parameter-uniform maximum error and the corresponding parameter-uniform convergence rate respectively by

$$E^{N,\Delta t} = \max_{\varepsilon_1,\varepsilon_2} E^{N,\Delta t}_{\varepsilon_1,\varepsilon_2}, \quad p^{N,\Delta t} = \log_2\left(\frac{E^{N,\Delta t}}{E^{2N,\Delta t/2}}\right). \tag{4.2.62}$$

From the above presentation in Table 4.2, we see the gradually decreasing behavior of the pointwise error $E^{N,\Delta t}_{\varepsilon_1,\varepsilon_2}$ as the number of spatial grid points N is increasing. We also observe that as the values of the perturbation parameters tend to be very small, the pointwise errors are still remaining to be bounded, which ensures the numerical stability of the proposed scheme. The pointwise and uniform rates of convergence $p^{N,\Delta t}_{\varepsilon_1,\varepsilon_2}$, $p^{N,\Delta t}$ displayed in the table clearly indicates the first-order parameter-uniform convergence, which is also graphically observed from the loglog plot in Figure 4.4.

4.3 Application of the ADI finite difference scheme: Case II

We have discussed the convergence analysis of the numerical solution for the first case $\varepsilon_2^2 \leq \frac{\gamma\varepsilon_1}{\beta}$ in Section 4.2. In this section, we study the analysis for the parameters satisfying the second case, *i.e.*, $\varepsilon_2^2 \geq \frac{\gamma\varepsilon_1}{\beta}$ and extend the results that we have proved in the previous section. For the present case, we have regular boundary layers of width $O(\varepsilon_2)$ near the inflow boundaries $x = 0$ and $y = 0$, while there are boundary layers of width $O\Big(\varepsilon_1/\varepsilon_2\Big)$ condensing

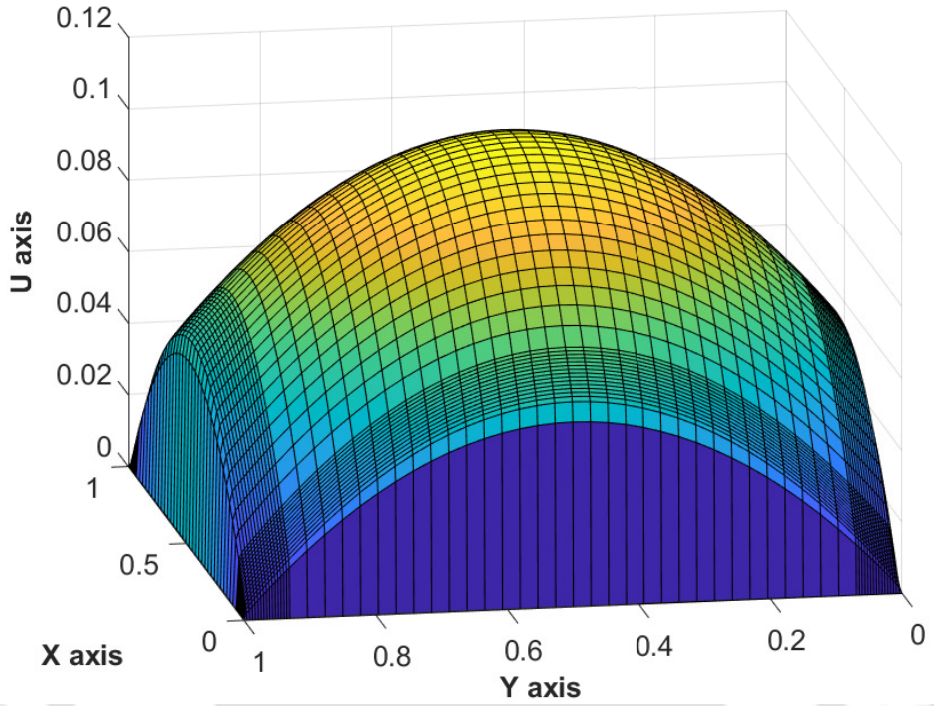

Figure 4.3: Surface plot of the numerical solution with $N = 64$ and $\varepsilon_1 = 10^{-7}$ at $t = 1$.

at the outflow boundaries $x = 1$ and $y = 1$. We proceed with the same numerical scheme discussed in the previous sections. We also apply the same Shishkin-type decomposition of the solution of (4.1.1) and the components of the solution in this case satisfy the following bounds: The boundary layer components of u satisfy the following bounds,

$$\left|\frac{\partial^{k_s+k_t} v}{\partial x^{k_1}\partial y^{k_2}\partial t^{k_t}}\right| \leq C, \tag{4.3.1}$$

$$\left|\frac{\partial^{k_s+k_t} w_L}{\partial x^{k_1}\partial y^{k_2}\partial t^{k_t}}\right| \leq C\varepsilon_2^{-k_1} e^{-\frac{\gamma x}{2\varepsilon_2}}, \tag{4.3.2}$$

$$\left|\frac{\partial^{k_s+k_t} w_R}{\partial x^{k_1}\partial y^{k_2}\partial t^{k_t}}\right| \leq C\left(\frac{\varepsilon_1}{\varepsilon_2}\right)^{-k_1} e^{-\frac{\beta\varepsilon_2}{2\varepsilon_1}(1-x)}, \tag{4.3.3}$$

$$\left|\frac{\partial^{k_s+k_t} w_B}{\partial x^{k_1}\partial y^{k_2}\partial t^{k_t}}\right| \leq C\varepsilon_2^{-k_2} e^{-\frac{\gamma y}{2\varepsilon_2}}, \tag{4.3.4}$$

$$\left|\frac{\partial^{k_s+k_t} w_T}{\partial x^{k_1}\partial y^{k_2}\partial t^{k_t}}\right| \leq C\left(\frac{\varepsilon_1}{\varepsilon_2}\right)^{-k_2} e^{-\frac{\beta\varepsilon_2}{2\varepsilon_1}(1-y)}, \tag{4.3.5}$$

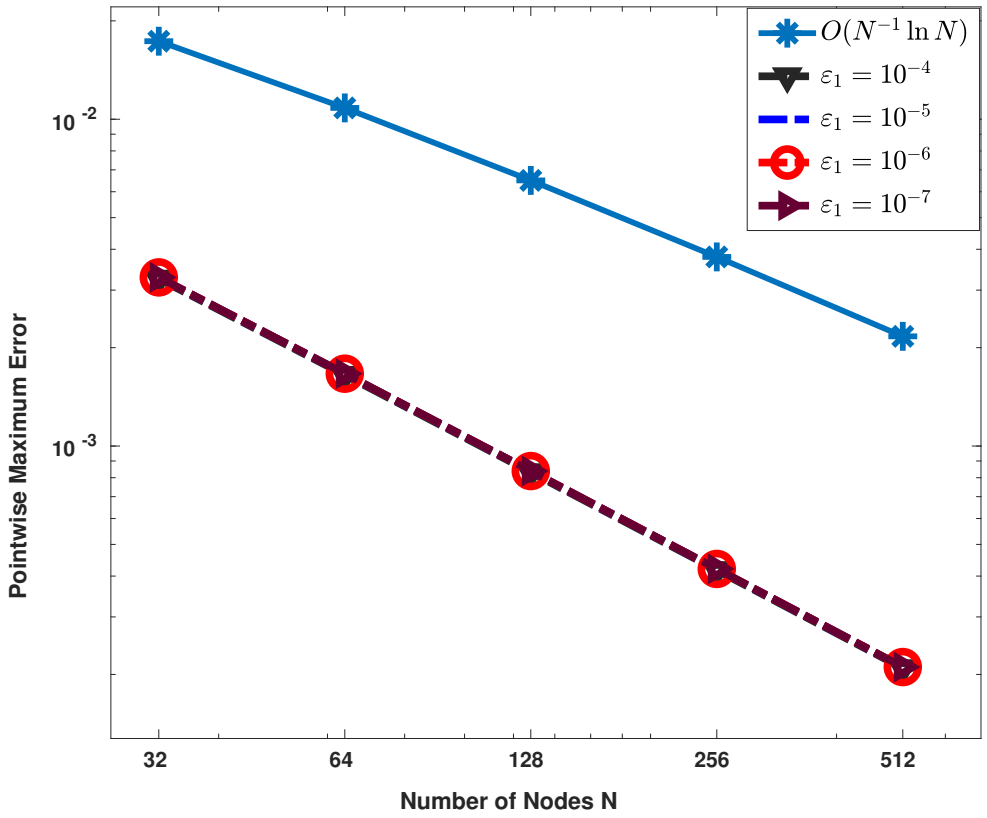

Figure 4.4: Graphical representation of the loglog plot of maximum pointwise errors in Table 4.2.

Table 4.1: Maximum pointwise error and corresponding rate of convergence for Example 4.2.11 for the parameters defined in (4.2.61) with $\Delta t = 1/N$.

ε_1	$N = 32$	64	128	256	512
	$\Delta t = 1/32$	$1/64$	$1/128$	$1/256$	$1/512$
10^{-2}	3.2224e-03	1.6369e-03	8.2476e-04	4.1394e-04	2.0736e-04
	0.9771	0.9889	0.9945	0.9972	-
10^{-3}	3.2700e-03	1.6590e-03	8.3550e-04	4.1925e-04	2.1001e-04
	0.9789	0.9895	0.9948	0.9974	-
10^{-4}	3.2771e-03	1.6627e-03	8.3740e-04	4.2024e-04	2.1051e-04
	0.9789	0.9895	0.9947	0.9973	-
10^{-5}	3.2803e-03	1.6640e-03	8.3801e-04	4.2050e-04	2.1063e-04
	0.9791	0.9896	0.9948	0.9974	-
10^{-6}	3.2815e-03	1.6646e-03	8.3828e-04	4.2064e-04	2.1069e-04
	0.9791	0.9896	0.9948	0.9974	-
10^{-7}	3.2818e-03	1.6648e-03	8.3837e-04	4.2068e-04	2.1071e-04
	0.9791	0.9896	0.9948	0.9974	-
$E^{N,\Delta t}$	**3.2818e-03**	**1.6648e-03**	**8.3837e-04**	**4.2068e-04**	**2.1071e-04**
$p^{N,\Delta t}$	**0.9791**	**0.9896**	**0.9948**	**0.9974**	-

while the corner layer components satisfy

$$\left|\frac{\partial^{k_s+k_t} w_{LB}}{\partial x^{k_1}\partial y^{k_2}\partial t^{k_t}}\right| \leq C \min\left\{\varepsilon_2^{-k_1} e^{-\frac{\gamma x}{2\varepsilon_2}},\ \varepsilon_2^{-k_2} e^{-\frac{\gamma y}{2\varepsilon_2}}\right\}, \tag{4.3.6}$$

$$\left|\frac{\partial^{k_s+k_t} w_{RB}}{\partial x^{k_1}\partial y^{k_2}\partial t^{k_t}}\right| \leq C \min\left\{\left(\frac{\varepsilon_1}{\varepsilon_2}\right)^{-k_1} e^{-\frac{\beta\varepsilon_2}{2\varepsilon_1}(1-x)},\ \varepsilon_2^{-k_2} e^{-\frac{\gamma y}{2\varepsilon_2}}\right\}, \tag{4.3.7}$$

$$\left|\frac{\partial^{k_s+k_t} w_{LT}}{\partial x^{k_1}\partial y^{k_2}\partial t^{k_t}}\right| \leq C \min\left\{\varepsilon_2^{-k_1} e^{-\frac{\gamma x}{2\varepsilon_2}},\ \left(\frac{\varepsilon_1}{\varepsilon_2}\right)^{-k_2} e^{-\frac{\beta\varepsilon_2}{2\varepsilon_1}(1-y)}\right\}, \tag{4.3.8}$$

$$\left|\frac{\partial^{k_s+k_t} w_{RT}}{\partial x^{k_1}\partial y^{k_2}\partial t^{k_t}}\right| \leq C \min\left\{\left(\frac{\varepsilon_1}{\varepsilon_2}\right)^{-k_1} e^{-\frac{\beta\varepsilon_2}{2\varepsilon_1}(1-x)},\ \left(\frac{\varepsilon_1}{\varepsilon_2}\right)^{-k_2} e^{-\frac{\beta\varepsilon_2}{2\varepsilon_1}(1-y)}\right\}, \tag{4.3.9}$$

where $k_s = k_1 + k_2$ and $0 \leq k_1 + k_2 + 2k_t \leq 4$. Note that the estimates here follow from the rigorous parameter-explicit bounds established by [68].

Table 4.2: Maximum pointwise error and the rate of convergence for Example 4.2.11 for the parameters defined in (4.2.61) with $\Delta t = 2/N$.

ε_1	$N = 32$	64	128	256	512
	$\Delta t = 1/16$	$1/32$	$1/64$	$1/128$	$1/256$
10^{-2}	6.2810e-03	3.2397e-03	1.6446e-03	8.2841e-04	4.1574e-04
	0.9551	0.9781	0.9893	0.9946	-
10^{-3}	6.3591e-03	3.2747e-03	1.6613e-03	8.3664e-04	4.1982e-04
	0.9574	0.9790	0.9896	0.9948	-
10^{-4}	6.3689e-03	3.2796e-03	1.6638e-03	8.3792e-04	4.2047e-04
	0.9575	0.9790	0.9895	0.9947	-
10^{-5}	6.3724e-03	3.2812e-03	1.6645e-03	8.3821e-04	4.2060e-04
	0.9576	0.9791	0.9896	0.9948	-
10^{-6}	6.3737e-03	3.2817e-03	1.6647e-03	8.3835e-04	4.2067e-04
	0.9576	0.9791	0.9896	0.9948	-
10^{-7}	6.3741e-03	3.2819e-03	1.6648e-03	8.3840e-04	4.2069e-04
	0.9576	0.9791	0.9896	0.9948	-
$E^{N,\Delta t}$	**6.3741e-03**	**3.2819e-03**	**1.6648e-03**	**8.3840e-04**	4.2069e-04
$p^{N,\Delta t}$	**0.9576**	**0.9791**	**0.9896**	**0.9948**	-

4.3.1 Temporal and spatial discretizations

Let us note that the error estimates proved for the semi-discrete problem (4.2.10) does not depend on the discretization of the domain and the constructed Shishkin mesh. Therefore, the lemmas and the theorems stated in Section 4.2 are also valid for Case II.

We discretize the time interval $[0, T]$ using uniform step size $\Delta t = T/M$ as

$$\overline{\Omega}_t^M := \big\{ t_{j+1} = t_j + \Delta t, \quad t_0 = 0, \quad 0 \le j \le M - 1 \big\}.$$

The semi-discrete problem in this case can be defined exactly as in (4.2.10) and assume that u^n is the solution semi-discrete problem. We also define $\widehat{u}^n$ similarly as we have done in (4.2.12). The following results can be obtained in the same manner. Therefore, we state the lemmas without any further proofs.

Lemma 4.3.1. *The local truncation error e_{n+1} defined in (4.2.13) satisfies the following*

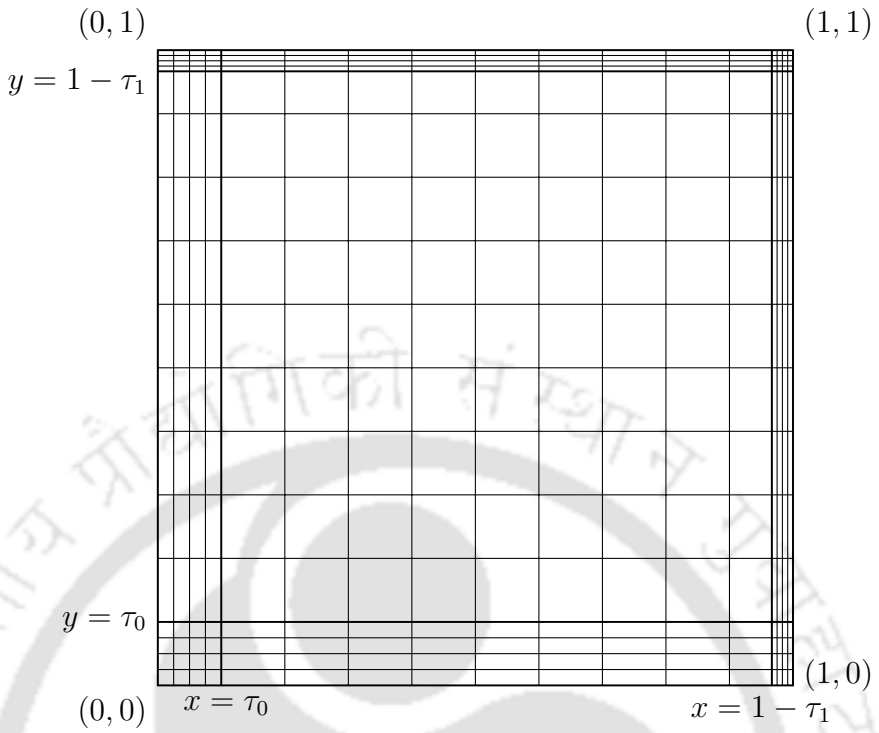

Figure 4.5: A sample Shishkin mesh for Case II with $N = 16$.

bound

$$\|e_{n+1}\|_{\infty,\overline{\Omega}} \leq C\Delta t^2, \quad 0 \leq n \leq M-1. \tag{4.3.10}$$

Theorem 4.3.2. *The global error E_n for the semi-discrete problem is bounded as*

$$\sup_{1\leq n\leq M} \|E_n\|_{\infty,\overline{\Omega}} \leq C\Delta t. \tag{4.3.11}$$

The spatial mesh is quite different from the one given in Section 4.3 due to the different layer structure at the various boundaries. We describe the grid for the x-direction and the same set of grids can be designed along the y-direction. In this case, we use the following transition parameters $\tau_0,\ \tau_1$ which are defined by

$$\tau_0 = \min\left\{\frac{1}{4},\ \frac{2}{\mu_0}\ln N\right\}, \quad \tau_1 = \min\left\{\frac{1}{4},\ \frac{2}{\mu_1}\ln N\right\}.$$

where $\mu_0,\ \mu_1$ are defined in (4.2.30).

To resolve the layers at the boundaries $x = 0$ and $x = 1$, we distribute the grids into the following subintervals $[0, \tau_0],\ [\tau_0, 1-\tau_1]$ and $[1-\tau_1, 1]$ in the ratio $1:2:1$. The Shishkin

mesh is defined by

$$x_i = \begin{cases} \dfrac{4i\tau_0}{N}, & 0 \le i \le N/4, \\ \tau_0 + 2\Big(i - \dfrac{N}{4}\Big)\dfrac{\Big(1-\tau_0-\tau_1\Big)}{N}, & N/4 < i \le 3N/4, \\ 1 - \tau_1 + 4\Big(i - \dfrac{3N}{4}\Big)\dfrac{\tau_1}{N}, & 3N/4 < i \le N. \end{cases} \tag{4.3.12}$$

4.3.2 Convergence analysis

Let us assume that the perturbation parameters satisfy the relation $\varepsilon_2^2 \ge \dfrac{\gamma\varepsilon_1}{\beta}$ and the functions in (4.1.1)-(4.1.2) possess sufficient smoothness and satisfy the compatibility conditions described in the previous sections. Then we can prove the following results in the same manner as in the previous sections.

Lemma 4.3.3. *Let $\widehat{u}^{n+1/2}$ be the solution of the equation (4.2.12) for $0 \le n \le M-1$ and the functions b_1, c_1, $f_1(\cdot,\cdot,t) \in C^2\big([0,1]^2\big)$. Let $p, \delta \in (0,1)$ be some arbitrary constants. Then, we have the following bounds for the derivatives of $\widehat{u}^{n+1/2}$ as*

$$\left|\frac{\partial^i \widehat{u}^{n+1/2}}{\partial x^i}\right| \le C\left[1 + \mu_0^i e^{-p\mu_0 x} + \mu_1^i e^{-p\mu_1(1-x)}\right], \quad 0 \le i \le 4, \tag{4.3.13}$$

when $2\varepsilon_2 \left\|\dfrac{\partial b_1}{\partial x}\right\|_{\infty,\Omega} \le \delta(1-p)$ and μ_0, μ_1 are defined in (4.2.30).

Proof. We observe that application of the maximum principle for the operator $\Big(I + \Delta t \mathcal{L}_{x,\varepsilon}\Big)$ ensures the boundedness of the semi-discrete solution $\widehat{u}^{n+1/2}$. Thus, the proof for (4.3.13) with $i = 0$ follows immediately.

In order to find the estimates in (4.3.13) for $1 \le i \le 4$, we consider the characteristic equation (4.2.29) again, with the constants μ_0, μ_1 defined similarly. In this case, the constants μ_0, μ_1 are found to be $\mu_0 = O(\varepsilon_2^{-1})$, $\mu_1 = O(\varepsilon_2/\varepsilon_1)$. Therefore, following the estimates given in Linß et al.[64], we obtain the bounds in (4.3.13) for $1 \le i \le 4$. □

The following bounds for the bounds of the derivatives of the semi-discrete solution $\widehat{u}^{n+1}$ with respect to y also holds analogously.

Lemma 4.3.4. *Let $\widehat{u}^{n+1}$ be the semi-discrete solution of (4.2.12) for $0 \le n \le M-1$, and the functions b_2, c_2, $f_2(\cdot,\cdot,t) \in C^2\big([0,1]^2\big)$. Then, we have the following bounds for the*

derivatives

$$\left|\frac{\partial^j \widehat{u}^{n+1}}{\partial y^j}\right| \leq C\left[1+\mu_0^j e^{-p\mu_0 y}+\mu_1^j e^{-p\mu_1(1-y)}\right], \quad 0\leq j\leq 4, \tag{4.3.14}$$

where $p,\delta\in(0,1)$ *and* $2\varepsilon_2\left\|\frac{\partial b_2}{\partial y}\right\|_{\infty,\Omega}\leq \delta(1-p)$.

Now we estimate the truncation error due to the discretization of (4.2.12) on Shishkin mesh defined in (4.3.12) for this case by rewriting the equation and using the main convergence result proved in [64].

Lemma 4.3.5. *Let* $\widehat{U}^{n+1/2}$ *be the solution of the fully-discrete equation* (4.2.34) *on* $\overline{\Omega}^N$ *and* $\widehat{u}^{n+1/2}$ *solves the problem (4.2.12.a). If* $\varepsilon_2\leq N^{-1}\ln N$, *then*

$$\left\|\widehat{U}^{n+1/2}-\widehat{u}^{n+1/2}\big|_{\overline{\Omega}^N}\right\|_{\infty,\overline{\Omega}^N}\leq C\Delta t\ N^{-1}\ln N. \tag{4.3.15}$$

Proof. We define the truncation error as in (4.2.38) by

$$\begin{aligned}\theta_i=&-\frac{\varepsilon_1\Delta t}{3}\big(h_{i+1}^x-h_i^x\big)\frac{\partial^3\widehat{u}^{n+1/2}}{\partial x^3}(x_i,y_j)+r_{ij}^+\ R_3\big(\widehat{u}^{n+1/2},x_i,x_{i+1}\big)\\&+r_{ij}^-\ R_3\big(\widehat{u}^{n+1/2},x_i,x_{i-1}\big)+\varepsilon_2\Delta t\ b_1(x_i,y_j)\bigg(-\frac{h_i^x}{2}\frac{\partial^2\widehat{u}^{n+1/2}}{\partial x^2}(x_i,y_j)\\&+\frac{(h_i^x)^2}{3!}\frac{\partial^3\widehat{u}^{n+1/2}}{\partial x^3}(x_i,y_j)\bigg),\end{aligned} \tag{4.3.16}$$

where the coefficients $r_{ij}^+,\ r_{ij}^-$ have the same definitions used in (4.2.23). We estimate the truncation error in the following three cases depending on the position of the grid point x_i.

Case (i): Let $0<x_i<\tau_0$.

From the definition of the generated Shishkin mesh given in (4.3.12), we have

$$h_i^x=h_{i+1}^x=\frac{4\tau_0}{N}\leq\ C\varepsilon_2\ N^{-1}\ln N.$$

One can easily simplify (4.3.16) to have

$$\begin{aligned}|\theta_i|\leq\ &C\Delta t\left[\varepsilon_2\int_{x_{i-1}}^{x_i}\left|\frac{\partial^2\widehat{u}^{n+1/2}}{\partial x^2}(s,y_j)\right|ds+\varepsilon_1\int_{x_{i-1}}^{x_{i+1}}\left|\frac{\partial^3\widehat{u}^{n+1/2}}{\partial x^3}(s,y_j)\right|ds\right]\\&=C\Delta t\ (I_1+I_2),\end{aligned} \tag{4.3.17}$$

where

$$I_1 = \varepsilon_2 \int_{x_{i-1}}^{x_i} \left| \frac{\partial^2 \widehat{u}^{n+1/2}}{\partial x^2}(s, y_j) \right| ds \leq C\varepsilon_2 \left[\int_{x_{i-1}}^{x_i} \left\{ 1 + \mu_0^2 \, e^{-p\mu_0 s} + \mu_1^2 \, e^{-p\mu_1(1-s)} \right\} ds \right]$$
$$\leq C\varepsilon_2 \left[h_i^x + \frac{\mu_0}{p} \left(e^{-p\mu_0 x_{i-1}} - e^{-p\mu_0 x_i} \right) + \frac{\mu_1}{p} \left(e^{-p\mu_1(1-x_i)} - e^{-p\mu_1(1-x_{i-1})} \right) \right].$$

Now, it is easy to check that

$$e^{-p\mu_0 x_{i-1}} - e^{-p\mu_0 x_i} = p\mu_0 h_i^x \, e^{-p\mu_0 x_i} + O\Big((h_i^x \mu_0)^2 \Big). \tag{4.3.18}$$

Since $h_i^x \mu_0 \leq C N^{-1} \ln N$ and $\varepsilon_2 \mu_0 \leq C$, we have

$$\begin{aligned} I_1 &\leq C\varepsilon_2 \left[h_i^x + \frac{\mu_0}{p} \, N^{-1} \ln N + \frac{\mu_1}{p} e^{-p\mu_1(1-x_i)} \right] \\ &\leq C\varepsilon_2 \left[\varepsilon_2 \, N^{-1} \ln N + \mu_0 \, N^{-1} \ln N + \frac{1}{1-x_i} \right] \\ &\leq C \Big(\varepsilon_2 + N^{-1} \ln N \Big). \end{aligned} \tag{4.3.19}$$

From (4.2.28), it follows that

$$\begin{aligned} \varepsilon_1 \frac{\partial^3 \widehat{u}^{n+1/2}}{\partial x^3} &= \varepsilon_2 \left(\frac{\partial b_1}{\partial x} \frac{\partial \widehat{u}^{n+1/2}}{\partial x} + b_1 \frac{\partial^2 \widehat{u}^{n+1/2}}{\partial x^2} \right) \\ &\quad + c_1 \frac{\partial \widehat{u}^{n+1/2}}{\partial x} + \widehat{u}^{n+1/2} \frac{\partial c_1}{\partial x} + \frac{\partial \hat{s}}{\partial x} \\ &= \varepsilon_2 b_1 \frac{\partial^2 \widehat{u}^{n+1/2}}{\partial x^2} + \left(\varepsilon_2 \frac{\partial b_1}{\partial x} + c_1 \right) \frac{\partial \widehat{u}^{n+1/2}}{\partial x} \\ &\quad + \widehat{u}^{n+1/2} \frac{\partial c_1}{\partial x} + \frac{\partial \hat{s}}{\partial x}. \end{aligned}$$

where $\hat{s} = \omega - f_1(x, y, t_{n+1})$ is a bounded function. Using the estimate in (4.3.19) and the boundedness of $\widehat{u}^{n+1/2}$, we deduce the following

$$\begin{aligned} I_2 &= \varepsilon_1 \int_{x_{i-1}}^{x_{i+1}} \left| \frac{\partial^3 \widehat{u}^{n+1/2}}{\partial x^3}(s, y_j) \right| ds \\ &\leq C\varepsilon_2 \int_{x_{i-1}}^{x_{i+1}} \left| \frac{\partial^2 \widehat{u}^{n+1/2}}{\partial x^2}(s, y_j) \right| ds + C \int_{x_{i-1}}^{x_{i+1}} \left(\gamma_0 \frac{\partial \widehat{u}^{n+1/2}}{\partial x} + g(s, y) \right) ds \\ &\leq C \Big(\varepsilon_2 + N^{-1} \ln N + h_i^x \Big) \leq C \Big(\varepsilon_2 + N^{-1} \ln N + \varepsilon_2 N^{-1} \ln N \Big). \end{aligned}$$

This gives

$$I_2 \leq C\bigg(\varepsilon_2 + N^{-1}\ln N\bigg), \tag{4.3.20}$$

where $\gamma_0 = \left\|\varepsilon_2\dfrac{\partial b_1}{\partial x} + c_1\right\|_{\infty,\overline{\Omega}}$, $g(x,y) = \left(\dfrac{\partial \hat{s}}{\partial x} + \widehat{u}^{n+1/2}\dfrac{\partial c_1}{\partial x}\right)$ and we used the property (4.3.18).

From the estimates in (4.3.19) and (4.3.20), one can easily conclude that

$$|\theta_i| \leq C\Delta t\bigg(\varepsilon_2 + N^{-1}\ln N\bigg). \tag{4.3.21}$$

If we assume that $\varepsilon_2 \leq N^{-1}\ln N$, then we have the desired estimate

$$|\theta_i| \leq C\Delta t N^{-1}\ln N. \tag{4.3.22}$$

Case (ii): Consider $1-\tau_1 < x_i < 1$.

Since $\varepsilon_2 \geq C\sqrt{\varepsilon_1}$, we have

$$h_i^x = h_{i+1}^x = \frac{4\tau_1}{N} \leq\ CN^{-1}\left(\frac{\varepsilon_1}{\varepsilon_2}\right)\ln N \leq\ C\varepsilon_1^{1/2}N^{-1}\ln N.$$

One can also verify that

$$\varepsilon_2 h_i^x \leq C\varepsilon_1 N^{-1}\ln N, \quad \varepsilon_2\left(h_i^x\right)^2 \leq C\varepsilon_1^{3/2}N^{-2}\ln^2 N. \tag{4.3.23}$$

Now, proceeding similarly as in Lemma 4.2.8, we get

$$|\theta_i| \leq C\Delta t N^{-1}\ln N. \tag{4.3.24}$$

Case (iii): Here, we consider $\tau_0 < x_i < 1-\tau_1$.

In this case, we have

$$h_i^x = \frac{2}{N}\left(1-\tau_0-\tau_1\right),$$

where $\tau_0+\tau_1 \leq C\varepsilon_2\ln N$. From the grid structure, it is clear that $\varepsilon_2\ln N \leq C$ and $h_i^x \leq CN^{-1}$. Using the inequality $e^{-t} \leq \dfrac{C}{1+t}$ for $t>0$, and the facts that $\varepsilon_2\ln N \leq C$ and

$\varepsilon_2 \leq C\varepsilon_1 \ln N$, one can show that

$$\left|r_{ij}^{+}R_3(\widehat{u}^{n+1/2}, x_i, x_{i+1})\right| \leq C\Delta t N^{-1}\ln N, \quad \left|r_{ij}^{-}R_3(\widehat{u}^{n+1/2}, x_i, x_{i-1})\right| \leq C\Delta t N^{-1}\ln N.$$

A set of similar calculations yield the following result:

$$\left|\varepsilon_2\Delta t\ b_1(x_i,y_j)\Big(-\frac{h_i^x}{2}\frac{\partial^2\widehat{u}^{n+1/2}}{\partial x^2}(x_i,y_j)+\frac{(h_i^x)^2}{3!}\frac{\partial^3\widehat{u}^{n+1/2}}{\partial x^3}(x_i,y_j)\Big)\right| \leq C\Delta t\ N^{-1}\ln N.$$

The estimate (4.3.24) follows by adding the above inequalities.

Case (iv): $x_i = \tau_0$ or $x_i = 1-\tau_1$

In case of $x_i = \tau_0$, the step-lengths on the left and right to x_i are either $h_i^x = \dfrac{4\tau_0}{N}$ or $h_i^x = \dfrac{2(1-\tau_0-\tau_1)}{N}$. Thus, $\left|h_i^x - h_{i+1}^x\right| \leq CN^{-1}$. From (4.2.38), we bound the truncation error as

$$\begin{aligned}&\left|\frac{\varepsilon_1\Delta t}{3}\big(h_{i+1}^x - h_i^x\big)\frac{\partial^3\widehat{u}^{n+1/2}}{\partial x^3}(x_i,y_j)\right| \\ &\leq \frac{C\varepsilon_1\Delta t}{N}\left[1+\mu_0^3 e^{-p\mu_0 x_i}+\mu_1^3 e^{-p\mu_1(1-x_i)}\right] \\ &\leq \frac{C\Delta t}{N}\left[1+C\mu_0^3\frac{1}{\mu_0^3}+C\mu_1^3\frac{1}{\mu_1^3}\right] \leq C\Delta t N^{-1},\end{aligned} \tag{4.3.25}$$

where we use the property $e^{-t} < C/t^k$, $t>0$, $k\in\mathbb{N}$. We also prove similarly as in **Case (i)** or **Case (ii)** the followings

$$\left|r_{ij}^{+}\ R_3\big(\widehat{u}^{n+1/2}, x_i, x_{i+1}\big)\right| \leq C\Delta t N^{-1}\ln N, \quad \left|r_{ij}^{-}\ R_3\big(\widehat{u}^{n+1/2}, x_i, x_{i-1}\big)\right| \leq C\Delta t\ N^{-1}\ln N, \tag{4.3.26}$$

$$\left|\varepsilon_2\Delta t\ b_1(x_i,y_j)\Big(-\frac{h_i^x}{2}\frac{\partial^2\widehat{u}^{n+1/2}}{\partial x^2}(x_i,y_j)+\frac{h_i^{x2}}{3!}\frac{\partial^3\widehat{u}^{n+1/2}}{\partial x^3}(x_i,y_j)\Big)\right| \leq C\Delta t\ N^{-1}\ln N. \tag{4.3.27}$$

It follows from (4.3.25)-(4.3.27) that

$$|\theta_i| \leq C\Delta t N^{-1}\ln N. \tag{4.3.28}$$

The proof for the case when $x_i = 1-\tau_1$ can also be carried out similarly.

So, combining all the cases, we have

$$|\theta_i| \leq \begin{cases} C\Delta t\ N^{-1}, & \tau_0 < x_i < 1-\tau_1 \\ C\Delta t\ N^{-1}\ln N, & x_i \leq \tau_0, \quad x_i \geq 1-\tau_1. \end{cases} \tag{4.3.29}$$

Thus, $|\theta_i| \leq C\Delta t\ N^{-1}\ln N, \quad x_i \in \overline{\Omega}_x^N$. Now following the exactly same arguments used in Lemma 4.3.5 and discrete maximum principle for the operator $\left(I + \Delta t L_{x,\varepsilon}^N\right)$, one can easily have

$$\left|\widehat{U}_i^{n+1/2} - \widehat{u}^{n+1/2}(x_i, y)\right| \leq C\Delta t\ N^{-1}\ln N, \quad x_i \in \overline{\Omega}_x^N. \tag{4.3.30}$$

Hence, the proof follows. □

Now, we can combine the above results and establish the following convergence results exactly the same way as we proceeded in the previous section. The results ensure that the method is robust convergent, which is not dependent on the conditions applied on the perturbation parameters.

Theorem 4.3.6. *Suppose $\varepsilon_2 \leq N^{-1}\ln N$ and let U^{n+1} be the solution of the fully-discrete problem (4.2.22) at $t = t_{n+1}$ and $\widehat{u}^{n+1}$ is the solution of (4.2.12). Then, we have*

$$\left\|U^{n+1} - \widehat{u}^{n+1}\big|_{\overline{\Omega}^N}\right\|_{\infty,\overline{\Omega}^N} \leq C\Delta t\ N^{-1}\ln N, \quad 0 \leq n \leq M-1. \tag{4.3.31}$$

Theorem 4.3.7. *Suppose $\varepsilon_2 \leq N^{-1}\ln N$ and let U^n be the solution of the fully-discrete problem (4.2.22) for $t = t_n$. If u is the exact solution of the given model problem (4.1.1), then the global error satisfies*

$$\left\|U^n - u(t_n)\big|_{\overline{\Omega}^N}\right\|_{\infty,\overline{\Omega}^N} \leq C\big(\Delta t + N^{-1}\ln N\big). \tag{4.3.32}$$

4.3.3 Numerical experiments

In this section, we present numerical experiments for the same test problem Example 4.2.11 with the following set of parameters

$$S_\varepsilon = \left\{\big(\varepsilon_1, \varepsilon_2\big) : \varepsilon_1 = 10^{-k-1}, \quad \varepsilon_2 = {\varepsilon_1}^{1/3}, \quad k = 1, 2, \ldots, 6\right\}. \tag{4.3.33}$$

which satisfies the conditions on the perturbation parameters for the present case. We calculate the maximum pointwise error and the corresponding order of convergence defined

in (4.2.59)-(4.2.60) for various values of N, Δt and present them in Table 4.3 with the parameters from set S_ε in (4.3.33). We also compute the parameter-uniform error and the corresponding rate of convergence for those values of N, Δt.

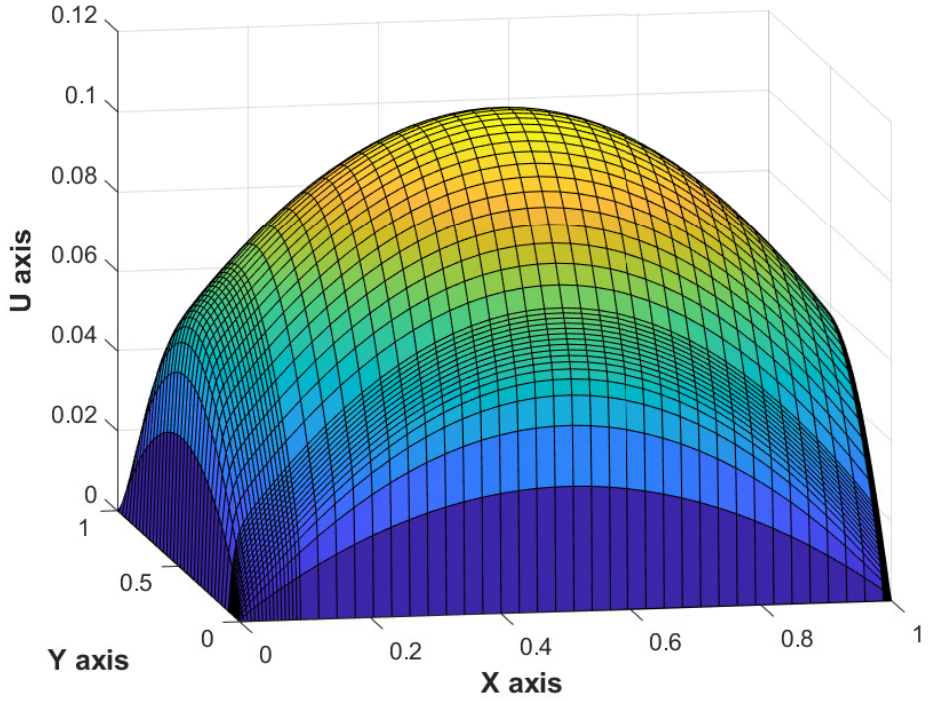

Figure 4.6: Numerical solution with $N = 64$ and $\varepsilon_1 = 10^{-7}$ at $t = 1$.

We observe that for each pair of fixed values of the parameters ε_1, ε_2, maximum pointwise error is decreasing monotonically as N is increasing. We also notice that these errors remain bounded as we keep on decreasing the parameters ε_1, ε_2. This ensures the parameter-uniform convergence of the proposed scheme, which is stated in Theorem 4.3.7. The table shows that the upwind scheme has almost first-order convergence in space and time variables. The loglog plot in Figure 4.7 clearly reveals the linear order convergence of the scheme, which validates the error estimates.

4.4 Conclusions

In this work, we proposed an ADI based finite difference scheme for the singularly perturbed 2D parabolic IBVPs with two parameters multiplying the diffusion and convection terms. To discretize the spatial domain, we used the piecewise-uniform Shishkin meshes. Truncation error is derived, stability of the proposed scheme is established. Parameter-uniform error

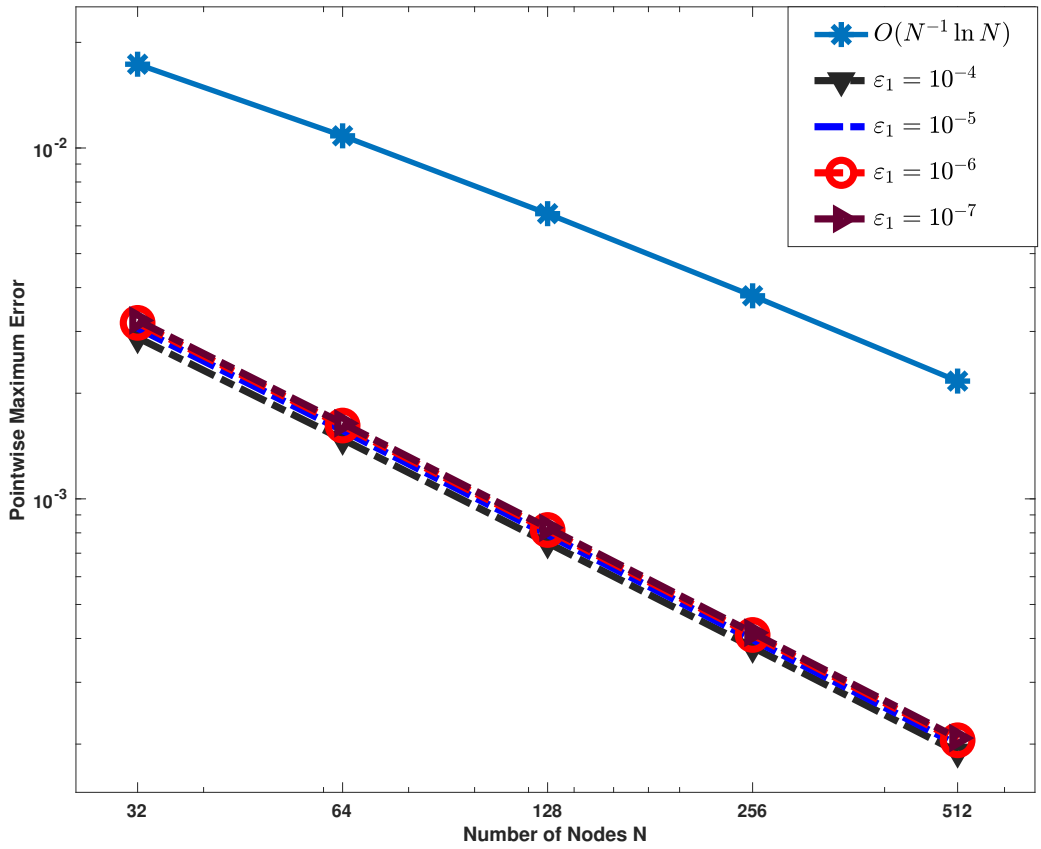

Figure 4.7: Visualization of the loglog plot of the maximum pointwise errors in Table 4.3.

estimates are obtained for both the cases. Numerical experiments reveal the theoretical order of convergence.

Table 4.3: Maximum pointwise error and corresponding rate of convergence for Example 4.2.11 for the parameters defined in (4.3.33) with $\Delta t = 1/N$.

ε_1	$N = 32$	64	128	256	512
	$\Delta t = 1/32$	$1/64$	$1/128$	$1/256$	$1/512$
10^{-2}	2.5370e-03	1.3370e-03	6.8439e-04	3.4573e-04	1.7370e-04
	0.9241	0.9661	0.9852	0.9931	-
10^{-3}	2.8806e-03	1.4789e-03	7.4942e-04	3.7765e-04	1.8988e-04
	0.9619	0.9806	0.9887	0.9920	-
10^{-4}	3.0657e-03	1.5669e-03	7.9050e-04	3.9711e-04	1.9903e-04
	0.9683	0.9871	0.9932	0.9966	-
10^{-5}	3.1738e-03	1.6179e-03	8.1518e-04	4.0933e-04	2.0506e-04
	0.9721	0.9889	0.9938	0.9972	-
10^{-6}	3.2248e-03	1.6416e-03	8.2742e-04	4.1537e-04	2.0807e-04
	0.9741	0.9884	0.9942	0.9973	-
10^{-7}	3.2316e-03	1.6500e-03	8.3295e-04	4.1811e-04	2.0948e-04
	0.9698	0.9862	0.9944	0.9971	-
$E^{N,\Delta t}$	**3.2316e-03**	**1.6500e-03**	**8.3295e-04**	**4.1811e-04**	**2.0948e-04**
$p^{N,\Delta t}$	**0.9698**	**0.9862**	**0.9944**	**0.9971**	-

Table 4.4: Maximum pointwise error and the rate of convergence for Example 4.2.11 for the parameters defined in (4.3.33) with $\Delta t = 2/N$.

ε_1	$N = 32$	64	128	256	512
	$\Delta t = 1/16$	$1/32$	$1/64$	$1/128$	$1/256$
10^{-2}	5.5261e-03	2.9516e-03	1.5172e-03	7.6806e-04	3.8629e-04
	0.9048	0.9600	0.9822	0.9915	-
10^{-3}	5.9615e-03	3.0995e-03	1.5791e-03	7.9710e-04	4.0075e-04
	0.9436	0.9730	0.9862	0.9921	-
10^{-4}	6.1359e-03	3.1834e-03	1.6169e-03	8.1512e-04	4.0918e-04
	0.9467	0.9773	0.9882	0.9943	-
10^{-5}	6.2506e-03	3.2337e-03	1.6412e-03	8.2706e-04	4.1507e-04
	0.9508	0.9784	0.9887	0.9946	-
10^{-6}	6.3037e-03	3.2570e-03	1.6535e-03	8.3306e-04	4.1804e-04
	0.9526	0.9780	0.9891	0.9948	-
10^{-7}	6.2974e-03	3.2635e-03	1.6593e-03	8.3579e-04	4.1945e-04
	0.9484	0.9759	0.9893	0.9946	-
$E^{N,\Delta t}$	**6.2974e-03**	**3.2635e-03**	**1.6593e-03**	**8.3579e-04**	**4.1945e-04**
$p^{N,\Delta t}$	**0.9484**	**0.9759**	**0.9893**	**0.9946**	-

CHAPTER 5

A parameter-uniform hybrid method for singularly perturbed parabolic 2D convection-diffusion-reaction problems

In this work, we construct and analyze a parameter-uniform operator-splitting ADI scheme to efficiently solve the parabolic SPPs with two positive parameters. The proposed model combines the backward-Euler method on a uniform mesh in time and a hybrid method in space. The developed numerical method on a layer-adapted piecewise-uniform Shishkin mesh has been proven to be first-order convergent in time and second-order convergent in space. The numerical experiments are performed to validate the theoretical convergence results and illustrate the efficiency of the current method.

5.1 Introduction

In this chapter, we propose to employ a hybrid numerical scheme for solving a class of singularly perturbed 2D parabolic convection-diffusion-reaction problems, where the diffusion and convection coefficients are multiplied by perturbation parameters. Basically, we combine the central difference and midpoint upwind technique on a piecewise-uniform mesh in space and we apply ADI method defined for time variable to find a efficient and accurate approximate solution to the model problem. We prove that the proposed method is first order convergent in time and second order convergent in space.

In this work, we consider a parabolic convection-diffusion-reaction problem in 2D:

$$\begin{cases} u_t - \varepsilon_1 \Delta u + \varepsilon_2 \mathbf{b}(x,y)\cdot\nabla u + c(x,y)u = f(x,y,t), \quad (x,y)\in\Omega=(0,1)^2, \quad 0<t\le T, \\ u(x,y,t) = 0, \quad \text{for } (x,y)\in\overline{\Omega}\backslash\Omega, \ t\in[0,T], \\ u(x,y,0) = g(x,y), \quad \text{for } (x,y)\in\Omega, \end{cases} \tag{5.1.1}$$

where $\varepsilon_1, \varepsilon_2$ are the perturbation parameters such that $0 < \varepsilon_1, \varepsilon_2 \ll 1$. The convection field $\mathbf{b}$ is of the form $\mathbf{b}(x,y) = \big(b_1(x,y),\ b_2(x,y)\big)$ such that $b_i \ge \beta_i > 0$, for $i = 1, 2$. The function g is assumed to be a continuous function in Ω. We also presume that the reaction coefficient $c(x,y) \ge c_0 > 0$ and $f = f_1 + f_2$ is the source function that is smooth enough and satisfies the compatibility condition

We denote $\beta = \min\big\{\beta_1, \beta_2\big\}$ and $\gamma < \min\limits_{\overline{\Omega}} \left\{ \dfrac{c(x,y)}{2b_1(x,y)},\ \dfrac{c(x,y)}{2b_2(x,y)} \right\}$. By using the relation between the perturbation parameters, we analyze the problem (5.1.1) separately for the following two cases:

$$\textbf{Case I:} \quad \varepsilon_2^2 \le \frac{\gamma\varepsilon_1}{\beta}, \quad \textbf{Case II:} \quad \varepsilon_2^2 \ge \frac{\gamma\varepsilon_1}{\beta}.$$

We note that $\|\eta\|_\infty = \max\limits_{x\in G} \eta(x)$ denotes the maximum norm of a continuous function $\eta(x)$ on a set G. We also use the notation

$$\|\eta\|_{\infty, G^N} = \max_{x_i \in G^N} S(x_i)$$

to denote the discrete maximum norm of a mesh function S on the mesh G^N. We use C to denote a generic positive constant, which is independent of the mesh sizes, perturbation parameters and associated functions throughout the paper.

We organize the rest of the chapter as follows: In Section 2, we introduce the singularly

perturbed 2D parabolic convection-diffusion-reaction problem containing the perturbation parameters $\varepsilon_1,\ \varepsilon_2$ with some assumptions on the coefficient functions as well as on the source function. We define some standard notations which we use to present our analysis of the method. Section 3 describes about the solution properties, semidiscrete problem, the proposed scheme and its convergence along with some illustrative example for the case $\varepsilon_2^2 \leq C\varepsilon_1$. In the next section, we discuss all these things for the other case, namely $\varepsilon_2^2 \geq C\varepsilon_1$. In the final section, we have concluded the article by summarizing the obtained theoretical results and the validation of them using numerical experiments.

5.2 Analysis of the hybrid scheme: Case I

We first discuss the analysis of the method when $\varepsilon_2^2 \leq \dfrac{\gamma\varepsilon_1}{\beta}$ in which the solution exhibit regular boundary layers of width $O(\sqrt{\varepsilon_1})$ condensing at the four edges along the corner layers at the corners of the domain. The boundaries of the domain are defined by

$$\Gamma_l = \big\{(0,y) \in \overline{\Omega} :\ 0 \leq y \leq 1\big\}, \quad \Gamma_r = \big\{(1,y) \in \overline{\Omega} :\ 0 \leq y \leq 1\big\},$$
$$\Gamma_b = \big\{(x,0) \in \overline{\Omega} :\ 0 \leq x \leq 1\big\}, \quad \Gamma_t = \big\{(x,1) \in \overline{\Omega} :\ 0 \leq x \leq 1\big\}.$$

For more rigorous analysis of the problem, we decompose the solution u of the problem (5.1.1) as in the following way,

$$u = v + w_L + w_R + w_T + w_B + w_{LT} + w_{RB} + w_{RT} + w_{LB}, \tag{5.2.1}$$

where v is the regular component of the solution; w_L, w_R, w_B, w_T are the boundary layer components appearing near the edges $\Gamma_l,\ \Gamma_r,\ \Gamma_b$ and Γ_t respectively; $w_{LB},\ w_{LT},\ w_{RB},\ w_{RT}$ are the associated corner layer functions near the corners $C_1(0,0),\ C_2(0,1),\ C_3(1,0),\ C_4(1,1)$ of Ω respectively.

We remark that under the compatibility conditions in (4.1.3), the layer components of the solution u for the problem (5.1.1) respect the following bounds (see [68] for details):

$$\left|\frac{\partial^{k_s+k_t} v}{\partial x^{k_1}\partial y^{k_2}\partial t^{k_t}}\right| \leq C, \tag{5.2.2}$$

$$\left|\frac{\partial^{k_s+k_t} w_L}{\partial x^{k_1}\partial y^{k_2}\partial t^{k_t}}\right| \leq C\varepsilon_1^{-k_1/2} e^{-\sqrt{\frac{\beta\gamma}{\varepsilon_1}}x}, \tag{5.2.3}$$

$$\left|\frac{\partial^{k_s+k_t} w_R}{\partial x^{k_1}\partial y^{k_2}\partial t^{k_t}}\right| \leq C\varepsilon_1^{-k_1/2} e^{-\sqrt{\frac{\beta\gamma}{\varepsilon_1}}(1-x)}, \tag{5.2.4}$$

$$\left|\frac{\partial^{k_s+k_t} w_B}{\partial x^{k_1}\partial y^{k_2}\partial t^{k_t}}\right| \leq C\varepsilon_1^{-k_2/2} e^{-\sqrt{\frac{\beta\gamma}{\varepsilon_1}}y}, \tag{5.2.5}$$

$$\left|\frac{\partial^{k_s+k_t} w_T}{\partial x^{k_1}\partial y^{k_2}\partial t^{k_t}}\right| \leq C\varepsilon_1^{-k_2/2} e^{-\sqrt{\frac{\beta\gamma}{\varepsilon_1}}(1-y)}, \tag{5.2.6}$$

and

$$\left|\frac{\partial^{k_s+k_t} w_{LB}}{\partial x^{k_1}\partial y^{k_2}\partial t^{k_t}}\right| \leq C\varepsilon_1^{-(k_1+k_2)/2} \min\left\{e^{-\sqrt{\frac{\beta\gamma}{\varepsilon_1}}x}, \ e^{-\sqrt{\frac{\beta\gamma}{\varepsilon_1}}y}, \right\} \tag{5.2.7}$$

$$\left|\frac{\partial^{k_s+k_t} w_{RB}}{\partial x^{k_1}\partial y^{k_2}\partial t^{k_t}}\right| \leq C\varepsilon_1^{-(k_1+k_2)/2} \min\left\{e^{-\sqrt{\frac{\beta\gamma}{\varepsilon_1}}(1-x)}, \ e^{-\sqrt{\frac{\beta\gamma}{\varepsilon_1}}y}\right\}, \tag{5.2.8}$$

$$\left|\frac{\partial^{k_s+k_t} w_{LT}}{\partial x^{k_1}\partial y^{k_2}\partial t^{k_t}}\right| \leq C\varepsilon_1^{-(k_1+k_2)/2} \min\left\{e^{-\sqrt{\frac{\beta\gamma}{\varepsilon_1}}x}, \ e^{-\sqrt{\frac{\beta\gamma}{\varepsilon_1}}(1-y)}\right\}, \tag{5.2.9}$$

$$\left|\frac{\partial^{k_s+k_t} w_{RT}}{\partial x^{k_1}\partial y^{k_2}\partial t^{k_t}}\right| \leq C\varepsilon_1^{-(k_1+k_2)/2} \min\left\{e^{-\sqrt{\frac{\beta\gamma}{\varepsilon_1}}(1-x)}, \ e^{-\sqrt{\frac{\beta\gamma}{\varepsilon_1}}(1-y)}\right\}, \tag{5.2.10}$$

where $k_s = k_1 + k_2$, $0 \leq k_1 + k_2 + 2k_t \leq 4$.

5.2.1 Temporal discretization and the semidiscrete problem

In this section, we study a time semidiscretization of model problem (5.1.1). To do that, we first denote the differential operator $\mathcal{L}_\varepsilon$ in (5.1.1) by

$$\mathcal{L}_\varepsilon u := -\varepsilon_1 \Delta u + \varepsilon_2 \mathbf{b}(x,y)\cdot\nabla u + c(x,y)u. \tag{5.2.11}$$

Then, we apply the operator-splitting ADI strategy on a uniform mesh and divide the operator $\mathcal{L}_\varepsilon$ in two components: $\mathcal{L}_\varepsilon = \mathcal{L}_{x,\varepsilon} + \mathcal{L}_{y,\varepsilon}$, where

$$\mathcal{L}_{x,\varepsilon} u := -\varepsilon_1 \frac{\partial^2 u}{\partial x^2} + \varepsilon_2 b_1(x,y)\frac{\partial u}{\partial x} + c_1(x,y)u,$$
$$\mathcal{L}_{y,\varepsilon} u := -\varepsilon_1 \frac{\partial^2 u}{\partial y^2} + \varepsilon_2 b_2(x,y)\frac{\partial u}{\partial y} + c_2(x,y)u,$$

and $c = c_1 + c_2$ with $c_1 > 0$, $c_2 > 0$. We now discretize the temporal domain as

$$\overline{\Omega}_t^M := \left\{t_k : t_k = k\Delta t, \quad k = 0, 1, \ldots, M, \quad \Delta t = T/M\right\}, \tag{5.2.12}$$

with uniform time step size Δt. Let $u^0 = g(x,y)$, then the discretization of the problem (5.1.1) in time is defined by the scheme: For $n = 0, 1, \ldots, M-1$, u^{n+1} is the solution of the

problem

$$\begin{cases} \begin{cases} \Big(I + \Delta t \mathcal{L}_{x,\varepsilon}\Big) u^{n+1/2} = u^n + \Delta t f_1(x, y, t_{n+1}), \\ u^{n+1/2}(0, y) = 0, \quad u^{n+1/2}(1, y) = 0, \quad 0 \le y \le 1, \end{cases} \\ \begin{cases} \Big(I + \Delta t \mathcal{L}_{y,\varepsilon}\Big) u^{n+1} = u^{n+1/2} + \Delta t f_2(x, y, t_{n+1}), \\ u^{n+1}(x, 0) = 0, \quad u^{n+1}(x, 1) = 0, \quad 0 \le x \le 1. \end{cases} \end{cases} \tag{5.2.13}$$

Before discussing the convergence of the above semidiscrete problem, we need to define a subproblem. For $n = 0, 1, \ldots, M-1$, let $\widehat{u}^{n+1}$ solve the next semidiscrete problem

$$\begin{cases} \begin{cases} \Big(I + \Delta t \mathcal{L}_{x,\varepsilon}\Big) \widehat{u}^{n+1/2} = u(t_n) + \Delta t f_1(x, y, t_{n+1}), \\ \widehat{u}^{n+1/2}(0, y) = 0, \quad \widehat{u}^{n+1/2}(1, y) = 0, \quad 0 \le y \le 1, \end{cases} \\ \begin{cases} \Big[I + \Delta t \mathcal{L}_{y,\varepsilon}\Big] \widehat{u}^{n+1} = \widehat{u}^{n+1/2} + \Delta t f_2(x, y, t_{n+1}), \\ \widehat{u}^{n+1}(x, 0) = 0, \quad \widehat{u}^{n+1}(x, 1) = 0, \quad 0 \le x \le 1. \end{cases} \end{cases} \tag{5.2.14}$$

We have the following properties of the semidiscrete solutions of the problem in (5.2.14).

Lemma 5.2.1. *Let $\varepsilon_1, \varepsilon_2$ satisfy the relation $\varepsilon_2^2 \le \dfrac{\gamma \varepsilon_1}{\beta}$ and $\widehat{u}^{n+1/2}$ satisfies the equation (5.2.14) for $0 \le n \le M-1$. Then for $p = 0, 1, \ldots, 4$, we get*

$$\left| \frac{\partial^p \widehat{u}^{n+1/2}}{\partial x^p} \right| \le C \left[1 + \varepsilon_1^{-p/2} \left(e^{-\sqrt{\frac{\beta\gamma}{\varepsilon_1}} x} + e^{-\sqrt{\frac{\beta\gamma}{\varepsilon_1}} (1-x)} \right) \right], \tag{5.2.15}$$

and for $q = 0, 1, \ldots, 4$, we have

$$\left| \frac{\partial^q \widehat{u}^{n+1}}{\partial y^q} \right| \le C \left[1 + \varepsilon_1^{-q/2} \left(e^{-\sqrt{\frac{\beta\gamma}{\varepsilon_1}} y} + e^{-\sqrt{\frac{\beta\gamma}{\varepsilon_1}} (1-y)} \right) \right]. \tag{5.2.16}$$

Proof. Proof of the above lemma can be found in the previous chapter. □

Now, we discuss the stability analysis and consistency result for the semidiscrete problem (5.2.13). In the next lemma, we clearly see that the operator $\big(I + \Delta t \mathcal{L}_{i,\varepsilon}\big)$, $i = x, y$ posses the maximum principle.

Lemma 5.2.2. *Let $\zeta(x, y) \in C^2(\Omega)$ be a function with $\zeta(x, y) \ge 0$ on the boundary $\partial\Omega$.*

Suppose that for $i = x, y$, the operators satisfy

$$\big(I + \Delta t \mathcal{L}_{i,\varepsilon}\big)\zeta(x,y) \geq 0, \quad (x,y) \in \Omega. \tag{5.2.17}$$

Then, $\zeta(x,y) \geq 0$ for all $(x,y) \in \overline{\Omega}$.

Consequently, the following stability estimates hold:

$$\left\|\big(I + \Delta t \mathcal{L}_{i,\varepsilon}\big)^{-1}\right\|_{\infty,\overline{\Omega}} \leq \frac{1}{1+\beta\Delta t} \text{ for } i = x, y, \tag{5.2.18}$$

$$\left\|\big(I + \Delta t \mathcal{L}_{x,\varepsilon} + \Delta t \mathcal{L}_{y,\varepsilon}\big)^{-1}\right\|_{\infty,\overline{\Omega}} \leq C. \tag{5.2.19}$$

Let us now define the local truncation error for the semidiscrete problem (5.1.1) at $t = t_n$ by $e_n = u(t_n) - \widehat{u}^n$, $1 \leq n \leq M$. Now, we state the consistency results which are given in the following lemmas and Theorem 5.2.4. For proof of all these results, one can refer to Mrityunjoy *et al.* [69].

Lemma 5.2.3. *Let u be the exact solution of the equation (5.1.1) and it satisfies $\left|\dfrac{\partial^k u}{\partial t^k}\right| \leq C$, $(x,y) \in \overline{\Omega}$, $0 \leq t \leq T$, for $0 \leq k \leq 2$. Then, we have the following estimate for e_{n+1}*

$$\|e_{n+1}\|_{\infty,\overline{\Omega}} \leq C\Delta t^2, \tag{5.2.20}$$

for each $n = 0, 1, \ldots, M-1$.

Theorem 5.2.4. *The global error $E_n = u(t_n) - u^n$, $1 \leq n \leq M$, satisfies the following bound*

$$\sup_{n\Delta t \leq T} \|E_n\|_{\infty,\overline{\Omega}} \leq C\Delta t. \tag{5.2.21}$$

This theorem proves that the global error associated with the semidiscretization method has first-order convergence in the time variable.

5.2.2 Spatial discretization: fully-discrete scheme

As a next step, we need to apply a hybrid numerical method to the semidiscrete problem (5.2.13) in order to find a fully discrete scheme. Let $N \geq 8$ be a natural number which is a

multiple of 4. The space domain $\overline{\Omega} = [0,1]^2$ can be discretized as $\overline{\Omega}^N := \overline{\Omega}_x^N \times \overline{\Omega}_y^N$, where

$$\overline{\Omega}_x^N = \Big\{ x_i : x_i = x_{i-1} + h_i^x, \quad x_0 = 0,\ x_N = 1, \quad 1 \le i \le N \Big\},$$
$$\overline{\Omega}_y^N = \Big\{ y_j : y_j = y_{j-1} + h_j^y, \quad y_0 = 0,\ y_N = 1, \quad 1 \le j \le N \Big\}.$$

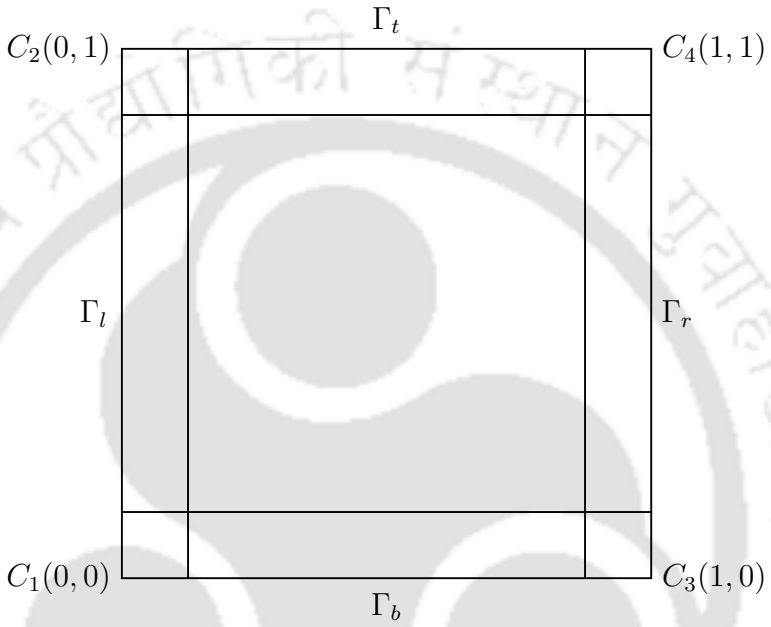

Figure 5.1: Partition of the domain Ω based on the boundary layer appearance at various edges.

First, we define the transition parameters τ_x and τ_y by

$$\tau_x = \tau_y = \min\left\{ \frac{1}{4},\ \sigma_0 \sqrt{\varepsilon_1} \ln N \right\},$$

where σ_0 is a positive constant. Since the problem has regular layers of width $O(\sqrt{\varepsilon_1})$ along every boundary of Ω, *i.e.*, along $x = 0,\ x = 1,\ y = 0$ and $y = 1$, we subdivide the domain as $\overline{\Omega} := \overline{\Omega}_x \times \overline{\Omega}_y$, where along the x-axis

$$\overline{\Omega}_x := \big\{ x :\ 0 \le x \le 1 \big\} = [0,\ \tau_x] \cup [\tau_x,\ 1-\tau_x] \cup [1-\tau_x,\ 1],$$

and along the y-axis

$$\overline{\Omega}_y := \big\{ y :\ 0 \le y \le 1 \big\} = [0,\ \tau_y] \cup [\tau_y,\ 1-\tau_y] \cup [1-\tau_y,\ 1].$$

We now equally distribute $N/2$ mesh points in each layer region and rest $N/2$ mesh points in the course region to construct a Shishkin mesh that is piecewise-uniform along each of the x-direction as well as the y-direction. The step-sizes along the x-direction are defined by $h_i^x = x_i - x_{i-1}$, $\widehat{h}_i^x = h_i^x + h_{i+1}^x$. Therefore, the Shishkin mesh points in $\overline{\Omega}_x$ can be defined by

$$x_i = \begin{cases} \dfrac{4i\tau_x}{N}, & 0 \le i \le N/4, \\ \tau_x + 2\left(i - \dfrac{N}{4}\right)\dfrac{1-2\tau_x}{N}, & N/4 < i \le 3N/4, \\ 1 - \tau_x + 4\left(i - \dfrac{3N}{4}\right)\dfrac{\tau_x}{N}, & 3N/4 < i \le N. \end{cases} \tag{5.2.22}$$

The step-size inside the layer regions is given by $h = \dfrac{4\tau_x}{N} \le 1/N$ and at the outside of layer regions by $H = \dfrac{2(1-2\tau_x)}{N}$. We see that the step-size at the outside of layer regions satisfies the following

$$1/N \le H \le 2/N.$$

We note that the mesh $\overline{\Omega}_y^N$ can be constructed in a similar way by taking $\tau_x = \tau_y$ as follows:

$$y_j = \begin{cases} \dfrac{4j\tau_y}{N}, & 0 \le j \le N/4, \\ \tau_y + 2\left(j - \dfrac{N}{4}\right)\dfrac{1-2\tau_y}{N}, & N/4 < j \le 3N/4, \\ 1 - \tau_y + 4\left(j - \dfrac{3N}{4}\right)\dfrac{\tau_y}{N}, & 3N/4 < j \le N, \end{cases} \tag{5.2.23}$$

where the step-sizes h_j^y, $\widehat{h}_i^y$ in along the y-axis are defined analogously.

Now, we briefly describe some notations to define the fully discrete problem. For the convection coefficient $\mathbf{b}(x,y) = (b_1,\ b_2)$, we define the followings:

$$b_{1,i-1/2} = \frac{b_1(x_i,y) + b_1(x_{i-1},y)}{2}, \quad b_{2,j-1/2} = \frac{b_2(x,y_j) + b_2(x,y_{j-1})}{2}.$$

We also use the following notations:

$$\widehat{U}_{x_i,y}^{n+1/2} = \widehat{U}^{n+1/2}(x_i,y), \quad \widehat{U}_{x,y_j}^{n+1} = \widehat{U}^{n+1}(x,y_j),$$
$$\widehat{U}_{i-1/2,y}^{n+1/2} = \frac{\widehat{U}_{x_i,y}^{n+1/2} + \widehat{U}_{x_{i-1},y}^{n+1/2}}{2}, \quad \widehat{U}_{x,j-1/2}^{n+1} = \frac{\widehat{U}_{x,y_j}^{n+1} + \widehat{U}_{x,y_{j-1}}^{n+1}}{2}.$$

In a similar way, one can define $f_{1_{x_i,y}}^{n+1}$, $f_{2_{x,y_j}}^{n+1}$, $f_{1,i-1/2}^{n+1}$, $f_{2,j-1/2}^{n+1}$ and $c_{1,i-1/2}$, $c_{2,j-1/2}$ in the

subsequent discrete equations. We denote the following standard operators by

$$\delta_x^2\ \psi_i = \frac{2}{\widehat{h}_i}\left(\frac{\psi_{i+1}-\psi_i}{h_{i+1}} - \frac{\psi_i-\psi_{i-1}}{h_i}\right),$$
$$\delta_x^c\ \psi_i = \frac{\psi_{i+1}-\psi_{i-1}}{\widehat{h}_i}, \quad \delta_x^-\ \psi_i = \frac{\psi_i-\psi_{i-1}}{h_i}.$$

Next, we define the midpoint upwind operators to be used in the proposed numerical scheme. For any function S, we have

$$L_{x,mu}^N\ S_{x_i,y} = -\varepsilon_1\Delta_x\ S_{x_i,y} + \varepsilon_2 b_{1,i-1/2}\ \delta_x^- S_{x_i,y} + c_{1,i-1/2}S_{1,i-1/2},$$
$$L_{y,mu}^N\ S_{x,y_j} = -\varepsilon_1\Delta_y\ S_{x,y_j} + \varepsilon_2 b_{2,j-1/2}\ \delta_y^- S_{x,y_j} + c_{2,j-1/2}S_{2,j-1/2},$$

and the central difference operators are given by

$$L_{x,cd}^N\ S_{x_i,y} = -\varepsilon_1\Delta_x\ S_{x_i,y} + \varepsilon_2 b_1(x_i,y)\ \delta_x^c S_{x_i,y} + c_1(x_i,y)S_{x_i,y},$$
$$L_{y,cd}^N\ S_{x,y_j} = -\varepsilon_1\Delta_y\ S_{x,y_j} + \varepsilon_2 b_2(x,y_j)\ \delta_y^c S_{x,y_j} + c_2(x,y_j)S_{x,y_j},$$

where $S_{x_i,y} = S(x_i,y)$ and $S_{x,y_j} = S(x,y_j)$.

Now, we are ready to describe the hybrid numerical method for the semidiscrete problem (5.2.14). Let $\widehat{U}^0 = g(x,y)$ and $n = 0,1,\ldots,M-1$, we find $\widehat{U}^{n+1}$ by solving the following problems:

For each fixed $y \in \overline{\Omega}_y^N$,

$$\begin{cases} \widehat{U}_{x_i,y}^{n+1/2} + \Delta t\ L_{x,cd}^N \widehat{U}_{x_i,y}^{n+1/2} = u(x_i,y,t_n) + \Delta t f_{1_{x_i,y}}^{n+1}, & 1 \le i \le \dfrac{N}{4},\ \dfrac{3N}{4} \le i \le N-1, \\ \widehat{U}_{i-1/2,y}^{n+1/2} + \Delta t\ L_{x,mu}^N \widehat{U}_{x_i,y}^{n+1/2} = \dfrac{1}{2}\Big(u(x_i,y,t_n) + u(x_{i-1},y,t_n)\Big) + \Delta t f_{1,i-1/2}^{n+1}, & \dfrac{N}{4} < i < \dfrac{3N}{4}, \end{cases} \tag{5.2.24}$$

with the boundary conditions $\widehat{U}_{0,y}^{n+1/2} = \widehat{U}_{1,y}^{n+1/2} = 0,\ y \in \overline{\Omega}_y^N$, and for each fixed $x \in \overline{\Omega}_x^N$,

$$\begin{cases} \widehat{U}_{x,y_j}^{n+1} + \Delta t\ L_{y,cd}^N \widehat{U}_{x,y_j}^{n+1} = \widehat{U}_{x,y_j}^{n+1/2} + \Delta t f_{2_{x,y_j}}^{n+1}, & 1 \le j \le N/4,\ 3N/4 \le j \le N-1, \\ \widehat{U}_{x,j-1/2}^{n+1} + \Delta t\ L_{y,mu}^N \widehat{U}_{x,y_j}^{n+1} = \widehat{U}_{x,j-1/2}^{n+1/2} + \Delta t f_{2,j-1/2}^{n+1}, & N/4 < j < 3N/4, \end{cases} \tag{5.2.25}$$

with the boundary conditions $\widehat{U}_{x,0}^{n+1} = \widehat{U}_{x,1}^{n+1} = 0,\ x \in \overline{\Omega}_x^N$.

The above numerical scheme can also be put in the simplified form:

For each fixed $1 \leq j \leq N-1$,

$$\begin{cases} \widehat{U}_{ij}^{n+1/2} + \Delta t L_{x,cd}^{N}\, \widehat{U}_{ij}^{n+1/2} = u(x_i, y_j, t_n) + \Delta t f_{1_{ij}}^{n+1}, \quad 1 \leq i \leq \dfrac{N}{4},\ \dfrac{3N}{4} \leq i \leq N-1, \\ \widehat{U}_{i-1/2,j}^{n+1/2} + \Delta t L_{x,mu}^{N}\, \widehat{U}_{ij}^{n+1/2} = \dfrac{u(x_i, y_j, t_n) + u(x_{i-1}, y_j, t_n)}{2} + \Delta t f_{1,i-1/2}^{n+1},\ \dfrac{N}{4} < i < \dfrac{3N}{4}, \end{cases} \tag{5.2.26}$$

with the boundary conditions $\widehat{U}_{0,j}^{n+1/2} = \widehat{U}_{N,j}^{n+1/2} = 0$, and for each fixed $1 \leq i \leq N-1$,

$$\begin{cases} \widehat{U}_{ij}^{n+1} + \Delta t\ L_{y,cd}^{N} \widehat{U}_{ij}^{n+1} = \widehat{U}_{ij}^{n+1/2} + \Delta t f_{2_{ij}}^{n+1}, \quad 1 \leq j \leq \dfrac{N}{4},\ \dfrac{3N}{4} \leq j \leq N-1, \\ \widehat{U}_{i,j-1/2}^{n+1} + \Delta t\ L_{y,mu}^{N} \widehat{U}_{ij}^{n+1} = \dfrac{1}{2}\left(\widehat{U}_{ij}^{n+1/2} + \widehat{U}_{i,j-1}^{n+1/2}\right) + \Delta t f_{2,j-1/2}^{n+1}, \quad \dfrac{N}{4} < i < \dfrac{3N}{4}, \end{cases} \tag{5.2.27}$$

with the boundary conditions $\widehat{U}_{i,0}^{n+1} = \widehat{U}_{i,N}^{n+1} = 0$.

5.2.3 Convergence analysis

In this section, we will study the convergence analysis of the fully-discrete scheme obtained by completely discretizing the semidiscrete problem (5.2.13). Before we define the fully-discrete solution, we introduce the simplified form of the discrete operators in the proposed hybrid scheme (5.2.26)-(5.2.27) as

$$\mathbb{L}_{1,\varepsilon}^{N} \widehat{U}_{ij}^{n+1/2} = \begin{cases} \left(I + \Delta t\ L_{x,cd}^{N}\right) \widehat{U}_{ij}^{n+1/2}, \quad 1 \leq i \leq N/4,\ 3N/4 \leq i \leq N-1, \\ \left(I + \Delta t\ L_{x,mu}^{N}\right) U_{ij}^{n+1/2}, \quad N/4 < i < 3N/4, \end{cases} \tag{5.2.28}$$

and

$$\mathbb{L}_{2,\varepsilon}^{N} \widehat{U}_{ij}^{n+1} = \begin{cases} \left(I + \Delta t\ L_{y,cd}^{N}\right) \widehat{U}_{ij}^{n+1}, \quad 1 \leq j \leq N/4,\ 3N/4 \leq j \leq N-1, \\ \left(I + \Delta t\ L_{y,mu}^{N}\right) \widehat{U}_{ij}^{n+1}, \quad N/4 < j < 3N/4. \end{cases} \tag{5.2.29}$$

With the discrete initial condition $U_{ij}^{0} = g(x_i, y_j)$, $0 \leq i, j \leq N$, the fully-discrete solution

U_{ij}^{n+1} can be solved from the following problems:

$$\begin{cases} \mathbb{L}_{1,\varepsilon}^{N} U_{ij}^{n+1/2} &= U_{ij}^{n} + \Delta t f_{1_{i,j}}^{n+1}, \quad 1 \le i \le N/4, \;\; 3N/4 \le i \le N-1, \\ \mathbb{L}_{1,\varepsilon}^{N} U_{ij}^{n+1/2} &= \dfrac{1}{2}\left[U_{i-1,j}^{n} + U_{ij}^{n}\right] + \dfrac{\Delta t}{2}\left[f_{1_{ij}}^{n+1} + f_{1_{i-1,j}}^{n+1}\right], \;\; N/4 < i < 3N/4, \\ U_{0,j}^{n+1/2} &= U_{N,j}^{n+1/2} = 0, \quad \text{for each fixed } j, \; 1 \le j \le N-1, \end{cases} \tag{5.2.30}$$

and

$$\begin{cases} \mathbb{L}_{2,\varepsilon}^{N} U_{ij}^{n+1} &= U_{ij}^{n+1/2} + \Delta t f_{2_{i,j}}^{n+1}, \quad 1 \le j \le N/4, \;\; 3N/4 \le j \le N-1, \\ \mathbb{L}_{2,\varepsilon}^{N} U_{ij}^{n+1} &= \dfrac{1}{2}\left[U_{i,j-1}^{n+1/2} + U_{ij}^{n+1/2}\right] + \dfrac{\Delta t}{2}\left[f_{2_{ij}}^{n+1} + f_{2_{i,j-1}}^{n+1}\right], \;\; N/4 < j < 3N/4, \\ U_{0,j}^{n+1} &= U_{N,j}^{n+1} = 0, \quad \text{for each fixed } i, \; 1 \le i \le N-1, \end{cases} \tag{5.2.31}$$

where

$$\mathbb{L}_{1,\varepsilon}^{N} U_{ij}^{n+1/2} := r_{ij}^{-}\, U_{i-1,j}^{n+1/2} + r_{ij}^{0}\, U_{ij}^{n+1/2} + r_{ij}^{+}\, U_{i+1,j}^{n+1/2}, \tag{5.2.32}$$

$$\mathbb{L}_{2,\varepsilon}^{N} U_{ij}^{n+1} := s_{ij}^{-}\, U_{i-1,j}^{n+1} + s_{ij}^{0}\, U_{ij}^{n+1} + s_{ij}^{+}\, U_{i+1,j}^{n+1}. \tag{5.2.33}$$

Here, the coefficients r_{ij} are given by,

$$r_{ij}^{-} = \begin{cases} -\dfrac{\Delta t}{\widehat{h}_i^x}\left(\dfrac{2\varepsilon_1}{h_i^x} + \varepsilon_2 b_{1,ij}\right), & 1 \le i \le N/4, \;\; 3N/4 \le i \le N-1, \\ -\dfrac{\Delta t}{h_i^x}\left(\dfrac{2\varepsilon_1}{\widehat{h}_i^x} + \varepsilon_2 b_{i-1/2,j}\right) + \dfrac{1 + \Delta t\; c_{i-1/2,j}}{2}, & N/4 < i < 3N/4, \end{cases} \tag{5.2.34}$$

$$r_{ij}^{+} = \begin{cases} \dfrac{\Delta t}{\widehat{h}_i^x}\left(-\dfrac{2\varepsilon_1}{h_{i+1}^x} + \varepsilon_2 b_{1,ij}\right), & 1 \le i \le N/4, \;\; 3N/4 \le i \le N-1, \\ -\dfrac{2\varepsilon_1 \Delta t}{h_{i+1}^x \widehat{h}_i^x}, & N/4 < i < 3N/4, \end{cases} \tag{5.2.35}$$

and

$$r_{ij}^{0} = \begin{cases} 1 + \Delta t\; c_{1,ij} - r_{ij}^{-} - r_{ij}^{+}, & 1 \le i \le N/4, \;\; 3N/4 \le i \le N-1, \\ 1 + \Delta t\; c_{i-1/2,j} - r_{ij}^{-} - r_{ij}^{+}, & N/4 < i < 3N/4, \end{cases} \tag{5.2.36}$$

where $b_{i-1/2,j} = \dfrac{b_1(x_i, y_j) + b_1(x_{i-1}, y_j)}{2}$, and $c_{i-1/2,j} = \dfrac{c_1(x_i, y_j) + c_1(x_{i-1}, y_j)}{2}$. The coefficients s_{ij} are given by,

$$s_{ij}^{-} = \begin{cases} -\dfrac{\Delta t}{\widehat{h}_j^y}\left(\dfrac{2\varepsilon_1}{h_j^y} + \varepsilon_2 b_{2,ij}\right), & 1 \le j \le N/4, \quad 3N/4 \le j \le N-1, \\ -\dfrac{\Delta t}{h_j^y}\left(\dfrac{2\varepsilon_1}{\widehat{h}_j^y} + \varepsilon_2 b_{i,j-1/2}\right) + \dfrac{1 + \Delta t\ c_{i,j-1/2}}{2}, & N/4 < j < 3N/4, \end{cases} \tag{5.2.37}$$

$$s_{ij}^{+} = \begin{cases} \dfrac{\Delta t}{\widehat{h}_j^y}\left(-\dfrac{2\varepsilon_1}{h_{j+1}^y} + \varepsilon_2 b_{2,ij}\right), & 1 \le j \le N/4,\ 3N/4 \le j \le N-1, \\ -\dfrac{2\varepsilon_1 \Delta t}{h_{j+1}^y \widehat{h}_j^y}, & N/4 < j < 3N/4, \end{cases} \tag{5.2.38}$$

$$s_{ij}^{0} = \begin{cases} 1 + \Delta t\ c_{2,ij} - s_{ij}^{-} - s_{ij}^{+}, & 1 \le j \le N/4,\ 3N/4 \le j \le N-1, \\ 1 + \Delta t\ c_{i,j-1/2} - s_{ij}^{-} - s_{ij}^{+}, & N/4 < j < 3N/4, \end{cases} \tag{5.2.39}$$

where $b_{i,j-1/2} = \dfrac{b_2(x_i, y_j) + b_2(x_i, y_{j-1})}{2}$ and $c_{i,j-1/2} = \dfrac{c_2(x_i, y_j) + c_2(x_i, y_{j-1})}{2}$.

Before proceeding to convergence analysis, we first deduce some inequalities which will be required for the proof of the subsequent results.

Lemma 5.2.5. *Let $N_0 \in \mathbb{N}$ be a number such that*

$$2\varepsilon_2 \left\|b_l\right\|_\infty \sigma_0 \le \frac{N_0\sqrt{\varepsilon_1}}{\ln N_0}, \tag{5.2.40}$$

$$\frac{1}{\Delta t} + \left\|c_l\right\|_\infty \le 2N_0\left(N_0\varepsilon_1 + \varepsilon_2\beta\right), \tag{5.2.41}$$

for $l = 1, 2$. Then, the matrices associated with the discrete equations (5.2.30) *and* (5.2.31) *are M-matrices for $N \ge N_0$.*

Proof. Let the coefficient matrix corresponding to the discrete problem in (5.2.30) is given by R_j which is a tridiagonal square matrix of size $N-1$ with super-diagonal entries r_{ij}^{+}, sub-diagonal entries r_{ij}^{-} and diagonal elements r_{ij}^{0} for each fixed j. In a similar way, let S_i be the coefficient matrix associated with the discrete problem (5.2.31) with the same structure as R_j for each i. We provide the proof only for the matrix R_j, and remark that similar arguments can be applied for the matrix S_i.

We start with the case when $1 \leq i \leq N/4$ and $3N/4 \leq i \leq N-1$. It is obvious that r_{ij}^- is negative for each j. Applying the inequality (5.2.40) we obtain $r_{ij}^+ < 0$ for each j. Thus, from (5.2.34)-(5.2.36), we can show that $r_{ij}^0 > 0$.

We remark that for such values of r_{ij}^- and r_{ij}^+, we have,

$$\left|r_{ij}^-\right| + \left|r_{ij}^+\right| = \frac{2\varepsilon_1 \Delta t}{\widehat{h}_i^x}\left(\frac{1}{h_i^x} + \frac{1}{h_{i+1}^x}\right) < \left|r_{ij}^0\right|, \quad \text{for } 1 < i \leq N/4,\ 3N/4 \leq i < N-1.$$

One can also verify that $\left|r_{1,j}^0\right| > \left|r_{1,j}^+\right|$ as well as $\left|r_{N-1,j}^0\right| > \left|r_{N-1,j}^-\right|$.

Now, consider the case when $N/4 < i < 3N/4$. In this case, we get $r_{ij}^+ < 0$ for each j. Applying the inequality (5.2.41) for $N \geq N_0$, we have $r_{ij}^- < 0$ which yields $r_{ij}^0 > 0$. Finally, we get,

$$\left|r_{ij}^-\right| + \left|r_{ij}^+\right| = \frac{2\varepsilon_1 \Delta t}{h_i^x h_{i+1}^x} + \varepsilon_2 \Delta t \frac{b_{i-1/2,j}}{h_i^x} - \frac{1 + \Delta t\ c_{i-1/2,j}}{2} < \left|r_{ij}^0\right|.$$

By combining the above results, we observe that the matrix R_j is an M-matrix for every j. Similarly, we can prove that S_i is also an M-matrix for every i. □

Now, we are ready to state the discrete maximum principle which is given in the next lemma.

Lemma 5.2.6. *Assume that S is an arbitrary function defined on $\overline{\Omega}_x^N$ (or on $\overline{\Omega}_y^N$) and $S_l \geq 0$ for $l = 0, N$. If the operators $\mathbb{L}_{i,\varepsilon}^N$, $i = 1, 2$ satisfy on $\overline{\Omega}_x^N$ (or on $\overline{\Omega}_y^N$)*

$$\mathbb{L}_{i,\varepsilon}^N\ S_l\ \geq 0,\ \ 1 \leq l \leq N-1, \quad i = 1, 2,$$

then we have, $S_l \geq 0,\ 0 \leq l \leq N$.

Remark 5.2.7. *Since the coefficient matrices of the above discrete equations are M-matrices, the operators $\mathbb{L}_{i,\varepsilon}^N$, $i = 1, 2$ satisfy the above proposition and the uniform stability of the proposed hybrid numerical method is therefore proved in the discrete maximum norm.*

We also use the following lemma to bound the local truncation error related to the above discrete equations.

Lemma 5.2.8. *Let $\psi \in C^4(\overline{\Omega}_x)$ with $\psi_i = \psi(x_i)$ on the discrete mesh $\overline{\Omega}_x^N$. Then, we have for $N/4 < i < 3N/4$,*

$$\left|L_{x,mu}^N\ \psi_i - (\mathcal{L}_{x,\varepsilon}\ \psi)_{i-1/2}\right| \leq\ C\left[\varepsilon_1 \int_{x_{i-1}}^{x_{i+1}} \left(h_i^x \left|\psi^{(4)}(\xi)\right| + \left|\psi^{(3)}(\xi)\right|\right) d\xi + \varepsilon_2 \int_{x_{i-1}}^{x_i} \left|\psi''(\xi)\right| d\xi\right], \tag{5.2.42}$$

and for $1 \le i \le N/4,\ 3N/4 \le i \le N-1,$

$$\left|L^N_{x,cd}\ \psi_i - \mathcal{L}_{x,\varepsilon}\ \psi(x_i)\right| \le Ch_i^x \int_{x_{i-1}}^{x_{i+1}} \left(\varepsilon_1 \left|\psi^{(4)}(\xi)\right| + \varepsilon_2 \left|\psi^{(3)}(\xi)\right|\right) d\xi. \tag{5.2.43}$$

Proof. The proof follows directly using the Taylor's series expansion of $g(x)$ about p at the point x with integral form of remainder term

$$R_n(\psi, p, x) = \frac{1}{n!}\int_p^x (x-\xi)^n \psi^{(n+1)}(\xi) d\xi.$$

Then, we obtain the following error bounds:

(i) Inside the layer regions: $1 \le i \le N/4$ and $3N/4 \le i \le N-1$.

We have

$$\left|\delta_x^2\ \psi_i - \psi''(x_i)\right| \le Ch_i^x \int_{x_{i-1}}^{x_{i+1}} \left|\psi^{(4)}(\xi)\right| d\xi,$$
$$\text{and}\ \ \left|\delta_x^c\ \psi_i - v'(x_i)\right| \le Ch_i^x \int_{x_{i-1}}^{x_{i+1}} \left|\psi^{(3)}(\xi)\right| d\xi.$$

(ii) Outside the layer regions $N/4 < i < 3N/4$:

We have

$$\left|\delta_x^2\ \psi_i - \frac{\psi''(x_i)+\psi''(x_{i-1})}{2}\right| \le C\int_{x_{i-1}}^{x_{i+1}} \left(h_i^x \left|\psi^{(4)}(\xi)\right| + \left|\psi^{(3)}(\xi)\right|\right) d\xi,$$
$$\text{and}\ \ \left|\delta_x^c\ \psi_i - \frac{\psi'(x_i)+\psi'(x_{i-1})}{2}\right| \le C\int_{x_{i-1}}^{x_i} \left|\psi''(\xi)\right| d\xi.$$

The result follows by combining the above estimates. □

The local truncation error associated with the first subproblem in (5.2.26) can be given by,

$$\mathbb{L}^N_{1,\varepsilon}\left(\widehat{U}^{n+1/2}(x_i,y) - \widehat{u}^{n+1/2}(x_i,y)\right) = \Delta t\ \theta_i(\widehat{u}^{n+1/2}, x_i), \tag{5.2.44}$$

for each fixed $y \in \overline{\Omega}^N_y$, where

$$\theta_i(\widehat{u}^{n+1/2}, x_i) = \begin{cases} L^N_{x,mu}\widehat{u}^{n+1/2}(x_i,y) - \mathcal{L}_{x,\varepsilon}\widehat{u}^{n+1/2}(x_{i-1/2},y), & N/2 < i < 3N/4, \\ L^N_{x,cd}\widehat{u}^{n+1/2}(x_i,y) - \mathcal{L}_{x,\varepsilon}\widehat{u}^{n+1/2}(x_i,y), & \text{otherwise.} \end{cases} \tag{5.2.45}$$

Therefore, inside layer regions, we have

$$\left|\theta_i(\widehat{u}^{n+1/2}, x_i)\right| \leq \left|L^N_{x,cd}\widehat{u}^{n+1/2}(x_i, y) - \mathcal{L}_{x,\varepsilon}\widehat{u}^{n+1/2}(x_i, y)\right| \leq Ch_i^x(\varepsilon_1 I_1 + \varepsilon_2 I_2), \tag{5.2.46}$$

where $y \in \overline{\Omega}_y^N$ remains fixed and

$$I_1 = \int_{x_{i-1}}^{x_{i+1}} \frac{\partial^4 \widehat{u}^{n+1/2}}{\partial x^4}(\xi, y)d\xi, \qquad I_2 = \int_{x_{i-1}}^{x_{i+1}} \frac{\partial^3 \widehat{u}^{n+1/2}}{\partial x^3}(\xi, y)d\xi.$$

We also have the followings when x_i lies outside of layer regions,

$$\left|\theta_i(\widehat{u}^{n+1/2}, x_i)\right| \leq \left|L^N_{x,mu}\widehat{u}^{n+1/2}(x_i, y) - \mathcal{L}_{x,\varepsilon}\widehat{u}^{n+1/2}(x_{i-1/2}, y)\right| \leq C(I_1 + I_2 + I_3), \tag{5.2.47}$$

where $y \in \overline{\Omega}_y^N$ is fixed and

$$I_1 = \varepsilon_1 \int_{x_{i-1}}^{x_{i+1}} \frac{\partial^3 \widehat{u}^{n+1/2}}{\partial x^3}(\xi, y)d\xi, \; I_2 = \varepsilon_1 h_i^x \int_{x_{i-1}}^{x_{i+1}} \frac{\partial^4 \widehat{u}^{n+1/2}}{\partial x^4}(\xi, y)d\xi,$$
$$\text{and } I_3 = \varepsilon_2 \int_{x_{i-1}}^{x_i} \frac{\partial^2 \widehat{u}^{n+1/2}}{\partial x^2}(\xi, y)d\xi.$$

Now, we are ready to provide an estimation of the local truncation error in the following lemma.

Lemma 5.2.9. *The local truncation error $\theta_i(\widehat{u}^{n+1/2}, x_i)$ at $x = x_i$ defined in* (5.2.45) *satisfies the following error bound:*

$$\left|\theta_i(\widehat{u}^{n+1/2}, x_i)\right| \leq \begin{cases} CN^{-2}, & \tau_x < x_i < 1 - \tau_x, \\ CN^{-2}\ln^2 N, & \textit{elsewhere.} \end{cases} \tag{5.2.48}$$

Proof. We find the estimates for θ_i for various values of x_i separately in each of the subdomains. Let us examine the next three typical cases in this regard.

Case (i): Inside the left layer region $1 \leq i \leq N/4$:

In this case, using (5.2.46) we have,

$$|I_1| \leq \int_{x_{i-1}}^{x_{i+1}} \left(1 + \varepsilon_1^{-2} e^{-\sqrt{\frac{\beta\gamma}{\varepsilon_1}}\xi} + \varepsilon_1^{-2} e^{-\sqrt{\frac{\beta\gamma}{\varepsilon_1}}(1-\xi)}\right) d\xi$$

$$\leq C\left[h_i^x+\frac{1}{\varepsilon_1^{3/2}}\left(e^{-\sqrt{\frac{\beta\gamma}{\varepsilon_1}}x_{i+1}}-e^{-\sqrt{\frac{\beta\gamma}{\varepsilon_1}}x_{i-1}}\right)+\frac{1}{\varepsilon_1^{3/2}}\left(e^{-\sqrt{\frac{\beta\gamma}{\varepsilon_1}}(1-x_{i+1})}-e^{-\sqrt{\frac{\beta\gamma}{\varepsilon_1}}(1-x_{i-1})}\right)\right]$$

$$\leq C\left[h_i^x+\frac{1}{\varepsilon_1^{3/2}}\frac{h_i^x}{\sqrt{\varepsilon_1}}e^{-\sqrt{\frac{\beta\gamma}{\varepsilon_1}}x_{i+1}}+\frac{1}{\varepsilon_1^{3/2}}e^{-\sqrt{\frac{\beta\gamma}{\varepsilon_1}}(1-x_{i+1})}\right]$$

$$\leq C\left[h_i^x+\frac{1}{\varepsilon_1^{3/2}}\frac{2\tau_x}{N}\frac{1}{\varepsilon_1^{3/2}}+\frac{1}{\varepsilon_1^{3/2}}e^{-\sqrt{\frac{\beta\gamma}{\varepsilon_1}}\tau_x}\right]$$

$$\leq C\left[h_i^x+\frac{1}{\varepsilon_1^{3/2}}N^{-1}\ln N+\frac{1}{\varepsilon_1^{3/2}}N^{-2}\right].$$

Combining the last inequality with the first term on the right hand side of (5.2.46), we get

$$h_i^x\varepsilon_1\left|I_1\right|\leq CN^{-2}\ln^2 N. \tag{5.2.49}$$

A similar estimate can be obtained for I_2, that is,

$$|I_2|\leq\int_{x_{i-1}}^{x_{i+1}}\left(1+\varepsilon_1^{-3/2}e^{-\sqrt{\frac{\beta\gamma}{\varepsilon_1}}\xi}+\varepsilon_1^{-3/2}e^{-\sqrt{\frac{\beta\gamma}{\varepsilon_1}}(1-\xi)}\right)d\xi$$

$$\leq C\left[h_i^x+\frac{1}{\varepsilon_1}\left(e^{-\sqrt{\frac{\beta\gamma}{\varepsilon_1}}x_{i+1}}-e^{-\sqrt{\frac{\beta\gamma}{\varepsilon_1}}x_{i-1}}\right)+\frac{1}{\varepsilon_1}\left(e^{-\sqrt{\frac{\beta\gamma}{\varepsilon_1}}(1-x_{i+1})}-e^{-\sqrt{\frac{\beta\gamma}{\varepsilon_1}}(1-x_{i-1})}\right)\right]$$

$$\leq C\left[h_i^x+\frac{1}{\varepsilon_1}\frac{h_i^x}{\sqrt{\varepsilon_1}}e^{-\sqrt{\frac{\beta\gamma}{\varepsilon_1}}x_{i+1}}+\frac{1}{\varepsilon_1}e^{-\sqrt{\frac{\beta\gamma}{\varepsilon_1}}(1-x_{i+1})}\right]$$

$$\leq C\left[h_i^x+\frac{1}{\varepsilon_1}\frac{2\tau_x}{N}\frac{1}{\sqrt{\varepsilon_1}}+\frac{1}{\varepsilon_1}e^{-\sqrt{\frac{\beta\gamma}{\varepsilon_1}}\tau_x}\right]$$

$$\leq C\left[h_i^x+\frac{1}{\varepsilon_1}N^{-1}\ln N+\frac{1}{\varepsilon_1}N^{-2}\right].$$

Combining the last inequality with the second term on the right hand side of (5.2.46), we get

$$h_i^x\varepsilon_2\left|I_2\right|\leq CN^{-2}\ln^2 N, \tag{5.2.50}$$

where we have used $\varepsilon_2^2\leq C\varepsilon_1$. Therefore, from (5.2.49) and (5.2.50) we obtain the desired estimate.

Case (ii): Inside the right layer region $3N/4\leq i\leq N-1$**:**

In this case, using (5.2.46), we have

$$
\begin{aligned}
|I_1| &\leq \int_{x_{i-1}}^{x_{i+1}} \left(1+\varepsilon_1^{-2}e^{-\sqrt{\frac{\beta\gamma}{\varepsilon_1}}\xi}+\varepsilon_1^{-2}e^{-\sqrt{\frac{\beta\gamma}{\varepsilon_1}}(1-\xi)}\right)d\xi \\
&\leq C\left[h_i^x+\frac{1}{\varepsilon_1^{3/2}}\left(e^{-\sqrt{\frac{\beta\gamma}{\varepsilon_1}}x_{i+1}}-e^{-\sqrt{\frac{\beta\gamma}{\varepsilon_1}}x_{i-1}}\right)+\frac{1}{\varepsilon_1^{3/2}}\left(e^{-\sqrt{\frac{\beta\gamma}{\varepsilon_1}}(1-x_{i+1})}-e^{-\sqrt{\frac{\beta\gamma}{\varepsilon_1}}(1-x_{i-1})}\right)\right] \\
&\leq C\left[h_i^x+\frac{1}{\varepsilon_1^{3/2}}e^{-\sqrt{\frac{\beta\gamma}{\varepsilon_1}}x_{i+1}}+\frac{1}{\varepsilon_1^{3/2}}\frac{h_i^x}{\sqrt{\varepsilon_1}}e^{-\sqrt{\frac{\beta\gamma}{\varepsilon_1}}(1-x_{i-1})}\right] \\
&\leq C\left[h_i^x+\frac{1}{\varepsilon_1^{3/2}}N^{-2}+\frac{1}{\varepsilon_1^{3/2}}(N^{-1}\ln N\sqrt{\varepsilon_1})\frac{1}{\sqrt{\varepsilon_1}}\right] \\
&\leq C\left[h_i^x+\frac{1}{\varepsilon_1^{3/2}}N^{-2}\ln N+\frac{1}{\varepsilon_1^{3/2}}N^{-1}\ln N\right].
\end{aligned}
$$

We observe that $h_i^x=\dfrac{8}{\mu_0}N^{-1}\ln N=O(\varepsilon_2 N^{-1}\ln N)$ when $x_i\in(0,\ \tau_0)$ for Case I. If we assume $\varepsilon_2\leq N^{-1}\ln N$, then combining with the last inequality, we get

$$
h_i^x\varepsilon_1\,|I_1|\leq CN^{-2}\ln^2 N. \tag{5.2.51}
$$

A similar estimate can be obtained for I_2, that is,

$$
\begin{aligned}
|I_2| &\leq C\left[h_i^x+\frac{1}{\varepsilon_1}\left(e^{-\sqrt{\frac{\beta\gamma}{\varepsilon_1}}x_{i+1}}-e^{-\sqrt{\frac{\beta\gamma}{\varepsilon_1}}x_{i-1}}\right)+\frac{1}{\varepsilon_1}\left(e^{-\sqrt{\frac{\beta\gamma}{\varepsilon_1}}(1-x_{i+1})}e^{-\sqrt{\frac{\beta\gamma}{\varepsilon_1}}(1-x_{i-1})}\right)\right] \\
&\leq C\left[h_i^x+\frac{1}{\varepsilon_1}N^{-2}+\frac{1}{\varepsilon_1}\frac{h_i^x}{\sqrt{\varepsilon_1}}e^{-\sqrt{\frac{\beta\gamma}{\varepsilon_1}}(1-x_{i-1})}\right] \\
&\leq C\left(h_i^x+\frac{1}{\varepsilon_1}N^{-2}+\frac{1}{\varepsilon_1}N^{-1}\ln N\right).
\end{aligned}
$$

We see that $h_i^x=\dfrac{8}{\mu_0}N^{-1}\ln N=O(\varepsilon_2 N^{-1}\ln N)$ when $x_i\in(0,\ \tau_0)$ for Case I. If we assume $\varepsilon_2\leq N^{-1}\ln N$, one can get

$$
h_i^x\varepsilon_2\,|I_2|\leq CN^{-2}\ln^2 N. \tag{5.2.52}
$$

where we have used $\varepsilon_2^2\leq C\varepsilon_1$. Therefore, from (5.2.51) and (5.2.52) we obtain the desired estimate.

Case (iii): Outside the layer regions: $N/4<i<3N/4$

In this case using (5.2.47), we have

$$
\begin{aligned}
|I_1| &\leq \varepsilon_1 \int_{x_{i-1}}^{x_{i+1}} \left(1 + \varepsilon_1^{-3/2} e^{-\sqrt{\frac{\beta\gamma}{\varepsilon_1}}\xi} + \varepsilon_1^{-3/2} e^{-\sqrt{\frac{\beta\gamma}{\varepsilon_1}}(1-\xi)}\right) d\xi \\
&\leq C\varepsilon_1 \left[h_i^x + \frac{1}{\varepsilon_1}\left|e^{-\sqrt{\frac{\beta\gamma}{\varepsilon_1}}x_{i+1}} - e^{-\sqrt{\frac{\beta\gamma}{\varepsilon_1}}x_{i-1}}\right| + \frac{1}{\varepsilon_1}\left|e^{-\sqrt{\frac{\beta\gamma}{\varepsilon_1}}(1-x_{i+1})} - e^{-\sqrt{\frac{\beta\gamma}{\varepsilon_1}}(1-x_{i-1})}\right|\right] \\
&\leq C\varepsilon_1 \left[h_i^x + \frac{1}{\varepsilon_1} e^{-\sqrt{\frac{\beta\gamma}{\varepsilon_1}}x_{i+1}} + \frac{1}{\varepsilon_1} e^{-\sqrt{\frac{\beta\gamma}{\varepsilon_1}}(1-x_{i+1})}\right] \\
&\leq C\varepsilon_1 \left[h_i^x + \frac{1}{\varepsilon_1} N^{-2} + \frac{1}{\varepsilon_1} N^{-2}\right] \leq CN^{-2}, \qquad (5.2.53)
\end{aligned}
$$

where we have used the followings: Since $x_{i+1} \geq \tau_x$, then we have

$$
e^{-\sqrt{\frac{\beta\gamma}{\varepsilon_1}}x_{i+1}} \leq e^{-\sqrt{\frac{\beta\gamma}{\varepsilon_1}}\tau_x} = e^{-\sqrt{\frac{\beta\gamma}{\varepsilon_1}}\sigma_0\sqrt{\varepsilon_1}\ln N} = N^{-2},
$$

for $\sigma_0 = \frac{2}{\sqrt{\beta\gamma}}$. A similar bound can be obtained by using $1 - x_{i+1} \geq \tau_x$.

Similarly, for I_2, we have

$$
\begin{aligned}
|I_2| &\leq \varepsilon_1 h_i^x \int_{x_{i-1}}^{x_{i+1}} \left(1 + \varepsilon_1^2 e^{-\sqrt{\frac{\beta\gamma}{\varepsilon_1}}\xi} + \varepsilon_1^2 e^{-\sqrt{\frac{\beta\gamma}{\varepsilon_1}}(1-\xi)}\right) d\xi \\
&\leq C\varepsilon_1 h_i^x \left[h_i^x + \frac{1}{\varepsilon_1^{3/2}}\left(e^{-\sqrt{\frac{\beta\gamma}{\varepsilon_1}}x_{i+1}} - e^{-\sqrt{\frac{\beta\gamma}{\varepsilon_1}}x_{i-1}}\right) + \frac{1}{\varepsilon_1^{3/2}}\left(e^{-\sqrt{\frac{\beta\gamma}{\varepsilon_1}}(1-x_{i+1})} - e^{-\sqrt{\frac{\beta\gamma}{\varepsilon_1}}(1-x_{i-1})}\right)\right] \\
&\leq C\varepsilon_1 h_i^x \left[h_i^x + \frac{1}{\varepsilon_1^{3/2}} \sinh(h_i^x) e^{-\sqrt{\frac{\beta\gamma}{\varepsilon_1}}x_i} + \frac{1}{\varepsilon_1^{3/2}} \sinh(h_i^x) e^{-\sqrt{\frac{\beta\gamma}{\varepsilon_1}}(1-x_i)}\right] \\
&\leq C\varepsilon_1 h_i^x \left[h_i^x + \frac{1}{\varepsilon_1^{3/2}} h_i^x e^{-\sqrt{\frac{\beta\gamma}{\varepsilon_1}}x_i} + \frac{1}{\varepsilon_1^{3/2}} h_i^x e^{-\sqrt{\frac{\beta\gamma}{\varepsilon_1}}(1-x_i)}\right] \\
&\leq C\varepsilon_1 h_i^x \left[h_i^x + \frac{h_i^x}{\varepsilon_1}\frac{1}{\varepsilon_1^{1/2}} e^{-\sqrt{\frac{\beta\gamma}{\varepsilon_1}}x_i} + \frac{h_i^x}{\varepsilon_1}\frac{1}{\varepsilon_1^{1/2}} e^{-\sqrt{\frac{\beta\gamma}{\varepsilon_1}}(1-x_i)}\right] \\
&\leq C\varepsilon_1 h_i^x \left[h_i^x + \frac{h_i^x}{\varepsilon_1}\frac{1}{x_i} + \frac{h_i^x}{\varepsilon_1}\frac{1}{1-x_i}\right] \\
&\leq C\left[\varepsilon_1 (h_i^x)^2 + (h_i^x)^2 \frac{1}{x_i} + (h_i^x)^2 \frac{1}{1-x_i}\right]. \qquad (5.2.54)
\end{aligned}
$$

Similarly, for I_3, we have

$$
\begin{aligned}
|I_3| &\leq \varepsilon_2 \int_{x_{i-1}}^{x_i} \left(1 + \varepsilon_1 e^{-\sqrt{\frac{\beta\gamma}{\varepsilon_1}}\xi} + \varepsilon_1 e^{-\sqrt{\frac{\beta\gamma}{\varepsilon_1}}(1-\xi)}\right) d\xi \\
&\leq C\varepsilon_2 \left[h_i^x + \frac{1}{\sqrt{\varepsilon_1}} \left| e^{-\sqrt{\frac{\beta\gamma}{\varepsilon_1}}x_i} - e^{-\sqrt{\frac{\beta\gamma}{\varepsilon_1}}x_{i-1}} \right| + \frac{1}{\sqrt{\varepsilon_1}} \left| e^{-\sqrt{\frac{\beta\gamma}{\varepsilon_1}}(1-x_i)} - e^{-\sqrt{\frac{\beta\gamma}{\varepsilon_1}}(1-x_{i-1})} \right| \right] \\
&\leq C\varepsilon_2 \left[h_i^x + \frac{1}{\sqrt{\varepsilon_1}} e^{-\sqrt{\frac{\beta\gamma}{\varepsilon_1}}x_i} + \frac{1}{\sqrt{\varepsilon_1}} e^{-\sqrt{\frac{\beta\gamma}{\varepsilon_1}}(1-x_i)}\right] \\
&\leq C\varepsilon_2 \left[h_i^x + \frac{1}{\sqrt{\varepsilon_1}} N^{-2} + \frac{1}{\sqrt{\varepsilon_1}} N^{-2}\right] \leq CN^{-2}. \qquad (5.2.55)
\end{aligned}
$$

Here we have used the fact $\varepsilon_2^2 \leq C\varepsilon_1$ along with the followings: Since $x_i \geq \tau_x$, we have

$$
e^{-\sqrt{\frac{\beta\gamma}{\varepsilon_1}}x_i} \leq e^{-\sqrt{\frac{\beta\gamma}{\varepsilon_1}}\tau_x} = e^{-\sqrt{\frac{\beta\gamma}{\varepsilon_1}}\sigma_0\sqrt{\varepsilon_1}\ln N} = N^{-2},
$$

for $\sigma_0 = \frac{2}{\sqrt{\beta\gamma}}$. A similar bound can be obtained by using $1 - x_i \geq \tau_x$.

From the above estimates of I_1, I_2 and I_3, it follows that $\left|\theta_i(\widehat{u}^{n+1/2}, x_i)\right| \leq CN^{-2}$, whenever $\tau_x < x_i < 1 - \tau_x$. □

Theorem 5.2.10. *Let $\varepsilon_2 \leq N^{-1}$ and $\widehat{u}^{n+1/2}$, $\widehat{U}^{n+1/2}$ be the solutions of the BVPs* (5.2.14) *and* (5.2.26) *respectively. Then we get:*

$$
\left\| \widehat{U}^{n+1/2} - \widehat{u}^{n+1/2}\big|_{\overline{\Omega}^N} \right\|_{\infty,\overline{\Omega}^N} \leq \begin{cases} C\Delta t N^{-2}, & \tau_x \leq x_i \leq 1 - \tau_x, \\ C\Delta t N^{-2} \ln^2 N, & \textit{otherwise.} \end{cases} \qquad (5.2.56)
$$

Proof. Using the inequality (5.2.44) and Lemma 5.2.9, it is clear that,

$$
\mathbb{L}_{1,\varepsilon}^N \left(\widehat{U}^{n+1/2}(x_i, y) - \widehat{u}^{n+1/2}(x_i, y)\right) = \Theta\left(\widehat{U}^{n+1/2}, x_i\right) \qquad (5.2.57)
$$

$$
\leq \begin{cases} C\Delta t N^{-2}, & N/4 < i < 3N/4, \\ C\Delta t N^{-2} \ln^2 N, & \text{otherwise.} \end{cases} \qquad (5.2.58)
$$

We use the discrete maximum principle for $\mathbb{L}_{1,\varepsilon}^N$, by choosing the following discrete barrier function

$$
\Phi(x_i) = \begin{cases} C_1 \Delta t N^{-2}, & N/4 < i < 3N/4, \\ C_1 \Delta t N^{-2} \ln^2 N, & \text{otherwise,} \end{cases}
$$

for some $C_1 > 0$. Thus, from the above, we easily get

$$\left|\widehat{U}^{n+1/2}(x_i,y) - \widehat{u}^{n+1/2}(x_i,y)\right| \leq \begin{cases} C\Delta t N^{-2}, & N/4 < i < 3N/4, \\ C\Delta t N^{-2}\ln^2 N, & \text{otherwise}, \end{cases}$$

for every $y \in \Omega_y^N$. This proves the result (5.2.56). □

Theorem 5.2.11. *Suppose $\widehat{U}^{n+1}$ solves the problem (5.2.27) at $t = t_{n+1}$ and the function $\widehat{u}^{n+1}$ solves (5.2.14). If $\varepsilon_2 \leq N^{-1}$, then we have:*

$$\left\|\widehat{U}^{n+1} - \widehat{u}^{n+1}|_{\overline{\Omega}^N}\right\|_{\infty,\overline{\Omega}^N} \leq \begin{cases} C\Delta t N^{-2}, & \tau_y < y_j < 1-\tau_y, \\ C\Delta t N^{-2}\ln^2 N, & \textit{otherwise.} \end{cases} \tag{5.2.59}$$

Proof. The proof can be carried out exactly in the same way as in Theorem 3.9 by Mrityunjoy *et al.* ([69], pp. 269). □

Now, we present the main convergence result for Case I in the next theorem.

Theorem 5.2.12. *Let U^n be the fully-discrete solution of the problem (5.2.30) for $t = t_n$ and u solves the equation (5.1.1). Then, the global error accomplish the following error estimate:*

$$\left\|U^n - u(t_n)|_{\overline{\Omega}^N}\right\|_{\infty,\overline{\Omega}^N} \leq \begin{cases} C\left(\Delta t + N^{-2}\right), & \tau_x < x_i < 1-\tau_x,\ \tau_y < y_j < 1-\tau_y, \\ C\left(\Delta t + N^{-2}\ln^2 N\right), & \textit{otherwise.} \end{cases} \tag{5.2.60}$$

Proof. We first observe that,

$$U^n - u(t_n)|_{\overline{\Omega}^N} = \left(U^n - \widehat{U}^n\right) + \left(\widehat{U}^n - \widehat{u}^n|_{\overline{\Omega}^N}\right) + \left(\widehat{u}^n|_{\overline{\Omega}^N} - u(t_n)|_{\overline{\Omega}^N}\right), \tag{5.2.61}$$

where $\widehat{U}^n$ is the solution obtained at the n-th iteration in the discrete version of the problem (5.2.14).

We now use Lemma 4.2.2 and Theorem 5.2.11 to get,

$$\left\|\widehat{u}^n|_{\overline{\Omega}^N} - u(t_n)|_{\overline{\Omega}^N}\right\|_{\infty,\overline{\Omega}^N} \leq C\Delta t^2,$$

$$\left\|\widehat{U}^n - \widehat{u}^n|_{\overline{\Omega}^N}\right\|_{\infty,\overline{\Omega}^N} \leq \begin{cases} C\Delta t N^{-2}, & \tau_x < x_i < 1-\tau_x,\ \tau_y < y_j < 1-\tau_y, \\ C\Delta t N^{-2}\ln^2 N, & \text{otherwise.} \end{cases}$$

By using these estimates, $n\Delta t \leq T$, and the inequality $\left\|\left(\mathbb{L}_{i,\varepsilon}^{N}\right)^{-1}\right\| \leq C, \quad i = 1, 2$, we have

$$\begin{aligned}\left\|U^n - u(t_n)|_{\overline{\Omega}^N}\right\|_{\infty,\overline{\Omega}^N} &\leq C\Delta t\big(\Delta t + N^{-2}\big) + C\left\|U^{n-1} - u(t_{n-1})|_{\overline{\Omega}^N}\right\|_{\infty,\overline{\Omega}^N} \\ &\leq Cn\Delta t\big(\Delta t + N^{-2}\big) \leq C\big(\Delta t + N^{-2}\big),\end{aligned}$$

for $\tau_x < x_i, y_j < 1 - \tau_x$. Similarly, using the same estimates, we can obtain the following

$$\begin{aligned}\left\|U^n - u(t_n)|_{\overline{\Omega}^N}\right\|_{\infty,\overline{\Omega}^N} &\leq C\Delta t\big(\Delta t + N^{-2}\ln^2 N\big) + C\left\|U^{n-1} - u(t_{n-1})|_{\overline{\Omega}^N}\right\|_{\infty,\overline{\Omega}^N} \\ &\leq Cn\Delta t\big(\Delta t + N^{-2}\ln^2 N\big) \leq C\big(\Delta t + N^{-2}\ln^2 N\big),\end{aligned}$$

for $x_i \leq \tau_x,\ y_j \leq \tau_y$ and $x_i \geq 1 - \tau_x,\ y_j \geq 1 - \tau_y$. □

5.2.4 Numerical experiments

In this section, we present the numerical results obtained with fully-discrete scheme proposed here to solve successfully some problems of type (5.1.1) with appropriate parameters for Case I.

Example 5.2.13. *We take the following example of a parabolic SPP in the domain* $G = (0,1)^2 \times (0,1]$.

$$\begin{cases} \dfrac{\partial u}{\partial t} - \varepsilon_1\left(\dfrac{\partial^2 u}{\partial x^2} + \dfrac{\partial^2 u}{\partial y^2}\right) + \dfrac{\varepsilon_2}{2}\Big(2 + xy\Big)\left(\dfrac{\partial u}{\partial x} + \dfrac{\partial u}{\partial y}\right) + \quad u = \Big(x^2 - x + y^2 - y\Big)t^2, \\ \qquad\qquad\qquad\qquad\qquad\qquad\qquad\qquad\qquad\qquad (x,y) \in (0,\ 1)^2,\ 0 < t \leq 1, \\ u = 0, \quad \textit{for } (x,y) \in \Gamma, \quad 0 \leq t \leq 1, \\ u = 0, \quad \textit{at } t = 0, \quad (x,y) \in (0,1)^2, \end{cases} \tag{5.2.62}$$

where $\Gamma = \Gamma_b \cup \Gamma_t \cup \Gamma_l \cup \Gamma_r$, *and the parameters are taken from*

$$S_1 = \left\{\big(\varepsilon_1, \varepsilon_2\big) : \varepsilon_1 = 10^{-k}, \quad \varepsilon_2 = \frac{\sqrt{\varepsilon_1}}{10}, \quad k = 1, 2, \ldots, 6\right\}. \tag{5.2.63}$$

We present the uniform error $E^{N,\Delta t}$ and the uniform rate of convergence $p^{N,\Delta t}$ in Table 5.1 and 5.2 with the loglog plot of maximum norm of the error in Figures 5.2-5.3. Although, the theoretical results suggest that the scheme has first-order convergence in time and second-order convergence in space, we are unable to observe it from Table 5.1. Therefore, we consider the temporal mesh parameter as $M = O(N^2)$ so that it reflects the true convergence rate

in the space variable (see Table 5 in Das and Natesan [54]). In Table 5.2, we show that the spatial convergence is second-order by taking $\Delta t = \frac{2}{N^2}$ for time discretization in each cases. The corresponding loglog plots in Figure (5.2) and Figure (5.3) represent the graphical validation of the error estimates for Case I.

Table 5.1: Error in max norm and rate of convergence for $\varepsilon_2 = \frac{\sqrt{\varepsilon_1}}{10}$ with $\Delta t = \frac{1}{N}$.

ε_1	$N = 32$	64	128	256	512
10^{-1}	2.6889e-03	1.3465e-03	6.7525e-04	3.3847e-04	1.6948e-04
	0.9978	0.9956	0.9963	0.9979	-
10^{-2}	9.8135e-03	3.1231e-03	1.3435e-03	6.2993e-04	3.0570e-04
	1.651	1.217	1.092	1.043	-
10^{-3}	1.8335e-02	5.9385e-03	1.9982e-03	8.5954e-04	4.0188e-04
	1.626	1.571	1.217	1.096	-
10^{-4}	4.6455e-02	2.4289e-02	1.0738e-02	3.8073e-03	1.3920e-03
	0.9354	1.177	1.495	1.451	-
10^{-5}	4.6452e-02	2.4298e-02	1.0743e-02	4.1636e-03	1.7402e-03
	0.9349	1.177	1.367	1.258	-
10^{-6}	4.6508e-02	2.4299e-02	1.0744e-02	4.1641e-03	1.7403e-03
	0.9365	1.177	1.367	1.258	-
$E^{N,\Delta t}$	**4.6508e-02**	**2.4299e-02**	**1.0744e-02**	**4.1641e-03**	**1.7403e-03**
$p^{N,\Delta t}$	**0.9371**	**1.177**	**1.367**	**1.258**	-

5.3 Analysis of the hybrid scheme: Case II

We have addressed the consistency and the stability of the hybrid scheme for the first case in the previous sections. In the subsequent part, we confine the analysis to the case when $\varepsilon_2^2 \geq \frac{\gamma\varepsilon_1}{\beta}$. For the current case, the problem (5.1.1) has regular boundary layers of width $O(\varepsilon_2)$ near the inflow boundaries, *i.*e. at the edges $x = 0$ and $y = 0$, and there are regular boundary layers of width $O\Big(\varepsilon_1/\varepsilon_2\Big)$ appearing at the outflow boundaries $x = 1$ and $y = 1$. We use the same solution decomposition (5.2.1) for the continuous solution, but the layer

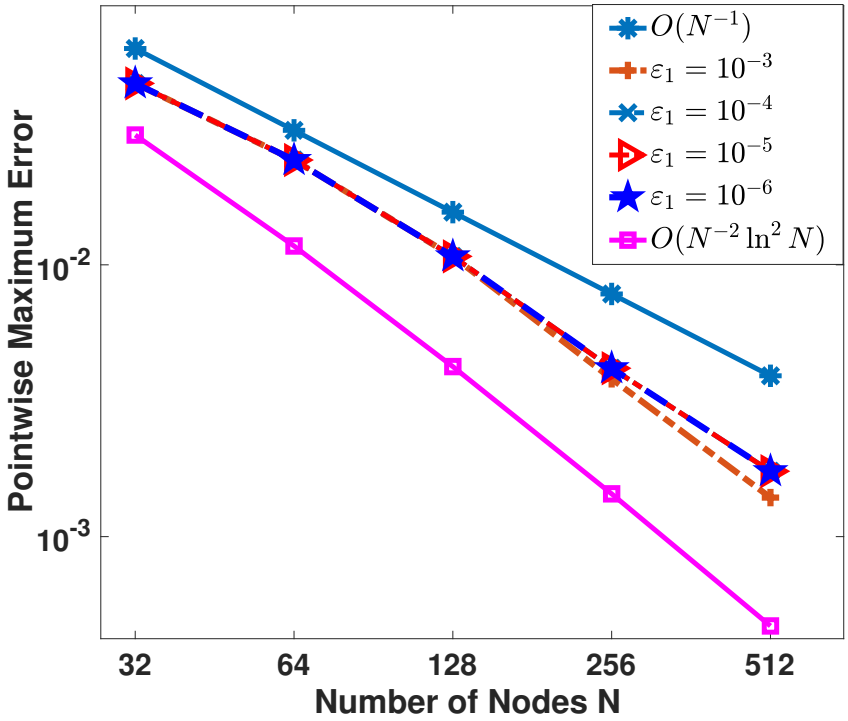

Figure 5.2: Visualization of the loglog plot of the maximum point-wise error with $\Delta t = \frac{1}{N}$.

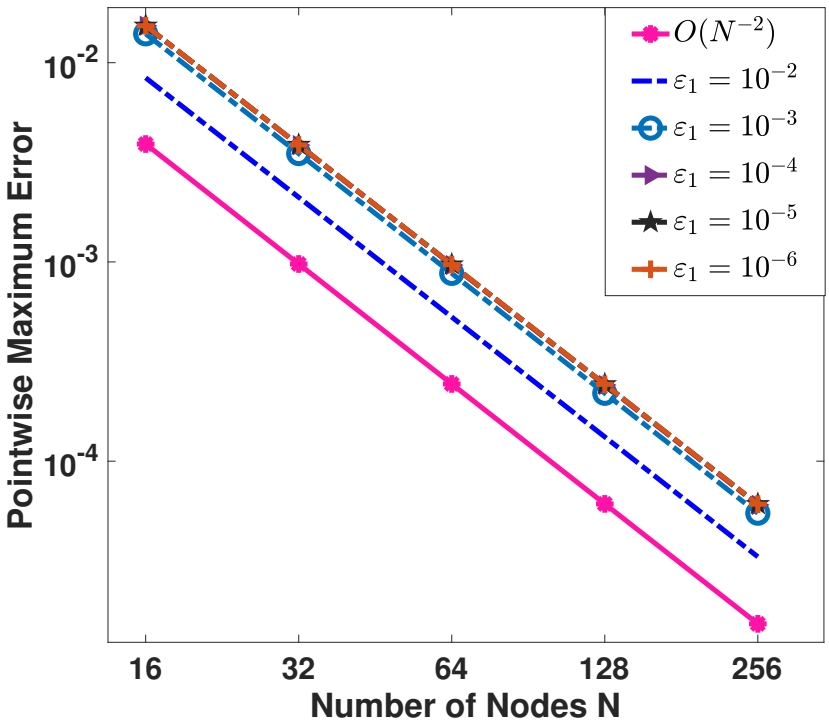

Figure 5.3: Visualization of the loglog plot for the maximum point-wise error with $\Delta t = \frac{1}{2N^2}$.

Table 5.2: Error in max norm and rate of convergence for $\varepsilon_2 = \dfrac{\sqrt{\varepsilon_1}}{10}$ with $\Delta t = \dfrac{2}{N^2}$.

ε_1	$N = 16$	32	64	128	256
10^{-1}	8.3986e-03	2.1105e-03	5.2896e-04	1.3241e-04	3.3122e-05
	1.992	1.996	1.998	1.999	-
10^{-2}	1.3961e-02	3.4999e-03	8.7619e-04	2.1920e-04	5.4819e-05
	1.996	1.998	1.999	1.999	-
10^{-3}	1.5325e-02	3.8564e-03	9.6459e-04	2.4121e-04	6.0309e-05
	1.990	1.999	1.999	1.999	-
10^{-4}	1.5324e-02	3.8653e-03	9.7018e-04	2.4305e-04	6.0838e-05
	1.987	1.994	1.997	1.998	-
10^{-5}	1.5324e-02	3.8653e-03	9.7018e-04	2.4305e-04	6.0838e-05
	1.987	1.994	1.997	1.998	-
10^{-6}	1.5324e-02	3.8653e-03	9.7018e-04	2.4305e-04	6.0838e-05
	1.987	1.994	1.997	1.998	-
$E^{N,\Delta t}$	**1.5324e-02**	**3.8653e-03**	**9.7018e-04**	**2.4305e-04**	**6.0838e-05**
$p^{N,\Delta t}$	**1.987**	**1.994**	**1.997**	**1.998**	-

components, however, respect the following bounds:

$$\left|\frac{\partial^{k_s+k_t} v}{\partial x^{k_1}\partial y^{k_2}\partial t^{k_t}}\right| \leq C, \tag{5.3.1}$$

$$\left|\frac{\partial^{k_s+k_t} w_L}{\partial x^{k_1}\partial y^{k_2}\partial t^{k_t}}\right| \leq C\varepsilon_2^{-k_1} e^{-\frac{\gamma x}{2\varepsilon_2}}, \tag{5.3.2}$$

$$\left|\frac{\partial^{k_s+k_t} w_R}{\partial x^{k_1}\partial y^{k_2}\partial t^{k_t}}\right| \leq C\left(\frac{\varepsilon_1}{\varepsilon_2}\right)^{-k_1} e^{-\frac{\beta\varepsilon_2}{2\varepsilon_1}(1-x)}, \tag{5.3.3}$$

$$\left|\frac{\partial^{k_s+k_t} w_B}{\partial x^{k_1}\partial y^{k_2}\partial t^{k_t}}\right| \leq C\varepsilon_2^{-k_2} e^{-\frac{\gamma y}{2\varepsilon_2}}, \tag{5.3.4}$$

$$\left|\frac{\partial^{k_s+k_t} w_T}{\partial x^{k_1}\partial y^{k_2}\partial t^{k_t}}\right| \leq C\left(\frac{\varepsilon_1}{\varepsilon_2}\right)^{-k_2} e^{-\frac{\beta\varepsilon_2}{2\varepsilon_1}(1-y)}, \tag{5.3.5}$$

and

$$\left|\frac{\partial^{k_s+k_t} w_{LB}}{\partial x^{k_1}\partial y^{k_2}\partial t^{k_t}}\right| \leq C \min\left\{\varepsilon_2^{-k_1} e^{-\frac{\gamma x}{2\varepsilon_2}},\ \varepsilon_2^{-k_2} e^{-\frac{\gamma y}{2\varepsilon_2}}\right\} \tag{5.3.6}$$

$$\left|\frac{\partial^{k_s+k_t} w_{RB}}{\partial x^{k_1}\partial y^{k_2}\partial t^{k_t}}\right| \leq C \min\left\{\left(\frac{\varepsilon_1}{\varepsilon_2}\right)^{-k_1} e^{-\frac{\beta\varepsilon_2}{2\varepsilon_1}(1-x)},\ \varepsilon_2^{-k_2} e^{-\frac{\gamma y}{2\varepsilon_2}}\right\}, \tag{5.3.7}$$

$$\left|\frac{\partial^{k_s+k_t} w_{LT}}{\partial x^{k_1}\partial y^{k_2}\partial t^{k_t}}\right| \leq C \min\left\{\varepsilon_2^{-k_1} e^{-\frac{\gamma x}{2\varepsilon_2}},\ \left(\frac{\varepsilon_1}{\varepsilon_2}\right)^{-k_2} e^{-\frac{\beta\varepsilon_2}{2\varepsilon_1}(1-y)}\right\}, \tag{5.3.8}$$

$$\left|\frac{\partial^{k_s+k_t} w_{RT}}{\partial x^{k_1}\partial y^{k_2}\partial t^{k_t}}\right| \leq C \min\left\{\left(\frac{\varepsilon_1}{\varepsilon_2}\right)^{-k_1} e^{-\frac{\beta\varepsilon_2}{2\varepsilon_1}(1-x)},\ \left(\frac{\varepsilon_1}{\varepsilon_2}\right)^{-k_2} e^{-\frac{\beta\varepsilon_2}{2\varepsilon_1}(1-y)}\right\}, \tag{5.3.9}$$

where $k_s = k_1 + k_2$ and $0 \leq k_1 + k_2 + 2k_t \leq 4$. We refer the reader to [68] for more details on the rigorous parameter-explicit bounds.

5.3.1 Temporal and spatial discretizations

In this case, the semidiscrete problem is exactly given as in the previous section, that is u^n is the solution of the semidiscrete problem in (5.2.13) and $\widehat{u}^n$ can be defined similarly as we have done in (5.2.14). We remark that the analysis for the semidiscrete problem (5.2.13) does not depend on the discretization of the domain in space. Moreover, we describe the grid with constant step-length Δt for time variable as in (5.2.12). Therefore, the results stated in previous part are also held for the current case. The following results can be established following a similar approach as we did in the previous case and hence, we simply state them without repeating their proofs.

Lemma 5.3.1. *The estimate for the local error e_{n+1} due to time discretization satisfies the following*

$$\|e_{n+1}\|_{\infty,\overline{\Omega}} \leq C\Delta t^2, \quad n = 0, 1, \ldots, M-1. \tag{5.3.10}$$

Lemma 5.3.2. *The global temporal error $E_n = u(t_n) - u^n,\ 1 \leq n \leq M$ satisfies the following estimate*

$$\sup_{n\Delta t \leq T} \|E_n\|_{\infty,\overline{\Omega}} \leq C\Delta t. \tag{5.3.11}$$

However, the spatial mesh is not same as the one described in the previous sections due to the different layer configuration. We first describe the mesh along x-direction and similarly, we create the mesh along the y-direction also.

Let us define the characteristic equation

$$-\varepsilon_1\eta^2(x) + \varepsilon_2\ b_1(x,y)\eta(x) + c_1(x,y) = 0 \tag{5.3.12}$$

by keeping y as a parameter. Next we define the constants

$$\mu_0 = \frac{-\varepsilon_2 B_1 + \sqrt{\varepsilon_2^2 B_1^2 + 4\varepsilon_1\gamma_1}}{2\varepsilon_1}, \quad \mu_1 = \frac{\varepsilon_2\beta + \sqrt{\varepsilon_2^2\beta^2 + 4\varepsilon_1\gamma_1}}{2\varepsilon_1}, \tag{5.3.13}$$

with $B_1 = \|b_1\|_\infty$, $c_1(x,y) \geq \gamma_1$. For the grid in x-direction, the transition parameters $\tau_0,\ \tau_1$ satisfy

$$\tau_0 = \min\left\{\frac{1}{4},\ \frac{2}{\mu_0}\ln N\right\}, \quad \tau_1 = \min\left\{\frac{1}{4},\ \frac{2}{\mu_1}\ln N\right\}.$$

Then, the domain $\overline{\Omega}_x = [0,1]$ is splitted into the following subintervals by,

$$\overline{\Omega}_x = [0,\ \tau_0] \cup [\tau_0,\ 1-\tau_1] \cup [1-\tau_1,\ 1].$$

Here also we distribute the grid points along the x-direction in a ratio of $1:2:1$ among these intervals. Thus, the Shishkin mesh described in this direction can explicitly be defined as

$$x_i = \begin{cases} \dfrac{4i\tau_0}{N}, & 0 \leq i \leq N/4, \\ \tau_0 + 2\left(i - \dfrac{N}{4}\right)\dfrac{1-\tau_0-\tau_1}{N}, & N/4 < i \leq 3N/4, \\ 1-\tau_1 + 4\left(i - \dfrac{3N}{4}\right)\dfrac{\tau_1}{N}, & 3N/4 < i \leq N. \end{cases} \tag{5.3.14}$$

We note that a similar set of meshpoints for $\overline{\Omega}_y^N$ can be constructed along the y-direction by using the following transition parameters

$$\tau_0 = \min\left\{\frac{1}{4},\ \frac{2}{\rho_0}\ln N\right\}, \quad \tau_1 = \min\left\{\frac{1}{4},\ \frac{2}{\rho_1}\ln N\right\},$$

where the constants $\rho_0,\ \rho_1$ satisfy

$$\rho_0 = \frac{-\varepsilon_2 B_2 + \sqrt{\varepsilon_2^2 B_2^2 + 4\varepsilon_1\gamma_2}}{2\varepsilon_1}, \quad \rho_1 = \frac{\varepsilon_2\beta + \sqrt{\varepsilon_2^2\beta^2 + 4\varepsilon_1\gamma_2}}{2\varepsilon_1}, \tag{5.3.15}$$

with $B_2 = \|b_2\|_\infty$, $c_2(x,y) \geq \gamma_2$.

Since the boundary layer structure at various boundaries are not the same and they depend on the constants $\mu_0,\ \mu_1$, we observe the following properties of the semidiscrete solutions of the problem in (5.2.14) for the present case.

Lemma 5.3.3. *Let $\varepsilon_1, \varepsilon_2$ satisfy the relation $\varepsilon_2^2 \geq \dfrac{\gamma\varepsilon_1}{\beta}$ and $\widehat{u}^{n+1/2}$ solves the equation* (5.2.14)

for $0 \le n \le M-1$. *Then for* $i = 0, 1, \ldots, \le 4$, *we obtain*

$$\left|\frac{\partial^i \widehat{u}^{n+1/2}}{\partial x^i}\right| \le C\left[1 + \mu_0^i e^{-p\mu_0 x} + \mu_1^i e^{-p\mu_1(1-x)}\right], \quad 0 \le x \le 1, \tag{5.3.16}$$

when $2\varepsilon_2 \left\|\frac{\partial b_1}{\partial x}\right\|_{\infty,\Omega} \le \delta(1-p)$ *and* μ_0, μ_1 *are defined and for* $0 \le j \le 4$, *we have*

$$\left|\frac{\partial^j \widehat{u}^{n+1}}{\partial y^j}\right| \le C\left[1 + \mu_0^j e^{-p\mu_0 y} + \mu_1^j e^{-p\mu_1(1-y)}\right], \quad 0 \le y \le 1, \tag{5.3.17}$$

with $p, \delta \in (0,1)$ *and* $2\varepsilon_2 \left\|\frac{\partial b_2}{\partial y}\right\|_{\infty,\Omega} \le \delta(1-p)$.

Proof. Proof of the above lemma is available in [69]. □

5.3.2 Convergence analysis

In this section, we will study the convergence analysis of the fully discrete problem in (5.2.30) and (5.2.31) for the Case II. As we mentioned earlier, the Lemma 5.2.5, Lemma 5.2.6 and Lemma 5.2.8 are valid for the current case as well. Now, we present the estimate for the local truncation error of (5.2.30) - (5.2.31) on a Shishkin mesh defined for Case II.

Lemma 5.3.4. *The local truncation error* $\theta_i(\widehat{u}, x_i)$ *at* $x = x_i$ *defined in* (5.2.45) *satisfies the following error bound:*

$$|\theta_i(\widehat{u}, x_i)| \le \begin{cases} CN^{-2}, & \tau_x \le x_i \le 1 - \tau_x, \\ CN^{-2}\ln^2 N, & \textit{otherwise.} \end{cases} \tag{5.3.18}$$

Proof. We find the estimate for θ_i separately for $x = x_i$ in each of the regions. We examine the following three typical cases one by one.

Case (i): Inside the layer regions: $1 \le i \le N/4$

In this case, using (5.2.46), we have

$$\begin{aligned}
|I_1| &\leq \varepsilon_1 \int_{x_{i-1}}^{x_i} \left(1 + \varepsilon_2^{-4} e^{-\frac{\beta\gamma}{\varepsilon_2}\xi} + \frac{\varepsilon_2^4}{\varepsilon_1^4} e^{-\frac{\beta\gamma\varepsilon_2}{\varepsilon_1}(1-\xi)}\right) d\xi \\
&\leq C\left[\varepsilon_1 h_i^x + \frac{\varepsilon_1}{\varepsilon_2^3}\left(e^{-\frac{\beta\gamma}{\varepsilon_2}x_i} - e^{-\frac{\beta\gamma}{\varepsilon_2}x_{i-1}}\right)\right] + C\frac{\varepsilon_2^3}{\varepsilon_1^2}\left[e^{-\frac{\beta\gamma\varepsilon_2}{\varepsilon_1}(1-x_i)} - e^{-\frac{\beta\gamma\varepsilon_2}{\varepsilon_1}(1-x_{i-1})}\right] \\
&\leq C\left(\varepsilon_1 h_i^x + \frac{\varepsilon_1}{\varepsilon_2^3}\frac{h_i^x}{\varepsilon_2} e^{-\frac{\beta\gamma}{\varepsilon_2}x_i} + \varepsilon_2 \frac{\varepsilon_2^2}{\varepsilon_1^2} e^{-\frac{\beta\gamma\varepsilon_2}{\varepsilon_1}(1-x_i)}\right) \\
&\leq C\left(\varepsilon_1 h_i^x + \frac{\varepsilon_2^2}{\varepsilon_2^3}\frac{h_i^x}{\varepsilon_2} e^{-\frac{\beta\gamma}{\varepsilon_2}x_i} + \varepsilon_2 \frac{\varepsilon_2^2}{\varepsilon_1^2} e^{-\frac{\beta\gamma\varepsilon_2}{\varepsilon_1}(1-x_i)}\right) \\
&\leq C\left(\varepsilon_1\varepsilon_2 N^{-1}\ln N + + \frac{1}{\varepsilon_2} N^{-1}\ln N + \varepsilon_2\right).
\end{aligned}$$

Combining the last inequality with the first term on the right hand side of (5.2.46), we get,

$$h_i^x\,|I_1| \leq CN^{-2}\ln^2 N. \tag{5.3.19}$$

A similar estimate can be obtained for I_2, that is,

$$\begin{aligned}
|I_2| &\leq \int_{x_{i-1}}^{x_i} \varepsilon_2\left(1 + \varepsilon_2^{-3} e^{-\frac{\beta\gamma}{\varepsilon_2}\xi} + \frac{\varepsilon_2^3}{\varepsilon_1^3} e^{-\frac{\beta\gamma\varepsilon_2}{\varepsilon_1}(1-\xi)}\right) d\xi \\
&\leq C\left[\varepsilon_2 h_i^x + \frac{\varepsilon_2}{\varepsilon_2^2}\left(e^{-\frac{\beta\gamma}{\varepsilon_2}x_i} - e^{-\frac{\beta\gamma}{\varepsilon_2}x_{i-1}}\right)\right] + C\left[\varepsilon_2\frac{\varepsilon_2^2}{\varepsilon_1^2}\left(e^{-\frac{\beta\gamma\varepsilon_2}{\varepsilon_1}(1-x_i)} - e^{-\frac{\beta\gamma\varepsilon_2}{\varepsilon_1}(1-x_{i-1})}\right)\right] \\
&\leq C\left[\varepsilon_2 h_i^x + \frac{1}{\varepsilon_2}\frac{h_i^x}{\varepsilon_2} e^{-\frac{\beta\gamma}{\varepsilon_2}x_i} + \varepsilon_2\frac{\varepsilon_2^2}{\varepsilon_1^2} e^{-\frac{\beta\gamma\varepsilon_2}{\varepsilon_1}(1-x_i)}\right] \\
&\leq C\left(\varepsilon_2^2 N^{-1}\ln N + \frac{1}{\varepsilon_2} N^{-1}\ln N + \varepsilon_2\right).
\end{aligned}$$

Combining the last inequality and the right hand side of (5.2.46), we get

$$h_i^x\,|I_2| \leq CN^{-2}\ln^2 N. \tag{5.3.20}$$

Therefore, from (5.3.19) and (5.3.20) we obtain the desired estimate.

Case (ii): Inside the layer regions: $3N/4 \leq i \leq N-1$

In this case, using (5.2.46), we have,

$$
\begin{aligned}
|I_1| &\leq \int_{x_{i-1}}^{x_i} \varepsilon_1 \left(1 + \varepsilon_2^{-4} e^{-\frac{\beta\gamma}{\varepsilon_2}\xi} + \frac{\varepsilon_2^4}{\varepsilon_1^4} e^{-\frac{\beta\gamma\varepsilon_2}{\varepsilon_1}(1-\xi)}\right) d\xi \\
&\leq C\left[\varepsilon_1 h_i^x + \frac{\varepsilon_1}{\varepsilon_2^3}\left(e^{-\frac{\beta\gamma}{\varepsilon_2}x_i} - e^{-\frac{\beta\gamma}{\varepsilon_2}x_{i-1}}\right)\right] + C\left[\varepsilon_1 \frac{\varepsilon_2^3}{\varepsilon_1^3}\left(e^{-\frac{\beta\gamma\varepsilon_2}{\varepsilon_1}(1-x_i)} - e^{-\frac{\beta\gamma\varepsilon_2}{\varepsilon_1}(1-x_{i-1})}\right)\right] \\
&\leq C\left(\frac{\varepsilon_1^2}{\varepsilon_2} N^{-1}\ln N + \frac{\varepsilon_1}{\varepsilon_2^3}\frac{h_i^x}{\varepsilon_2} e^{-\frac{\beta\gamma}{\varepsilon_2}x_{i-1}} + \varepsilon_1 \frac{\varepsilon_2^3}{\varepsilon_1^3} h_i^x \frac{\varepsilon_2}{\varepsilon_1} e^{-\frac{\beta\gamma\varepsilon_2}{\varepsilon_1}(1-x_i)}\right) \\
&\leq C\left(\frac{\varepsilon_1^2}{\varepsilon_2} N^{-1}\ln N + \frac{\varepsilon_1^2}{\varepsilon_2^5} N^{-1}\ln N + \varepsilon_1 \frac{\varepsilon_2^3}{\varepsilon_1^3}\frac{\varepsilon_1}{\varepsilon_2} N^{-1}\ln N \frac{\varepsilon_2}{\varepsilon_1} e^{-\frac{\beta\gamma\varepsilon_2}{\varepsilon_1}(1-x_i)}\right) \\
&\leq C\left(\frac{\varepsilon_1^2}{\varepsilon_2} N^{-1}\ln N + \frac{\varepsilon_1^2}{\varepsilon_2^5} N^{-1}\ln N + \varepsilon_2 \frac{\varepsilon_2}{\varepsilon_1} N^{-1}\ln N\right) \\
&\leq C\left(\varepsilon_2^3 N^{-1}\ln N + \frac{\varepsilon_1^2}{\varepsilon_2^5} N^{-1}\ln N + \frac{\varepsilon_2}{\varepsilon_1} N^{-1}\ln N\right).
\end{aligned}
$$

From the last inequality and the equation (5.2.46), we get

$$
h_i^x\,|I_1| \leq \frac{\varepsilon_2}{\varepsilon_1} N^{-1}\ln N\,|I_1| \leq C N^{-2}\ln^2 N. \tag{5.3.21}
$$

A similar estimate can be obtained for I_2, that is,

$$
\begin{aligned}
|I_2| &\leq \int_{x_{i-1}}^{x_i} \varepsilon_2 \left(1 + \varepsilon_2^{-3} e^{-\frac{\beta\gamma}{\varepsilon_2}\xi} + \frac{\varepsilon_2^3}{\varepsilon_1^3} e^{-\frac{\beta\gamma\varepsilon_2}{\varepsilon_1}(1-\xi)}\right) d\xi \\
&\leq C\left[\varepsilon_2 h_i^x + \frac{1}{\varepsilon_2}\left(e^{-\frac{\beta\gamma}{\varepsilon_2}x_i} - e^{-\frac{\beta\gamma}{\varepsilon_2}x_{i-1}}\right)\right] \\
&\quad + C\left[\varepsilon_2 \frac{\varepsilon_2^2}{\varepsilon_1^2}\left(e^{-\frac{\beta\gamma\varepsilon_2}{\varepsilon_1}(1-x_i)} - e^{-\frac{\beta\gamma\varepsilon_2}{\varepsilon_1}(1-x_{i-1})}\right)\right] \\
&\leq C\left[\varepsilon_1 N^{-1}\ln N + \frac{1}{\varepsilon_2}\frac{h_i^x}{\varepsilon_2}\left(e^{-\frac{\beta\gamma}{\varepsilon_2}x_{i-1}}\right)\right] + C\left[\varepsilon_2 \frac{\varepsilon_2^2}{\varepsilon_1^2} h_i^x \frac{\varepsilon_2}{\varepsilon_1}\left(e^{-\frac{\beta\gamma\varepsilon_2}{\varepsilon_1}(1-x_{i-1})}\right)\right] \\
&\leq C\left(\varepsilon_1 N^{-1}\ln N + \frac{\varepsilon_1}{\varepsilon_2^3} N^{-1}\ln N + \frac{\varepsilon_2^4}{\varepsilon_1^3}\frac{\varepsilon_1}{\varepsilon_2} N^{-1}\ln N \frac{\varepsilon_1}{\varepsilon_2}\right) \\
&\leq C\left(\varepsilon_1 N^{-1}\ln N + \frac{\varepsilon_1}{\varepsilon_2^3} N^{-1}\ln N + \frac{\varepsilon_2}{\varepsilon_1} N^{-1}\ln N\right).
\end{aligned}
$$

From the last inequality and the equation (5.2.46), we get

$$h_i^x\,|I_2| \leq \frac{\varepsilon_1}{\varepsilon_2} N^{-1} \ln N\,|I_2| \leq C N^{-2} \ln^2 N. \tag{5.3.22}$$

Therefore, from (5.3.21) and (5.3.22) we obtain the desired estimate.

Case (iii): Outside the layer regions: $N/4 < i < 3N/4$

In this case, using (5.2.47), we have,

$$\begin{aligned}
|I_1| &\leq \int_{x_{i-1}}^{x_{i+1}} \varepsilon_1 \left(1 + \varepsilon_2^{-3} e^{-\frac{\beta\gamma}{\varepsilon_2}\xi} + \frac{\varepsilon_2^3}{\varepsilon_1^3} e^{-\frac{\beta\gamma\varepsilon_2}{\varepsilon_1}(1-\xi)}\right) d\xi \\
&\leq C\left[\varepsilon_1 h_i^x + \frac{\varepsilon_1}{\varepsilon_2^2}\left(e^{-\frac{\beta\gamma}{\varepsilon_2}x_{i+1}} - e^{-\frac{\beta\gamma}{\varepsilon_2}x_{i-1}}\right)\right] \\
&+ C\left[\varepsilon_1 \frac{\varepsilon_2^2}{\varepsilon_1^2}\left(e^{-\frac{\beta\gamma\varepsilon_2}{\varepsilon_1}(1-x_{i+1})} - e^{-\frac{\beta\gamma\varepsilon_2}{\varepsilon_1}(1-x_{i-1})}\right)\right] \\
&\leq C\left[\varepsilon_2^2 N^{-1} + e^{-\frac{\beta\gamma}{\varepsilon_2}\tau_0} + \varepsilon_1 h_i^x \frac{\varepsilon_2^3}{\varepsilon_1^3}\left(e^{-\frac{\beta\gamma\varepsilon_2}{\varepsilon_1}(1-x_{i+1})}\right)\right] \\
&\leq C\left(\varepsilon_2^2 N^{-1} + N^{-2} + \varepsilon_1 h_i^x\right) \leq C N^{-2}.
\end{aligned} \tag{5.3.23}$$

Similarly, for I_2, we obtain

$$\begin{aligned}
|I_2| &\leq \int_{x_{i-1}}^{x_i} \varepsilon_2 \left(1 + \varepsilon_2^{-2} e^{-\frac{\beta\gamma}{\varepsilon_2}\xi} + \frac{\varepsilon_2^2}{\varepsilon_1^2} e^{-\frac{\beta\gamma\varepsilon_2}{\varepsilon_1}(1-\xi)}\right) d\xi \\
&\leq C\left[\varepsilon_2 h_i^x + \left(e^{-\frac{\beta\gamma}{\varepsilon_2}x_i} - e^{-\frac{\beta\gamma}{\varepsilon_2}x_{i-1}}\right)\right] \\
&+ C\left[\varepsilon_2 \frac{\varepsilon_2}{\varepsilon_1}\left(e^{-\frac{\beta\gamma\varepsilon_2}{\varepsilon_1}(1-x_i)} - e^{-\frac{\beta\gamma\varepsilon_2}{\varepsilon_1}(1-x_{i-1})}\right)\right] \\
&\leq C\left[\varepsilon_2 h_i^x + e^{-\frac{\beta\gamma}{\varepsilon_2}x_{i+1}} + \varepsilon_2 \frac{\varepsilon_2}{\varepsilon_1}\left(e^{-\frac{\beta\gamma\varepsilon_2}{\varepsilon_1}(1-x_i)} - e^{-\frac{\beta\gamma\varepsilon_2}{\varepsilon_1}(1-x_{i-1})}\right)\right] \\
&\leq C\left[\varepsilon_2 h_i^x + N^{-2} + \varepsilon_1 h_i^x \frac{\varepsilon_2^3}{\varepsilon_1^3}\frac{\varepsilon_2}{\varepsilon_1} e^{-\frac{\beta\gamma\varepsilon_2}{\varepsilon_1}(1-x_{i-1})}\right] \\
&\leq C\left(\varepsilon_2 h_i^x + N^{-2} + \varepsilon_1 h_i^x\right) \leq C N^{-2}.
\end{aligned}$$

So, we have

$$|I_2| \leq CN^{-2}. \tag{5.3.24}$$

Similarly, for I_3, we also have

$$\begin{aligned}
|I_3| &\leq \int_{x_{i-1}}^{x_i} h_i^x \left(1 + \varepsilon_2^{-2} e^{-\frac{\beta\gamma}{\varepsilon_2}\xi} + \frac{\varepsilon_2^2}{\varepsilon_1^2} e^{-\frac{\beta\gamma\varepsilon_2}{\varepsilon_1}(1-\xi)}\right) d\xi \\
&\leq C\left[(h_i^x)^2 + \frac{h_i^x}{\varepsilon_2}\left(e^{-\frac{\beta\gamma}{\varepsilon_2}x_i} - e^{-\frac{\beta\gamma}{\varepsilon_2}x_{i-1}}\right)\right] \\
&\quad + C\left[h_i^x \frac{\varepsilon_2}{\varepsilon_1}\left(e^{-\frac{\beta\gamma\varepsilon_2}{\varepsilon_1}(1-x_i)} - e^{-\frac{\beta\gamma\varepsilon_2}{\varepsilon_1}(1-x_{i-1})}\right)\right] \qquad (5.3.25) \\
&\leq C\left[(h_i^x)^2 + h_i^x \varepsilon_2^2 \frac{1}{\varepsilon_2^3} e^{-\frac{\beta\gamma}{\varepsilon_2}x_i} + h_i^x \frac{\varepsilon_2}{\varepsilon_1} h_i^x \frac{\varepsilon_2}{\varepsilon_1}\left(e^{-\frac{\beta\gamma\varepsilon_2}{\varepsilon_1}(1-x_{i+1})}\right)\right] \\
&\leq C\left[(h_i^x)^2 + h_i^x \varepsilon_2^2 \frac{1}{x_i} + (h_i^x)^2 \frac{\varepsilon_1^2}{\varepsilon_2^2}\frac{1}{x_{i-1}}\right] \\
&\leq C\left[(h_i^x)^2 + h_i^x \varepsilon_2^2 \frac{1}{\varepsilon_2 \ln N} + (h_i^x)^2 \frac{\varepsilon_1^2}{\varepsilon_2^2}\frac{\varepsilon_2}{\varepsilon_1 \ln N}\right] \\
&\leq C\left[(h_i^x)^2 + h_i^x N^{-1} + (h_i^x)^2 N^{-1}\right] \leq CN^{-2}. \qquad (5.3.26)
\end{aligned}$$

Using the inequalities (5.3.23) - (5.3.25) in (5.2.47), we obtain the desired estimate. □

Theorem 5.3.5. *Assuming $\widehat{U}^{n+1/2}$ be the function defined in the semidiscrete problem* (5.2.26) *and $\widehat{u}^{n+1/2}$ be the solution defined in* (5.2.14) *on $\overline{\Omega}^N$, the following bound holds:*

$$\left\| \widehat{U}^{n+1/2} - \widehat{u}^{n+1/2}\big|_{\overline{\Omega}^N} \right\|_{\infty,\overline{\Omega}^N} \leq \begin{cases} C\Delta t N^{-2}, & \tau_0 \leq x_i \leq 1-\tau_1, \\ C\Delta t N^{-2}\ln^2 N, & \text{otherwise.} \end{cases} \tag{5.3.27}$$

Proof. The proof is based on the truncation error estimate given in Lemma 5.3.4 and can be done exactly in a similar approach as Theorem 4.2.9. □

An analogous proof for the following theorem follows for the second subproblem as well.

Theorem 5.3.6. *Let $\widehat{U}^{n+1}$ solves the semidiscrete problem* (5.2.27) *at $t = t_{n+1}$ and $\widehat{u}^{n+1}$*

solves the problem (5.2.14). *Then the following bounds are valid:*

$$\left\| \widehat{U}^{n+1} - \widehat{u}^{n+1}\big|_{\overline{\Omega}^N} \right\|_{\infty,\overline{\Omega}^N} \leq \begin{cases} C\Delta t N^{-2}, & \tau_0 \leq y_j \leq 1-\tau_1, \\ C\Delta t N^{-2}\ln^2 N, & \text{otherwise.} \end{cases} \tag{5.3.28}$$

Now we present the main convergence theorem of this section for Case II.

Theorem 5.3.7. *Let U^n be the fully-discrete solution of the problem* (5.2.30) *at $t = t_n$ and let u be the exact solution of* (5.1.1). *Then, the global error can be estimated by*

$$\|U^n - u(t_n)\|_{\infty,\overline{\Omega}^N} \leq \begin{cases} C\left(\Delta t + N^{-2}\right), & \tau_0 \leq x_i, y_j \leq 1-\tau_1, \\ C\left(\Delta t + N^{-2}\ln^2 N\right), & \text{otherwise.} \end{cases} \tag{5.3.29}$$

5.3.3 Numerical experiments

Here, we illustrate the numerical experiments obtained by applying the fully-discrete scheme to efficiently solve the problem (5.1.1) with appropriate parameters for Case II. We take the test problem as in Example 5.2.13 with the following configuration:

$$S_2 = \left\{ \left(\varepsilon_1, \varepsilon_2\right) : \varepsilon_1 = 10^{-k-2}, \quad \varepsilon_2 = {\varepsilon_1}^{1/4}, \quad k = 1, 2, \ldots, 6 \right\}. \tag{5.3.30}$$

We present the parameter-uniform error $E^{N,\Delta t}$ and the parameter-independent rate of convergence $p^{N,\Delta t}$ in Table 5.3 and Table 5.4 with the diagram of the plot of the maximum norm of the error in logarithmic scale in Figures 5.4-5.5. Although, the theoretical results suggest that the scheme has first-order convergence in time and second-order accurate in space, we are unable to observe it directly from Table 5.3. Therefore, in order to reveal the actual convergence order in space, we take $M = O(N^2)$ (see Table 5 in Das and Natesan [54]). By taking $\Delta t = \dfrac{2}{N^2}$ in Table 5.4, we show that the spatial convergence is also of second-order. The corresponding loglog plots in Figure (5.4) and Figure (5.5) represent the graphical validation of the error estimates for Case II.

5.4 Conclusions

In this work, we construct and analyze an efficient ADI-based hybrid numerical method for a class of IBVPs of parabolic type in two dimensions with two perturbation parameters appearing in the diffusion and convection terms. A Shishkin mesh that is piecewise-uniform

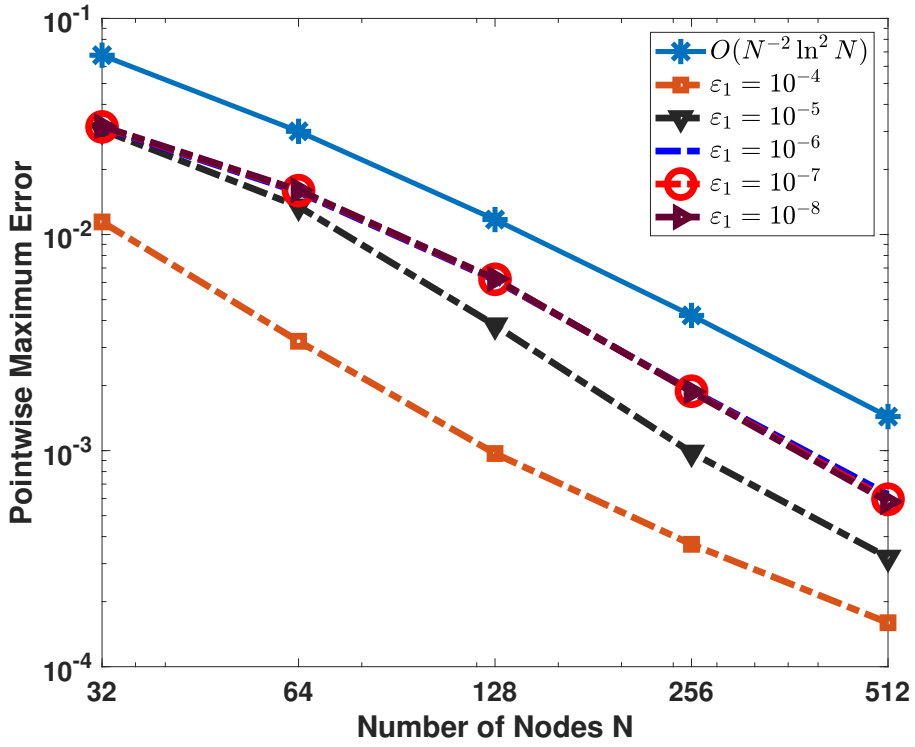

Figure 5.4: Visualization of the loglog plot of the maximum pointwise error with $\Delta t = \frac{1}{N}$.

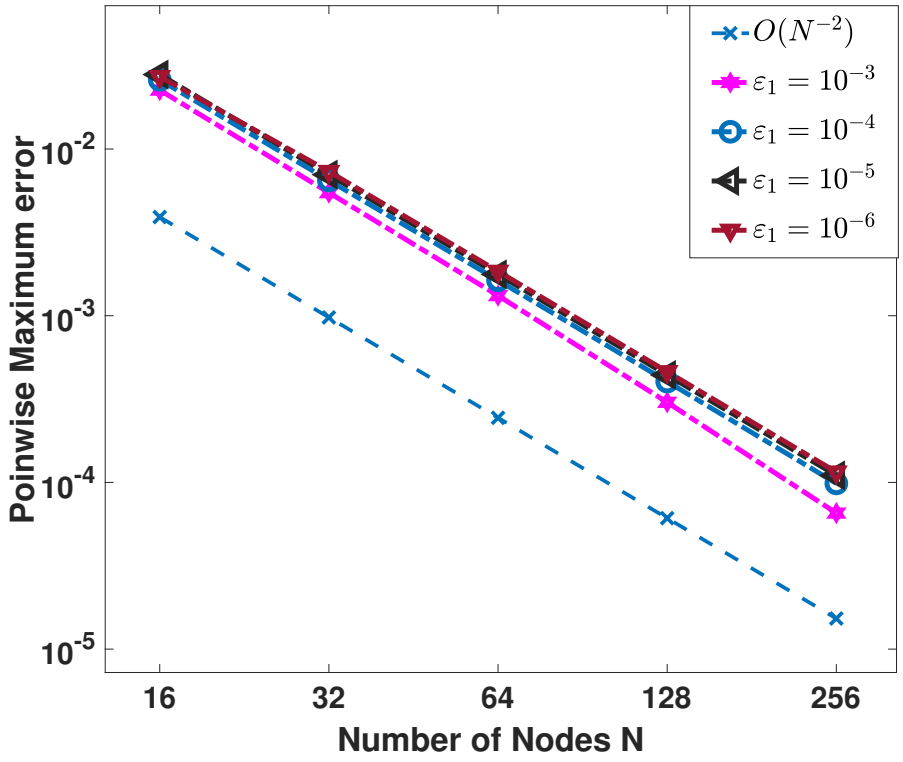

Figure 5.5: Visualization of the loglog plot for the pointwise error with $\Delta t = \frac{2}{N^2}$.

Table 5.3: *Error in discrete maximum norm and rate of convergence for* $\varepsilon_2 = {\varepsilon_1}^{1/4}$ with $\Delta t = \dfrac{1}{N}$.

ε_1	$N = 32$	64	128	256	512
10^{-3}	2.6384e-03	1.0144e-03	4.4362e-04	2.1165e-04	1.0592e-04
	1.3790	1.1932	1.0676	0.9987	-
10^{-4}	1.1437e-02	3.2067e-03	9.6936e-04	3.6841e-04	1.5976e-04
	1.8345	1.7260	1.3957	1.2054	-
10^{-5}	3.0478e-02	1.3491e-02	3.8035e-03	9.7979e-04	3.1984e-04
	1.1757	1.8266	1.9568	1.6151	-
10^{-6}	3.1220e-02	1.5739e-02	6.1459e-03	1.8989e-03	6.2574e-04
	0.9881	1.3567	1.6945	1.6016	-
10^{-7}	3.1482e-02	1.5954e-02	6.2044e-03	1.8831e-03	5.9559e-04
	0.9806	1.3626	1.7202	1.6607	-
10^{-8}	3.1702e-02	1.6042e-02	6.2324e-03	1.8742e-03	5.7995e-04
	0.9827	1.3640	1.7335	1.6923	-
$E^{N,\Delta t}$	**3.1702e-02**	**1.6042e-02**	**6.2324e-03**	**1.8989e-03**	**6.2574e-04**
$p^{N,\Delta t}$	**0.9827**	**1.3640**	**1.7146**	**1.6015**	-

and adapts to the layer characteristics of the solution has been used to construct the spatial grid. The present hybrid scheme has been established to be consistent as well as stable with respect to the perturbation parameters. Appropriate error estimates are achieved separately for two different cases having different structures of the layer. The numerical experiments are performed to validate the theoretical convergence results and illustrate the efficiency of the proposed strategy.

Table 5.4: *Error in discrete maximum norm and rate of convergence for* $\varepsilon_2 = \varepsilon^{1/4}$ *with* $\Delta t = \dfrac{2}{N^2}$.

ε_1	$N = 16$	32	64	128	256
10^{-3}	1.1486e-02	2.9178e-03	7.3170e-04	1.8306e-04	4.5774e-05
	1.976	1.995	1.998	1.999	-
10^{-4}	1.5099e-02	3.5688e-03	8.8353e-04	2.2029e-04	5.4958e-05
	2.080	2.014	2.003	2.003	-
10^{-5}	2.2552e-02	5.4735e-03	1.3195e-03	3.0228e-04	6.5451e-05
	2.042	2.052	2.126	2.207	-
10^{-6}	2.6002e-02	6.4810e-03	1.6301e-03	4.0277e-04	9.8641e-05
	2.0043	1.991	2.016	2.029	-
10^{-7}	2.7967e-02	7.0189e-03	1.7690e-03	4.4095e-04	1.1015e-04
	1.994	1.988	2.004	2.001	-
10^{-8}	2.7184e-02	7.3289e-03	1.8462e-03	4.6116e-04	1.1538e-04
	1.891	1.989	2.001	1.998	-
$E^{N,\Delta t}$	**2.7967e-02**	**7.3289e-03**	**1.8462e-03**	**4.6116e-04**	**1.1538e-04**
$p^{N,\Delta t}$	**1.891**	**1.989**	**2.001**	**1.998**	-

CHAPTER 6

The summary and future scope of the thesis

6.1 Summary of the thesis

In this thesis, we have proposed some computationally efficient, yet very simple numerical algorithms for a class of degenerate SPPs and a class of parabolic non-degenerate SPPs with two parameters in two dimensions. The numerical methods discussed here are not only convergent, they are uniformly stable with respect to the perturbation parameters also. We can summarize the works in this thesis as follows.

In Chapter 2, we have considered a singularly perturbed degenerate BVP with two parameters $\varepsilon_1,\ \varepsilon_2$. Depending on the relations between the parameters, we studied the problems in two different cases, namely $\varepsilon_2^2 \leq C\varepsilon_1$ and $\varepsilon_2^2 \geq C\varepsilon_1$, due to the difference in the boundary layer structures. In each of these cases, we have discussed the a prori estimates on the derivatives of the regular and layer components of the exact solution. We have considered the characteristic equation of the problem and defined the transition points based on that in order to design the Shishkin mesh. We have used an standard upwind scheme for solving the problem numerically and achieved first-order accuracy in the approximation. We also have studied the Richardson extrapolation method for improving the approximate solution of the same model problem considered in the previous chapter. The extrapolation scheme is derived from the existing numerical solution U^N on a Shishkin mesh $\overline{\Omega}^N$ and the solution $\widehat{U}^N$ obtained on the refinement of the same mesh by keeping the same transition points. The truncation error estimates are computed for every singular and smooth components of the solution to prove the consistency of the scheme. We also discuss the parameter-uniform stability to establish the second-order convergence of the method.

In Chapter 3, we have considered a time-dependent convection-diffusion-reaction problem with parameters with smooth initial data. To define the semidiscrete problem, we used backward-Euler scheme to approximate the time derivative on a uniformly spaced temporal grid. For spatial mesh, we have formed Shishkin mesh with the transition points defined in the same way as we did the previous works. Then, a uniformly convergent upwind finite difference method has been used to discretize the spatial derivatives for describing the fully-discrete problem. The resulting scheme has been established to be first-order accurate in both space and time variables. We also employed Richardson extrapolation scheme to enhance the spatial convergence of this solution to second-order. Suitable numerical examples are included for validation of the theoretical estimates for both schemes.

In Chapter 4, we have studied a first-order convergent upwind scheme for a 2D parabolic SPP of convection-diffusion-reaction type with two parameters. In this work, we used backward-Euler scheme for the time variable and an ADI-type operator splitting method for the space variables. While the temporal mesh has been taken as equispaced, the piecewise-

uniform Shishkin mesh was considered for spatial discretization. The scheme was proved uniformly convergent and first-order accurate in both time and space variables. Appropriate examples are discussed to support the convergence results at the end of the chapter.

The last work in this thesis discusses a hybrid numerical scheme for the same model problem in Chapter 5. Here we use ADI-type finite difference scheme which is a combination of a midpoint upwind scheme and a central difference scheme for the spatial derivatives. Backward-Euler approximation of time derivatives ensures first-order accuracy for time variable, while the hybrid scheme has second-order convergence for the space variables. The consistency and stability of this scheme has been numerically established with the help of some suitable examples in the end.

6.2 Future scope of the thesis

6.2.1 Numerical approximations for a two-parameter singularly perturbed parabolic problem of convection-diffusion type with a discontinuous initial condition

In this work, we study the SPP of the following type

$$\begin{cases} u_t - \varepsilon_1 u_{xx} + \varepsilon_2 a(x,t) u_x = f(x,t), \quad x \in \Omega = (0,1), \quad t \in (0,T], \\ u(x,t) = 0, \quad x \in \partial\Omega = \overline{\Omega}\backslash\Omega, \quad 0 \le t \le T, \\ u(x,0) = \phi(x) \notin C(\Omega), \quad x \in \Omega. \end{cases} \tag{6.2.1}$$

We assume that the functions a, f, ϕ satisfy the bellow conditions:

$$a,\ f \in C^{4+\gamma}(\Omega) \text{ for some } \gamma > 0,\ a(x,t) \ge \alpha > 0, \text{ and that } \phi^{(l)}(0) = 0 = \phi^{(l)}(1),\ 0 \le l \le 4.$$

Let there be a point $d \in (0,1)$ such that ϕ is not continuous at $x = d$, but $\phi \in C^4(\overline{\Omega} \setminus \{d\})$. Due to the presence of this non-smoothness in the initial condition, the solution exhibits an interior layer along with a boundary layer. Since the problem is parabolic in nature, the location of the initial layer moves in time in case of a convection-diffusion problem, while in case of a reaction-diffusion equation, it remains fixed. In this model problem, the formed interior layer moves along a characteristic curve which, is associated with the corresponding reduced problem. Gracia and O'Riordan [11, 70] discussed about the movement of the interior layer for convection-diffusion SPPs. This affects the convergence rate of the numerical scheme

for convection-diffusion problems in the original domain. Therefore, we need to transform the space variable x into s so that the characteristic curve can be transformed into a straight line, around which we can construct the required Shishkin mesh for the computation. The following map $S : (x,t) \longrightarrow (s,t)$ is a possible transformation which will serve our purpose.

$$s(x,t) = \begin{cases} \dfrac{xd}{d(t)}, & x \le d(t), \\ 1 - \dfrac{1-d}{1-d(t)}(1-x), & else. \end{cases} \tag{6.2.2}$$

However, no such transformation is necessary if $a(x,t)$ is only time-dependent. We plan to solve this problem using a uniformly convergent finite difference method in the transformed domain.

6.2.2 A comparative study of singularly perturbed parabolic convection-diffusion-reaction problems on some layer-adapted meshes using streamline-diffusion finite element methods

We study the following parabolic SPP:

$$\begin{cases} \dfrac{\partial u}{\partial t} - \varepsilon \dfrac{\partial^2 u}{\partial x^2} + b(x)\dfrac{\partial u}{\partial x} + c(x)u(x,t) = f(x,t), \quad x \in \Omega = (0,1), \quad t \in (0,T], \\ u(0,t) = 0, \quad u(1,t) = 0, \quad 0 \le t \le T, \\ u(x,0) = \phi(x), \quad x \in \Omega, \end{cases} \tag{6.2.3}$$

where the perturbation parameter ε satisfies $0 < \varepsilon \ll 1$. The coefficient functions b, c as well as the given functions ϕ, f are assumed to be sufficiently smooth. To construct the computational mesh, we use the idea of original Bakhvalov mesh. The mesh generating function $\lambda(t)$, associated with the exponential boundary layer at $x = 0$, is defined as

$$\lambda(t) = \begin{cases} \psi(t) := \sigma\varepsilon\phi(t), & 0 \le t < \alpha \\ \psi(\alpha) + \psi'(\alpha)(t-\alpha), & \alpha \le t \le 1, \end{cases} \tag{6.2.4}$$

where $\phi(t) = \ln \dfrac{q}{q-t}$, $0 \le t < q$ and $\sigma > 0$, $q \in (0,1)$ are user chosen parameters. It is not difficult to see that the mesh is graded inside the layer region, while we see uniform spacing outside the region. To create the mesh, we also assume $\psi'(0) < 1$, which gives $\sigma\varepsilon < q$. The

mesh transition point α corresponds to the point $(\alpha, \psi(\alpha))$ where the tangent from the point $(1,1)$ touches the curve $\psi(t)$. Thus, α is given by the following implicit relation

$$\frac{1-\psi(\alpha)}{1-\alpha} = \psi'(\alpha). \tag{6.2.5}$$

The generated modified-Bakhvalov mesh points are defined by

$$x_i = \lambda(t_i),\ t_i = i/N, \quad 0 \le i \le N.$$

Now, since the relation (6.2.5) does not give α explicitly, we therefore need to approximate it suitably to construct the computational mesh. We follow the idea of construction of the mesh described in [71], and our goal is to present the analysis of the method on this special mesh. We plan to solve the parabolic problem using a uniformly convergent streamline-diffusion finite element method (SDFEM).

6.2.3 Higher-order accurate numerical method for singularly perturbed parabolic problems of degenerate type with two perturbation parameters in 2D

We consider the following singularly perturbed degenerate parabolic problem:

$$\begin{cases} u_t + \mathcal{L}_\varepsilon u = f(x,y,t), \quad (x,y) \in \Omega = (0,1)^2, \quad t \in (0,T], \\ u(x,y,t) = 0, \quad (x,y) \in \partial\Omega = \overline{\Omega}\backslash\Omega, \quad 0 \le t \le T, \\ u(x,y,0) = \phi(x,y), \quad (x,y) \in \overline{\Omega}, \end{cases} \tag{6.2.6}$$

where $0 < \varepsilon_1, \varepsilon_2 \ll 1$ and

$$\mathcal{L}_\varepsilon u := -\varepsilon_1 \Delta u + \varepsilon_2 \widehat{\mathbf{b}}(x,y) \cdot \nabla u + c(x,y)u, \tag{6.2.7}$$

$$\widehat{\mathbf{b}} = (\widehat{b}_1, \widehat{b}_2), \quad \widehat{b}_1(x,y) = b_1(x,y)x^p, \quad \widehat{b}_2(x,y) = b_2(x,y)y^q,\ p,q \ge 1, \tag{6.2.8}$$

$$b_1(x,y) \ge \beta_1 > 0, \quad b_2(x,y) \ge \beta_2 > 0, \quad c(x,y) \ge c_0 > 0, \quad x \in \overline{\Omega}. \tag{6.2.9}$$

We also assume that the associated functions $b_1,\ b_2,\ c$ are all smooth enough and the source function $f = f_1 + f_2$ satisfies the compatibility property,

$$f_1(x,0,t) = f_1(x,1,t) = f_2(0,y,t) = f_2(1,y,t) = 0. \tag{6.2.10}$$

We will complete the analysis of the convergence of an standard upwind method for solving this degenerate problem in two separate cases based on the boundary layer formation at the boundaries of the domain. For grid construction, we propose to use the modified-Bakhvalov mesh for a better resolution of the layer structure which depend on the relations between the parameters $\varepsilon_1,\ \varepsilon_2$.

Bibliography

[1] J. Miller, E. O'Riordan, G. Shishkin, Fitted Numerical Methods for Singular Perturbation Problems, World Scientific, Singapore, 1996.

[2] P. Farrell, A. Hegarty, J. Miller, E. O'Riordan, G. Shishkin, Robust Computational Techniques for Boundary Layers, Chapman & Hall/CRC Press, Boco Raton, 2000.

[3] H.-G. Roos, M. Stynes, L. Tobiska, Robust Numerical Methods for Singularly Perturbed Differential Equations: Convection-Diffusion-Reaction and Flow Problems, Vol. 24, Springer Science & Business Media, 2008.

[4] T. Linß, Layer-adapted meshes for reaction-convection-diffusion problems, Vol. 1985 of Lecture Notes in Mathematics, Springer-Verlag, Berlin, 2010.

[5] M. C. Natividad, M. Stynes, Richardson extrapolation for a convection–diffusion problem using a shishkin mesh, Applied Numerical Mathematics 45 (2-3) (2003) 315–329.

[6] C. Clavero, J. Jorge, F. Lisbona, G. Shishkin, A fractional step method on a special mesh for the resolution of multidimensional evolutionary convection-diffusion problems, Applied Numerical Mathematics 27 (3) (1998) 211–231.

[7] P. Das, S. Natesan, Higher-order parameter uniform convergent schemes for robin type reaction-diffusion problems using adaptively generated grid, International Journal of Computational Methods 9 (04) (2012) 1250052.

[8] P. Das, V. Mehrmann, Numerical solution of singularly perturbed convection-diffusion-reaction problems with two small parameters, BIT Numerical Mathematics 56 (1) (2016) 51–76.

[9] D. Avijit, S. Natesan, SDFEM for singularly perturbed boundary-value problems with two parameters, Journal of Applied Mathematics and Computing 64 (2020) 591–614.

[10] M. K. Kadalbajoo, A. S. Yadaw, Parameter-uniform finite element method for two-parameter singularly perturbed parabolic reaction-diffusion problems, International Journal of Computational methods 9 (04) (2012) 1250047.

[11] J. Gracia, E. O'Riordan, A singularly perturbed convection diffusion parabolic problem with an interior layer, in: BAIL 2010-Boundary and Interior Layers, Computational and Asymptotic Methods, Springer, 2011, pp. 139–146.

[12] J. M.-S. Lubuma, K. C. Patidar, Non-standard methods for singularly perturbed problems possessing oscillatory/layer solutions, Applied Mathematics and Computation 187 (2) (2007) 1147–1160.

[13] K. C. Patidar, K. K. Sharma, Uniformly convergent non-standard finite difference methods for singularly perturbed differential-difference equations with delay and advance, International Journal for Numerical Methods in Engineering 66 (2) (2006) 272–296.

[14] J. B. Munyakazi, K. C. Patidar, Novel fitted operator finite difference methods for singularly perturbed elliptic convection–diffusion problems in two dimensions, Journal of Difference Equations and Applications 18 (5) (2012) 799–813.

[15] K. C. Patidar, A robust fitted operator finite difference method for a two-parameter singular perturbation problem1, Journal of Difference Equations and Applications 14 (12) (2008) 1197–1214.

[16] E. Bashier, K. Patidar, A second-order fitted operator finite difference method for a singularly perturbed delay parabolic partial differential equation, Journal of Difference Equations and Applications 17 (05) (2011) 779–794.

[17] R. O'Malley, Introduction to Singular Perturbations, Academic Press, New York, 1974.

[18] R. O'Malley, Singular Perturbation Methods for Ordinary Differential Equations, Springer, New York, 1991.

[19] E. Doolan, J. Miller, W. Schildres, Uniform Numerical Methods for Problems with Initial and Boundary Layers, Boole Press, Dublin, 1980.

[20] S. Gowrisankar, S. Natesan, Robust numerical scheme for singularly perturbed convection–diffusion parabolic initial–boundary-value problems on equidistributed grids, Computer Physics Communications 185 (7) (2014) 2008–2019.

[21] K. Mukherjee, S. Natesan, Richardson extrapolation technique for singularly perturbed parabolic convection–diffusion problems, Computing 92 (2011) 1–32.

[22] K. Mukherjee, S. Natesan, ε-uniform error estimate of hybrid numerical scheme for singularly perturbed parabolic problems with nterior layers, Numerical Algorithms 58 (1) (2011) 103–141.

[23] J. Mohapatra, S. Natesan, Uniformly convergent second-order numerical method for singularly perturbed delay differential equations, Neural, Parallel and Scientific Computations 16 (3) (2008) 353.

[24] J. Mohapatra, S. Natesan, Uniformly convergent numerical method for singularly perturbed differential-difference equation using grid equidistribution, International Journal for Numerical Methods in Biomedical Engineering 27 (9) (2011) 1427–1445.

[25] N. Kopteva, E. O'Riordan, Shishkin meshes in the numerical solution of singularly perturbed differential equations, Int. J. Numer. Anal. Model. 7 (3) (2010) 393–415.

[26] H.-G. Roos, Error estimates for linear finite elements on bakhvalov-type meshes, Applications of Mathematics 51 (2006) 63–72.

[27] H.-G. Roos, L. Teofanov, Z. Uzelac, A modified bakhvalov mesh, Applied Mathematics Letters 31 (2014) 7–11.

[28] R. Kellogg, T. Linss, M. Stynes, A finite difference method on layer-adapted meshes for an elliptic reaction-diffusion system in two dimensions, Mathematics of computation 77 (264) (2008) 2085–2096.

[29] M. Brdar, H. Zarin, A singularly perturbed problem with two parameters on a bakhvalov-type mesh, Journal of Computational and Applied Mathematics 292 (2016) 307–319.

[30] J. Zhang, X. Liu, Supercloseness of linear finite element method on bakhvalov-type meshes for singularly perturbed convection–diffusion equation in 1d, Applied Mathematics Letters 111 (2021) 106624.

[31] E. O'Riordan, M. Pickett, G. Shishkin, Numerical methods for singularly perturbed elliptic problems containing two perturbation parameters, Mathematical Modelling and Analysis 11 (2) (2006) 199–212.

[32] A. Jha, M. K. Kadalbajoo, A robust layer adapted difference method for singularly perturbed two-parameter parabolic problems, International Journal of Computer Mathematics 92 (6) (2015) 1204–1221.

[33] V. Gupta, M. K. Kadalbajoo, R. K. Dubey, A parameter-uniform higher order finite difference scheme for singularly perturbed time-dependent parabolic problem with two small parameters, International Journal of Computer Mathematics 96 (3) (2019) 474–499.

[34] V. Shanthi, N. Ramanujam, S. Natesan, Fitted mesh method for singularly perturbed reaction-convection-diffusion problems with boundary and interior layers, Journal of Applied Mathematics and Computing 22 (1) (2006) 49–65.

[35] Y. Qiu, D. Sloan, Analysis of difference approximations to a singularly perturbed two-point boundary value problem on an adaptively generated grid, Journal of computational and applied mathematics 101 (1-2) (1999) 1–25.

[36] N. Kopteva, M. Stynes, A robust adaptive method for a quasi-linear one-dimensional convection-diffusion problem, SIAM Journal on Numerical Analysis 39 (4) (2001) 1446–1467.

[37] T. Linß, Uniform pointwise convergence of finite difference schemes using grid equidistribution, Computing 66 (1) (2001) 27–39.

[38] N. Kopteva, N. Madden, M. Stynes, Grid equidistribution for reaction–diffusion problems in one dimension, Numerical Algorithms 40 (3) (2005) 305–322.

[39] P. Das, Robust numerical schemes for singularly perturbed boundary-value problems on adaptive meshes, Ph.D. thesis, Indian Institute of Technology Guwahati (2013).

[40] S. Gowrisankar, Uniformly convergent numerical schemes for singularly perturbed parabolic partial diffrential equations on adaptive grid, Ph.D. thesis, Indian Institute of Technology Guwahati (2013).

[41] G. Shishkin, V. Titov, A difference scheme for a differential equation with two small parameters at the derivatives, Chisl. Metody Meh. Sploshn. Sredy 7 (2) (1976) 145–155.

[42] M. Stynes, H.-G. Roos, The midpoint upwind scheme, Applied Numerical Mathematics 23 (3) (1997) 361–374.

[43] G. I. Shishkin, Grid approximation of a singularly perturbed elliptic equation with convective terms in the presence of various boundary layers, Zhurnal Vychislitel'noi Matematiki i Matematicheskoi Fiziki 45 (1) (2005) 110–125.

[44] A. Jha, M. K. Kadalbajoo, Hybrid method for two parameter singularly perturbed elliptic boundary value problems, Computational and Mathematical Methods 3 (6) (2021) e1210.

[45] M. Kadalbajoo, A. Jha, Analysis of fitted spline in compression for convection diffusion problems with two small parameters, Neural Parallel and Scientific Computations 19 (3) (2011) 307.

[46] M. K. Kadalbajoo, A. Jha, Exponentially fitted cubic spline for two-parameter singularly perturbed boundary value problems, International Journal of Computer Mathematics 89 (6) (2012) 836–850.

[47] W. Zahra, M. El-Azab, A. M. E. Mhlawy, Spline difference scheme for two-parameter singularly perturbed partial differential equations, Journal of applied mathematics & informatics 32 (1–2) (2014) 185–201.

[48] C. Clavero, J. L. Gracia, G. I. Shishkin, L. P. Shishkina, An efficient numerical scheme for 1d parabolic singularly perturbed problems with an interior and boundary layers, Journal of Computational and Applied Mathematics 318 (2017) 634–645.

[49] M. Chandru, T. Prabha, P. Das, V. Shanthi, A numerical method for solving boundary and interior layers dominated parabolic problems with discontinuous convection coefficient and source terms, Differential Equations and Dynamical Systems 27 (2019) 91–112.

[50] D. Kumar, P. Kumari, Uniformly convergent scheme for two-parameter singularly perturbed problems with non-smooth data, Numerical Methods for Partial Differential Equations 37 (1) (2021) 796–817.

[51] K. Mukherjee, S. Natesan, Parameter-uniform hybrid numerical scheme for time-dependent convection-dominated initial-boundary-value problems, Computing 84 (3) (2009) 209–230.

[52] K. Mukherjee, S. Natesan, Parameter-uniform fractional step hybrid numerical scheme for 2D singularly perturbed parabolic convection–diffusion problems, Journal of Applied Mathematics and Computing 60 (1) (2019) 51–86.

[53] K. Mukherjee, S. Natesan, Optimal error estimate of upwind scheme on shishkin-type meshes for singularly perturbed parabolic problems with discontinuous convection coefficients, BIT Numerical Mathematics 51 (2011) 289–315.

[54] A. Das, S. Natesan, Uniformly convergent hybrid numerical scheme for singularly perturbed delay parabolic convection-diffusion problems on shishkin mesh, Applied Mathematics and Computation 271 (2015) 168–186.

[55] A. Das, S. Natesan, Higher-order convergence with fractional-step method for singularly perturbed 2D parabolic convection–diffusion problems on shishkin mesh, Computers & Mathematics with Applications 75 (7) (2018) 2387–2403.

[56] A. Das, S. Natesan, Fractional step method for singularly perturbed 2D delay parabolic convection diffusion problems on shishkin mesh, International Journal of Applied and Computational Mathematics 4 (2) (2018) 1–23.

[57] A. Das, S. Natesan, Parameter-uniform numerical method for singularly perturbed 2d delay parabolic convection–diffusion problems on shishkin mesh, Journal of Applied Mathematics and Computing 59 (1-2) (2019) 207–225.

[58] A. Majumdar, S. Natesan, Alternating direction numerical scheme for singularly perturbed 2D degenerate parabolic convection-diffusion problems, Applied Mathematics and Computation 313 (2017) 453–473.

[59] A. Majumdar, S. Natesan, An ε-uniform hybrid numerical scheme for a singularly perturbed degenerate parabolic convection-diffusion problem, International Journal of Computer Mathematics 96 (7) (2019) 1313–1334.

[60] A. Majumdar, S. Natesan, Second-order uniformly convergent richardson extrapolation method for singularly perturbed degenerate parabolic pdes, International Journal of Applied and Computational Mathematics 3 (2017) 31–53.

[61] A. Majumdar, S. Natesan, A higher-order hybrid numerical scheme for singularly perturbed convection-diffusion problem with boundary and weak interior layers, International Journal of Mathematical Modelling and Numerical Optimisation 10 (1) (2020) 68–101.

[62] A. Majumdar, S. Natesan, Parameter-uniform numerical method for singularly perturbed 2-d parabolic convection–diffusion problem with interior layers, Mathematical Methods in the Applied Sciences 45 (5) (2022) 3039–3057.

[63] J. Gracia, E. O'Riordan, M. Pickett, A parameter robust second order numerical method for a singularly perturbed two-parameter problem, Applied Numerical Mathematics 56 (7) (2006) 962–980.

[64] T. Linß, H.-G. Roos, Analysis of a finite-difference scheme for a singularly perturbed problem with two small parameters, Journal of Mathematical Analysis and Applications 289 (2) (2004) 355–366.

[65] E. O'Riordan, M. L. Pickett, G. I. Shishkin, Singularly perturbed problems modeling reaction-convection-diffusion processes, Computational Methods in Applied Mathematics 3 (3) (2003) 424–442.

[66] C. Clavero, J. Jorge, F. Lisbona, G. Shishkin, An alternating direction scheme on a nonuniform mesh for reaction-diffusion parabolic problems, IMA Journal of Numerical Analysis 20 (2) (2000) 263–280.

[67] C. Clavero, J. L. Gracia, J. C. Jorge, A uniformly convergent alternating direction HODIE finite difference scheme for 2D time-dependent convection–diffusion problems, IMA Journal of Numerical Analysis 26 (1) (2006) 155–172.

[68] E. O'Riordan, M. Pickett, A parameter-uniform numerical method for a singularly perturbed two parameter elliptic problem, Advances in Computational Mathematics 35 (1) (2011) 57–82.

[69] B. Mrityunjoy, S. Natesan, A. Sendur, Alternating direction implicit method for singularly perturbed 2D parabolic convection–diffusion–reaction problem with two small parameters, International Journal of Computer Mathematics 100 (2) (2023) 253–282.

[70] J. L. Gracia, E. O'Riordan, Parameter-uniform approximations for a singularly perturbed convection-diffusion problem with a discontinuous initial condition, Applied Numerical Mathematics 162 (2021) 106–123.

[71] T. A. Nhan, R. Vulanović, The bakhvalov mesh: a complete finite-difference analysis of two-dimensional singularly perturbed convection-diffusion problems, Numerical Algorithms 87 (1) (2021) 203–221.

Status of the works communicated/published:

- **Mrityunjoy, B., Natesan, S., Sendur, A.**, Alternating direction implicit method for singularly perturbed 2D parabolic convection–diffusion–reaction problem with two small parameters, *International Journal of Computer Mathematics*, 100, 253–282, 2023.
- **Mrityunjoy, B., Natesan, S., Sendur, A.**, Parameter-uniform Numerical Solution of a Singularly Perturbed 2D Parabolic Convection-Diffusion-Reaction Problem using ADI Hybrid Scheme **(Under revision)**.
- **Mrityunjoy B., Natesan S., Majumdar A.**, Second-order accurate numerical solution of a singularly perturbed degenerate problem with two perturbation parameters on a layer adapted Shishkin Mesh, **(Under revision)**.
- **Mrityunjoy B., Natesan S., Majumdar A.**, Richardson extrapolation of the numerical solution of singularly perturbed parabolic problems of degenerate type with two parameters, **(Under revision)**.